
Lab Medicine

Editorial

Is It Time for a Broader Call to Learn the Language of Pathology and Laboratory Medicine?

Laboratory Medicine 2021;52:415-419

DOI: 10.1093/labmed/lmab017

The fields of pathology and laboratory medicine have a long-standing pipeline problem.[1,2] Most students do not have medical laboratory sciences or pathology on their list of possible future careers, partly because their exposure to those fields as careers is extremely limited.[3–5] Confounding this problem are the incorrect and contradictory impressions that pathology might be an "inferior" specialty within medicine (due to lack of direct patient contact), chosen by only those with poor communication skills or those who are not doing well academically. Others believe incorrectly that pathology requires only the highest level of scientific knowledge and skills, such that students who are not in the top tiers of their basic science courses need not apply.[6,7]

Similarly, because most university and college academic advisors are unaware of the many career opportunities in the laboratory, they might not actively encourage science and math majors to consider these professions. Everyone has personal or media exposure to physicians and nurses in typical patient-facing roles (on television shows, etc). However, aside from forensic pathologists and crime scene investigators, who are often portrayed in unrealistic settings and roles, there are few media depictions of pathologists or laboratorians to inspire the next generation. Most patients have never toured laboratories or met the laboratory professionals and pathologists who are central to diagnostic patient care. Further, information regarding the lifestyle, reimbursement, and career opportunities in pathology and laboratory medicine/science are not widely available.

How do we address these problems? Many have previously discussed the importance of building pipelines for engaging students earlier in their education and creating inroads into the fields of pathology and laboratory medicine/science. These approaches have been developed, by collaborations with student interest groups, to offer symposia and other events exposing students to laboratory careers. The students selected for these "interventions" are often the same—biology, chemistry, and life sciences majors who do not have a clear understanding of pathology and laboratory careers.

Doing this makes sense, to address the gaps in their understanding of the opportunities that laboratory and pathology careers offer. However, we also suggest considering and reaching out to the "not-so-usual" candidates, among untapped pools of gifted people who would bring uncommon but much-needed skills and perspectives to our profession. Why don't we reach out to arts, music, or history majors? The obvious, traditional answer has been that they lack scientific training, which might seemingly put them at a disadvantage for the profession. However, assuming that they fulfill the usual prerequisites required to enter laboratory-professional training programs or medical school, this would not be an issue. Let us consider the other skills and training that they would bring.

Music Majors

Serious music students typically have extensive training in music theory, a discipline requiring complex spatial memory and analysis of abstract relationships. Music students develop reading, listening, and writing skills, and they approach problems differently from classical cognitive-scientific methods. The tonality and rhythm structures of classical Western music are often quite different from those of Asian and Middle Eastern music, and from some forms of indigenous music and jazz. Performance experiences and courses in music theory require students to set aside their learned preferences to understand and analyze ideas presented in significantly varying forms.[8]

Also, music students are extensively trained in teamwork, professionalism, and discipline. Performing requires listening to others, patience, staying in the present, timing,

taking turns with expressing one's "voice", and sometimes interpreting a score (a set of "rules" or "guidelines") in fresh and innovative ways.[9] These experiences and skills are integrally important in ensemble courses and performance groups, where students learn how to handle conflict and miscommunication professionally. Because a musician's reputation is central to future employment, professionalism and the ability to work with others are critical.

Also, musicians must use their extramural time wisely to reach tangible goals of musical performance proficiency. This work ethic and discipline would extend well to laboratory medicine, such as when scientists agree to take on quality improvement or research projects. These students would be accustomed to working on a team, performing professionally and efficiently to help the laboratory run more smoothly.

Finally, universities around the country have been introducing music double-major options and "music with elective studies" options for students hoping to develop their musical abilities while gaining the education required to enter graduate school in a different topic. These programs are challenging but offer the opportunity for students to balance their scientific studies with a passion for music. This approach could help prevent future burnout and enhance students' ability to maintain a healthy life balance as they progress through their academic and professional careers. These student might bring new approaches to help our profession address wellness and life balance wisely and creatively.[10] It is worth nothing, anecdotally, that many physicians and laboratory scientists are also accomplished musicians. There is considerable overlap in the skill sets involved in medicine and music.

Visual Art Majors

Whether analyzing the subtle strokes of a paintbrush in a work of art or the hues of crystals in joint fluid, many an art-oriented brain has found a home in pathology and the laboratory sciences.[11] Numerous laboratorians have mentioned that their career focus choices had (at one time) hinged on the decision between art vs science. Fine-tuning the assessment of subtle morphological findings in the white blood cells of a peripheral blood smear or analyzing the variations in cytoplasmic content of a sarcoma cell are akin to critiquing brush strokes and colors in a painting—they both require a keen eye, an understanding of the medium, and knowledge of the technique.

Students of the visual arts are taught to observe nuances that may not be obvious to the untrained eye—this is similar to the process of visual recognition of pathological processes grossly and under the microscope. They are also encouraged to innovate in their use of media and technique, developing rigorous knowledge in service of new forms of expression. These attitudes and skills translate well to rethinking and recreating approaches to disease recognition and diagnostic testing. The visual arts (including graphic arts) are mostly about translating thought into visual representations, whether in painting a landscape or designing an effective advertisement. Recognizing meaningful features of visual representations is the common denominator between visual arts and pathology.

Language Majors

All modern pathology laboratories must employ informatic approaches to reporting patient results, processing large data sets, and connecting separate diagnostic and testing instruments to the patient medical record.[12] At a fundamental level, this requires language fluency in converting digital events into human language or linguistic text into digital information amenable to numerical processing. Students with aptitudes and interest in languages are often highly gifted, creative, and indispensable for helping us connect human beings, whether they are health care providers or patients, to information provided by instruments used in our technologically intensive discipline.

Modern health care delivery needs more people who are competent in languages, linguistics, and medical science for a variety of roles, in addition to informatics. In laboratory medicine, these individuals could be even more valuable if they earn medical interpreter certification. Because clinical laboratorians are trained in phlebotomy, scientists with diagnostic understanding and language competency can assist in the patient-facing functions of the laboratory by

delivering patient-centered, culturally competent laboratory care, and in providing patient materials to improve health literacy and understanding of test results. These skills are especially important when establishing or maintaining laboratories or clinics in underserved communities.

Also, medical laboratorians with advanced cultural and language training can serve as cultural liaisons to the laboratory or members of ethics committees specializing in community needs and health initiatives. Pathology is dependent on effective communication at every level. Anecdotally, if you ask scientists what the most difficult part of their job is, many will say writing—yet it is, in many respects, the most important part of their profession.

Engineering Majors

Engineering comprises a diverse collection of majors, including biological, industrial, chemical, electrical, environmental, civil, and computer engineering, among others. Engineering, no matter which path the student chooses, is a challenging major, and along the way, students receive advanced training in the sciences, mathematics, and even business. Because many engineering degrees cover biological sciences and chemistry, these students might not need any additional coursework before pursuing a medical laboratory science graduate degree or medical school.

Central to the training of engineers is the application of science to solve real-world problems. Not only are engineering graduates impressive scientists, but they also bring an advanced understanding of process improvement in the medical laboratory and to the design or improvement of diagnostic testing. Similar to how engineering firms and manufacturing facilities strive to improve profit margins along with technical innovations, clinical laboratories strive to decrease overhead, enhance the interaction between the staff and the instruments, improve efficiency and safety, deliver more and updated pathology and diagnostic services, and enhance the value and quality of services without increasing costs.[13,14] In addition, recent focus in engineering schools on environmental considerations allows graduating students to bring specialized skills to help clinical laboratories address environmental sustainability, an area of increasingly critical need and regulatory burden.

Social Science Majors: History, Anthropology, Sociology, and Psychology

The work of a medical laboratory is to serve patients—this complex process requires working in teams of people with diverse skills and backgrounds. Also, diagnostic testing and applications of guidelines are most likely to be applied correctly and safely when designed by professionals who understand the complexity of human behaviors, particularly when addressing human factors that can lead to error, misinterpretation of results, or implicit biases in decision-making. Social science students bring knowledge of human decision making and preferences to health care, and they are also often trained in the complex, sometimes chaotic factors that lead to choices and behaviors.[15]

In the current era of personalized and precision diagnostics, one fundamental challenge in laboratory medicine is how to address personalized care to an individual patient while incorporating each patient's data points into evidence-based approaches that also ensure diagnostic precision. If psychology and sociology students pursue medical laboratory science or pathology, their training in human behavior could help the laboratory team improve patient care while bringing more attention to the humanistic side of laboratory medicine practice.

In addition to the understanding of the human experience that these students have, they also have training in research methods and statistics. During their training as social scientists, they gain experience with developing and leading research projects, which further develops their leadership skills associated with project management. Some social scientists would bring experience from working with diverse populations during their research. Addressing health equity in laboratory practice requires us to include people with these skills on our teams.

Summary

As mentioned earlier herein, recruiting students with diverse educational backgrounds can improve the practice of pathology and laboratory medicine by inviting, and deliberately including, different approaches and skills to tackling the problems facing the clinical laboratory. This concept has

Lab Medicine 2021;52;415–419 417
DOI: 10.1093/labmed/lmab017

been introduced into admissions initiatives in some medical schools and other medical graduate programs but has yet to be explicitly introduced into medical laboratory science graduate programs. However, if similar holistic admissions and outreach programs were implemented, the field of pathology and laboratory medicine could be enriched by innovative approaches. As a side benefit, increasing the visibility and the intellectual and cultural diversity in laboratory medicine could bring about a better understanding of the field to the public.

To increase broader knowledge about opportunities in the fields of pathology and laboratory medicine/science, we need to improve outreach to high school students who are considering their future majors at the time that they are making university choices. We also need to provide middle-school students and their parents with an "educational roadmap" informing them of the breadth of opportunities in those fields, from phlebotomy through the MD/PhD level, as well as the prerequisites needed, because students may need to select a college prep track that will provide them with the skills needed to enter training programs in those fields. There will also likely need to be a radical shift in how medical laboratory scientists are trained, given that most students pursue 4-year degrees before deciding on their profession.

Thinking critically about enhancing recruitment into the field requires institutions to develop creative solutions like a professional Master's program or an advanced postbaccalaureate training program. Still, these programs must consider the amount of debt that students are likely to carry before entry. Because some training programs are not linked to a college or university (ie, a hospital-linked training program), it may be difficult to pay for the program and one's other living expenses while making required payments on undergraduate loans. We may need to develop creative work-study programs by which students gain tuition reimbursement through work in our laboratories, or by developing state and national loan-forgiveness programs with placement of our graduates in areas with high need.

*To whom correspondence should be addressed.
Kamran.Mirza@LUMC.edu

Kamran M. Mirza, MD, PhD, FASCP, MLS(ASCP)^{CM},[1,*] Cullen M. Lilley, MS, MB(ASCP), MDxT(AAB),[1] Melissa P. Upton, MD, FASCP[2]

[1]Department of Pathology and Laboratory Medicine, Loyola University Chicago Stritch School of Medicine, Maywood, Illinois, [2]Department of Laboratory Medicine and Pathology, University of Washington, Seattle, Washington

Cullen M. Lilley, MS, MB(ASCP), MDxT(AAB) is a current MD/MA candidate studying medicine and bioethics/health policy at Loyola University Chicago Stritch School of Medicine. Before medical school, Cullen was a microbiologist at the Centers for Disease Control and Prevention contracted through IHRC, inc. and received a Master of Science in microbiology from the University of Florida. Cullen received his Bachelor of Music and Bachelor of Science from Loyola University New Orleans. You can follow him on twitter @Cullen_Lilley.

Kamran Mirza, MD PhD FCAP MLS(ASCP)^{CM} is an Associate Professor of Pathology and Laboratory Medicine, Medical Education and Applies Health Sciences at Loyola University Chicago Stritch School of Medicine and Parkinson School of Health Sciences and Public Health. Kamran serves as the Vice-Chair of Education in the Department of Pathology and Laboratory Medicine and is the founding Program Director of the M.S. degree in Medical Laboratory Science at LUC Parkinson School of Health Sciences and Public Health. Kamran can be found on Twitter @KMirza.

Dr. Upton is board certified in Anatomic Pathology and Cytology and directed an autopsy service and forensic pathology fellowship program at Beth Israel Deaconess Medical Center in Boston, Massachusetts. She has also practiced cytopathology and general surgical pathology, and has focused on genitourinary pathology, head and neck pathology, and gastroenterology (GI) and liver pathology. From 1982-85 and 1987-2002, Dr. Upton lived in Boston and taught at Tufts, Boston, and Harvard Universities. Since 2002, she has been at the University of Washington in Seattle, where she formerly directed the GI and Hepatic Pathology Service the Pathology Residency Program and the UW GI and Hepatic Pathology Fellowship. Currently Emeritus Professor of Pathology, she continues to practice Surgical Pathology, Autopsy Pathology, and Cytopathology, and she is one of the specialists at UW in the areas of GI, liver, and pancreatic pathology.

References

1. Naritoku WY, Timmons CF. The pathologist pipeline: Implications of changes for programs and post-sophomore fellowships-program directors' section perspective. *Acad Pathol.* 2016;3:2374289516646117.
2. Zafar N, Baccon J. So you want to be a pathologist. Accessed on April 25, 2021. https://thepathologist.com/outside-the-lab/so-you-want-to-be-a-pathologist
3. Bennett A, Garcia E, Schulze M, et al. Building a laboratory workforce to meet the future: ASCP Task Force on the Laboratory Professionals Workforce. *Am J Clin Pathol.* 2014;141(2):154–167.
4. Ahmed A, Mirza K. Pathology: a clinical specialty. Accessed on April 25, 2021. https://thepathologist.com/outside-the-lab/pathology-a-clinical-specialty
5. McHenry A, Mirza K. The case for a universal clerkship. Accessed on April 25, 2021. https://thepathologist.com/outside-the-lab/the-case-for-a-universal-clerkship
6. Hung T, Jarvis-Selinger S, Ford JC. Residency choices by graduating medical students: why not pathology? *Hum Pathol.* 2011;42(6):802–807.
7. Raphael S, Lingard L. Choosing pathology: a qualitative analysis of the changing factors affecting medical career choice. *J Int Assoc Med Sci Educ*. 2005;15:81–91.
8. Onu BO. Music and Intercultural Communicaiton. In: N Iheanacho, ed. *Intercultural Communication and Public Policy*. M & J Grand Orbit Communications; 2016:195–212.
9. Urbain O. Business and music in peacebuilding activities. *Coll Music Symp*. 2018;58:1–15.
10. Reed K, Cochran KL, Edelblute A, et al. Creative arts therapy as a potential intervention to prevent burnout and build resilience in health care professionals. *AACN Adv Crit Care.* 2020;31(2):179–190.
11. DeLue RZ. Art and science in America. *Am Art*. 2009;23(2):2–9.
12. Liao KP, Cai T, Savova GK, et al. Development of phenotype algorithms using electronic medical records and incorporating natural language processing. *BMJ.* 2015; 350:h1885.
13. Jimmerson C, Weber D, Sobek DK 2nd. Reducing waste and errors: piloting lean principles at Intermountain Healthcare. *Jt Comm J Qual Patient Saf.* 2005;31(5):249–257.
14. Jensen K, Haniff R, Kamarinos A, Rosenberg A, Santiago M, Laser J. Improving turnaround times through a process improvement initiative involving barcoding, floorplans, dual measuring cells, chemistry analyzers, and staff shifts. *J Appl Lab Med.* 2019;4(3): 311–322.
15. Phillips JH. "Classics and the science undergraduate major" revisited: three decades of a successful and relevant pedagogical approach. *Class Outlook*. 2015;90(4):121–126.

DOI: 10.1093/labmed/lmab017

Special Report

Strategies for Sustainability of University-Based Medical Laboratory Sciences Programs

Kristina Jackson Behan, PhD, MLS(ASCP)[CM]*

Laboratory Medicine 2021;52:420-425

DOI: 10.1093/labmed/lmaa109

ABSTRACT

The COVID-19 pandemic has taken a major toll on the economy and funding for public education. For that reason, the pandemic has a worrisome effect on the sustainability of university/college based Medical Laboratory Sciences MLS training programs. Stakeholders of university-based MLS programs include university administrators, students, clinical affiliates and faculty. Each group has specific goals and challenges that affect the sustainability of the program. This report details strategies that can be used to satisfy the goals specific to key stakeholders that lead to sustainability. These strategies apply in pandemic times and in the back-to-normal future.

Keywords: COVID-19, enrollment, pandemic, education, management/administration, sustainability, economy

The COVID-19 pandemic has put a spotlight on the role of medical laboratories. Even before the pandemic, the projected employment growth for medical laboratory scientists from 2019 to 2029 was expected to be 7%, higher than the average.[1] Whether medical laboratory sciences (MLS) programs in their current construct will be able to keep up with the projected growth remains to be seen. The number of National Accrediting Agency for Clinical Laboratory Sciences accredited MLS programs increased only slightly in the past 10 years, from 230 in 2009 to 235 in 2019.[2,3] The American Association for Clinical Chemistry recently asked Congress for funding to expand clinical laboratory training programs for future pandemic preparedness.[4] These efforts will take time to see fruition. In the meantime, the economy has suffered greatly, and so has funding for public education. Colleges and universities across the nation are making drastic budget cuts, restructuring their units and eliminating some degrees.[5] For that reason, the pandemic has a worrisome effect on the sustainability of university-/college-based MLS training programs.

Stakeholders of university-based MLS programs include university administrators, students, clinical affiliates, and faculty. Each group has specific goals and challenges that affect the sustainability of the program. This report details strategies that are being used by 1 institution to satisfy the goals of those stakeholders, leading to a sustainable university-based MLS program. These strategies include changes made because of the COVID-19 pandemic. Herein they are organized by stakeholder, but there is significant overlap between the groups.

Abbreviations:

MLS, medical laboratory sciences; BMS, biomedical science; ASCP, American Society for Clinical Pathology; MLT, medical laboratory technician; CLEC, Clinical Laboratory Educators' Conference; SIM, simulated

University of West Florida Medical Laboratory Sciences Department, Pensacola, Florida, USA

*To whom correspondence should be addressed.
kbehan@uwf.edu

Administrators

University administrators scrutinize programs when the economy suffers. Criteria used to evaluate programs include demand (enrollment), quality, relevance to the workforce, compatibility with the university mission, and program cost.[6,7] It is important to ensure that administrators know about program quality, including the program outcomes of graduation rate, board examination pass rate, job placement rate, and community support. Administrators should be reminded of the university's National Accrediting Agency for Clinical Laboratory Sciences accreditation. These are

significant criteria to justify program cost, but program faculty must be aware that enrollment may be the final determinant.

Strategy 1

Administrators and faculty must determine the minimum annual number of graduates or student credit hours that their program needs to be fiscally sound to their home institution and aim to exceed it. Increasing the number of students requires student recruitment and expansion of clinical affiliates. It also puts a major onus on the faculty for student success.

Students

The MLS profession has low visibility to the public at large.[8,9] Many students report that they have never heard of the major.

Strategy 2

Faculty can promote their program to similar majors, eg, biomedical science (BMS)/biology, at their institution. An ideal method is to insert 1 or more MLS courses into the BMS curriculum, preferably as a required course. This strategy requires significant buy-in if the MLS program is not housed in the same department or college as the BMS program. Faculty can attend each others' faculty meetings, provide syllabi, and show how MLS course content will benefit the BMS students in their ultimate careers. In addition faculty can invite BMS faculty to tour a medical laboratory with them. As fellow scientists, this will help them gain an appreciation of the laboratory skills that the MLS courses provide. At the author's institution, the MLS and BMS programs had the same dean. The programs worked side by side to align their curricula.

Faculty should identify the goals of the nonmajor students early in the course and regularly relate course content to those goals. One way to do this is to ask students to introduce themselves early in the class and state their career goals. During the introduction process, the instructor can immediately relate the overall goals of the course to the student. Faculty may return to these goals when discussing specific topics and consider the lens through which a nonmajor is viewing the course while teaching. For example, premedical students taking hematology are more interested in the disease acute myelogenous leukemia than in the difference between a metamyelocyte and a myelocyte. Faculty can discuss the big picture and how a physician will utilize the results of complete blood counts, cytogenetics, and flow cytometry in making a diagnosis. Prepharmacy students taking microbiology are interested in how antimicrobials work, and predental students should be tuned in to the importance of oropharyngeal flora and pathogens. Instructors should keep their learning goals aligned with the career goals of their audience, and show all their students that instructors respect their students' goals.

When nonmajors are incorporated into MLS courses, it benefits the program in 3 ways. First, it increases enrollment in courses. In spring 2020 at the author's institution, there were 24 MLS majors and 23 BMS majors taking diagnostic microbiology (a required course for BMS) and 24 BMS majors taking hematology (an elective). The BMS majors provided a significant increase in credit hours that was viewed favorably by upper administration. Second, nonmajor students may select MLS as an alternate career or change majors. Third, one expects that the students who become doctors, dentists, physician assistants, and pharmacists will have a deeper appreciation for the role and training of medical laboratory scientists. The author's institution has received thank-you cards from past students attending those professional schools in which they expressed appreciation for the deep learning they received from their MLS courses.

Strategy 3

Faculty can recruit BMS/biology alumni to their MLS program and advertise MLS as a second degree on the departmental website. Earning a second degree appeals to many students. At the author's institution, the BMS degree aligns with the MLS degree, so that all of the MLS prerequisite courses have been completed by BMS graduates. Postbaccalaureate students are admitted to the program in the same manner as transfer students and complete the core courses to earn the second degree. Administrators can obtain the email list of those alumni from the registrar and contact them 1, 2, and 3 semesters after graduation. It is important to turn around phone and email queries quickly.

Strategy 4

Faculty should add more start dates to their program, once in each semester if possible, which will minimize the amount of

Lab Medicine 2021;52;420–425 421
DOI: 10.1093/labmed/lmaa109

time a prospective student has to wait to start, which leads to retention. Faculty at the author's institution realized the retention implication at a time when they were struggling to increase their student numbers. Historically, the program had begun in January only. Two students who missed the start date reported that they were applying to other programs. To retain them, the institution opened the second start date in May. They consequently gained 5 students that year from that modification. Multiple start dates also improve retention by providing wiggle room for students who get off-track for personal reasons.

The author's MLS program offers its courses once per year, and laboratory sections run in the same semester as the lectures. Instructors may need to revise certain aspects of their MLS core courses and repeat key topics accordingly so that courses do not have to be taken in a particular sequence. For example, some students will take hematology before hemostasis, but others will not. Faculty must keep this in mind when they design lectures and experiments. The nonsequential course design fits well with BMS students, because they do not have the advantage of an MLS background. Some laboratory skills are repeated every semester, such as laboratory safety and microscopy. Phlebotomy and specimen types are discussed in every laboratory section. The reiteration about preanalytical, analytical, and postanalytical issues is beneficial to students.

Strategy 5

Faculty may consider adding categorical training to their program. Students with a bachelor of science degree can qualify for American Society for Clinical Pathology (ASCP) categorical training in microbiology, hematology, chemistry, or immunohematology by completing a structured program of the categorical requirements from an MLS curriculum. A survey of MLS program directors conducted in 2016 found that 29.0% of university programs accepted categorical students.[10]

Strategy 6

Faculty can create opportunities to support community within the student groups. Students in their second or third semester of the program can lead study groups. This activity provides teaching practice for more seasoned students and support for new students, nonmajors, and faculty members. Its aim is to improve student retention in the course and to extend the reputation of the program to nonmajors. Study groups can be set up during laboratory time where attendance is graded. Study groups held outside class time are poorly attended without incentive, and a small amount of extra credit will increase participation. Weekly study groups help students stay on track, especially if classes are online and self-paced. Students also improve their communication and organizational skills by their participation. **Image 1** shows a student-led study group at the author's institution. Zoom, WebEx, and other virtual platforms are a convenient mechanism for student groups to meet. Virtual platforms became very popular after March 2020 because of COVID-19.

Image 1

Building community. Students in their third semester (term 3) host weekly study sessions.

Clinical Affiliates

The number of clinical seats is a limiting factor for program growth.[10] Some training hospitals accommodate MLS and medical laboratory technician (MLT) students from other programs. Local hospitals may not have a sufficient test menu to train students.

Strategy 7

It is important to recruit more clinical sites. Faculty can use their state's hospital database to search out prospective sites for training, including Veterans Administration and military hospitals. Faculty should look outside of their own state, especially if they are located near the state border. Many hospitals will make the argument that they cannot train students because they have a personnel shortage themselves. This is an opportunity, not a drawback. The 2018 ASCP vacancy

survey[11] reported that the second and third top difficulties in hiring result from increased competition for well-trained personnel and because of applicants who do not have the necessary certification, education, and skills to perform the work. Faculty can emphasize to prospective affiliates that graduates are more likely to be hired by the hospital that trains them. Hospital human resources departments can be very helpful with this argument. Matching student profiles to training sites will facilitate their retention as employees. For example, if a student wants to be involved in research, then that student should be placed at a research institution. If a student is a veteran, then that student should be placed at a Veterans Administration facility. It is vital not to overlook smaller facilities. Hospitals that have a limited menu (eg, no microbiology training) can be paired with larger hospitals to complete student internship training. Courting new sites takes time, effort, training, and of course, an affiliation agreement. This may take more than 6 months to accomplish, so faculty should plan ahead.

Strategy 8

Clinical affiliate training capacity should be increased, with staggered start dates for clinical rotations. Large facilities that take 4 students in a traditional program may be able to expand to 6 students when the start dates are staggered. Employers who are part of the author's institution's Program Advisory Committee initially resisted this idea but now express their appreciation for having prospective employees graduating every 4 months.

Strategy 9

Faculty should consider how to shorten onsite training time. Four presentations at the February 2020 Clinical Laboratory Educators' Conference (CLEC) conference reported the benefits of a hybrid program that paired simulated (SIM) laboratories with shortened onsite training, and the presenters expressed their satisfaction with student outcomes.[12-15] The idea is to create a nonclinical semester on campus that utilizes robust SIM laboratory experiences that is paired with a second semester onsite. Utilizing this strategy, a program can double its student placement with the same number of affiliates. Designing SIM labs and supporting them is a significant effort in time and expense. Facilities, faculty, and materials must be considered and supported. Affiliate buy-in is essential to these changes. Program faculty can create a framework for discussion with their advisory board and maximize the utility of their suggestions in the ultimate curriculum redesign.

In 2020, the COVID-19 pandemic has led to a rapid redesign of many programs as educators have held to their mission of graduating qualified medical laboratory scientists. A survey was sent to the MLS and MLT program directors who attended CLEC 2020 regarding changes they made because of the pandemic. Thirty-four out of the 46 programs that participated in the survey applied a hybrid approach, substituting virtual laboratories for some of the onsite clinical training. Many respondents provided comments that expressed their pride in their simulated laboratory sessions and their virtual meetings.[16]

Faculty

Strategy 10

Curriculum design is an exciting and creative task. Faculty can strategize curriculum change as a group and expect that brainstorming will take several sessions over at least a semester. It is important to set an overarching schedule and a smaller agenda for each session. The following questions can be included: What are the essential skills that should be offered every semester? What can be offered as SIM laboratories? What can be offered as a virtual laboratory? How can instructors keep track of students in different cohorts? Which courses can be offered online, and which courses must be face-to-face? What clinical sites should be courted, and who will make the contact? Which courses best fit nonmajor students? What have other programs done that worked? A faculty member can be assigned as the devil's advocate during the strategizing. This assigned duty highlights potential pitfalls and avoids hard feelings. The program director can set timelines for task completion and assign faculty as needed to accomplish goals. Faculty should be encouraged to present their work at conferences and as publications on the scholarship of teaching and learning, an added benefit for tenure-track faculty members.

Note that the strategies for sustainability must satisfy all stakeholders. **Table 1** lists the strategies and relates them to specific stakeholders. The following case study discusses the author's program before and after utilizing these strategies.

Lab Medicine 2021;52;420–425 423
DOI: 10.1093/labmed/lmaa109

Table 1. Eleven Strategies for Sustainability (and their stakeholders)

Strategy	Stakeholders
Fulfill enrollment goal of institution	Administrators
Promote the program to students in similar majors at institution	Students
Recruit alumni of similar majors from institution	Students
Add additional start dates to program	Students
Consider categorical training	Students
Create community within student groups to aid retention and expand program reputation	Students
Add clinical sites	Affiliates
Stretch clinical site capacity	Affiliates
Shorten onsite clinical training	Affiliates
Strategize curriculum changes creatively	Faculty and affiliates
Be flexible	Everyone

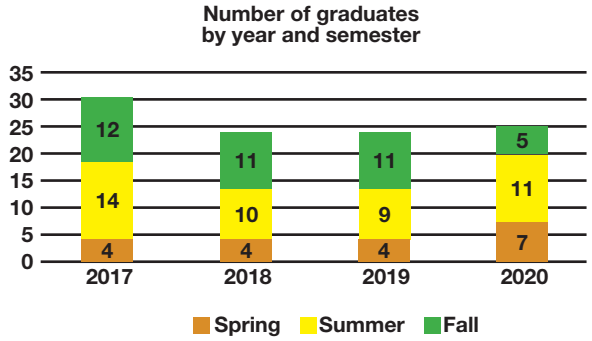

Figure 1

Four-year summary of graduates of case study MLS program stratified by semester of graduation. Spring is orange, summer is yellow, and fall is green. Note the variability in enrollment across semesters. MLS, medical laboratory sciences.

Case Study: Strategies in Action

Before the recession of 2008, the author's MLS program graduated 12 to 16 students per year. The program was 2 + 2, part of a bachelor of science degree. It was 5 semesters long; the clinical year started in January. There were 6 full-service affiliates who took 1 to 4 students for a 29-week rotation. In 2008, university administrators threatened program closure because of the economy. The criterion for closure was low enrollment. Administrators and faculty followed a number of strategies to sustain the program.

The university's formula was used to determine that the minimum graduate number for sustainability was 24 students. A second start date in May was opened, enrolling postbaccalaureate students and students who were off-track by a semester. Eventually, another start date in August was added. To keep track of student cohorts, they were grouped by term and were oriented to specific requirements relevant to each term. Term 1 students had just joined, term 3 students were preparing for clinicals, and term 5 students were getting ready to graduate. A limit of 40 students per year was set, but no limit was set on the size of each cohort. **Figure 1** shows 4 years of enrollment by the semester that students graduated from the program. The fluctuation of the numbers by year is notable.

Nonmajor (BMS, biology, and chemistry) alumni were recruited with direct emails sent twice, at 6 months and at 12 months after their graduation. The MLS course in diagnostic microbiology was added as a required course, and hematology was added as an elective to the BMS curriculum; these additions increased the program's visibility and added more student credit hours to the department. The exposure to the MLS curriculum has caused some students to change majors or come back to the MLS program postgraduation. Three more laboratory sections were added to select core courses because of the boost in enrollment, which also boosted the program's credit hours. The website advertises clinical laboratory sciences as a second degree.

Program faculty courted more clinical sites, especially focusing on hospitals in major cities that were experiencing workforce shortages. In addition, they expanded their geographic range; the program has 22 active affiliates that span more than 500 miles from east to west in 2 states. The program pairs large and small hospitals to fulfill curricular requirements. Faculty and administrators attempt to match student preferences to the sites, and so far, every student has been placed without a delay in progression to graduation. The larger affiliates take up to 6 students per year. Students with personal or health issues who need time off can more easily return, which reduces attrition. A recurring snag is that clinical sites cannot always accommodate the same number of students, and the number of students varies each semester. This variability can make scheduling clinical internships more difficult, but it is not insurmountable.

The COVID-19 pandemic has forced some rapid changes to program delivery and to the clinical internships. From

mid-March to July 2020, the university phase of the program pivoted to total online delivery. Virtual laboratories were purchased and/or developed, and alternate assignments were made. Students and faculty met regularly over WebEx, Google Hangouts, and Zoom. Several clinical sites were no longer able to accept students, and 3 students chose to postpone clinical training. Some of the affiliate hospitals that were experiencing workforce shortages recognized this crisis as a hiring opportunity, integrating the displaced trainees and eventually hiring them. Administrators and faculty shortened the onsite training time and created robust SIM laboratories and online practical exams for the clinical students. The customary end of program ASCP preparation "Review Week" was held using WebEx. The feedback from clinical affiliates during the redesign was considered, and alterations based on their input were made.

The MLS program has graduated 2 cohorts during the pandemic with a total of 20 students. All students took the ASCP Board of Certification examination, with a 95% pass rate on the first attempt. The median overall score for these students was 537, compared to the national mean scaled score of 503. It was also higher than the median score for the students who took the examination in 2019. All of the graduates who sought employment found it. Program faculty and administrators will continue to evaluate employer feedback through the Advisory Committee.

Conclusion

For university-based MLS programs to remain viable, they must satisfy the demands of their stakeholders. To satisfy university administrators, they must meet certain enrollment goals. To boost enrollment, they must recruit more qualified applicants. To train applicants, they must increase the number of clinical training sites. This report shares multiple strategies that were used by the author's MLS program to meet these requirements. These strategies take time and effort to put them in place. The COVID-19 pandemic has added additional constraints in 2020, especially regarding hands-on experience, and has required a rapid response. The impact of this response is still being evaluated, but so far it appears successful, leading to the final strategy: be flexible. **LM**

References

1. Occupational Outlook Handbook: clinical laboratory technologists and technicians. U.S. Bureau of Labor Statistics website. https://www.bls.gov/ooh/healthcare/clinical-laboratory-technologists-and-technicians.htm. Accessed September 28, 2020.
2. NAACLS 2019 annual report. National Accrediting Agency for Clinical Laboratory Sciences website. https://naacls.org/NAACLS/media/Documents/AnnualReport.pdf. Accessed September 28, 2020.
3. Hunt W. NAACLS update 2018. American Society for Clinical Laboratory Science website. http://www.ascls.org/images/Meetings/CLEC/CLEChandouts/Thursday_230pm_NAACLS-Update_Handout.pdf. Accessed September 28, 2020.
4. AACC urges Congress to fund lab training programs to prepare US for future pandemics. American Association for Clinical Chemistry website. https://www.aacc.org/media/press-release-archive. Published September 17, 2020. Accessed September 29, 2020.
5. Hubler S. Colleges slash budgets in the pandemic, with "nothing off-limits." *The New York Times*, November 2, 2020. https://www.nytimes.com/2020/10/26/us/colleges-coronavirus-budget-cuts.html. Accessed November 24, 2020.
6. Mangan K. A college weighs its priorities before making cuts. *The Chronicle of Higher Education*. https://www.chronicle.com/article/a-college-weighs-its-priorities-before-making-cuts/. Published November 17, 2017. Accessed November 24, 2020.
7. Will M. The anatomy of an academic program cut. *The Chronicle of Higher Education*. https://www.chronicle.com/article/the-anatomy-of-an-academic-program-cut/. Published February 6, 2015. Accessed November 24, 2020.
8. Beazer K, Cummins K. Effective marketing strategies for a medical laboratory science program. *American Society for Clinical Laboratory Science*. Published online February 2020. doi: 10.29074/ascls.119.002154.
9. Doby CF. *Awareness of Clinical Laboratory Sciences and Shortage of Clinical Laboratory Scientists in the 21st Century*. *Walden Dissertations and Doctoral Studies*; 2016. Accessed November 24, 2020. https://scholarworks.waldenu.edu/dissertations/3095
10. Brown K, Parker Fenn J, Fong K, et al. ASCP Board of Certification survey of medical laboratory science faculty. *Lab Med.* 2019;50(4):e75–e81.
11. Garcia E, Kundu I, Kelly M, Soles R. The American Society for Clinical Pathology's 2018 vacancy survey of medical laboratories in the United States. *Am J Clin Pathol.* 2019;152(2):155–168.
12. deRegnier D, Ruskin L. Simulation in laboratory education: best practices, models, and future. Paper presented at: ASCLS Clinical Laboratory Educators Conference Program; February 27, 2020; Orlando, FL. https://www.ascls.org/images/Meetings/CLEC/2020Orlando/2020_CLEC_PG_Final_WEBv2.pdf
13. Mantini J, Natter A. Measuring the success of a shortened clinical rotation. Paper presented at: ASCLS Clinical Laboratory Educators Conference Program; February 27, 2020; Orlando, FL. https://www.ascls.org/images/Meetings/CLEC/2020Orlando/2020_CLEC_PG_Final_WEBv2.pdf
14. Conway-Klaassen J, Tille P. Best practices in laboratory simulation: eliminating the need for rotations. Paper presented at: ASCLS Clinical Laboratory Educators Conference Program; February 28, 2020; Orlando, FL. https://www.ascls.org/images/Meetings/CLEC/2020Orlando/2020_CLEC_PG_Final_WEBv2.pdf
15. O'Shields A, Porter J. Bringing clinical microbiology training to campus: our MLT programs are making it work. Paper presented at: ASCLS Clinical Laboratory Educators Conference Program; February 28, 2020; Orlando, FL. https://www.ascls.org/images/Meetings/CLEC/2020Orlando/2020_CLEC_PG_Final_WEBv2.pdf
16. Behan K, Cavnar K, Biswas-Fiss E. Medical lab training programs response to COVID-19. *ASCLS Education Digest*. Published August 6, 2020. www.ascls.org.

DOI: 10.1093/labmed/lmaa109

Overview

Smudge Cells in Chronic Lymphocytic Leukemia: Pathophysiology, Laboratory Considerations, and Clinical Significance

Steven M. Marionneaux, MS, MT(ASCP),[1,2] Elaine M. Keohane, PhD,[1] Nicole Lamanna, MD,[3] Thomas C. King, MD, PhD,[1,4] Shashi R. Mehta, PhD[1,]*

Laboratory Medicine 2021;52:426-438

DOI: 10.1093/labmed/lmaa119

ABSTRACT

Chronic lymphocytic leukemia (CLL) is the most commonly encountered leukemia in the clinical laboratory. Cytoskeletal defects in CLL lymphocytes can result in the formation of up to 75% smudge cells (SCs) during blood film preparation. Failure to account for these damaged lymphocytes in the white blood cell (WBC) differential diminishes the accuracy and reproducibility of the results. Lacking clear practice standards on handling SCs in CLL, different laboratories may employ different methods to mitigate SC-induced errors. This review explores the pathophysiology of SCs, their effect on WBC differentials in CLL, and how these results can impact clinical decisions. The pros and cons of various SC corrective methods are described to assist laboratories in developing an optimized protocol to reduce errors and inconsistencies in WBC differentials. Finally, the potential utility of SC enumeration as an indicator of CLL prognosis is discussed in terms of laboratories with differing access to technology.

Keywords: chronic lymphocytic leukemia, smudge cells, WBC differential, lymphocyte doubling time, absolute lymphocyte count, lymphocyte cytoskeleton, CLL prognosis, CLL

Chronic lymphocytic leukemia (CLL) is the most common leukemia in the Western world.[1] It is characterized by the proliferation and accumulation of a malignant clone of mature B lymphocytes in the bone marrow, blood, lymph nodes, and spleen. It is primarily a disease of older adults, and the incidence increases with age. The median age at diagnosis is 70 years.[1] The clinical behavior of the disease is heterogeneous. Whereas some patients never require treatment, others have aggressive, treatment-refractory disease and drastically reduced survival. There are numerous predictive and prognostic biomarkers available to stratify patients with CLL and help guide treatment decisions.

Abbreviations:

CLL, chronic lymphocytic leukemia; SC, smudge cell; WBC, white blood cell; ALC, absolute lymphocyte count; CBC, complete blood count; ANC, absolute neutrophil count; mDIFF, manual WBC differential; aDIFF, automated WBC differential; CLSI, Clinical and Laboratory Standards Institute; LDT, lymphocyte doubling time.

[1]Clinical Laboratory and Medical Imaging Sciences, School of Health Professions, Rutgers University, Newark, New Jersey, USA, [2]Scientific Affairs, Cellavision AB, Lund, Sweden, [3]Division of Hematology and Oncology, Department of Medicine, New York Presbyterian/Columbia University Medical Center, New York, New York, USA, [4]Immunovia, Inc, Marlborough, Massachusetts, USA

*To whom correspondence should be addressed.
mehtas1@shp.rutgers.edu

Most patients with CLL are asymptomatic at diagnosis. The disease is often discovered as an incidental finding during routine laboratory testing when the absolute lymphocyte count (ALC) is increased. The diagnosis is based on a sustained increase in peripheral blood B lymphocytes ≥ 5.0×10^9/L and a characteristic immunophenotype indicated by flow cytometry.[2] The ALC frequently serves as a surrogate test for the B lymphocyte count in CLL. The complete blood count (CBC) and white blood cell (WBC) differential is performed at regular intervals on all patients with CLL to measure the ALC, the absolute neutrophil count (ANC), hemoglobin, platelet count, and other parameters. A peripheral blood film review with or without manual WBC differential (mDIFF) is frequently required because of increased ALC, cytopenias, and/or hematology analyzer flags.[3]

Smudge cells (SCs), also known as Gumprecht shadows, smear cells, or basket cells, are a common finding on blood films of patients with CLL. In CLL, nearly all SCs represent damaged lymphocytes and are sometimes excluded from the mDIFF. However, doing so can significantly affect the accuracy and reproducibility of the WBC differential cell counts.[4-6] Although laboratory accreditation agencies such as the College of American Pathologists and the New York State Department of Health do not require laboratories to address the inaccuracies caused by SCs, many laboratories nonetheless use various corrective methods that are associated with advantages and disadvantages. Unfortunately, there is no universally recognized approach, and peer-reviewed publications on this topic are scarce. As a result, this review includes information obtained from peer-reviewed and non-peer-reviewed articles, print and online textbooks, statistical databases, practice guidelines, conference proceedings, hematology analyzer company websites, health organization websites, blogs, and other materials from the internet. What follows is an in-depth review of SCs seen in CLL, including their cause and clinical and laboratory significance and the methods used to analyze specimens containing SCs that best conserve the accuracy and reproducibility of the WBC differential.

Pathophysiology of SCs

One can readily observe SCs on the blood films of nearly all patients with CLL; they typically comprise 20% to 30% of total lymphocytes. However, SC concentration can vary, ranging from 1% to 75% or higher between patients.[7-10] In an individual patient with CLL, although there can be minor fluctuations, the percentage of SCs tends to remain stable over time, despite changes in the ALC.[9,11] There are characteristic intracellular abnormalities in lymphocytes along with other factors that lead to SC formation and influence the number of SCs observed on the blood films of patients with CLL.

Normal Lymphocyte Cytoskeleton

Normally, circulating lymphocytes are stressed by mechanical and hydrodynamic forces and thus require an intact and dynamic cytoskeleton to survive. This cytoskeleton enables the lymphocytes to be rigid in circulation yet deformable when they transmigrate into tissues.[12] Vimentin is an intermediate filament protein that is a primary component of the cytoskeleton and is important for membrane integrity. Along with other structural proteins, vimentin forms a network that encases the nucleus and extends throughout the cytoplasm.[13,14] A normal functioning cytoskeleton is also required for the lymphocyte to endure the mechanical forces involved in making a blood film.

CLL Lymphocyte Cytoskeleton

Quantitative and qualitative abnormalities in the proteins that make up the nuclear envelope and plasma membrane cause CLL lymphocytes to be stiffer, less deformable, and more fragile than normal lymphocytes.[15] These defects appear to be heterogeneously expressed among CLL lymphocytes both within and between patients[9,16] and include decreased but variable levels of cytoskeletal vimentin.[7,9] In addition, vimentin filaments are abnormally organized within the cytoskeleton.[16] Vimentin abnormalities in CLL lymphocytes lead to impairment and instability in the cytoplasmic membrane and subcellular structures, including the nuclear envelope.[17] In addition to vimentin defects, CLL lymphocytes are deficient in actin, another cytoskeletal protein that is important for maintaining structural integrity.[18] However, some researchers have suggested that the deformability and fragility of CLL lymphocytes may be more related to vimentin defects rather than to low levels of actin.[19]

When a normal lymphocyte comes into contact with a glass slide, vimentin filaments polymerize and form a cap on one side of the cell.[16] Capping helps the cell adhere and maintain its shape. Cap formation has been shown to be defective in CLL lymphocytes. Stark, Liebes, Shelanski, et al[16] found that 21% of lymphocytes in patients with CLL versus 47% of lymphocytes in healthy donors exhibited capping when the cells were exposed to a glass surface (P <.002). In addition, CLL lymphocytes have shown heterogeneity in the ability to form caps. Because capping is needed for structural stability on a glass surface, the degree of the vimentin defect and thus the inhibition of capping at least partially determines whether a CLL lymphocyte will stay intact or smudge as blood is spread along a glass slide.

Apoptosis and Smudging

Lymphocytes in CLL exhibit decreased expression of CD45, which has been shown to be inversely proportional to SC concentration.[20] The fragility of CLL lymphocytes as measured by osmotic shock–induced cell lysis is also inversely

DOI: 10.1093/labmed/lmaa119

proportional to CD45 expression.[20] There does not appear to be any direct evidence that links CD45 with cytoskeletal proteins in B cells. Studies of T cells, however, have shown that CD45 is related to the protein fondrin, which links CD45 with the cytoskeleton and induces apoptosis-related morphologic changes.[21] Further, CD45 is a receptor for galectin-1, which can initiate apoptosis.[22] Decreased vimentin has also been shown to promote apoptosis of lymphocytes.[23] Although they are protected from apoptosis in vivo, a variable number of CLL lymphocytes undergo spontaneous apoptosis in vitro.[24] Fumi et al[25] found a linear correlation between the number of apoptotic CLL lymphocytes and SCs using an Abbott Sapphire hematology analyzer (Abbott, Santa Clara, CA), which utilizes propidium iodide to identify nonviable, or apoptotic, WBCs. Rusak et al[26] also observed a correlation between SCs and apoptotic cells. The smudging of CLL lymphocytes occurs in cells with physical defects, and fragility that may develop during in vitro apoptosis is at least partially initiated by deficiencies in vimentin and CD45.

Process of SC Formation

The SCs in CLL exist as intact lymphocytes in vivo. These lymphocytes remain whole during blood collection and processing on the hematology analyzer. This structural integrity is evidenced by CBC and automated WBC differential (aDIFF) results, which are dependent on intact cells. The results of these tests would be compromised if some lymphocytes disintegrated during testing. This theory is supported by studies in which aDIFF agreed with mDIFF results when SCs were added to the lymphocytes counted in the mDIFF.[5,27]

The lymphocytes in CLL do not smudge because of delays in staining the blood film, the type of stain, or the staining process, including fixation.[28] Rather, SCs are produced when the blood film is made. The cytoplasmic and nuclear membranes of CLL lymphocytes fail because of the force used to spread the blood on the slide. A more thorough investigation of this process has been lacking. **Image 1**, from a case report of a patient aged 64 years with CLL, provides visual evidence of the proposed steps involved in SC formation.[17] **Image 2** shows a group of SCs in a patient with CLL.

The mechanical compression between the stationary slide and the spreader slide causes fragile CLL lymphocytes to rupture.[28,29] The amount of pressure applied is directly related to the number of SCs.[28] In addition, speed and slide angle can impact SC quantity. A 40° to 60° angle, less force, and quick spreading produces fewer SCs compared with a 20° to 30° angle, more force, and a slower process.[30]

It is unclear whether the method of slide preparation influences the SC number in patients with CLL because published data are limited and nonconcordant. Bron et al[31] compared the automated slide maker and the manual method in 10 patients with CLL with various concentrations of SCs. The automated device generated more SCs in all patients; in some there were 2 to 3 times more SCs vs the number found when using the manual method. On the other hand, Wenk[32]compared a semiautomated device, the Hemaprep (Sedona Lab Products), with the manual method and found an average of 28 SCs vs 44 SCs per 100 WBCs, respectively, in 8 patients with lymphocytic leukemias and atypical lymphocytes. With respect to reproducibility, automated and semiautomated devices, as opposed to the manual method, use consistent amounts of force on each slide. Therefore, automation results in better inter- and intraobserver agreement in the number of SCs counted on CLL blood films.[9]

Other Conditions with SCs

A SC most often refers to the remnant of a lymphocyte seen on the blood film from a patient with CLL; however, any WBC subtype can become fragile and susceptible to smudging.[33] Smudged or disintegrated WBCs are common in specimens stored for a long time before blood film preparation.[34-36] However, in fresh specimens from most individuals without CLL, the vast majority of WBCs are structurally sound. According to the Clinical and Laboratory Standards Institute (CLSI), SCs usually represent < 2% of the WBCs present.[37] Osgood[38] and Herishanu, Kay, Joffe, et al[39] reported 0% to 12% and 0% to 10% SCs on routine blood films, respectively. Using automated slide makers, Bron et al[31] found 2% to 12% damaged cells in 10 patients without CLL. Using the same specimens, the manual slide method yielded 1% to 4% damaged cells. On the other hand, Simson et al[40] reported that manual and automated methods produced similar numbers of SCs in 139 patients with a variety of diseases. Wenk[32] also observed consistent results between use of the manual method (6 SCs) and use of the Hemaprep (8 SCs) in 22 healthy individuals and patients with granulocytic leukemia.

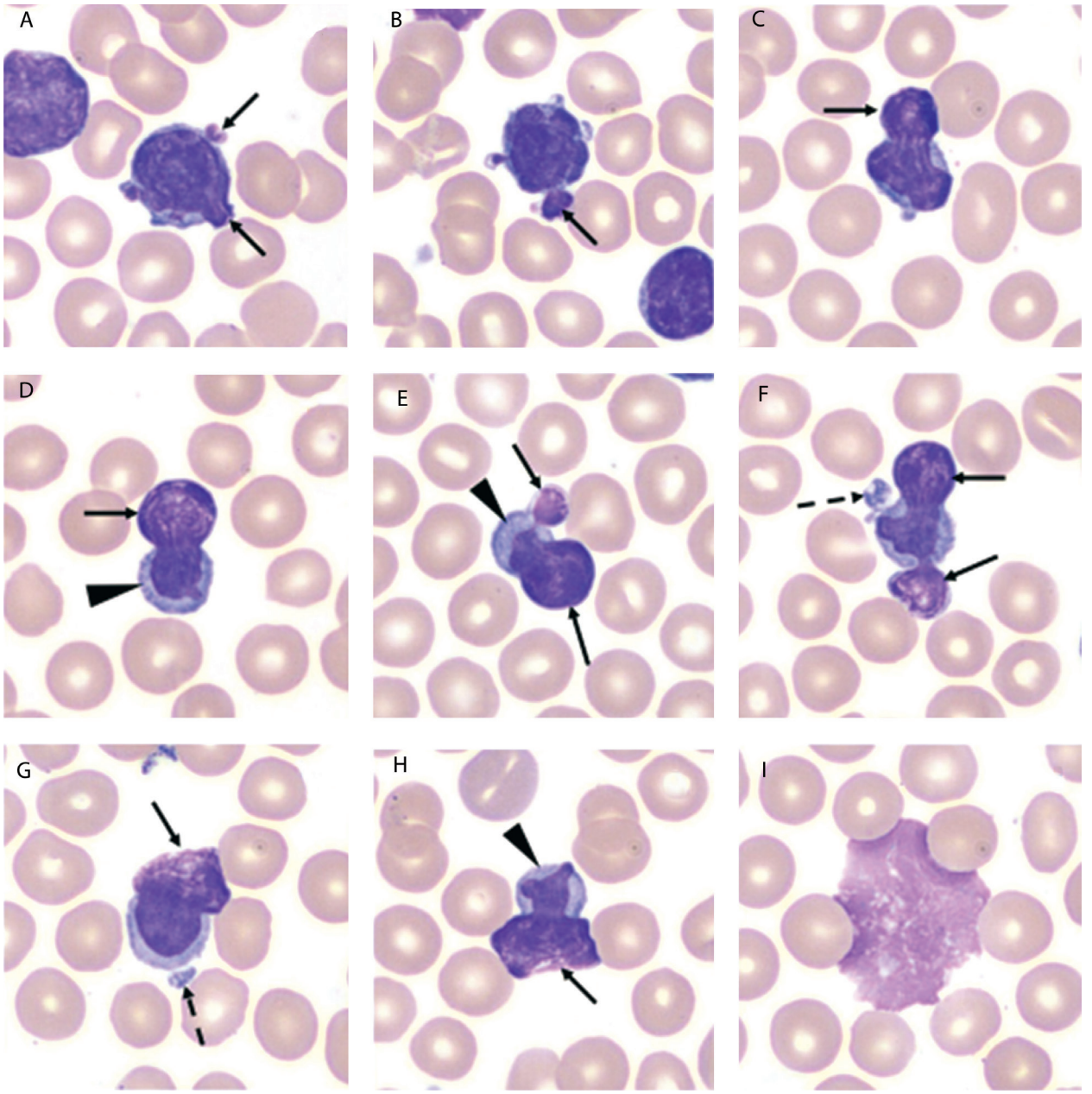

Image 1

Process of SC formation. Intact CLL cells exhibit membrane protrusions infiltrated by chromatin (**A, B,** arrows). In some of these cells, the plasma membrane is breached and the chromatin has spilled outside the cells (**C–E,** arrows), occasionally via multiple egresses (**E, F,** arrows). Chromatin extrusion is occasionally accompanied by the release of plasma membrane fragments (**F, G,** dashed arrows). After the spread of extracellular chromatin, the empty membrane shell shrinks (**D, E, H,** arrowheads). In some cells, the color of the chromatin turns from a nuclear-condensed purple to a reticulated pink spreading among erythrocytes (**G, H,** arrows), similar to that seen in SCs. Typical SCs contain only diffuse pink chromatin, with no other remnants (**I**). May Grunwald Giemsa stain ×1000. This research was originally published in Katz and Herishanu.[17] CLL, chronic lymphocytic leukemia; SCs, smudge cells.

Lab Medicine 2021;52;426–438
DOI: 10.1093/labmed/lmaa119

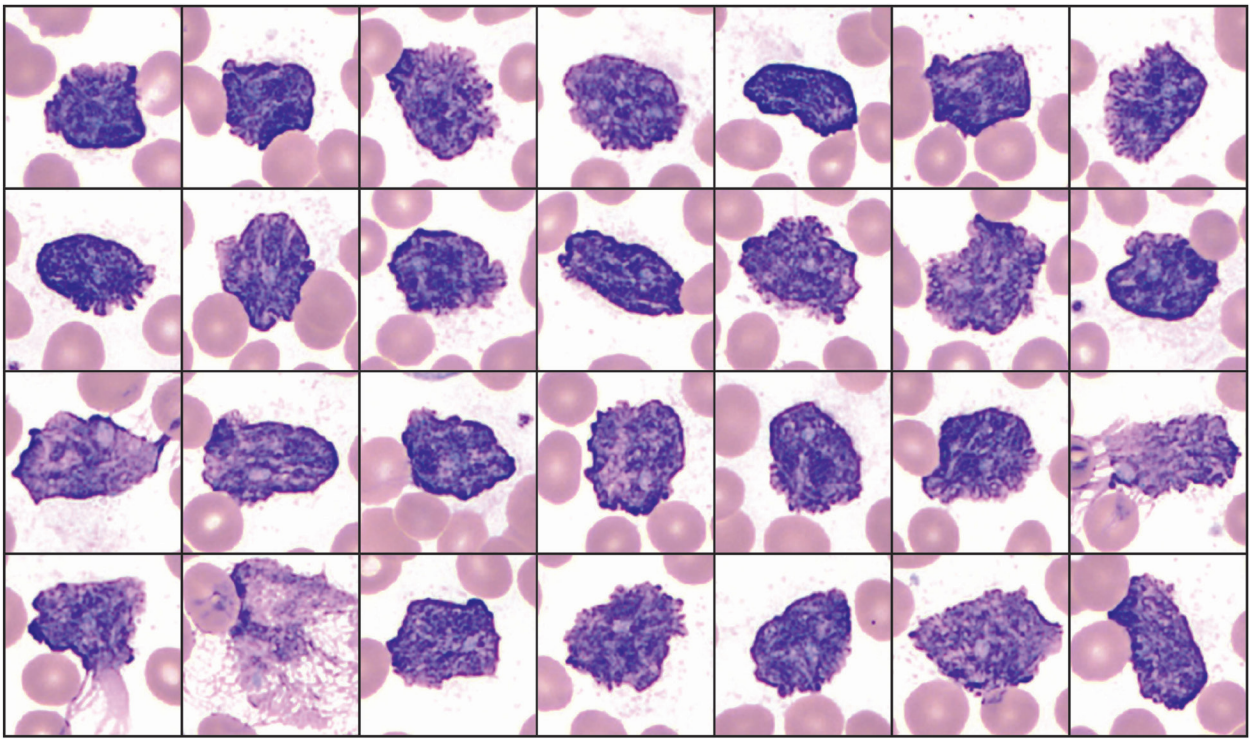

Image 2

SCs in a patient with CLL. SC formation begins with rupture of the CLL lymphocyte's nuclear and plasma membranes and ends with an amorphous purple blob or splotch on the slide. Bits of cytoplasm can be seen spread around the smudges. Wright-Giemsa stain ×1000 viewed on a Cellavision DM96 digital imaging analyzer. CLL, chronic lymphocytic leukemia; SCs, smudge cells.

An increase in SCs has been reported on the blood films of patients with a history of cardiac arrest, solid tumor, and infection, including infectious mononucleosis and a rare patient with SARS-CoV-2.[36,41,42] Higher concentrations of SCs have also been associated with hematologic neoplasms other than CLL, including natural killer–cell leukemia/lymphoma, myelodysplastic syndrome, acute leukemia, and mantle-cell lymphoma.[40,41,43,44]

Investigators have attempted to use the SC number to differentiate CLL from other lymphoid malignancies. Wong et al[44] were not successful using SC concentration to rule out CLL in 14 patients with mantle-cell lymphoma in the leukemic phase. They found SCs in 13 of the 14 patients at concentrations of 2% to 30% of WBCs. In a related study, Matos et al[45] found a significant difference between the average number of SCs in patients with CLL vs patients with other B-cell neoplasms (26% vs 14%, respectively; $P < .001$). However, a threshold could not be established with adequate sensitivity, specificity, and positive predictive value to differentiate CLL from other B-cell neoplasms.

The strong association between CLL and SCs has been well known among clinicians for many years. The term "smudge cell" has been known to cause confusion when reported in individuals without CLL. Thus, some laboratories will use the term only for patients with suspected or confirmed CLL to avoid an incorrect impression of CLL and unfounded patient anxiety and confusion.[43,46,47] To help ensure appropriate reporting, laboratories may use criteria in patients with suspected CLL as outlined below (all 3 conditions must be present to report SCs)[30,43]:

- Lymphocytosis > 5.0×10^9/L
- Age > 30 years
- SCs > 10 per 100 WBCs

Impact of SCs on Cell Counts and Implications for CLL Management

The mDIFF directly measures the relative concentrations (%) of each WBC subtype. The absolute cell counts are calculated by multiplying these results (%) by the WBC count. With few exceptions, SCs in patients with CLL represent lymphocytes and therefore should be classified as such. Failure to do so reduces the accuracy of the relative and absolute counts of all cell types in the mDIFF. The degree of the inaccuracies is related to SC number, concentrations of WBC subclasses, and total WBC count.

Falsely Decreased Lymphocyte Counts

The ALC is a key test for all patients with CLL. The ALC is often the first sign of disease and is used to diagnose CLL.[2] The ALC is tested regularly to monitor the progress of the disease and to assess treatment efficacy. It can also predict survival after therapy.[48] In addition, to determine whether a patient with CLL has achieved complete remission, the ALC must be $< 4 \times 10^9$/L, the upper reference interval for adults.[2] In serial measurements of patients with untreated CLL, the ALC may fluctuate slightly but will show a steady increase over time. The rate of this increase is calculated as the lymphocyte doubling time (LDT), the time required for the ALC to increase by 100%. Various CLL management guidelines include the LDT to determine when treatment should be initiated.[2] The LDT is an inexpensive and accurate predictor of disease aggressiveness and patient outcomes.[2,49]

To use serial calculations of LDT for all these purposes, the ALC must be accurate and precise. However, the ALC is falsely decreased when SCs, which represent lymphocytes in patients with CLL, are not counted as lymphocytes in the WBC differential. Further, monitoring the LDT over time can be negatively impacted when laboratories do not consistently correct for the presence of SCs or use incompatible corrective methods to include SCs in serial WBC differentials.[43,50] Therefore, laboratories should strive to utilize procedures that produce compatible WBC differential results both within and between laboratories. It is not uncommon for a patient with CLL to have a CBC performed at both a central hospital laboratory and a different laboratory near the patient's residence. These laboratories may have conflicting practices regarding SCs, which can cause irregular trending of ALCs.

When omitting SCs in the WBC differential lowers an ALC from elevated to normal in a patient with CLL, posttreatment assessments can also be affected. For example, a negatively biased ALC may lead to an incorrect designation of complete remission in a patient with residual disease.

Falsely Increased Nonlymphocyte Cell Counts

Whenever SCs are not included in the mDIFF, the relative and absolute concentrations of nonlymphocyte WBC subclasses, most notably neutrophils, are falsely increased.[4,5,27,43] The ANC is an important component in patient assessment and can dictate treatment decisions, particularly in oncology patients. Myelosuppressive chemotherapies can cause life-threatening neutropenia. In CLL, neutropenia may be disease- and/or treatment-related. Febrile patients seen in the emergency department with an ANC $<1 \times 10^9$/L are often admitted and administered antibiotics.[51] Patients with an ANC between 1×10^9/L and 1.5×10^9/L should be closely monitored. A falsely increased ANC can instill a false sense of security in which a clinician may fail to admit the patient and administer antibiotics when they are truly needed. The potential implications of inappropriate clinical decisions based on laboratory error underscores the need for the laboratory to produce reliable ANC results in patients with CLL.

Methods to Mitigate SC Impact on ALC and ANC

Publications that discuss laboratory approaches for handling SCs in patients with CLL are limited. There does not seem to be a consensus among clinical laboratory professionals on whether SCs should be included in the WBC differential.[52] Laboratory medicine textbooks have historically stated that SCs should generally be disregarded.[29] In 2017, in a proficiency test from the American Proficiency Institute and the American Society for Clinical Pathologists, the educational commentary stated that most laboratories do not report the presence of SCs in the WBC differential.[36] In addition, directors from several leading clinical laboratories have indicated that pathologists differ about whether SCs should be reported.[36] A survey of Canadian laboratories found that SCs are most often not included in CLL mDIFFs.[50] However, in 2014, a question was posted

Lab Medicine 2021;52;426–438 431
DOI: 10.1093/labmed/lmaa119

on a Cellavision (Lund, Sweden) user group blog: "Smudge cells—include or exclude?"[53] Feedback from 16 of 20 respondents indicated that their laboratories used procedures to include SCs in the WBC differential. Given the potential impact of SCs, laboratory professionals who encounter patients with CLL may want to consider adopting one of the methods described below to prevent the reporting of inaccurate results.

Four methods that ensure that SCs are included in the WBC differentials of CLL patients and the advantages and disadvantages of each are discussed in the sections below and outlined in **Table 1**. They include (1) using albumin to prevent smudging of lymphocytes, (2) using the aDIFF to count SCs as lymphocytes, (3) counting SCs as lymphocytes in the mDIFF, and (4) counting SCs as a separate population within the mDIFF.

Use Albumin to Prevent Smudging of Lymphocytes

The formation of SCs can be dramatically reduced by adding a drop of 22% bovine serum albumin to 4 to 5 drops of EDTA anticoagulated blood before making the blood film.[6,52,54,55] Albumin seems to stabilize and support the defective cytoskeletons of CLL lymphocytes during blood film preparation.[55] The cell counts obtained on albumin films agree with other methods to remediate SCs.[5,27] The use of albumin is widely recommended for obtaining accurate cell counts when SCs are present[37,56] and seems to be a preferred method among clinical laboratories.[52,53]

As outlined in **Table 1**, the albumin method has drawbacks, including the additional time and effort required to manipulate the specimen and to prepare, stain, and examine the albumin blood film. Consequently, turnaround times are longer for mDIFFs performed on albumin films. For these reasons, some laboratories prepare an albumin film only in patients with CLL who have "significant" numbers of SCs that could lead to erroneous WBC differential results with clinically significant consequences.[4,5] To determine whether albumin will be used, a standard (no-albumin) blood film is first reviewed to estimate the number of SCs present.[5] If SCs are greater than 20%, >1+ or other threshold, then an albumin film is prepared and used for the mDIFF. However, applying a threshold is problematic because estimating SC concentration can be subjective; human nature may lead the morphologist to err on the side of underestimation. In addition, determining a clinically significant cutoff

Table 1. Methods for Including CLL SCs in the WBC Differential

Method	Advantages	Disadvantages/Limitations
Use aDIFF	Fastest TAT compared with other methods Counts thousands of cells, better precision than mDIFF Minimal blood exposure Correlates with mDIFF method that counts SCs as lymphocytes and albumin method	Not reportable in approximately 25% of patients because of, eg, missing data, flags Abnormal lymphoid cells can be missed Blood film review may still be needed for morphology assessment and to confirm and comment on presence of SCs
Count SCs as lymphocytes on mDIFF	Same TAT as routine mDIFF Correlates with aDIFF and albumin methods	Applicable only in patients with CLL Must not count other lineage SCs as lymphocytes
Perform mDIFF on albumin blood film	Correlates with aDIFF and mDIFF method that counts SCs as lymphocytes Abnormal lymphoid cells are better distinguished	Slowest TAT Additional specimen manipulation and blood exposure No-albumin blood film may still be needed to determine if albumin will be used and evaluate morphology Criteria for deciding when to use albumin can be subjective and confusing Failure to always use albumin can impact consistency/trending of differential cell counts
Count SC as "others" on mDIFF	Nonlymphocyte differential cell counts are corrected for SCs "Others" count can be used to determine SC percentage in the prognosis calculation	Lymphocyte count is not corrected for SCs; will be falsely low "Others" category can cause confusion Results are not consistent with aDIFF and other SC correction methods

aDIFF, automated white blood cell differential; CLL, chronic lymphocytic leukemia; mDIFF, manual white blood cell differential; SCs, smudge cells; TAT, turnaround time; WBC, white blood cell.

for SCs can be challenging because total WBC count and concentration of WBC subtypes can widely vary. Furthermore, the inconsistent use of albumin is itself an issue. For patients who do not meet the SC threshold, the mDIFF is often performed on the no-albumin slide and SCs are ignored. The resulting cell counts will consequently be inaccurate, potentially affecting patient care, such as in patients with an ANC that is near decision limits. Trending of WBC differential results will be less reliable if albumin is used for some mDIFFs and not for others.

Some laboratories that use albumin also review a no-albumin blood film to assess morphology because albumin may induce morphologic artifacts including stomatocytes and target cells.[5,53,54] The no-albumin blood film can also be used to comment on the presence of SCs[56] and count SCs to assess prognosis.[5]

In addition to inhibiting smudging, albumin has been shown to reduce other artifactual morphologic changes in CLL lymphocytes related to cytoskeletal defects.[55] It can be difficult on no-albumin blood films to confidently recognize and quantitate abnormal and immature lymphoid cells because in vitro distortions in typical CLL lymphocytes can mimic these cells.[55] The presence of abnormal and immature lymphoid cells can be clinically significant in CLL, and an albumin blood film may provide a clearer picture. Gulati, Ly, et al[5] suggested an algorithm in 2017 to guide the use of albumin when a no-albumin blood film shows ≥ 1% blasts or > 10% activated, abnormal, or immature lymphoid cells. Using such criteria is prudent because accurate recognition and counting of these cells can be clinically valuable.

Implementing separate criteria for using albumin based on the number of SCs and blasts/abnormal/immature lymphoid cells seems complicated. And given the drawbacks of the inconsistent use of albumin, laboratories may want to consider a simpler approach and use albumin for all patients with CLL (or suspected CLL) who need an mDIFF. This approach is more streamlined and less confusing. All patients with CLL, including those with fewer SCs, would benefit from more accurate and reproducible WBC differential results obtained with the consistent use of albumin. The mDIFF and aDIFF results would be interchangeable, leading to the dependable and seamless trending of the LDT. Moreover, the ANC would not be impacted by SCs because there would be no instances of biased results from mDIFFs performed without albumin. Finally, increasing numbers of abnormal and immature lymphoid cells could be better detected and trended with consistent use of albumin.

If preparing an albumin blood film in all patients with CLL is not practical, and abnormal/immature lymphoid cells are not a concern, then there are other suitable approaches. For specimens containing SCs in which albumin will not be used, reliable results can be obtained using other corrective methods. Namely, the aDIFF and standard mDIFF in which SCs are counted as lymphocytes produce results that are comparable with the albumin method.[5,27]

Use the aDIFF to Count SCs as Lymphocytes

Modern hematology analyzers evaluate thousands of WBCs in the aDIFF, including the entire population of CLL lymphocytes, counting those that smudge during the making of the blood film. The aDIFF is reported in <30 seconds and most often the results are immediately available to the clinician. However, in approximately 10% to 30% of patients, a mDIFF is performed and replaces the aDIFF.[57] A mDIFF or blood smear verification of the aDIFF is generally performed when the accuracy of the aDIFF is suspect and/or when certain quantitative limits have been exceeded, ie, an ALC >4.0 × 10^9/L or >5.0 × 10^9/L in adults.[3,58] Using such criteria, all patients with CLL and active disease would need a mDIFF or aDIFF verification because the ALC will, by definition, exceed these limits.[2] However, the reportable range of the aDIFF ALC can often reach up to 400 × 10^9/L.[59,60] In addition, the analysis of thousands of cells in the aDIFF yields better precision compared with the mDIFF.

Because CLL lymphocytes are intact during aDIFF analysis,[27] it has been recommended that laboratories report the aDIFF in patients with CLL, including those with elevated ALC counts.[50,56] In appraising the reportable range of the aDIFF in CLL, Gulati, Bourne, et al[27] found accurate ALCs in 79 CLL (or suspected) specimens containing up to 285.3 × 10^9/L lymphocytes; mDIFFs performed on albumin blood films served as the reference method. Using regression statistics, they compared relative and absolute lymphocyte counts from Sysmex XE-series hematology analyzers (Mundelein, IL) against the reference method and showed consistent

DOI: 10.1093/labmed/lmaa119

results ($y = 0.98x - 0.32$, $R2 = 0.93$ and $y = 0.98x - 0.26$, $R2 = 1.00$, respectively). The investigators concluded that the aDIFF was a suitable replacement for the mDIFF in patients with CLL. Using the aDIFF ensured that SCs were included in the WBC differential as intact lymphocytes. An exception noted in the study was that in approximately one-fourth of patients the aDIFF could not be used because of incomplete/missing results. Additional technological limitations that precluded using the aDIFF included instances when CLL lymphocytes were counted as monocytes and/or basophils by the aDIFF.[27]

This issue has been reported in other publications.[5,27,61] To identify these specimens and prevent the reporting of biased aDIFF results in CLL patients, a mDIFF has been recommended when a relative monocytosis or relative basophilia is noted in the aDIFF.[61-64] Other potential exceptions to using the aDIFF in patients with CLL include aDIFF suspect flags that suggest the presence of immature/abnormal cells or other causes of potential inaccuracies in the aDIFF results. Laboratory accreditation standards and guidelines require laboratories to investigate and validate flagged aDIFF results.[37,65] This requirement often involves using microscopic verification, which may result in replacing the aDIFF with an mDIFF.

To summarize, the aDIFF is not reportable in approximately 25% of CLL specimens, for which a suitable alternate method is needed. One practice guideline on remediating SCs in CLL recommends using the aDIFF in all patients, even in the presence of flags.[50] However, this suggestion is not advised for the reasons stated above. The risk of reporting erroneous aDIFF results when suspect flags are present is too great.

A routine blood film review is still recommended when the aDIFF is used in patients with CLL to assess and comment on the presence of SCs and evaluate morphology if needed.[27,50,56] A blood film review also enables a scan for abnormal and immature lymphocytes. These cells may be an indication of more aggressive disease especially when they are increasing in concentration. In some CLL specimens with abnormal and immature lymphoid cells present, a related suspect flag will be reported with the aDIFF indicating the need for blood film review. Hematology analyzers with effective flagging/screening for suspicious cells can be helpful in developing efficient mDIFF criteria.

Count SCs as Lymphocytes in the mDIFF

When a mDIFF is being performed, guidelines advise that when a SC can be identified as to its cell of origin it should be classified as such and counted with this population.[37,56] It is commonly accepted in the clinical laboratory that SCs in CLL originate from lymphocytes. Objective evidence that SCs represent lymphocytes in CLL was found in a study using 100 specimens from patients with CLL in a 3-way comparison of results obtained by aDIFF vs counting SCs as lymphocytes in the mDIFF vs mDIFF performed on albumin blood films.[5] The results showed that the mDIFF in which SCs were counted as lymphocytes compared well with the aDIFF results for relative lymphocyte and neutrophil concentrations ($y = 0.95x + 1.93$, $R2 = 0.94$ and $y = 0.98x + 0.76$, $R2 = 0.97$, respectively). In addition, when the mDIFF with SCs counted as lymphocytes was compared with the albumin blood film mDIFF, similar agreement was found for the relative lymphocyte and neutrophil concentrations ($y = 1.01x - 0.54$, $R2 = 0.92$ and $y = 0.99x + 0.45$, $R2 = 0.94$, respectively).

In laboratories that use the aDIFF for patients with CLL, the method of counting SCs as lymphocytes in the mDIFF has been proposed as a backup for patients with unreportable aDIFFs (eg, because of flags or missing data).[50] Similar to using the aDIFF in patients with CLL, a benefit of counting SCs as lymphocytes in the mDIFF is that WBC differential results on all patients with CLL will be corrected for SCs, including those with lower numbers of SCs. The results are more consistent than the albumin method because albumin is often used only for CLL specimens with higher numbers of SCs.

However, a potential drawback of this method is the possibility of using it in individuals who do not have CLL. Although most true incidences of CLL will seem obvious from the data presented, it may be helpful to use criteria for patients with suspected CLL to lower the risk of the inappropriate use of the method. For example, as described earlier, patient age, ALC, and SC percentage have been utilized as criteria.[30,43] Another disadvantage is the possibility that using this method will miss abnormal CLL lymphocytes, which are also susceptible to smudging.

Digital imaging analyzers commonly used in hematology laboratories can facilitate counting SCs as lymphocytes. For example, Cellavision systems classify and count SCs as a separate population outside of the WBC differential.

To reclassify SCs, the cut-and-paste function can be used to combine the SCs with the lymphocytes. The differential results will be automatically adjusted, and an updated lymphocyte percentage will be reported. Before reclassifying the SCs, they should visually inspected to identify nonlymphocyte SCs. When possible, these SCs should be reclassified with the appropriate lineage.[37,56]

Count SCs as a Separate Population in the mDIFF

The CLSI H20-A2 standard states that SCs should be classified separately and counted as "others".[37] The working group for laboratory diagnostics of the German Society of Haematology and Oncology has also endorsed using a separate category in the mDIFF for SCs.[47] However, this method is controversial: CLSI delegate comments noted the discrepancy with other published guidelines.[37] Classifying SCs as "others" ensures an accurate ANC, but relative lymphocyte counts and ALCs are falsely decreased because SCs are not counted as lymphocytes. The LDT is also impacted when this method is used. However, a corrected ALC and LDT can be calculated manually by adding together the absolute number of "others" and the ALC. The clinician who desires a reliable LDT would be responsible for performing these calculations to fix what is essentially a laboratory-created problem. Another drawback with this method is the potential confusion caused by reporting an "other" cell population in the mDIFF. Given these issues, counting SCs as a separate population within the mDIFF may not be an appropriate method of remediating SCs for most laboratories.

Prognostic Significance of SCs in CLL

Counting the number of SCs present on peripheral blood films can be valuable for assessing prognosis in CLL, particularly in laboratories without ready access to advanced technology. Multiple studies have shown that patients with higher numbers of SCs experience less aggressive disease, fewer adverse disease features, and better outcomes as compared with patients with lower numbers of SCs. The quantity of SCs also correlates with genetic and biologic indicators of prognosis. **Table 2** summarizes the findings of these studies.

Table 2. Markers of Favorable Prognosis and Disease Features Associated with >30% SCs

Prognostic Marker/Disease Feature	References
Decreased expression of CD38	7,8,11,66,67
Decreased expression of ZAP 70	7,11,67,68
TP53 abnormalities not detected	66
Mutated *IgVH*	7,9
ATM mutations not detected	66
Lower risk Rai stage	10,11,66,69
Lower risk Binet stage	8,10,67
Slower lymphocyte doubling time	66
Less/no lymphadenopathy and organomegaly	66
Longer time to first treatment	7,9
Longer progression-free survival	10
Longer overall survival	7,9-11

SC, smudge cells.
Johansson[7] used a threshold of >20% SCs. In all studies, SC concentration is expressed as a percentage of total lymphocytes.

Although these studies found a threshold SC concentration to define 2 distinct prognostic groups, there is evidence that SC concentration correlates with overall survival as a continuous variable.[9-11] Additional work is needed to understand the clinical implications of SC concentration expressed on a continuous scale.

Studies cited in **Table 2** determined SC concentration not as a percentage of total WBC but as a percentage of total lymphocytes using the calculation shown below. Thus, to implement such a test with similar conclusions about prognosis, the same calculation should be used.

$$\frac{\text{Number of SCs} \times 100}{\text{Total lymphocytes (SCs + intact lymphocytes)}}$$

Counting SCs to assess prognosis can usually be performed quickly, easily, and at little cost even in laboratories without hematology analyzers. And because SC concentration remains relatively stable over time, patients do not require repeated measurements. Therefore, archived blood films can be used if a current slide is unavailable, the patient is undergoing chemotherapy, or the patient is on a clinical trial.[11]

The general CLL community has been slow to adopt this novel test seemingly because of the plethora of prognostic tests already available. Other potential hindrances include methodological limitations associated with manual microscopic cell counts such as inter-/intraobserver variability, sampling errors/statistical probabilities, and technical

Lab Medicine 2021;52;426–438 435
DOI: 10.1093/labmed/lmaa119

issues related to blood film quality. Nevertheless, genetic and immunophenotypic measures of prognosis may not be accessible in some geographic locations or at centers with limited resources. Sall[8] published the findings of a Senegalese study that correlated SC percentage with biological markers and Binet stage. The results are included in **Table 2**. The SC prognostic marker was noted as a solution to tests that are expensive and require sophisticated instrumentation and technical expertise that may not be available in some areas.

Conclusion

SCs are often found on peripheral blood films of patients with CLL, which is the most common leukemia. Specimens from these patients are frequently tested in most clinical laboratories. There has been a long history of morphologists passing over SCs when performing an mDIFF. This practice has been discredited because it results in falsely decreased measurements of ALC and positive biases in other cell classes. Despite the clinical significance of reporting erroneous results, regulatory agencies have been slow to issue guidelines to address this issue using a standard approach to promote accurate, precise, and consistent results across laboratories. This review sought to highlight the potential clinical impact of overlooking SCs and describe various approaches that include SCs in the WBC differential. Choosing the most appropriate method should consider the benefits and drawbacks of each, clinical needs, staff expertise, type(s) of hematology analyzer used and technological limitations, patient population, regulatory requirements, guidelines, and personal preferences. Finally, multiple studies have shown the significance of using SC concentration as a quick, simple, and reliable predictor of prognosis in patients with CLL. This potential use may be particularly attractive for institutions in remote locations and/or those with limited resources. **LM**

Acknowledgments

We thank Becky Socha, MS, MT(ASCP) for sharing expertise in methods to mitigate the impact of SCs on WBC differentials.

All authors met the following criteria: made substantial contributions to the conception or design of the work or the acquisition, analysis, or interpretation of data for the work; drafted the work or revised it critically for important intellectual content; gave final approval of the version to be published; and agreed to be accountable for all aspects of the work in ensuring that questions related to the accuracy or integrity of any part of the work are appropriately investigated and resolved.

Study concept and design, information acquisition, drafting of manuscript: Marionneaux. Study supervision: Mehta. Analysis and interpretation of information; critical revision for important intellectual content; administrative, technical, or material support: all authors.

References

1. Cancer stat facts: leukemia—chronic lymphocytic leukemia (CLL). Surveillance, Epidemiology, and End Results Program, National Cancer Institute website. https://seer.cancer.gov/statfacts/html/clyl.html. Accessed March 3, 2020.
2. Hallek M, Cheson BD, Catovsky D, et al. iwCLL guidelines for diagnosis, indications for treatment, response assessment, and supportive management of CLL. *Blood.* 2018;131(25):2745–2760.
3. Barnes PW, McFadden SL, Machin SJ, Simson E; International Consensus Group for Hematology. The International Consensus Group for Hematology review: suggested criteria for action following automated CBC and WBC differential analysis. *Lab Hematol.* 2005;11(2):83–90.
4. Socha B. Smudge cells: artifacts or clinically significant? *Lablogatory* blog. April 17, 2019. Accessed January 4, 2021. https://labmedicineblog.com/2019/04/17/smudge-cells-artifacts-or-clinically-significant/.
5. Gulati G, Ly V, Uppal G, Gong J. Feasibility of counting smudge cells as lymphocytes in differential leukocyte counts performed on blood smears of patients with established or suspected chronic lymphocytic leukemia/small lymphocytic lymphoma. *Lab Med.* 2017;48(2):137–147.
6. Densmore CM. Eliminating disintegrated cells on hematologic smears. *Lab Med.* 1981;12(10):640–641.
7. Johansson P, Eisele L, Klein-Hitpass L, et al. Percentage of smudge cells determined on routine blood smears is a novel prognostic factor in chronic lymphocytic leukemia. *Leuk Res.* 2010;34(7):892–898.
8. Sall S, Touré AO, Sall FB, et al. Using smudge cells percentage on routine blood smear in chronic lymphoytic leukemia as prognostic factor: Senegalese experience. *Blood.* 2015;126(23):5273.
9. Nowakowski GS, Hoyer JD, Shanafelt TD, et al. Using smudge cells on routine blood smears to predict clinical outcome in chronic lymphocytic leukemia: a universally available prognostic test. *Mayo Clin Proc.* 2007;82(4):449–453.
10. Gogia A, Raina V, Gupta R, et al. Prognostic and predictive significance of smudge cell percentage on routine blood smear in chronic lymphocytic leukemia. *Clin Lymphoma Myeloma Leuk.* 2014;14(6):514–517.
11. Nowakowski GS, Hoyer JD, Shanafelt TD, et al. Percentage of smudge cells on routine blood smear predicts survival in chronic lymphocytic leukemia. *J Clin Oncol.* 2009;27(11):1844–1849.
12. Brown MJ, Hallam JA, Colucci-Guyon E, Shaw S. Rigidity of circulating lymphocytes is primarily conferred by vimentin intermediate filaments. *J Immunol.* 2001;166(11):6640–6646.

13. Danielsson F, Peterson MK, Caldeira Araújo H, et al. Vimentin diversity in health and disease. *Cells.* 2018;7(10):147.
14. Patteson A, Vahabikashi A, Pogoda K, et al. Vimentin protects the structural integrity of the nucleus and suppresses nuclear damage caused by large deformations. Preprint. Posted online March 3, 2019. *bioRxiv 566174*. doi: 10.1101/566174.
15. Zheng Y, Wen J, Nguyen J, Cachia MA, Wang C, Sun Y. Decreased deformability of lymphocytes in chronic lymphocytic leukemia. *Sci Rep.* 2015;5:7613.
16. Stark RS, Liebes LF, Shelanski ML, Silber R. Anomalous function of vimentin in chronic lymphocytic leukemia lymphocytes. *Blood.* 1984;63(2):415–420.
17. Katz BZ, Herishanu Y. Fragility of sub-cellular structures in chronic lymphocytic leukemia. *Int J Hematol.* 2017;105(6):707–708. https://link.springer.com/journal/12185
18. Stark R, Liebes LF, Nevrla D, Conklyn M, Silber R. Decreased actin content of lymphocytes from patients with chronic lymphocytic leukemia. *Blood.* 1982;59(3):536–541.
19. Terriac E, Schütz S, Lautenschläger F. Vimentin intermediate filament rings deform the nucleus during the first steps of adhesion. *Front Cell Dev Biol.* 2019;7:106.
20. Rizzo D, Lotay A, Gachard N, et al. Very low levels of surface CD45 reflect CLL cell fragility, are inversely correlated with trisomy 12 and are associated with increased treatment-free survival. *Am J Hematol.* 2013;88(9):747–753.
21. Martin SJ, O'Brien GA, Nishioka WK, et al. Proteolysis of fodrin (non-erythroid spectrin) during apoptosis. *J Biol Chem.* 1995;270(12):6425–6428.
22. Dupéré-Minier G, Desharnais P, Bernier J. Involvement of tyrosine phosphatase CD45 in apoptosis. *Apoptosis.* 2010;15(1):1–13.
23. Su L, Pan P, Yan P, et al. Role of vimentin in modulating immune cell apoptosis and inflammatory responses in sepsis. *Sci Rep.* 2019;9(1):5747.
24. Oliveira GB, Pereira FG, Metze K, Lorand-Metze I. Spontaneous apoptosis in chronic lymphocytic leukemia and its relationship to clinical and cell kinetic parameters. *Cytometry.* 2001;46(6):329–335.
25. Fumi M, Martins D, Pancione Y, Sale S, Rocco V. Automated quantification of apoptosis in B-cell chronic lymphoproliferative disorders: a prognostic variable obtained with the Cell-Dyn Sapphire (Abbott) automated hematology analyzer. *Int J Lab Hematol.* 2014;36(6):628–635.
26. Rusak M, Osada J, Pawlus J, Chociej-Stypułkowska J, Dąbrowska M, Kłoczko J. Utility of laboratory tests in B-CLL patients in different clinical stages. *Int J Hematol.* 2011;93(6):736–744.
27. Gulati GL, Bourne S, El Jamal SM, Florea AD, Gong J. Automated lymphocyte counts vs manual lymphocyte counts in chronic lymphocytic leukemia patients. *Lab Med.* 2011;42(9):545–548.
28. Heinivaara O. Smudge cells in lymphocytic leukemia. *Ann Med Intern Fenn.* 1959;48:69–75.
29. Binet JL, Baudet S, Mentz F, et al. Basket cells or shadow cells of Gumprecht: a scanning electron microscope study, and the correlation between percentages of basket cells, and cells with altered chromatin structure (dense cells), in chronic lymphocytic leukemia. *Blood Cells.* 1993;19(3):573–581.
30. Constantino BT. Smudge cells: what technologists need to know. *Can J Med Lab Sci.* 2002;46(3):114–120.
31. Bron J, Jellema GI, Noordervliet R, et al. Improved performance of the automated slide preparation unit, Sysmex SP-100. *Sysmex J Int*. 2000;10(2):71–76.
32. Wenk RE. Comparison of five methods for preparing blood smears. *Am J Med Technol.* 1976;42(3):71–78.
33. *Hematology and clinical microscopy glossary*. College of American Pathologists website. https://documents.cap.org/documents/2019-hematology-clinical-microscopy-glossary.pdf. Accessed January 4, 2021.
34. Zini G; International Council for Standardization in Haematology (ICSH). Stability of complete blood count parameters with storage: toward defined specifications for different diagnostic applications. *Int J Lab Hematol.* 2014;36(2):111–113.
35. Vives-Corrons JL, Briggs C, Simon-Lopez R, et al. Effect of EDTA-anticoagulated whole blood storage on cell morphology examination. A need for standardization. *Int J Lab Hematol.* 2014;36(2):222–226.
36. Educational commentary—smudge cells: useless artifact or prognostic indicator? American Proficiency Institute website. http://www.api-pt.com/Reference/Commentary/2017Ascope.pdf. Accessed January 4, 2021.
37. *Reference leukocyte (WBC) differential count (proportional) and evaluation of instrumental methods*, 2nd ed. Clinical and Laboratory Standards Institute website. https://clsi.org/standards/products/hematology/documents/h20/. Accessed January 4, 2021.
38. Osgood EE. *A Textbook of Laboratory Diagnosis; with Clinical Applications for Practitioners and Students*. Philadelphia: The Blakiston Company; 1940.
39. Herishanu Y, Kay S, Joffe E, et al. Integration of automated morphological features resolves a distinct group of atypical chronic lymphocytic leukemias with chromosomal aberrations. *Leuk Res.* 2014;38(4):484–489.
40. Simson E, Gascon-Lema MG, Brown DL. Performance of automated slidemakers and stainers in a working laboratory environment—routine operation and quality control. *Int J Lab Hematol.* 2010;32(1 Pt 1):e64–e76.
41. Chang CC, Sun JT, Liou TH, et al. Clinical significance of smudge cells in peripheral blood smears in hematological malignancies and other diseases. *Asian Pac J Cancer Prev.* 2016;17(4):1847–1850.
42. Mitra A, Dwyre DM, Schivo M, et al. Leukoerythroblastic reaction in a patient with COVID-19 infection. *Am J Hematol.* 2020;95(8):999–1000.
43. Mehta D, Desai NJ. Smudge cells or basket cells—a diagnostic pitfall. *Indian J Res.* 2013;2(3):256–257.
44. Wong KF, Chan JK, So JC, Yu PH. Mantle cell lymphoma in leukemic phase: characterization of its broad cytologic spectrum with emphasis on the importance of distinction from other chronic lymphoproliferative disorders. *Cancer.* 1999;86(5):850–857.
45. Matos DM, Perini G, Kruzich CR, Eduardo M, Falcão RP. Smudge cells in peripheral blood smears did not differentiate chronic lymphocytic leukemia from other B-cell chronic lymphoproliferative diseases. *Rev Bras Hematol Hemoter.* 2009;31(5):333–336.
46. Dusse LMSA, Silva TP, Freitas LG, Vieira LM, Sabino ADP, Carvalho MDG. Gumprecht shadows: when to use this terminology? *J Bras Patol Med Lab.* 2013;49(5):320–323.
47. Baurmann H, Bettelheim P, Diem H. Lymphocyte morphology in the peripheral blood film: proposal of a revised nomenclature and systematics. *J Lab Med.* 2011;35(5):1–9.
48. Joffe E, Ariela Arad N, Bairey O, et al. Persistently low lymphocyte counts after FCR therapy for chronic lymphocytic leukemia are associated with longer overall survival. *Hematol Oncol.* 2018;36(1):128–135.
49. Montserrat E, Sanchez-Bisono J, Viñolas N, Rozman C. Lymphocyte doubling time in chronic lymphocytic leukaemia: analysis of its prognostic significance. *Br J Haematol.* 1986;62(3):567–575.
50. Macdonald D, Richardson H, Raby A. Practice guidelines on the reporting of smudge cells in the white blood cell differential count. *Arch Pathol Lab Med.* 2003;127(1):105.
51. Smellie WS, Forth J, Smart SR, et al. Best practice in primary care pathology: review 7. *J Clin Pathol.* 2007;60(5):458–465.
52. Kiechle FL, ed. Smudge cells Q & A. *CAP Today*. http://www.captodayonline.com/Archives/0610/0610_qa.html. Published June 2010. Accessed January 4, 2021.
53. *Smudge cells—include or exclude?* Cellavision blog. Published March 25, 2014. Accessed January 4, 2021. http://blog.cellavision.com/smudge-cells-include-or-exclude/.

54. George TI. Diagnostic approach to lymphocytosis. *The Hematol.* 2015;12(6):1.
55. Lunning MA, Zenger VE, Dreyfuss R, et al. Albumin enhanced morphometric image analysis in CLL. *Cytometry B Clin Cytom.* 2004;57(1):7–14.
56. Palmer L, Briggs C, McFadden S, et al. ICSH recommendations for the standardization of nomenclature and grading of peripheral blood cell morphological features. *Int J Lab Hematol.* 2015;37(3):287–303.
57. Novis DA, Walsh M, Wilkinson D, St. Louis M, Ben-Ezra J. Laboratory productivity and the rate of manual peripheral blood smear review: a College of American Pathologists Q-Probes study of 95,141 complete blood count determinations performed in 263 institutions. *Arch Pathol Lab Med.* 2006;130(5):596–601.
58. Gulati G, Song J, Florea AD, Gong J. Purpose and criteria for blood smear scan, blood smear examination, and blood smear review. *Ann Lab Med.* 2013;33(1):1–7.
59. Siemens. *Operator's Guide*. Vol. 067D0157-01 Rev. C, 2010-04. Tarrytown, NY: Siemens Healthcare Diagnostics Inc.; 2010.
60. Beckman Coulter. *UniCel DxH 800 Coulter Cellular Analysis System Instructions for Use*. Vol. PN 629743AC. Fullerton, CA: Beckman Coulter; 2008.
61. Gibbs G, Campbell G, Christie I. Pseudobasophilia and the Advia 120. *Hematology.* 2009;14(3):159–163.
62. Furundarena JR, Sainz M, Uranga A, et al. Comparison of abnormal cell flagging of the hematology analyzers Sysmex XN and Sysmex XE-5000 in oncohematologic patients. *Int J Lab Hematol.* 2017;39(1):58–67.
63. Herishanu Y, Kay S, Sarid N, et al. Absolute monocyte count trichotomizes chronic lymphocytic leukemia into high risk patients with immune dysregulation, disease progression and poor survival. *Leuk Res.* 2013;37(10):1222–1228.
64. Lai AP, Martin PJ, Cawley JC, Richards JD, Goldstone AH. Automated leucocyte differential counts in chronic lymphocytic and hairy-cell leukaemias: a comparison of the Hemalog D, H6000 and Coulter S Plus IV. *Clin Lab Haematol.* 1987;9(2):169–174.
65. *Hematology and coagulation checklist*. College of American Pathologists Laboratory Accreditation Program. https://elss.cap.org/elss/ShowProperty?nodePath=/UCMCON/Contribution%20Folders/DctmContent/education/OnlineCourseContent/2017/LAP-TLTM/checklists/cl-hem.pdf. Published August 21, 2017. Accessed January 4, 2021.
66. Mohamed AA, Safwat NA. New insights into smudge cell percentage in chronic lymphocytic leukemia: a novel prognostic indicator of disease burden. *Egypt J Med Hum Genet.* 2018;19(4):409–415.
67. Szerafin L, Jakó J, Riskó F, Hevessy Z. The prognostic value of smudge cells (Gumprecht shadows) in chronic lymphocytic leukaemia. *Orv Hetil.* 2012;153(44):1732–1737.
68. Al-Kahiry W, Tawfik HS, Sharshira H, Ghanem A, El-Gammal M, Mikhael IL. Smudge cell percentage as a surrogate marker for ZAP-70 expression in patients with chronic lymphocytic leukemia. *Blood Res.* 2018;53(3):218–222.
69. Bhanshe P. Prognostic value of smudge cell percentages on peripheral blood smear in chronic lymphocytic leukemia. Abstract presented at: 55th Annual Conference of Indian Society of Haematology & Blood Transfusion; 2014.

MicroRNA-138 Regulates T-Cell Function by Targeting PD-1 in Patients with Hepatitis B Virus–Related Liver Diseases

Wei Liu, MD,[1] Xianzhao Zheng, MD,[1] Jie Wang, MD,[2] Quanli He, MD,[1] Junmin Li, MD,[1] Zengzeng Zhang, MD,[1] Hongchun Liu, MD, PhD[3,]*

Laboratory Medicine 2021;52:439-451

DOI: 10.1093/labmed/lmaa110

ABSTRACT

Objective: T-cell exhaustion in hepatitis B virus (HBV) infection, which results from upregulation of programmed cell death-1 (PD-1), leads to persistent HBV infection and related disease progression. Therefore, agents targeting PD-1 may prove beneficial in the treatment of this condition. MicroRNA-138 (miR-138) possesses an anti-tumor ability in that it targets immune checkpoints, including PD-1. However, the function and underlying mechanisms of miR-138 in patients with HBV infection remains unclear.

Methods: Specimens were collected from healthy volunteers (n = 43) and patients with chronic hepatitis B (CHB; n = 52), liver cirrhosis (LC; n = 26), and hepatocellular carcinoma (HCC; n = 31); carriers of HBV who were asymptomatic (n = 51); and patients with CHB receiving antivirus treatment (n = 11). These specimens were then used to study the expression and relationship among miR-138, PD-1, and HBV DNA viral load. To investigate the role of miR-138 in regulating PD-1 expression and determine the effect of miR-138 in regulating T-cell function, a luciferase assay and a transfection assay were each performed with primary $CD3^+$ T cells.

Results: We found that PD-1 was upregulated and miR-138 was downregulated in patients with CHB, LC, and HCC. Correlations analysis revealed that PD-1 expression was positively correlated with HBV DNA viral load whereas miR-138 was negatively correlated. Luciferase assay results showed that miR-138 directly inhibited PD-1 expression by interacting with the 3'-untranslated region of PD-1. As a result of miR-138 overexpression in primary T cells, PD-1 in these T cells was downregulated and antivirus cytokines secreted by T cells were significantly upregulated. In addition, the expression levels of PD-1 and miR-138 were reversed in patients with CHB who received antivirus treatments.

Conclusion: Results showed that miR-138 can promote T-cell responses within patients with HBV infection by inducing a PD-1 blockade. Such an effect suggests that miR-138 may serve as a new therapeutic target for the treatment of HBV infection.

Keywords: HBV-related liver diseases, miR-138, T cells, PD-1

Abbreviations:

HBV, hepatitis B virus; PD-1, programmed cell death-1; miR-138, microRNA-138; CHB, chronic hepatitis B; LC, liver cirrhosis; HCC, hepatocellular carcinoma; miRNAs, microRNAs; 3'-UTR, 3'-untranslated region; HV, healthy volunteers; AsC, HBV asymptomatic carriers; HCV, hepatitis C virus; HDV, hepatitis D virus; HBsAg, hepatitis B surface antigen; ALT, aminotransaminase; CT, computed tomography; AFP, α-fetoprotein; HBeAg, hepatitis B e antigen; AST, aminotransferase; ALB, albumin; TBIL, total bilirubin; PBMCs, peripheral blood monocytes cells; anti-PD-1; PD-blocking antibody; PBS, phosphate-buffered saline; Mut, mutated; PCR, polymerase chain reaction, qRT-PCR, quantitative reverse-transcription polymerase chain reaction; IFN-γ, interferon- γ; TNF-α, tumor necrosis factor-α.

[1]Department of Clinical Laboratory, The People's Hospital of Jiaozuo, China, [2]Department of Nephrology, The Affiliated Hospital of Henan Polytechnic University, China, [3]Department of Clinical Laboratory, The First Affiliated Hospital of Zhengzhou University, China

*To whom correspondence should be addressed.
999longway@gmail.com

Hepatitis B virus (HBV) is a leading cause of liver hepatitis, liver cirrhosis (LC), and hepatocellular carcinoma (HCC) worldwide. The World Health Organization estimates that approximately 257 million adults, or 3.5% of the world population in 2015, were living with chronic HBV infection at that time. Furthermore HBV-related liver diseases, such as LC and HCC, are responsible for more than 900,000 deaths each year.[1,2] Although vaccines and treatment strategies for HBV infection, including interferon-based therapy and nucleotide/nucleoside analogues, are available and can be effective, the complete eradication of HBV remains challenging.[3] Therefore, novel and effective targets to improve the treatment of HBV infection are urgently needed.

Cell-mediated immunity represents a critical process involved with the clearance of HBV infection from hepatocytes.[4] Based upon results obtained with chimpanzee models of

HBV infection, $CD8^+$ and $CD4^+$ T cells have been shown to be indispensable for the resolution of HBV infection.[5] However, although T cells are effective in clearing HBV infection during the acute phase, they become unresponsive because of exhaustion in the chronic phase.[6] One of the main reasons for this change in T-cell responsiveness is the robust expression of immune checkpoint markers in T cells, including programmed cell death-1 (PD-1),[7,8] an immunomodulatory receptor expressed in T-cell membranes.[9] Research has shown that PD-1 engagement by its ligands, PD-L1 or PD-L2, inhibits T-cell receptor-mediated proliferation and cytokine production in activated T lymphocytes.[10,11] Because T cells are the key mediators of HBV clearance, the blocking of inhibitory receptors on T cells in patients with chronic HBV could serve as a means to trigger or enhance T-cell function in response to infected hepatocytes and thus a potentially effective treatment strategy.

The modulatory effects of microRNAs (miRNAs) in HBV-related liver diseases have received considerable attention of late.[12] Research has shown that MiRNAs are a class of endogenous noncoding RNA molecules with 19 to 25 nucleotides in length and can modulate gene expression by binding to the 3'-untranslated region (3'-UTR) messenger RNA (mRNA) of target genes, effects that lead to mRNA decay or transcriptional repression. Increasing evidence has revealed that miRNAs are involved in a number of T-cell processes, including their development, differentiation, activation, proliferation, and aging.[13,14] The miRNA known as miR-138 has been reported to serve as a tumor suppressor in multiple cancers and regulate different biological process, including cell differentiation and inflammation processes.[15-19] A recent study showed that miR-138 could directly interact with immune checkpoints and regulate their expression.[20]

Of particular relevance to the present report are the findings from a bioinformatics analysis showing that downregulation of miR-138 is strongly related to HBV-associated HCC tumorigenesis.[21] However, the specific role of miR-138 in the progression of chronic HBV infection remains unknown. Therefore, the present report examined the role of miR-138 in HBV-related liver diseases in specimens from patients with various HBV-related diseases. Our results indicated that miR-138 was downregulated and that PD-1 was upregulated during HBV infection, whereas these expression levels of miR-138 and PD-1 were reversed after antivirus treatment in these patients. Moreover, we have shown that miR-138 enhanced the function of T cells by directly inhibiting PD-1. Taken together, these results suggest that miR-138 could promote T-cell responses within patients with HBV infection by inducing a PD-1 blockade. Such an effect suggests that miR-138 may serve as a new therapeutic target for the treatment of HBV infection.

Methods and Materials

Patients and Specimen Collection

The recruited participants included healthy volunteers (HV; n = 43), HBV asymptomatic carriers (AsC; n = 51), patients with chronic hepatitis B (CHB; n = 52), HBV-related LC (n = 26), and HCC (n = 31). Patients coinfected with hepatitis C virus (HCV), hepatitis D virus (HDV), HIV, acute hepatitis B infection, or other causes of liver diseases were excluded from the study. For this study, HV were also negative for HBV, HCV, HDV, and HIV infection and for other related liver diseases. Participants who were AsC were defined as having a persistent positive expression of hepatitis B surface antigen (HBsAg) but normal alanine aminotransaminase (ALT) levels for 6 months. Participants with CHB were defined by a persistent positive expression of HBsAg plus persistent or elevated ALT levels present for 6 months.[22] An LC diagnosis was established as based on computed tomography (CT) images and laboratory findings. HCC was diagnosed as based upon histological analysis, α-fetoprotein (AFP) levels and findings of CT imaging.

No significant differences in terms of age or sex were present among all patient groups and HV (**Table 1**). Also contained in **Table 1** are the hepatitis B e antigen (HBeAg) serostatus, serum HBV DNA concentrations, liver functions (ALT and aspartate aminotransferase [AST]), albumin (ALB), total bilirubin (TBIL), and AFP levels. On the basis of the tumor-node-metastasis system of the 2010 International Union Against Cancer by the American Joint Committee, 17 patients with HCC were at level I/II and 14 patients were at level III/IV. Moreover, specimens from 11 patients with CHB receiving antivirus treatment for 1, 3, or 6 months were collected. The study was approved by the ethical committee of the People's Hospital of Jiaozuo (China), and informed consent forms were signed by all participants.

Serological Assays for HBV Markers, Viral Load, and Basic Clinical Features

Serological markers of HBV, including HBsAg and HBeAg, were determined using enzyme-linked immunosorbent assay kits (Livzon Pharmaceutical Group Inc, Zhuhai,

Table 1. Clinical and Virological Data of Patients

Variable	HV (n = 43)	AsC (n = 51)	CHB (n = 52)	LC (n = 26)	HCC (n = 31)	*P* Value
Age, y	49.0 (31.0–65.0)	49.0 (33.0–65.0)	52.0 (31.0–65.0)	49.5 (34.0–65.0)	51.0 (36.0–65.0)	.922
Sex (M/F)	25/18	30/21	30/22	15/11	18/13	.956
HBsAg+/-	0/43	51/0	52/0	26/0	31/0	<.001
HBeAg+/-	0/43	0/51	38/14	20/6	24/7	<.001
HBV DNA Log10copies/mL	NA	NA	5.715 (2.630–8.740)	5.655 (2.440–8.410)	5.650 (2.380–8.590)	.3457
ALT, IU/L	12.0 (5.0–47.0)	19.0 (4.0–47.0)	201.0 (70.0–752.0)	175.5 (70.0–611.0)	231.4 (85.0–552.0)	<.0001
AST, IU/L	23.0 (13.0–49.0)	21.0 (13.0–47.0)	244.5 (77.0–568.0)	258.0 (83.0–642.0)	241.0 (89.0–632.0)	<.0001
ALB, g/L	45.4 (41.0–49.7)	45.5 (40.8–50.2)	33.8 (22.9–33.9)	32.1 (25.8–36.8)	34.3 (21.7–38.3)	<.0001
TBIL, umol/L	8.4 (0.9–20.2)	10.7 (3.6–20.1)	59.55 (10.5–139.0)	69.5 (10.5–139.0)	61.6 (25.4–124.0)	<.0001
AFP, ng/mL	1.56 (0.5–4.4)	1.2 (0.7–5.3)	46.1 (6.0–498.4)	218.2 (8.2-1305.0)	72783.0 (2159.0–156,382.0)	<.0001
PLT	217.8 (91–397)	207.7 (52–442)	188.7 (22–482)	164.9 (42–320)	165.9 (26–437)	.0323
TNM I II/III IV	NA	NA	NA	NA	17/14	NA

Data presented as number or median (range). Data were analyzed using the Kruskal-Wallis test or the χ^2 test and statistically significant differences among the groups are indicated (P values). HV, healthy volunteers; AsC, HBV asymptomatic carriers; CHB, chronic hepatitis B; LC, liver cirrhosis; HCC, hepatocellular carcinoma; HBsAg, hepatitis B surface antigen; HBeAg, hepatitis B e antigen; HBV, hepatitis B virus; ALT, alanine aminotransaminase; AST, aspartate aminotransferase; ALB, albumin; TBIL, total bilirubin; AFP, α-fetoprotein; TNM, tumor node metastasis; PLT, Platelets.

China). The HBV viral load was determined using the HBV LC PCR Kit (Daan Technology Co, Guangzhou, China). Routine biochemical assays, including liver function, ALB, TBIL, and tumor marker-AFP were also determined.

Isolation of Peripheral Blood Monocytes Cells and Purification of CD3$^+$ T Cells

Peripheral blood monocytes cells (PBMCs) were isolated from freshly heparinized blood of different groups using Ficoll-Histopaque (Sigma-Aldrich, St. Louis, MO, USA). CD3$^+$ T cells were purified from PBMCs of HV with magnetic-activated cell-sorting using a human CD3$^+$ T-cell isolation kit (Miltenyi Biotec, Germany) following the manufacturers' protocols. The purity of CD3$^+$ T cells was 95.63%.

Cell Culture and Transfection

Primary CD3$^+$ T cells were cultured in 6-well plates at 2×10^6 cells/well or in 12-well plates at 1×10^6 cells/well in Roswell Park Memorial Institute (RPMI) 1640 medium (Gibco, Grand Island, NY). The medium was supplemented with 10% heat-inactivated fetal calf serum (Biochrom, Berlin, Germany), penicillin (100 IU/mL), and streptomycin (100 μg/mL) and maintained at 37°C in a humidified atmosphere of 5% CO_2. Subsequently, T cells were transiently transfected with either (1) miR-138 control mimics, (2) miR-138 mimics, (3) an miR-138 control inhibitor, or (4) an miR-138 inhibitor (Genechem, Shanghai, China) in the presence or absence of the PD-1 blocking antibody (anti-PD-1; Merck, Whitehouse Station, NJ) using Lipofectamine 2000 (Invitrogen; Thermo Fisher Scientific, Inc., CA) according to the manufacturers' instructions. The concentrations were designed as follows: 2 μL miR-138 or control (10 mg/mL) + 48 μL phosphate-buffered saline (PBS) mixed with the vehicle (40 μL PBS + 10 μL Lipofectamine 2000) or the vehicle control (90 μL PBS + 10 μL Lipofectamine 2000). Cells or protein lysates were collected at 24 hours after transfection.

Luciferase Reporter Assay

Bioinformatics analysis by Target Scan (http://www.targetscan.org) was performed to predict potential targets for miR-138. DNA fragments of the PD-1 3'-UTR regions contained putative miR-138-binding sites or mutated (Mut) miR-138 binding sites, which were amplified by polymerase chain reaction (PCR) from genomic DNA and inserted into the UTR downstream of the luciferase gene in the pMIR-report vector (The pMIR-REPORT miRNA Expression Reporter Vector System

DOI: 10.1093/labmed/lmaa110

consists of an experimental firefly luciferase reporter vector and an associated β-gal reporter control plasmid; Thermo Fisher Scientific, Inc., Waltham, MA). Mutations of the putative miR-138 target sequence within the PD-1 3'-UTR were generated using the MutanBEST Kit (Takara, Toyota, Japan). The plasmids were termed as wild-type (pMIR-report-PD-1-WT) or Mut (pMIR-report-PD-1-Mut) sequences. Luciferase reporter plasmids (WT or Mut) and miR-138 mimics and negative controls were cotransfected into purified $CD3^+$ T cells using Lipofectamine 2000 (Thermo Fisher Scientific). Purified $CD3^+$ T cells were grown in RPMI 1640 medium (Gibco, Grand Island, NY) supplemented with 10% heat-inactivated fetal calf serum (Biochrom, Berlin, Germany), penicillin (100 IU/mL), and streptomycin (100 μg/mL) and maintained at 37°C in a humidified atmosphere of 5% CO_2. Luciferase activities were determined at 48 hours after transfection using the Dual Luciferase Reporter Assay kit (Promega Corporation, Madison, WI; catalog number E1910). The primers were as follows: PD-1-XhoI forward, 5'-CCGCTCGAGCAGTAAGCGGGCAGGC-3' and PD-1-NotI reverse, 5'-ATTTGCGGCCGCTCCTTAGCATGC TCTCATATTT-3'; PD-1-MUT forward 5'-CCTTCCCTGTGGTTC GCACTGGTTATAATTATAA-3' and PD-1-MUT reverse, 5'-TTAT AATTATAACCAGTGCGAACCACAGGGAAGG-3'.

Flow Cytometric Analysis

The following antibodies were used for surface or intracellular cytokine staining for flow cytometry: CD3-FITC, CD4-PerCP, PD-1-PE, TNF-α-PE, IL-10-PE, IFN-γ-PE, and CD8-APC (BD Biosciences, San Diego, CA). For all clinical specimen staining, isolated PBMCs were incubated with antibodies against cell surface markers (CD3, CD4, CD8, PD-1) for 15 minutes at room temperature. For transfected purified T-cell staining, purified T cells were harvested after transfection, centrifuged at 1000 × g for 5 minutes, and then washed with PBS. The concentration of cells was then adjusted to 1×10^7 cells/mL, and 100 μL of cell suspension was then followed by cell permeabilization (FOXP3 Fix/Perm Buffer; eBioscience, San Diego, CA) for 45 minutes at room temperature and the addition of antibodies for intracellular markers for 45 minutes at room temperature. Subsequently, stained specimens were washed with PBS, fixed, and eventually assessed using BD FACSCanto with the BD FACSDiva software program (BD FACSDiva v9.0 Software; BD Biosciences, San Diego, CA). Data were analyzed using FlowJo7.6 (Tree Star Inc., San Carlos, CA).

Quantitative Reverse Transcription PCR Analysis

Total RNA was isolated from serum from different participant groups (HV, AsC, CHB, LC, and HCC) or from miR-138 transfected purified $CD3^+$ T cells using TRIzol reagent (Invitrogen, Carlsbad, CA) according to the manufacturer's instructions. Complementary DNAs were synthesized with the miRcute miRNA First-Strand cDNA Synthesis Kit (Tiangen, Beijing, China). Expression levels of miRNAs were analyzed using the miRcute miRNA qPCR Detection Kit (Synergy Brands Synergy Brands green; Tiangen) on a CFX96 Real Time PCR system (Bio-Rad, Feldkirchen, Germany) specific for hsa-miR-138. The U6 small RNA was used as an internal control.[23,24] The primers were as follows: miR-138 sense, 5'-AGCTGGTGTTGTGAATCAGGCCG-3' and anti-sense, 5'-TGGTGTCGTGGAGTCG-3'; U6 sense, 5'-TTCACGAATTTGCGTGTCAT-3' and anti-sense, 5'-TTCACGAATTTGCGTGTCAT-3'. The PCR cycling conditions were 94°C for 2 minutes, 40 cycles at 94°C for 20 seconds, and 60°C for 34 seconds, followed by an annealing/elongation step at 72°C for 8 minutes. All experiments were performed in triplicate.

Western Blot Analysis

After transfection, purified T cells were harvested and total protein was extracted using Cell Lysis Buffer (Beyotime, Beijing, China) supplemented with a protease inhibitor cocktail (Beyotime) according to the manufacturer's instructions. Antibodies used for WB were PD-1 (Cell Signaling Technology, Danvers, MA) and β-actin (Ray Biotech, Beijing, China). All primary antibodies were used at 1:1,000 dilutions and secondary antibodies were used at 1:5,000 dilutions. The resulting immune complexes were visualized using enhanced chemiluminescence detection reagents (Bio-Rad). Data were analyzed using β-actin for normalization.

Statistical Analysis

Flow cytometry data were analyzed using FlowJo software 7.6 (Tree Star Inc, San Carlos, CA), and statistical analysis was performed using GraphPad Prism 5 software (GraphPad Software Inc, La Jolla, CA). For clinical specimens, the expression of HBV DNA viral load, miR-138, and PD-1 among different groups was analyzed using the Kruskal-Wallis test; data from cell cultures were expressed as means ± standard deviation and analyzed using Student's *t*-tests. Correlations analysis was performed using

the Spearman correlation test. A *P* value of <.05 was required for results to be considered statistically significant.

Results

Positive Correlation of HBV DNA Level with PD-1 Expression in Peripheral T Cells

Upregulation of PD-1 has been found to be associated with regulatory functions in the progression of various diseases.[25,26] To study the relationship between PD-1 expression and HBV virus level, we first used a flow cytometer assay to detect PD-1 expression in circulating $CD3^+$, $CD4^+$, and $CD8^+$ T cells of patients with HBV infection (**Figure 1A**). Our data showed that significant expressions of PD-1 were present in $CD3^+$, $CD4^+$, and $CD8^+$ T cells of the CHB, LC, and HCC groups as compared with those of the HV or AsC groups, which showed no statistically significant differences from each other (**Figure 1B**). These results indicate that PD-1 expression is regulated by HBV DNA level. To further analyze the relationship between PD-1 expression and HBV DNA level, correlations analysis were performed within $CD3^+$, $CD4^+$, and $CD8^+$ T cells of patients with CHB, LC, and HCC, respectively. The results showed that HBV DNA level was associated with an upregulated expression of PD-1 in $CD3^+$, $CD4^+$, and $CD8^+$ T cells in both the CHB and the LC groups (**Figures 1C and 1D**), whereas no significant correlation between HBV DNA level and PD-1 expression was found within the HCC group (**Figure 1E**).

Negative Correlation of miR-138 Expression with HBV DNA Level in Patients with HBV

Increasing evidence has provided support for the concept that miRNAs play important roles in the regulation of host immune responses.[27] With regard to HBV-related liver diseases, various types of miRNAs have been identified as being related to the progression of HBV-related liver diseases and thus may serve as potential new targets for HBV treatment.[28] Findings from recent studies have revealed that miR-138 is downregulated in cancer diseases, and this overexpression displays anticancer activity by targeting immune checkpoints.[20] To study the role of miR-138 in HBV-related liver diseases, a quantitative reverse-transcription PCR (qRT-PCR) assay was used to determine the relative expression of miR-138 in serum within the different groups. Our data showed that miR-138 expression was decreased in patients with CHB, LC, and HCC as compared with that in the HV and AsC groups (**Figure 2A**). Moreover, results from the correlation tests showed that miR-138 expression was inversely correlated with HBV DNA level within the CHB, LC, and HCC groups (**Figures 2B, 2C**, and **2D**). Such results provide further evidence indicating that HBV DNA level inhibits miR-138 expression.

Inverse Correlation of miR-138 Expression with PD-1 in Patients with HBV

Because miR-138 expression was negatively regulated whereas PD-1 was upregulated in patients with HBV infection, we speculated that a correlation would be present between miR-138 and PD-1 in these patients. As expected, the results of the Spearman correlation analysis showed that miR-138 expression in patients with CHB (**Figure 3A**), LC (**Figure 3B**), and HCC (**Figure 3C**) was inversely correlated with PD-1 in $CD3^+$, $CD4^+$, and $CD8^+$ T cells. These findings suggest that the upregulation of miR-138 has the potential for a new treatment strategy in patients with HBV infection through its capacity to regulate PD-1 expression.

Direct Regulation of PD-1 Expression in T Cells by miR-138

Research has shown that MiRNAs posttranscriptionally modulate target gene expressions by binding to 3'-UTR regions. Our bioinformatic analysis result indicated that PD-1 is one of the targets of miR-138. To functionally verify the interaction between miR-138 and PD-1, a luciferase expression assay was conducted in purified $CD3^+$ T cells, including mutating the predicted 3'-UTRs of the PD-1 binding site of miR-138. In cotransfected purified $CD3^+$ T cells, miR-138 significantly inhibited PD-1 luciferase activity, whereas the mutated miR-138 binding site of the 3'-UTR of PD-1 resulted in diminished luciferase activity when normalized to baseline (**Figure 4A**). These findings indicate a direct binding between miR-138 and PD-1, which is consistent with results reported in another study.[20] To verify a regulatory function of miR-138 in PD-1 expression, we next conducted a cell transfection assay with the miR-138 inhibitor and miR-138 mimics along with the corresponding control in purified $CD3^+$ T cells from HV. Effects of the miR-138 mimic and inhibitor transfection were determined using qRT-PCR (**Figure 4B**). The $CD3^+$ T cell lysate was then harvested at 24 hours after transfection for Western Blot analysis. The results showed that PD-1 expression was significantly downregulated by miR-138 (**Figures 4C** and **4D**). Accordingly, miR-138 directly modulates PD-1 expression by targeting the 3'-UTR region of PD-1.

DOI: 10.1093/labmed/lmaa110

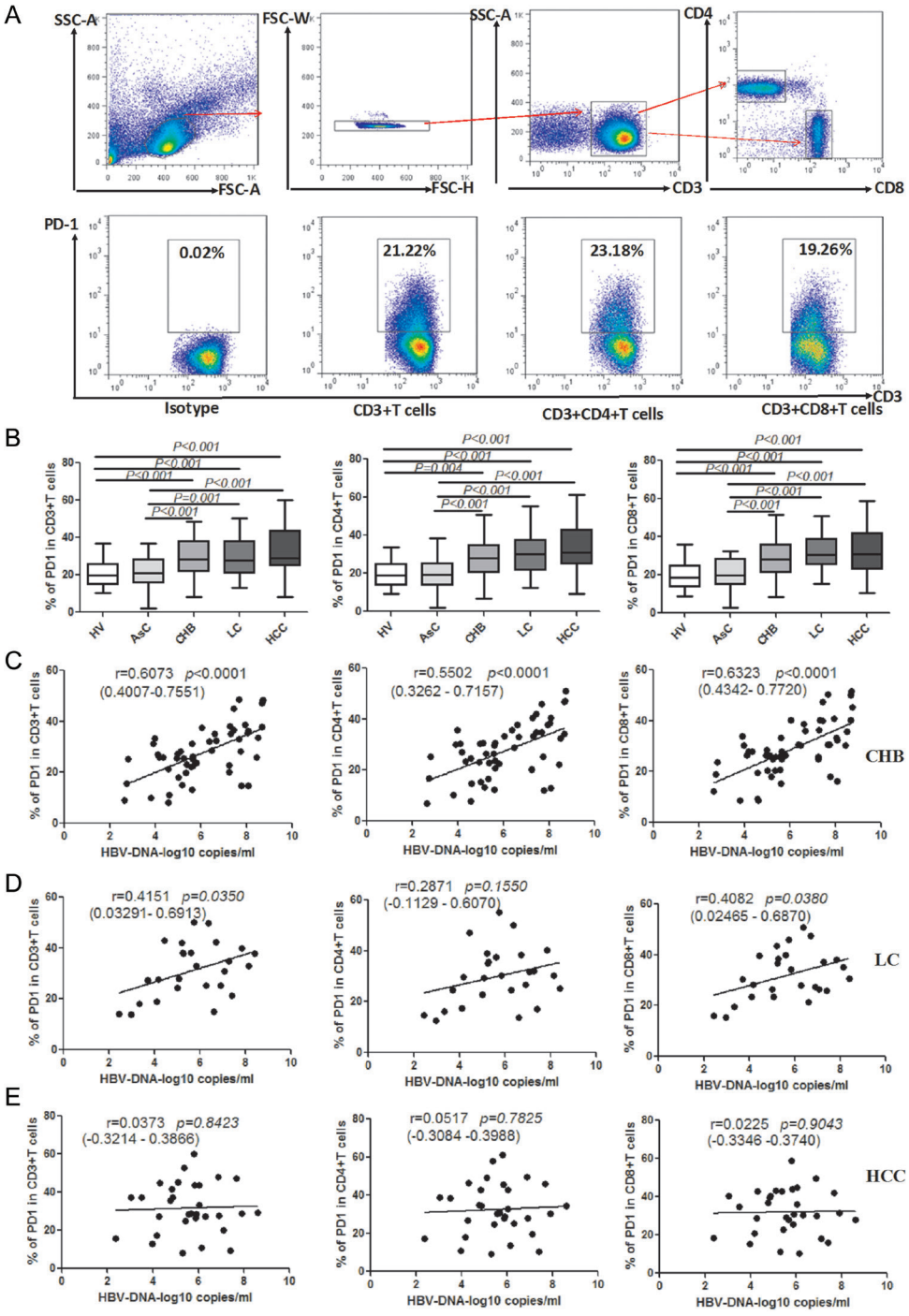

Figure 1

Expression profiles of PD-1 in peripheral T cells in patients with HBV and correlations between PD-1 expression and HBV level. **(A)** Gating strategies and representative results of PD-1 expression in circulating $CD3^+$, $CD4^+$, and $CD8^+$ T cells. **(B)** Histogram showing PD-1 expression in circulating $CD3^+$, $CD4^+$, and $CD8^+$ T cells from the different groups: HV (n = 43), AsC (n = 51), CHB (n = 52), LC (n = 26), and HCC (n = 31). **(C–E)** Spearman correlations between HBV DNA level and PD-1 expression within the CHB, LC and HCC groups. PD-1, programmed cell death-1; HBV, hepatitis B virus; HV, healthy volunteers; AsC, HBV asymptomatic carrier; CHB, chronic hepatitis B; LC, liver cirrhosis; HCC, hepatocellular carcinoma.

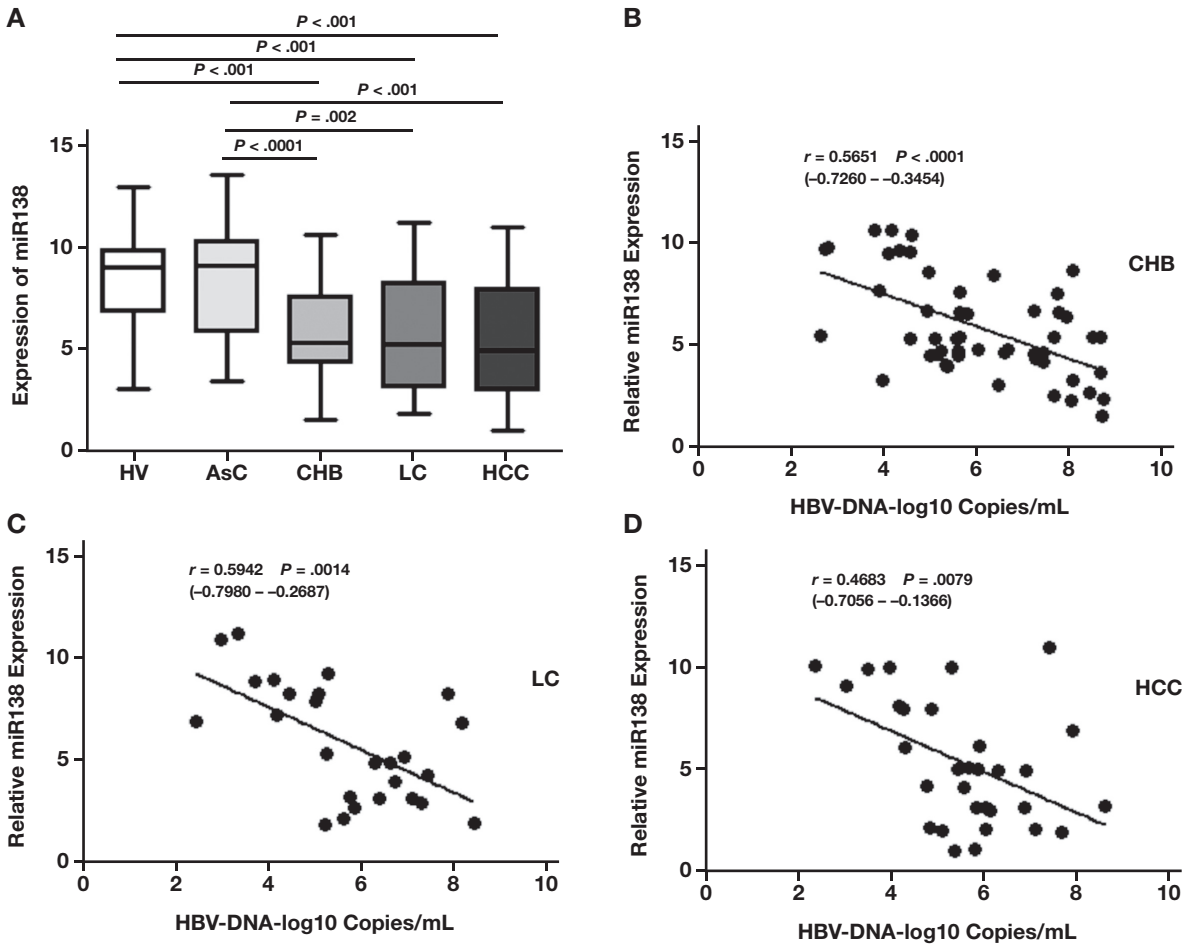

Figure 2

Correlations between HBV DNA level and miR-138 expression in patients with HBV. **(A)** qRT-PCR analysis of miR-138 expression levels in serum from the different groups: HV (n = 43), AsC (n = 51), CHB (n = 52), LC (n = 26), and HCC (n = 31). **(B–D)** Spearman correlations between HBV DNA level and miR-138 expression within the CHB, LC, and HCC groups. HBV, hepatitis B virus; miR-138, microRNA-138; qRT-PCR, quantitative real-time polymerase chain reaction; HV, healthy volunteers; AsC, HBV asymptomatic carrier; CHB, chronic hepatitis B; LC, liver cirrhosis; HCC, hepatocellular carcinoma.

MiR-138 Regulating Cytokine Secretion of T Cells by Blocking PD-1

Because miR-138 can directly regulate PD-1 expression in T cells, we next examined whether an alteration in miR-138 would affect T-cell function via targeting PD-1. To test for this possibility, we first upregulated and downregulated miR-138 in purified T cells by transfecting cells with an miR-138 mimic or miR-138 inhibitor. The flow cytometer results showed that miR-138 mimics resulted in substantially increased interferon-γ and tumor necrosis factor-α expressions, whereas interleukin-10 expression was markedly decreased. In contrast, the miR-138 inhibitor led to an opposite result in the expression of these cytokines (**Figures 5A**, **5B**, and **5C**). With the addition of anti-PD-1 to these cells during transfection with the miR-138 inhibitor, the expression of these cytokines was similar to those that had been treated with miR-138 mimics (**Figures 5D**, **5E**, and **5F**). These results suggest that the regulatory effects of miR-138 upon T-cell cytokine secretion develop through inhibiting PD-1 expression. Collectively, these findings imply that miR-138 regulates T-cell function by blocking PD-1.

DOI: 10.1093/labmed/lmaa110

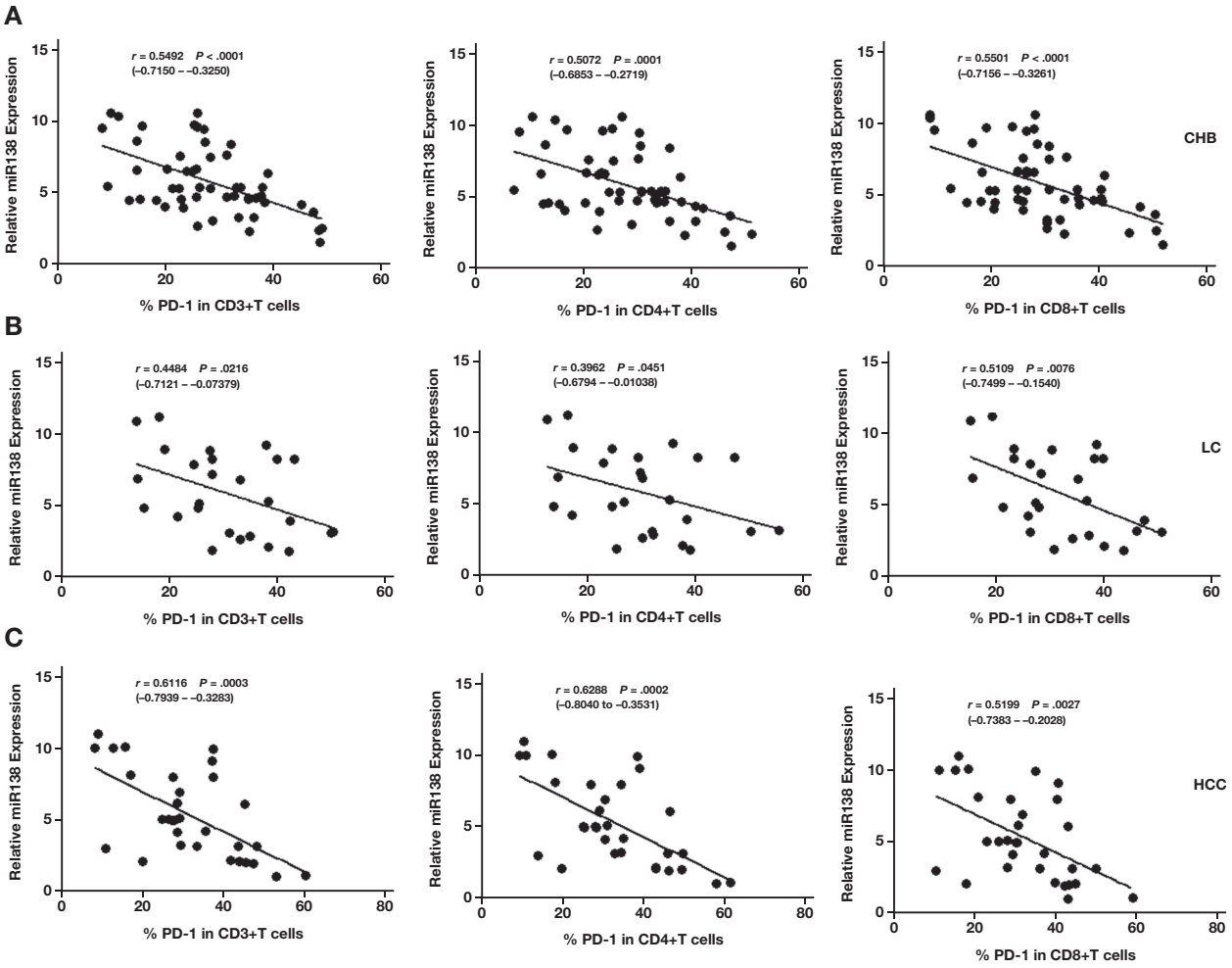

Figure 3

Correlations between PD-1 and miR-138 in patients with CHB (n = 52), LC (n = 26), and HCC (n = 31). Relative expressions of miR-138 in serum and percentage of PD-1 in peripheral T cells from patients with CHB, LC, and HCC are detected. **(A–C)** Spearman correlations between miR-138 and PD-1 expression in circulating $CD3^+$, $CD4^+$, and $CD8^+$ T cells in patients with CHB, LC, and HCC, respectively. PD-1, programmed cell death-1; CHB, chronic hepatitis B; LC, liver cirrhosis; HCC, hepatocellular carcinoma; miR-138, microRNA-138.

Antivirus Treatment for CHB Followed by Increased Expression of miR-138 and Decreased PD-1

To further verify the role of miR-138 in HBV infection, specimens from 11 patients with CHB receiving antivirus treatment for 1, 3, or 6 months were collected for analysis. As shown in **Figure 6A**, PD-1 expression in $CD3^+$, $CD4^+$, and $CD8^+$ T cells was remarkably decreased after antivirus treatment whereas miR-138 expression displayed a trend for a steady increase. Taken together, these data suggest that miR-138 may improve T-cell immune responses by inhibiting HBV DNA level via interactions with PD-1. These findings indicate a potential new strategy for the treatment of HBV (**Figure 6B**).

Discussion

Cell-mediated immune responses represent a prominent component of anti-HBV infection. For example, depletion of $CD4^+$ T cells before HBV infection results in a persistence

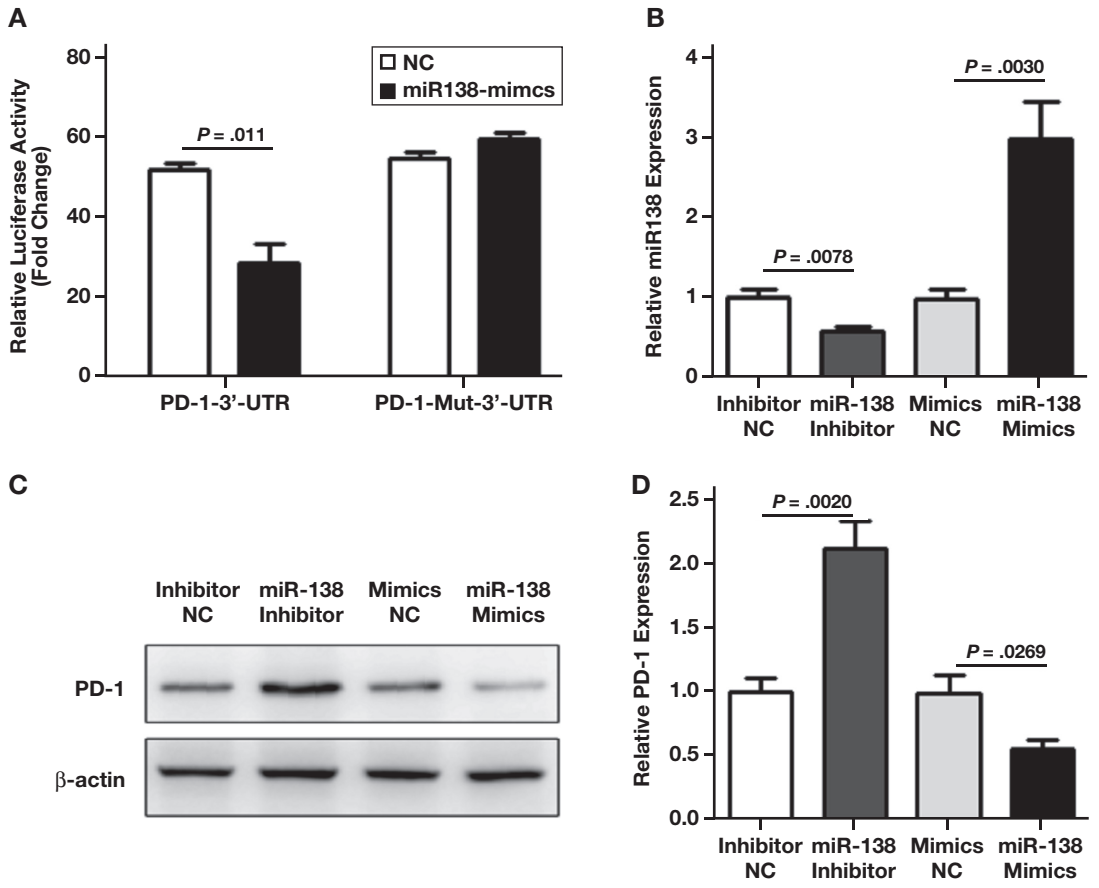

Figure 4

MiR-138 inhibits PD-1 expression by directly binding to its 3'-UTRs. Peripheral blood specimens from HV (n = 3) were collected and $CD3^+$ T cells were purified using a human $CD3^+$ T cell isolation kit. **(A)** Purified T cells were cotransfected with the designated PD-1 luciferase reporter plasmid and miR-138 or control miRNA molecules. Image shows the relative luciferase expression in purified $CD3^+$ T cells of HV transfected with miR-138 vs control cells. **(B)** Purified T cells were transfected either with miR-138 inhibitor controls, miR-138 inhibitors, miR-138 mimics controls, or miR-138 mimics. Expression levels of miR-138 were determined using qRT-PCR. **(C)** Expression levels of PD-1 in purified $CD3^+$ T cells after transfection were determined using Western blot assay. Image shows a representative experiment of the 3 experiments performed. **(D)** Histogram showing the relative expression of PD-1 in each group. miR-138, microRNA-138; PD-1, programmed cell death-1; 3'-UTR, 3'-untranslated region; HV, healthy volunteers; qRT-PCR, quantitative reverse-transcription polymerase chain reaction.

of HBV infection.[29] Moreover, depending on the secreting cytokines involved, such as IFN-γ or TNF-α, $CD8^+$ T cells also play a crucial role in the clearance of HBV virus within hepatocytes, especially in the clearance of HBV covalently closed circular DNA.[30] However, it has been reported that in patients with CHB, T-cell responses are much weaker and are often barely detectable because of immune-cell exhaustion as compared with the vigorous and broad T-cell responses observed in patients with acute self-limited hepatitis B.[31] It seems that upregulation and coexpression of multiple inhibitory receptors in T cells represent one of the main factors leading to T-cell exhaustion.[32] Such effects are consistent with our current data showing that PD-1 in T cells is upregulated in patients with HBV infection, with expression levels being positively correlated with the HBV viral load. Interestingly, this positive correlation is only present in patients with CHB and LC, but not in patients with HBV-related HCC. These effects may result from the capacity of not only HBV but also tumor cells to be involved in deregulating the expression of inhibitory receptors in immune cells. Immune checkpoints can exert a substantial effect upon T cells to suppress the HBV level, and by blocking

DOI: 10.1093/labmed/lmaa110

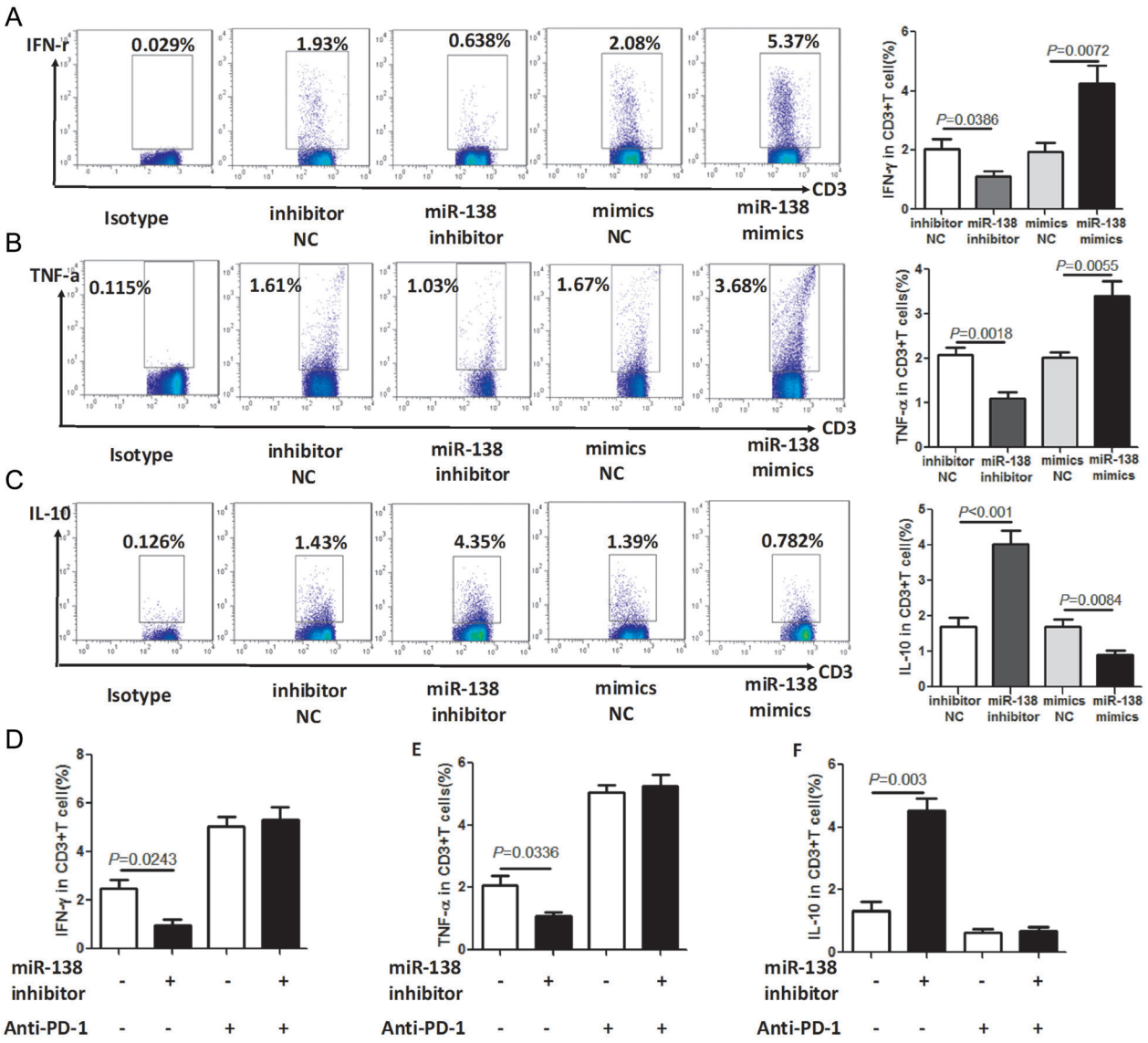

Figure 5

MiR-138 influences T-cell cytokine expression by regulating PD-1. $CD3^+$ T cells of HV (n = 5) were purified and processed for transfection as described in **Figure 4B**. After 24 hours, T cells were harvested for flow cytometry analysis. Figure shows representative percentages and histograms of IFN-γ **(A),** TNF-α **(B)**, and IL-10 **(C)** in T cells. **(D–F)** Purified T cells transfected with the miR-138 inhibitor or miR-138 inhibitor control with or without anti-PD-1. After transfection, IFN-γ, TNF-α, and IL-10 were determined using flow cytometry. miR-138, microRNA-138; PD-1, programmed cell death-1; HV, healthy volunteers; IFN-γ, interferon- γ; TNF-α, tumor necrosis factor-α; IL-10, interleukin 10; anti-PD-1, PD-1-blocking antibody.

these immune checkpoints can reinvigorate antiviral T-cell function.

Significant interest has accrued regarding the development of miRNA-based immunotherapeutics for the treatment of liver disease because expressions of miRNA are dysregulated in almost all types of liver diseases, including cancer. For example, miR-720 expression is upregulated in HBV-specific $CD8^+$ T cells and the overexpression of miR-720 in primary human $CD8^+$ T cells inhibits T-cell receptor stimulation-induced proliferation.[33] Zhang et al[34] reported that miR-4717 could directly regulate PD-1 expression on

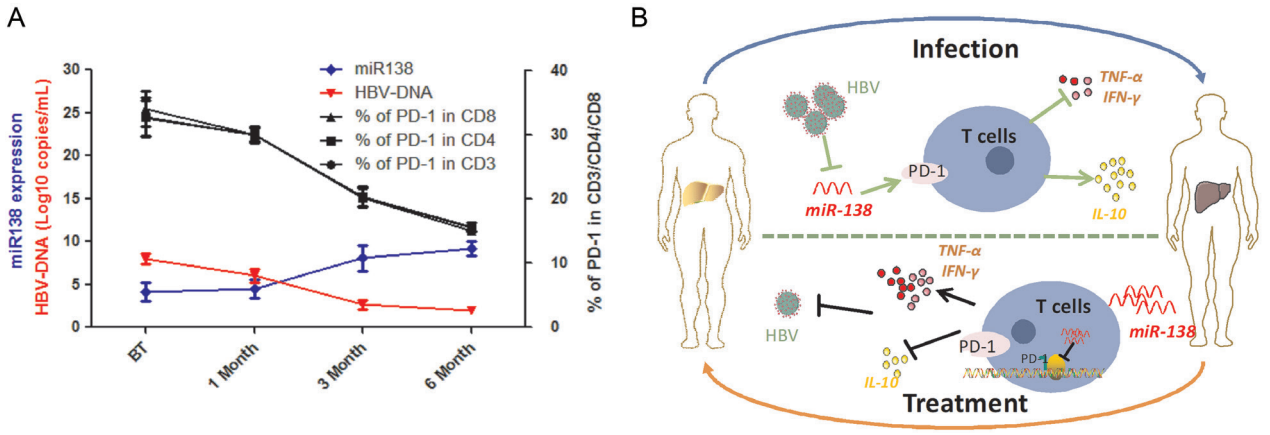

Figure 6

MiR-138 expression in patients with CHB is upregulated whereas PD-1 is downregulated after antivirus treatment. **(A)** Specimens from patients with CHB were collected after treatment for 1, 3, or 6 months (n = 11) and relative expressions of miR-138 in serum, HBV DNA level, and the percentage of PD-1 in circulating $CD3^+$, $CD4^+$, and $CD8^+$ T cells from the different treated stages were determined. "HBV-DNA LLOD" indicates the lowest detection limit, which was 2Log10 copies/mL. **(B)** Schematic representation of biological and functional interactions between PD-1 and HBV virus level through the miR-138 regulatory cascade. miR-138, microRNA-138; CHB, chronic hepatitis B; PD-1, programmed cell death-1; HBV, hepatitis B virus.

peripheral lymphocytes, leading to an alteration in immune regulation and exerting effects upon the susceptibility and disease course of chronic HBV infection. Such findings have 2 salient implications, the first being that alterations in miRNA expression are related to chronic HBV infection, and the second being that miRNAs may serve as promising therapeutic targets for HBV treatment. Results from genome identification studies have led to the suggestion that the HBV-HBx regulatory protein (required for HBV replication and involved in HBV-related carcinogenesis) contributes to the transcriptional repression of miRNAs, including miR-138, miR-224, miR-576, and miR-596, all of which possess the capacity to inhibit HBV level.[35]

In our current study, we found that miR-138 was downregulated in patients with CHB, LC, and HBV-associated HCC and that miR-138 expression levels were inversely correlated with HBV viral load, suggesting a potential involvement of miR-138 in HBV-related diseases. We also found that miR-138 can directly inhibit PD-1 expression by targeting the 3'-UTR of PD-1, a result consistent with a report indicating that miR-138 can exert anti-glioma efficacy by enhancing T-cell function.[20] Moreover, the overexpression of miR-138 in primary T cells could activate $CD3^+$ T cells by facilitating the expression of antivirus cytokines, such as IFN-γ and TNF-α, indicating that miR-138 may possess antivirus effects during HBV infection via enhancing T-cell function.

Although the tumor suppression effect of miR-138 has been validated in glioma cancer, this is the first report indicating the immune regulatory effects of miR-138 in HBV-related diseases as shown with clinical specimens rather than with cell cultures or transgenic mouse models. Wang, Zhao, et al[21] predicted an important role for miR-138 in HBV-related HCC tumorigenesis as achieved by targeting cyclin D3, whereas our current data suggest that miR-138 exerts anti-HBV effects by enhancing T-cell function. Collating these findings leads to the conclusion that miR-138 may exert antivirus effects not only by directly interacting with virus target cells but also by upregulating host immune responses.

Conclusion

Our data show that PD-1 expression is upregulated in T cells of patients with CHB, LC, and HCC, whereas miR-138 is downregulated. This downregulation of miR-138 results in an increase in PD-1 and induces aberrant T-cell activation

Lab Medicine 2021;52;439–451
DOI: 10.1093/labmed/lmaa110

in patients with HBV infection. Accordingly, the findings of this study offer new insights into the regulation of PD-1 by miRNAs and suggest that miR-138 may serve as a promising therapeutic intervention for use in the treatment of chronic infectious diseases such as HBV. However, we have only focused on the regulation effect of miR-138 on T cells by targeting immune checkpoints in vitro, but the effect on hepatocytes have not been studied and further animal experiments should be conducted to verify these data.

This study was supported by grants from the National Natural Science Foundation of China (81870016), the Science and Technology Tackling Project of the Henan Provincial Department of Education (2013020036), and the Science and Technology Project of Jiaozuo (2014196). All funding bodies had no role in the study design, data collection and analysis, decision to publish, or preparation of the manuscript.

The datasets used and/or analyzed during this study are available from the corresponding author on reasonable request.

WL and XZ conceived and designed the idea of the study. WL performed the experiments. WL and JW analyzed most of the data and wrote the initial draft. JL and QH contributed materials and analysis tools and performed statistical analysis. JL, SY, and HL contributed to discussions, interpretation of data, and manuscript revision. The remaining authors contributed to refining the ideas, carrying out additional analyses, and finalizing the manuscript.

This study was reviewed and approved by the People's Hospital of Jiaozuo under protocol number 2017-03. All the procedures in this study were in accordance with the 1975 Declaration of Helsinki, updated in 2013. Informed consent was obtained from all participants included in the study; written informed consent was obtained from the patients for publication of this study and accompanying statistics. **LM**

Acknowledgments

We thank the nurses, doctors, and staff in the Department of Respiration at the People's Hospital of Jiaozuo, China, and the Department of Clinical Medicine Laboratory, First Affiliated Hospital, Zhengzhou University, China for the collection of clinical specimens and data.

References

1. Schweitzer A, Horn J, Mikolajczyk RT, Krause G, Ott JJ. Estimations of worldwide prevalence of chronic hepatitis B virus infection: a systematic review of data published between 1965 and 2013. *Lancet.* 2015;386(10003):1546–1555.
2. Zeng JC, Lin DZ, Yi LL, et al. BTLA exhibits immune memory for αβ T cells in patients with active pulmonary tuberculosis. *Am J Transl Res.* 2014;6(5):494–506.
3. Allweiss L, Dandri M. The role of cccDNA in HBV maintenance. *Viruses*. 2017;9(6):156.
4. Gehring AJ, Xue SA, Ho ZZ, et al. Engineering virus-specific T cells that target HBV infected hepatocytes and hepatocellular carcinoma cell lines. *J Hepatol.* 2011;55(1):103–110.
5. Ferrari C, Penna A, Bertoletti A, et al. Cellular immune response to hepatitis B virus-encoded antigens in acute and chronic hepatitis B virus infection. *J Immunol.* 1990;145(10):3442–3449.
6. Sandhu P, Haque M, Humphries-Bickley T, Ravi S, Song J. Hepatitis B virus immunopathology, model systems, and current therapies. *Front Immunol.* 2017;8:436.
7. Peng G, Li S, Wu W, Tan X, Chen Y, Chen Z. PD-1 upregulation is associated with HBV-specific T cell dysfunction in chronic hepatitis B patients. *Mol Immunol.* 2008;45(4):963–970.
8. Schurich A, Khanna P, Lopes AR, et al. Role of the coinhibitory receptor cytotoxic T lymphocyte antigen-4 on apoptosis-prone CD8 T cells in persistent hepatitis B virus infection. *Hepatology.* 2011;53(5):1494–1503.
9. Petrovas C, Casazza JP, Brenchley JM, et al. PD-1 is a regulator of virus-specific CD8+ T cell survival in HIV infection. *J Exp Med.* 2006;203(10):2281–2292.
10. Yokosuka T, Takamatsu M, Kobayashi-Imanishi W, Hashimoto-Tane A, Azuma M, Saito T. Programmed cell death 1 forms negative costimulatory microclusters that directly inhibit T cell receptor signaling by recruiting phosphatase SHP2. *J Exp Med.* 2012;209(6):1201–1217.
11. Hui E, Cheung J, Zhu J, et al. T cell costimulatory receptor CD28 is a primary target for PD-1-mediated inhibition. *Science.* 2017;355(6332):1428–1433.
12. Wei YF, Cui GY, Ye P, Chen JN, Diao HY. MicroRNAs may solve the mystery of chronic hepatitis B virus infection. *World J Gastroenterol.* 2013;19(30):4867–4876.
13. Amaral AJ, Andrade J, Foxall RB, et al. miRNA profiling of human naive CD4 T cells links miR-34c-5p to cell activation and HIV replication. *EMBO J.* 2017;36(3):346–360.
14. Kroesen BJ, Teteloshvili N, Smigielska-Czepiel K, et al. Immuno-miRs: critical regulators of T-cell development, function and ageing. *Immunology.* 2015;144(1):1–10.
15. Liu X, Jiang L, Wang A, Yu J, Shi F, Zhou X. MicroRNA-138 suppresses invasion and promotes apoptosis in head and neck squamous cell carcinoma cell lines. *Cancer Lett.* 2009;286(2):217–222.
16. Mitomo S, Maesawa C, Ogasawara S, et al. Downregulation of miR-138 is associated with overexpression of human telomerase reverse transcriptase protein in human anaplastic thyroid carcinoma cell lines. *Cancer Sci.* 2008;99(2):280–286.
17. Yamasaki T, Seki N, Yamada Y, et al. Tumor suppressive microRNA-138 contributes to cell migration and invasion through its targeting of vimentin in renal cell carcinoma. *Int J Oncol.* 2012;41(3):805–817.
18. Yeh YM, Chuang CM, Chao KC, Wang LH. MicroRNA-138 suppresses ovarian cancer cell invasion and metastasis by targeting SOX4 and HIF-1α. *Int J Cancer.* 2013;133(4):867–878.
19. Zhou X, Luan X, Chen Z, et al. MicroRNA-138 inhibits periodontal progenitor differentiation under inflammatory conditions. *J Dent Res.* 2016;95(2):230–237.

20. Wei J, Nduom EK, Kong LY, et al. MiR-138 exerts anti-glioma efficacy by targeting immune checkpoints. *Neuro Oncol.* 2016;18(5):639–648.
21. Wang W, Zhao LJ, Tan YX, Ren H, Qi ZT. Identification of deregulated miRNAs and their targets in hepatitis B virus-associated hepatocellular carcinoma. *World J Gastroenterol.* 2012;18(38):5442–5453.
22. Gerlich WH. Medical virology of hepatitis B: how it began and where we are now. *Virol J.* 2013;10:239.
23. Crossland RE, Norden J, Bibby LA, Davis J, Dickinson AM. Evaluation of optimal extracellular vesicle small RNA isolation and qRT-PCR normalisation for serum and urine. *J Immunol Methods.* 2016;429:39–49.
24. Occhipinti G, Giulietti M, Principato G, Piva F. The choice of endogenous controls in exosomal microRNA assessments from biofluids. *Tumour Biol.* 2016;37(9):11657–11665.
25. Salmaninejad A, Khoramshahi V, Azani A, et al. PD-1 and cancer: molecular mechanisms and polymorphisms. *Immunogenetics.* 2018;70(2):73–86.
26. Chinai JM, Janakiram M, Chen F, Chen W, Kaplan M, Zang X. New immunotherapies targeting the PD-1 pathway. *Trends Pharmacol Sci.* 2015;36(9):587–595.
27. Yin Y, Cai X, Chen X, et al. Tumor-secreted miR-214 induces regulatory T cells: a major link between immune evasion and tumor growth. *Cell Res.* 2014;24(10):1164–1180.
28. Xie KL, Zhang YG, Liu J, Zeng Y, Wu H. MicroRNAs associated with HBV infection and HBV-related HCC. *Theranostics.* 2014;4(12):1176–1192.
29. Asabe S, Wieland SF, Chattopadhyay PK, et al. The size of the viral inoculum contributes to the outcome of hepatitis B virus infection. *J Virol.* 2009;83(19):9652–9662.
30. Phillips S, Chokshi S, Riva A, Evans A, Williams R, Naoumov NV. CD8(+) T cell control of hepatitis B virus replication: direct comparison between cytolytic and noncytolytic functions. *J Immunol.* 2010;184(1):287–295.
31. Bertoletti A, Ferrari C. Adaptive immunity in HBV infection. *J Hepatol.* 2016;64(1 Suppl):S71–S83.
32. Gehring AJ. New treatments to reach functional cure: rationale and challenges for emerging immune-based therapies. *Best Pract Res Clin Gastroenterol.* 2017;31(3):337–345.
33. Wang Y, Zhang Z, Ji D, et al. Regulation of T cell function by microRNA-720. *Sci Rep.* 2015;5:12159.
34. Zhang G, Li N, Li Z, et al. microRNA-4717 differentially interacts with its polymorphic target in the PD1 3' untranslated region: a mechanism for regulating PD-1 expression and function in HBV-associated liver diseases. *Oncotarget.* 2015;6(22):18933–18944.
35. Guerrieri F, Belloni L, D'Andrea D, et al. Genome-wide identification of direct HBx genomic targets. *BMC Genomics.* 2017;18(1):184.

DOI: 10.1093/labmed/lmaa110

Methodology to Evaluate Clinical Impact of 0/3 Hour High-Sensitivity Cardiac Troponin T Protocol on Managing Acute Coronary Syndrome in Daily Emergency Department Practice

Claudia Bellini, MD,[1,2,*] *Francesca Cinci, MD,*[1,2] *Giovanni Bova, MD,*[3] *Monica Mascarucci, MD,*[3] *Roberto Leoncini, MSc,*[1,2] *Carlo Scapellato, MD,*[2] *Roberto Guerranti, PhD*[1,2]

Laboratory Medicine 2021;52:452-459

DOI: 10.1093/labmed/lmaa118

ABSTRACT

Objective: Sex-/age-differentiated cutoffs and the magnitude of serial changes in high-sensitivity cardiac troponins (hs-cTn) for acute coronary syndrome (ACS) diagnosis algorithms are still under discussion. This study presents a methodology to evaluate decision-making limits and to assess whether sex-specific cutoffs could improve diagnostic accuracy.

Methods: A high-sensitivity cardiac troponin T (hs-cTnT) 0-/3-hour protocol was adopted, applying the 2015 European Society of Cardiology Guidelines. Decision-making limits (99th percentile: 14 ng/L; delta change ≥ 30%) were agreed upon with the emergency department (ED) at the University Hospital of Siena in Siena, Italy. One-year requests (5177) for hs-cTnT serial determination were compared with the final International Classification of Diseases, 9th revision, clinical modifications diagnosis (contingency tables; receiver operating characteristic curves).

Results: The algorithm's capability to exclude or confirm ACS was verified by remarkable negative predictive value (97%) and high areas under the curve for the first troponin sampling (0.712), troponin sampling at 3 hours (0.789), and delta (0.744). The clinical utility for the general population—even those with comorbidities—accessing the ED was verified. Our data did not support a sex-differentiated cutoff utility because it would not have affected patient management.

Conclusion: This methodology allowed us to confirm the effectiveness of our decision-making limits.

Keywords: troponin T, high-sensitivity cardiac troponin, acute coronary syndrome, NSTEMI, evidence-based practice, diagnostic accuracy

Abbreviations:

Hs-cTn, high-sensitivity cardiac troponin; ACS, acute coronary syndrome; hs-cTnT, high-sensitivity cardiac troponin T; ED, emergency department; AMI, acute myocardial infarction; cTn, cardiac troponin; CV, coefficient of variation; UHS, University Hospital of Siena; T0h, first sampling at presentation; T3h, sampling after 3 hours; LIS, laboratory information system; eGFR, estimated glomerular filtration rate; HDC, hospital discharge card; STEMI, ST-segment elevation myocardial infarction; NSTEMI, non-ST-segment elevation myocardial infarction; CKD, chronic kidney disease; IFCC, International Federation for Clinical Chemistry; ROC, receiver operating characteristic; AUC, area under the curve; NPV, negative predictive value; PPV, positive predictive value.

[1]Department of Medical Biotechnologies, University of Siena, Siena, Italy, [2]Clinical Pathology Unit, Innovation, Experimentation and Clinical and Translational Research Department, University Hospital of Siena, Siena, Italy, [3]Emergency-Urgency and Transplants Department, University Hospital of Siena, Siena, Italy

*To whom correspondence should be addressed.
claudia.bellini@dbm.unisi.it

The differential diagnosis of acute chest pain is one of the most complex challenges in emergency departments (ED) because acute coronary syndrome (ACS) is associated with high mortality and morbidity. Therefore it is necessary to manage both the risk of missing an ACS diagnosis, with its medical, social, and legal consequences and the risk of inappropriate hospitalization of low-risk patients, resulting in increased health care costs.

High-sensitivity cardiac troponins (hs-cTn) have significantly improved the diagnosis of patients presenting in the ED with chest pain who are suspected to have ACS and have completely replaced the old biomarkers of acute myocardial infarction (AMI). High-sensitivity methods are defined by the ability to measure cardiac troponin (cTn) values with a coefficient of variation (CV) ≤10% at the upper reference limit, ie, the 99th percentile cTn concentration of

a healthy population, and to detect cTn amounts above the limit of detection in more than 50% of the male and female healthy reference population.[1]

cTn serum increases are noted in many cardiac conditions, such as heart failure, along with conditions that are not primarily cardiac, such as renal failure, because there is debate as to whether these increases represent a decreased elimination or myocyte damage induced by renal disease.[2] In fact, cTns are very sensitive to myocardial damage, but they are not specific to ACS. For this reason, several algorithms have been developed to evaluate cTn variations in consecutive determinations to highlight acute injury.[3] According to the Fourth Universal Definition of Myocardial Infarction,[4] hs-cTn values exceeding the 99th percentile of a healthy reference population with an increase/decrease pattern are only indicative of acute myocardial damage. To identify AMI, it is necessary to evaluate 2 other factors: whether there is a specific kinetics of variation (delta change), typical of ACS, and whether there is an ischemic condition that can be detected by symptomatology or other tests, such as electrocardiogram or imaging.[4]

The debate on decision-making limits is always topical, and numerous studies are underway to assess the clinical utility of sex- or age-differentiated cutoffs[5]: since the Third Universal Definition of Myocardial Infarction was issued,[6] it has been recognized that upper reference limits for females are lower than for males, and the Fourth Definition recommends the use of sex-differentiated cutoffs because diagnostic performances are improved for some methods.[4] However, precisely because the clinical usefulness of sex-differentiated cutoffs has not yet been proven for all methods, the same guideline reports that there is still no consensus on the sex-specific approach. In fact, although a single threshold simplifies cTn clinical application, it may lead to an excess of false positives for AMI in males and to underdiagnosis in females.[7]

A similar risk may occur by applying a higher cutoff in the older adult population: healthier individuals may be underdiagnosed. On the contrary, a single lower cutoff, undifferentiated by age, may increase false positives among older adults, who carry more ACS risk factors and comorbidities.[8] Therefore, the Fourth Definition states that on the basis of the current evidence, it is not possible to recommend age-differentiated cutoffs for clinical use.[4]

Furthermore, there is no "universal" delta; even a small variation (>20%) can be significant in the appropriate clinical context, ie, when the basal cTn value is already high (>99th percentile), whereas it is suggested to use a larger variation (>50%) when the cTn is low (<99th percentile) at the first sampling.[9,10] Therefore, in selecting the delta, we must consider the objective we intend to achieve in terms of a balance between sensitivity and specificity and therefore between false positives and false negatives.[11,12]

For some years now, at the University Hospital of Siena (UHS), a high-sensitivity cardiac troponin T (hs-cTnT) 0-/3-hour protocol has been adopted, applying the principles of clinical use expressed in the 2015 European Society of Cardiology Guidelines.[10] The following decision limits were agreed upon with emergency physicians for ACS rule-in: a ≥30% increase or decrease of hs-cTnT in serial population samples with at least 1 of the values exceeding 14 ng/L, which is the cutoff for myocardial injury, corresponding to the 99th percentile declared by the manufacturer of the method. A cutoff of 50 ng/L is used for immediate ACS rule-in at the first sampling (T0h). It is noteworthy that our 99th percentile is lower compared with the U.S. Food & Drug Administration–approved overall 99th percentile (19 ng/L) used in the United States, because the latter was determined in a reference population matched to the age of patients presenting to the ED with suspected AMI.[13]

Because our decision limits are not derived from a population study, it was decided, in agreement with emergency physicians, to evaluate them in a retrospective study of diagnostic accuracy. In fact, although hs-cTns are no longer dichotomous markers but rather continuous variables related to pathophysiology and prognosis, it is still important and necessary to research and refine decision levels and algorithms for their effective use in clinical practice for the diagnosis of ACS.[14,15] The analysis of the results of diagnostic assays, correlated to the actual diagnoses issued, can be very useful to optimize the predictive capacity of the test: even small changes made to such a protocol can lead to benefits on waiting times and reduction of ED overcrowding, with considerable savings in health care spending.

Therefore, in the present study we aimed to provide a practical methodology for the evaluation of decision limits for ACS diagnosis in a "real-world" population. The population sample under examination included all possible cases of patients presenting in the ED with suspected ACS, regardless of their comorbidities, as happens in real life. We retrospectively examined the diagnostic accuracy of the decision

DOI: 10.1093/labmed/lmaa118

limits in use, even including those patients with impaired renal function whose basal hs-cTnT values were higher. For this reason, we evaluated the diagnostic accuracy of the hs-cTnT algorithm not only on the entire selected population but also on the "cleaned" subgroup of patients who did not have impaired renal function, and we made a comparison. Moreover, we assessed whether the application of sex-specific cutoffs could have improved the diagnostic accuracy for ACS in ED.

Materials and Methods

This monocentric retrospective study includes the analysis of data from patients presenting with acute chest pain at the UHS ED during the period of 1 year for whom serial determination of hs-cTnT, which we indicate with "hs-cTnT curve," was required. Thanks to a specific computerized acceptance code, clinicians require the contextual determination of hs-cTnT in serial blood withdrawals. Appropriate barcodes are generated for the labeling of the relevant test tubes (at presentation: T0h; after 3 hours: T3h), and the results are noted in a single report that also includes the calculation of the delta change. Hence, for our purposes, all hs-cTnT curve requests (n = 5177) were extracted from the laboratory information system (LIS). The computerized curve acceptance code made it possible to exclude requests for a single determination of hs-cTnT, which was not programmed for suspected ACS. Together with the hs-cTnT curve, the creatinine values, from which the estimated glomerular filtration rate (eGFR) was calculated using the Chronic Kidney Disease Epidemiology Collaboration formula, were also extracted.[16] The data were processed guaranteeing the anonymity of the patients and respecting their privacy.

The hs-cTnT was measured in serum specimens with the Elecsys Troponin T hs method performed on the Cobas 6000, e601system (Roche Diagnostics GmbH, Mannheim, Germany). Assay specifications were as follows[17]:

(i) 3 ng/L: limit of blank
(ii) 5 ng/L: limit of detection
(iii) 14 ng/L: 99th percentile cutoff
(iv) CV <10% at 13 ng/L

The diagnostic performance of the protocol (0/3h) was evaluated through contingency tables in which the classification of patients according to the hs-cTnT algorithm was compared to the final diagnosis considered as the gold standard, retrieved from the hospital discharge card (HDC). Patients were grouped according to the International Classification of Diseases, 9th revision, clinical modification final diagnosis framework into 5 categories:

(i) ST-segment elevation myocardial infarction (STEMI)
(ii) non-ST-segment elevation myocardial infarction (NSTEMI)
(iii) unstable angina
(iv) other cardiac syndrome
(v) noncardiac syndrome

The first 3 categories represented ACS and were brought together in the AMI group. The others included all other causes of chest pain, cardiac or noncardiac, which led to diagnoses other than ACS (non-AMI).

Those patients lacking the T3h sampling (n = 2436) were analyzed separately, and the rule-in cutoff of 50 ng/L was evaluated for them (**Figure 1**). First, the algorithm in use (unique cutoff of 14 ng/L and delta of 30%) was applied to the population that had performed the hs-cTnT curve (T0h–T3h; n = 2741). For the same population, an algorithm with unique cutoff of 14 ng/L and delta of 100% was applied to detect any changes in predictivity.

To eliminate a source of possible misclassification related to the fact that patients with chronic kidney disease

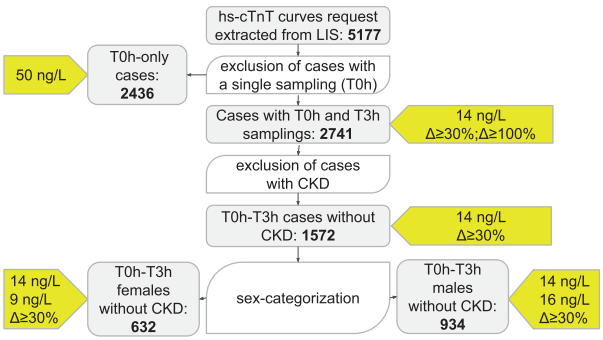

Figure 1

Study design. The arrow-shaped boxes include the decision limits that were assessed for that group of patients. CKD, chronic kidney disease; hs-cTnT, high-sensitivity cardiac troponin T; LIS, laboratory information system; T0h, first sampling at presentation; T3h, sampling after 3 hours.

(CKD) have higher baseline cTn values,[4,18,19] the algorithm was also tested in the subgroup of patients (n = 1572) with eGFR ≥ 60 mL/min/1.73m^2, because a value of eGFR < 60 mL/min/1.73m^2 is the threshold for the definition of CKD.

Subsequently, the same algorithm (unique cutoff of 14 ng/L and delta of 30%) was applied in the population without CKD, divided between males and females. Sex-differentiated cutoffs were then applied to verify a possible reclassification of patients: for females (n = 632), a cutoff of 9 ng/L was applied and for males (n = 934), a cutoff of 16 ng/L was applied. These thresholds were derived from the existing literature on hs-cTnT by the International Federation for Clinical Chemistry (IFCC) Committee on Clinical Applications of Cardiac Bio-Markers.[20]

For the diagnostic accuracy assessment with respect to ACS diagnosis and the calculation of the desirable cutoffs, receiver operating characteristic (ROC) curves were constructed for the T0h and T3h values of hs-cTnT and for the percentage variation in all the above groups. Data processing was carried out with SPSS Statistics software version 21.0.

Results

To assess the diagnostic accuracy of the hs-cTnT 0/3h protocol in use at the UHS, all the hs-cTnT curves requested from the ED during the period of 1 year (for 5177 patients) were extracted from the LIS: Approximately half (2741) of the patients received both T0h and T3h sampling, and the other half (2436) received only T0h (**Table 1**). The population examined was mostly older adults—63.07% of patients were aged >65 years. Both sexes were well represented (females:males = 1:1.15). The STEMI:NSTEMI ratio was 1:1, in accordance with the 2017 Tuscan Regional Health Agency Report on the Regional Programme for the Observation of Outcomes, which reported a similar diagnostic capacity in Tuscany.[21] There were 280 patients with ACS out of 5177 patients, of whom 159 were among the 2741 patients with both T0h and T3h specimens, representing 5.4% and 5.8% of requests from the ED, respectively, whereas the average pretest probability of patients in the ED with suspicious chest pain who have ACS ranges from 10% to 20%.[22]

Table 1. Characteristics of the Study Population

Characteristics	Number of Patients	Percentage of All Patients
Age (0–105 y)	5177	
Age > 50 y	4279	82.65
Age > 65 y	3265	63.07
Female	2411	46.60
Male	2766	53.40
Non-AMI	4897	94.59
AMI	280	5.41
STEMI	108	2.09
NSTEMI	106	2.05
UA	66	1.27

AMI, acute myocardial infarction; NSTEMI, non-ST-segment elevation myocardial infarction; STEMI, ST-segment elevation myocardial infarction; UA, unstable angina.

Figure 2 shows the final diagnosis distribution of patients for whom hs-cTnT was found to be higher than the cutoff of 14 ng/L at T0h (n = 2463; 48%); among these patients, only 229 (9.3%) had a final diagnosis of AMI and 2234 (90.7%) had a diagnosis of non-AMI. On the other hand, studies have reported that the probability of ACS in the population presenting in the ED with suspected chest pain and with their first hs-cTn value above the 99th percentile is approximately 30%.[23]

Table 2 summarizes the results of all the contingency tables analyzed in the various groups and subgroups, and **Table 3** lists the respective areas under the curve (AUCs) and cutoffs obtained from the ROC curves.

Discussion

The aim of this study was to provide a methodology to verify whether the information given by the 0/3h protocol of the hs-cTnT test was satisfactory in the detection or exclusion of AMI in the real-world setting of our ED, including those situations in which impaired kidney function could have complicated the interpretation of cTn results. In addition, the study evaluated whether the application of sex-specific cutoffs could have improved the diagnostic accuracy for ACS. Results are discussed in the following sections, separately for each group.

Lab Medicine 2021;52;452–459 455
DOI: 10.1093/labmed/lmaa118

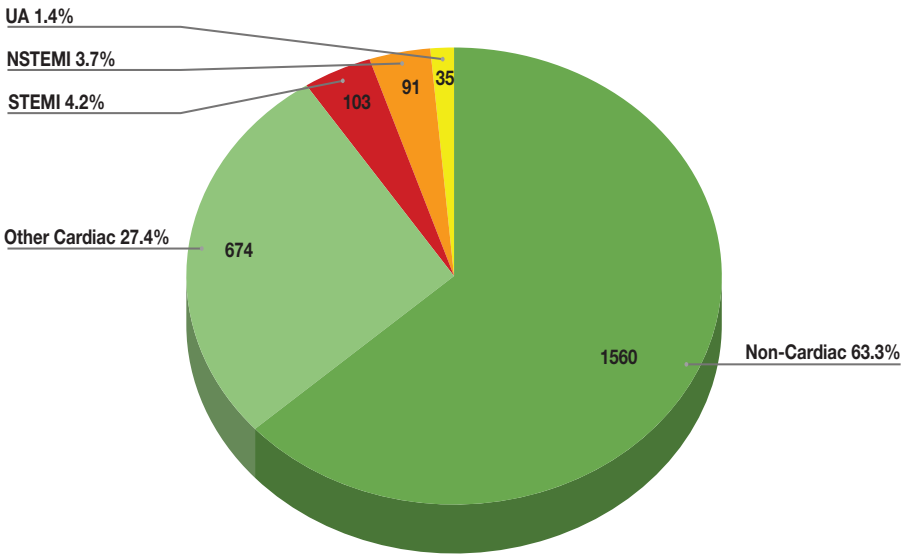

Figure 2

Final diagnosis in patients with T0h >14 ng/L. NSTEMI, non-ST-segment elevation myocardial infarction; STEMI, ST-segment elevation myocardial infarction; T0h, first sampling at presentation; UA, unstable angina.

Table 2. Summary of SE, SP, PPV, and NPV

n	eGFR (mL/min/1.73 m^2)	Sex	Cutoff (ng/L)	Delta (%)	TP	FP	FN	TN	SE (%)	SP (%)	PPV (%)	NPV (%)	Pr (%)
2741	U	U	14	30	85	268	74	2314	53 (52–55)	90 (88–91)	24 (22–26)	97 (96–98)	5.8 (5.0–6.8)
2741	U	U	14	100	60	108	99	2474	38 (36–40)	96 (95–97)	36 (34–38)	96 (95–97)	5.8 (5.0–6.8)
2436	U	U	50		69	284	52	2031	57 (55–59)	88 (86–89)	20 (18–21)	98 (97–98)	5.0 (4.2–5.9)
1572	≥60	U	14	30	41	123	41	1367	50 (47–53)	92 (90–93)	25 (23–27)	97 (96–98)	5.2 (4.2–6.5)
632	≥60	F	14	30	12	62	8	550	60 (56–64)	90 (87–92)	16 (13–19)	99 (97–99)	3.2 (2.0–4.9)
632	≥60	F	9	30	13	76	7	536	65 (61–69)	88 (85–90)	15 (12–18)	99 (97–99)	3.2 (2.0–4.9)
934	≥60	M	14	30	29	59	33	813	47 (44–50)	93 (91–95)	33 (30–36)	96 (95–97)	6.6 (5.1–8.5)
934	≥60	M	16	30	29	58	33	814	47 (44–50)	93 (92–95)	33 (30–36)	96 (95–97)	6.6 (5.2–8.5)

Delta, percentage of delta change considered; eGFR, estimated glomerular filtration rate; FP, false positive; FN, false negative; NPV, negative predictive value; Pr, prevalence; PPV, positive predictive value; SE, sensitivity; SP, specificity; TN, true negative; TP, true positive; U, unchecked.
Values in parentheses are 95% confidence intervals.

Total Population assessed at T0h and T3h (n = 2741)

The AUCs for T0h (0.712), T3h (0.789), and delta (0.744) confirmed a good discriminatory capacity and, as expected for biomarker kinetics at least in the majority of patients presenting at the ED within the first 6 hours after pain onset, this capacity was greater on T3h sampling and on the delta change with respect to T0h.[24,25]

The best T0h cutoff obtained from the ROC curve (29.92 ng/L) was higher than the decision limit in use corresponding to the 99th percentile (14 ng/L), in accordance with the fact that the 99th percentile itself corresponded to a lower value than the ROC-derived cutoff.[26,27] The ROC-derived best cutoff of T3h (44.54 ng/L) was higher than that of T0h, consistent with the kinetics of cTn release from the necrotic myocardium.

In our protocol, we adopted a minimum variation of 30%, although according to the ROC-derived delta best cutoff, a variation of approximately 18% should be already considered indicative of acute process. Using this delta, we would certainly have an increase in the negative predictive value (NPV) related to the algorithm but also an increase in

Table 3. Summary of AUCs and Cutoffs Derived from ROC Curves for Examined Groups

n	eGFR (mL/min/1.73 m^2)	Sex	Decision Limit	AUC	Best Cutoff	Unit of Measure
2741	U	U	T0h	0.712 (0.671–0.753)	29.92	ng/L
			T3h	0.789 (0.749–0.830)	44.54	ng/L
			Delta	0.744 (0.698–0.790)	17.85	%
2436	U	U	T0h	0.812 (0.772–0.852)	27.02	ng/L
1572	≥60	U	T0h	0.762 (0.706–0.817)	18.48	ng/L
			T3h	0.810 (0.752–0.867)	29.47	ng/L
			Delta	0.744 (0.682–0.807)	23.55	%
632	≥60	F	T0h	0.802 (0.693–0.912)	22.22	ng/L
			T3h	0.847 (0.736–0.958)	41.57	ng/L
			Delta	0.787 (0.669–0.905)	31.15	%
934	≥60	M	T0h	0.746 (0.681–0.812)	14.12	ng/L
			T3h	0.798 (0.730–0.866)	29.47	ng/L
			Delta	0.733 (0.659–0.807)	23.55	%

AUC, area under the curve; delta, percentage of delta change considered; eGFR, estimated glomerular filtration rate; ROC, receiver operating characteristic; T0h, first sampling at presentation; T3h, sampling after 3 hours.
Values in parentheses are 95% confidence intervals.

false positives. Because with our protocol we obtained a remarkable NPV (97%), we believe that the cutoffs for the 99th percentile and the delta adopted are already properly balanced and therefore allow clinicians to exclude the diagnosis of AMI with relative safety if after 3 hours a patient presents with hs-cTnT < 14 ng/L, has no pain, and has a low risk of intrahospital mortality (quantified using a Global Registry of Acute Coronary Events Score < 140). This NPV was slightly lower than we might expect from the literature data (99%–100%), but we must consider the bias resulting from the retrospective nature of the study.

To verify whether a higher variation could increase the positive predictive value (PPV), a delta of 100% was applied to the same population (n = 2741) and corresponded to the better specificity obtainable from the ROC curve carried out on patients with NSTEMI compared with patients in the non-AMI category. The increase of the delta threshold did not assure the desired increase in specificity and caused a reduction in sensitivity, so the PPV was only slightly increased. This value was too low for the rule-in and was justified by the low prevalence of ACS in our study.

Subgroup of Patients Assessed at T0h and T3h Without CKD

Patients with eGFR within normal limits (n = 1572) had higher AUCs for T0h and T3h compared with the nonselected sample of patients (ie, those without CKD; T0h AUC = 0.762 vs 0.712; T3h AUC = 0.810 vs 0.789), with a ROC-derived cutoff closer to the 99th percentile (T0h = 18.48 ng/L vs 29.92 ng/L; T3h = 29.47 ng/L vs 44.54 ng/L), reflecting an increase in diagnostic accuracy in the subgroup of patients without CKD. The delta AUC was instead in line with that of the nonselected population, and there was only a small improvement (1%–2%) in specificity and predictive values compared with the nonselected sample of patients, confirming that although basal cTn is higher in patients with CKD, serial changes are effective in diagnosing ACS even in these patients and are therefore clinically usable.[28]

Subgroup of Patients Assessed at T0h and T3h Without CKD Divided by Sex with Unique Cutoff

The distribution of the population without CKD by sex showed a greater discriminatory capacity in the group of female patients compared to male patients (higher AUCs in female patients than in male patients, as shown in **Table 3**). As for the best cutoffs determined by the ROC curves, higher values were found in female patients. This result may be unexpected considering that cTn values are generally lower in females than in males, but older age is another factor to consider: In the group of female patients (n = 632), 62% (393) were aged > 65 years, whereas in the group of male patients (n = 934), only 47% (445) were aged> 65 years. This difference may have affected the results at least in part because sex differences in cardiovascular diseases described for younger patients tend to disappear in the older adult population.[29] Moreover, the prevalence of ACS in our study was higher in male

patients (6.6%) than in female patients (3.2%), although it was related to a few patients with AMI in absolute numbers. Although both of prevalences are underestimates of the prevalence of AMI in populations who generally present in the ED with chest pain (10%–20%),[22] even this lower prevalence in female patients may have influenced the different pattern of the ROC curves. Regarding the values calculated for the 0/3h algorithm with unique cutoffs (14 ng/L; delta 30%), sensitivity and NPV were higher in female patients and specificity and PPV were higher in male patients, compared with the sex-undifferentiated group, but these differences were small and could be purely coincidental, related to age distribution and sample size.

Subgroup of Patients Assessed at T0h and T3h Without CKD Divided by Sex with Differentiated Cutoffs

The application of sex-differentiated cutoffs did not change the diagnostic accuracy of the test because the ROC curves were clearly derived from the same populations divided by sex. In terms of reclassification, the application of sex-specific cutoffs only led to a minimal difference: for female patients, by lowering the cutoff from 14 ng/L to 9 ng/L, we would have had 1 more diagnosed patient as the true positives increased from 12 to 13, whereas there would have been an increase of 14 units in false positives; for male patients, by raising the cutoff from 14 ng/L to 16 ng/L, the number of patients diagnosed would have been the same.

Therefore, according to the American Association of Clinical Chemistry and the IFCC Recommendations on the Clinical Application of Cardiac Bio-Markers,[30] our data do not show the clinical utility of sex-differentiated cutoffs because they would not have affected patient management, apart from the 1 additional true positive among the female patients.

Population with a Single Sampling: Patients Assessed at T0h Only (n = 2436)

Concerning the diagnostic performance single hs-cTnT value for the straight rule-in at presentation (T0h) with the cutoff of 50 ng/L, in the 2436 patients who were assessed only at the first point of the hs-cTnT curve, a poor positive predictivity resulted (PPV = 20%). Assay predictivity is linked to the clinical context of suspected ACS, and in the retrospectively selected population a number of patients with low pretest probability were likely to be included because of prescriptive inappropriateness. However, the ROC curve of this group of patients had a good AUC (0.812), confirming the discriminatory capacity of the test.

Limitations

The retrospective design of this study allowed us to assess the actual use of the biomarker and its accuracy in a situation of clinical practice, different from the trial setting, which also included the eventual inappropriate use. In fact, although the inclusion criterion was the request for serial determination of hs-cTnT that has a specific reason, ie, suspected ACS, the prevalence data showed that the hs-cTnT curve was probably requested even in situations with low pretest probability, such as in patients with atypical pain or as an exclusion marker, and therefore because of poor prescriptive appropriateness. The application of a biomarker in a pretest probability condition that differs from the one for which it has been validated could change the diagnostic performance in terms of positive predictivity. In fact, the inappropriate use led to a false reduction in the prevalence of AMI in our study and consequently an unexpectedly lower number of true positives, with an unexpected reduction in PPV.

These findings are in agreement with a recent study that showed, on the basis of 2 clinical scenarios examined in different countries (the United States and the United Kingdom), that the prevalence of the disease significantly affects the PPV of hs-cTn for the diagnosis of AMI.[31]

Moreover, in the various groups examined in this study, there were a good number of false positives, which affected the PPV and, unfortunately, also a number of false negatives, which reduced the NPV. The false positives and negatives could have been derived, as in most retrospective studies, from the lack of standardization in the formulation of the final diagnoses, retrieved from the HDC, and from the lack of standardization in the time of pain onset among the patients included. It was not possible to verify these data, so there could have been some patients who although they had a final diagnosis of ACS were in the plateau phase of the biomarker increment curve at the time of the sampling. Nevertheless, high NPVs were obtained, in accordance with the literature, which guarantee the safety of ruling out patients who do not have ACS.

Conclusion

This study provides a simple methodology by which each organization can evaluate the performance of their decision limits. Our findings show that the application of sex-specific cutoffs does not seem to improve accuracy and confirm that the thresholds adopted by the UHS have the best possible accuracy regarding the hs-cTnT algorithm for the diagnosis of AMI. **LM**

References

1. Apple FS, Collinson PO; IFCC Task Force on Clinical Applications of Cardiac Biomarkers. Analytical characteristics of high-sensitivity cardiac troponin assays. *Clin Chem*. 2012;58:54–61.
2. Januzzi JL Jr, Filippatos G, Nieminen M, Gheorghiade M. Troponin elevation in patients with heart failure: on behalf of the third Universal Definition of Myocardial Infarction Global Task Force: heart failure section. *Eur Heart J.* 2012;33(18):2265–2271.
3. Twerenbold R, Boeddinghaus J, Nestelberger T, et al. How to best use high-sensitivity cardiac troponin in patients with suspected myocardial infarction. *Clin Biochem.* 2018;53:143–155.
4. Thygesen K, Alpert JS, Jaffe AS, et al. Fourth Universal Definition of Myocardial Infarction (2018). *J Am Coll Cardiol.* 2018;72(18):2231–2264.
5. Mueller T, Egger M, Peer E, Jani E, Dieplinger B. Evaluation of sex-specific cut-off values of high-sensitivity cardiac troponin I and T assays in an emergency department setting—results from the Linz Troponin (LITROP) study. *Clin Chim Acta.* 2018;487:66–74.
6. Thygesen K, Alpert JS, Jaffe AS, et al. Third Universal Definition of Myocardial Infarction. *J Am Coll Cardiol.* 2012;60(16):1581–1598.
7. Ramos HR, López LE, Castro WQ, Serra CM. High-sensitivity cardiac troponins: sex-specific values in clinical practice. Precision or confusion? *Hellenic J Cardiol.* 2019;60(3):171–177.
8. Olivieri F, Galeazzi R, Giavarina D, et al. Aged-related increase of high sensitive troponin T and its implication in acute myocardial infarction diagnosis of elderly patients. *Mech Ageing Dev*. 2012;133:300–305.
9. Thygesen K, Mair J, Giannitsis E, et al.; on behalf of the Study Group on Biomarkers in Cardiology of ESC Working Group on Acute Cardiac Care. How to use high-sensitivity cardiac troponins in acute cardiac care. *Eur Heart J*. 2012;33:2252–2257.
10. Roffi M, Patrono C, Collet JP, et al. 2015 ESC Guidelines for the management of acute coronary syndromes in patients presenting without persistent ST-segment elevation: Task Force for the Management of Acute Coronary Syndromes in Patients Presenting without Persistent ST-Segment Elevation of the European Society of Cardiology (ESC). *Eur Heart J.* 2016;37(3):267–315.
11. Korley FK, Jaffe AS. Preparing the United States for high-sensitivity cardiac troponin assays. *J Am Coll Cardiol.* 2013;61(17):1753–1758.
12. Apple FS, Jaffe AS, Collinson P, et al.; International Federation of Clinical Chemistry (IFCC) Task Force on Clinical Applications of Cardiac Bio-Markers. IFCC educational materials on selected analytical and clinical applications of high sensitivity cardiac troponin assays. *Clin Biochem.* 2015;48(4–5):201–203.
13. Rubini Gimenez M, Badertscher P, Twerenbold R, et al. Impact of the US Food and Drug Administration-approved sex-specific cutoff values for high-sensitivity cardiac troponin T to diagnose myocardial infarction. *Circulation*. 2018;137:1867–1869.
14. Mueller-Hennessen M, Mueller C, Giannitsis E, et al. Serial sampling of high sensitivity cardiac troponin T may not be required for prediction of acute myocardial infarction diagnosis in chest pain patients with highly abnormal concentrations at presentation. *Clin Chem*. 2017;63:542–551.
15. Body R. Acute coronary syndromes diagnosis, version 2.0: tomorrow's approach to diagnosing acute coronary syndromes? *Turk J Emerg Med.* 2018;18(3):94–99.
16. Levey AS, Stevens LA. Estimating GFR using the CKD Epidemiology Collaboration (CKD-EPI) creatinine equation: more accurate GFR estimates, lower CKD prevalence estimates, and better risk predictions. *Am J Kidney Dis.* 2010;55(4):622–627.
17. Giannitsis E, Kurz K, Hallermayer K, et al. Analytical validation of a high-sensitivity cardiac troponin T assay. *Clin Chem*. 2010;56:254–261.
18. Levin A, Stevens PE, Bilous RW, et al.; Kidney Disease: Improving Global Outcomes (KDIGO) CKD Work Group. KDIGO 2012 clinical practice guideline for the evaluation and management of chronic kidney disease. *Kidney Int Suppl*. 2013;3(1):1–150.
19. Parikh RH, Seliger SL, deFilippi CR. Use and interpretation of high sensitivity cardiac troponins in patients with chronic kidney disease with and without acute myocardial infarction. *Clin Biochem.* 2015;48(4–5):247–253.
20. High-sensitivity cardiac troponin I and T assay analytical characteristics designated by manufacturer. International Federation for Clinical Chemistry Committee on Clinical Applications of Cardiac BioMarkers. https://www.ifcc.org/media/478231/high-sensitivity-cardiac-troponin-i-and-t-assay-analytical-characteristics-designated-by-manufacturer-v122019.pdf. Accessed December 29, 2020.
21. Forni S. Il programma di osservazione degli esiti—ARS Toscana [Programme for the Observation of Outcomes - Tuscan Regional Health Agency (ARS)]. https://www.ars.toscana.it/files/eventi/eventi_2017/PNE/Forni.pdf. Accessed December 29, 2020.
22. Kohn MA, Kwan E, Gupta M, Tabas JA. Prevalence of acute myocardial infarction and other serious diagnoses in patients presenting to an urban emergency department with chest pain. *J Emerg Med.* 2005;29(4):383–390.
23. Giannitsis E, Katus HA. Cardiac troponin level elevations not related to acute coronary syndromes. *Nat Rev Cardiol.* 2013;10(11):623–634.
24. Guangquan L, Hualan H, Xin N, et al. Time from symptom onset influences high-sensitivity troponin T diagnostic accuracy for the diagnosis of acute myocardial infarction. *Clin Chem Lab Med* 2015;54:133–142.
25. Peacock WF, Baumann BM, Bruton D, et al. Efficacy of high-sensitivity troponin T in identifying very-low-risk patients with possible acute coronary syndrome. *JAMA Cardiol.* 2018;3(2):104–111.
26. Alpert JS, Thygesen K, Antman E, Bassand JP. Myocardial infarction redefined—a consensus document of the Joint European Society of Cardiology/American College of Cardiology Committee for the redefinition of myocardial infarction. *J Am Coll Cardiol.* 2000;36(3):959–969.
27. Brush JE Jr, Kaul S, Krumholz HM. Troponin testing for clinicians. *J Am Coll Cardiol.* 2016;68(21):2365–2375.
28. Stacy SR, Suarez-Cuervo C, Berger Z, et al. Role of troponin in patients with chronic kidney disease and suspected acute coronary syndrome: a systematic review. *Ann Intern Med.* 2014;161(7):502–512.
29. Haider A, Bengs S, Luu J, et al. Sex and gender in cardiovascular medicine: presentation and outcomes of acute coronary syndrome. *Eur Heart J.* 2020;41(13):1328–1336.
30. Wu AHB, Christenson RH, Greene DN, et al. Clinical laboratory practice recommendations for the use of cardiac troponin in acute coronary syndrome: expert opinion from the Academy of the American Association for Clinical Chemistry and the Task Force on Clinical Applications of Cardiac Bio-Markers of the International Federation of Clinical Chemistry and Laboratory Medicine. *Clin Chem.* 2018;64(4):645–655.
31. Shah ASV, Sandoval Y, Noaman A, et al. Patient selection for high sensitivity cardiac troponin testing and diagnosis of myocardial infarction: prospective cohort study. *BMJ.* 2017;359:j4788.

Direct Amplification of Whole Blood and Amniotic Fluid Specimens for Prenatal and Postnatal Diagnosis of Hb E-β^0-Thalassemia Diseases

Phongsathorn Wichian, MSc,[1,2] *Supawadee Yamsri, PhD,*[2,*] *Kanokwan Sanchaisuriya, PhD,*[2] *Supan Fucharoen, DSc*[2]

Laboratory Medicine 2021;52:460-468

DOI: 10.1093/labmed/lmaa117

ABSTRACT

Objective: Prenatal and postnatal diagnosis of hemoglobin E-β^0-thalassemia can be made using polymerase chain reaction (PCR) analysis mostly on purified DNA. We have establihed a direct amplification method without DNA extraction on whole blood (WB) and amniotic fluid (AF) specimens to diagnose the disease.

Methods: Three reactions of WB PCR assays and 7 reactions of AF PCR tests were developed for postnatal and prenatal diagnosis, respectively. Assays were validated against routine tests in a blinded trial.

Results: The results showed 100% concordance with routine DNA PCR assays. Among 309 β-thalassemia carriers, 191 patients (61.8%) carried common β-thalassemia mutations. Among 448 AF specimens, 116 (25.9%) fetuses were found to be affected, 247 (55.1%) fetuses were carriers, and 85 (19%) fetuses were unaffected.

Conclusion: We found that WB and AF PCR assays are simple, rapid, and reliable. The developed techniques could be applicable in routine settings.

Keywords: direct amplification, whole blood, amniotic fluid, carrier identification, prenatal diagnosis, Hb E-β^0-thalassemia

Hemoglobin (Hb) E-β^0-thalassemia disease is one of the most common severe thalassemia diseases found in Thailand. The patients with this disease exhibit varied clinical expression from mild thalassemia intermedia to severe transfusion-dependent thalassemia. However, most patients need a blood transfusion to survive.[1-3] Hb E-β^0-thalassemia disease is one of the targeted diseases in the prevention and control program for thalassemia in Thailand.

Abbreviations:

HGVS, The Human Genome Variation Society; PCR, polymerase chain reaction; WB, whole blood; AF, amniotic fluid; Hb, hemoglobin; TSU, Thalassemia Service Unit; dNTP, deoxynucleotide triphosphate; $MgCl_2$, magnesium chloride; UV, ultraviolet; bp, base pair.

[1]Medical Science Program, Graduate School, Khon Kaen University, Khon Kaen, Thailand, [2]Centre for Research and Development of Medical Diagnostic Laboratories, Faculty of Associated Medical Sciences, Khon Kaen University, Khon Kaen, Thailand

*To whom correspondence should be addressed.
supawadee@kku.ac.th

One objective of this program is to reduce the number of patients newly diagnosed with severe thalassemia disease. The strategies of the program for preventing Hb E-β^0-thalassemia disease include carrier identification and prenatal diagnosis for identifying affected fetuses.[4]

Identification of β-thalassemia mutations is necessary for genetic counseling and prenatal diagnosis. Parents who have an affected child are counseled to either continue or terminate the pregnancy. In Thailand, the termination of pregnancy is legally accepted when gestational age less than 28 weeks. Therefore, rapid and accurate molecular techniques for mutation analysis play an essential role in the success of the prevention and control program.[5-7]

β-thalassemia is caused by an absence of (β^0) or reduced (β^+) production of the β-globin chain. Although more than 30 β-thalassemia mutations have been reported in Thailand, 7 mutations are commonly found in the region

including NT-28 (A-G), CD 41/42 (-TTCT), CD 17 (A-T), CD 71/72 (+A), IVSI#1 (G-T), IVSI#5 (G-C), and IVSII#654 (C-T).[7-9] Identification of the β-thalassemia mutation is crucial for the prediction of clinical outcomes and for prenatal diagnosis. For prenatal diagnosis, fetal specimens, including amniotic fluid (AF), chorionic villus sampling, and cord blood, are used in DNA analysis. Based on our data from the Thalassemia Service Unit (TSU) in the Centre for Research and Development of Medical Diagnostic Laboratories of the Faculty of Associated Medical Sciences at Khon Kaen University, Khon Kaen, Thailand, the most frequent fetal specimen received is an AF specimen.

Rapid detection and double-check methods for identification of β-thalassemia mutations in whole blood (WB) and AF specimens would be favorable. Hence, we have established rapid WB polymerase chain reaction (PCR) testing for carrier identification of β-thalassemia mutation and AF PCR testing for the prenatal diagnosis of severe thalassemia diseases in Thailand without DNA extraction.

Methods

Study Design and Patients

Our initial developments of direct PCR assays were done on WB and AF specimens. First, known WB specimens of the 7 common β-thalassemia mutations in Thailand were selectively recruited from the TSU. The β-thalassemia mutations included the β^0-thalassemia mutations; CD 41/42 (-TTCT), CD 17 (A-T), CD 71/72 (+A), IVSI#1 (G-T), IVSI#5 (G-C), and IVSII#654 (C-T) and the β^+-thalassemia mutations; NT-28 (A-G). Similarly, AF specimens with known thalassemia genotypes were selectively recruited from at-risk couples for Hb E-β^0-thalassemia disease, including 6 common β^0-thalassemia mutations, as mentioned earlier. Validation was assessed on leftover WB specimens of β-thalassemia carriers and AF specimens from at-risk couples for Hb E-β^0-thalassemia disease recruited from the TSU in a blinded trial from January 2018 to May 2020. The results were compared with the standard PCR method using purified DNA specimens in our routine setting. Ethical approval of the study protocol was obtained from the Institutional Review Board of Khon Kaen University (HE612063).

Carrier Identification of 7 Common β-Thalassemia Mutations Using WB PCR

We successfully developed 3 reactions of multiplex WB PCR for the identification of 7 common β-thalassemia mutations according to the frequency of each mutation. β-thalassemia mutations in each PCR reaction included reaction A: CD 41/42 (-TTCT), CD 17 (A-T), and NT-28 (A-G); reaction B: CD 71/72 (+A) and IVSI#5 (G-C); and reaction C: IVSI#1 (G-T) and IVSII#654 (C-T). The locations, orientations of primers, and representative agarose gel electrophoresis of each WB PCR reaction mixture are shown in **Figure 1**. The sequence of primers, the primer concentration, and the PCR cycling condition of each WB PCR reaction mixture are shown in **Table 1**.

Multiplex WB PCR was carried out in a total volume of 50 μL. The PCR mixture contained a high-pH PCR buffer,[10] 8 mM deoxynucleotide triphosphate (dNTP), 3 mM magnesium chloride ($MgCl_2$), 1.005 M betaine, 2% dimethyl sulfoxide, each primer as shown in **Table 1**, 2 units of *Taq* DNA polymerase (Biotools, B&M Labs, Madrid, Spain), and 3 μL of WB mixture. The WB mixture was readily prepared by mixing 3 μL of WB specimens with 15 μL of pre-PCR reagent as previously developed[10] for 5 seconds and adding this mixture directly to the PCR reaction mixture. The WB PCR was carried out on a SimpliAmp Thermal Cycler (Applied Biosystems, Waltham, MA, USA). The PCR amplicon was analyzed on 2% agarose gel electrophoresis and visualized under ultraviolet (UV) light after staining with ethidium bromide (**Figure 1**).

Prenatal Diagnosis of Hb E-β^0-Thalassemia Disease Using AF PCR Assay

Two most common β^0-thalassemia mutations are CD 41/42 (-TTCT) and CD 17 (A-T), therefore, we developed 2 reactions of multiplex AF PCR for identifying CD 41/42 (-TTCT) and the Hb E gene and CD 17 (A-T) and the Hb E gene, respectively. For the 4 remaining β^0-thalassemia mutations, CD 71/72 (+A), IVSI#5 (G-C), IVSI#1 (G-T), and IVSII#654 along with th Hb E gene, the monoplex AF PCR assay was developed. The locations and orientations of primers and a representative agarose gel electrophoresis of each AF PCR reaction mixture are shown in **Figure 2**. The sequences of primers, the primer concentration, and the PCR cycling condition of each AF PCR reaction mixture are shown in **Table 2**.

DOI: 10.1093/labmed/lmaa117

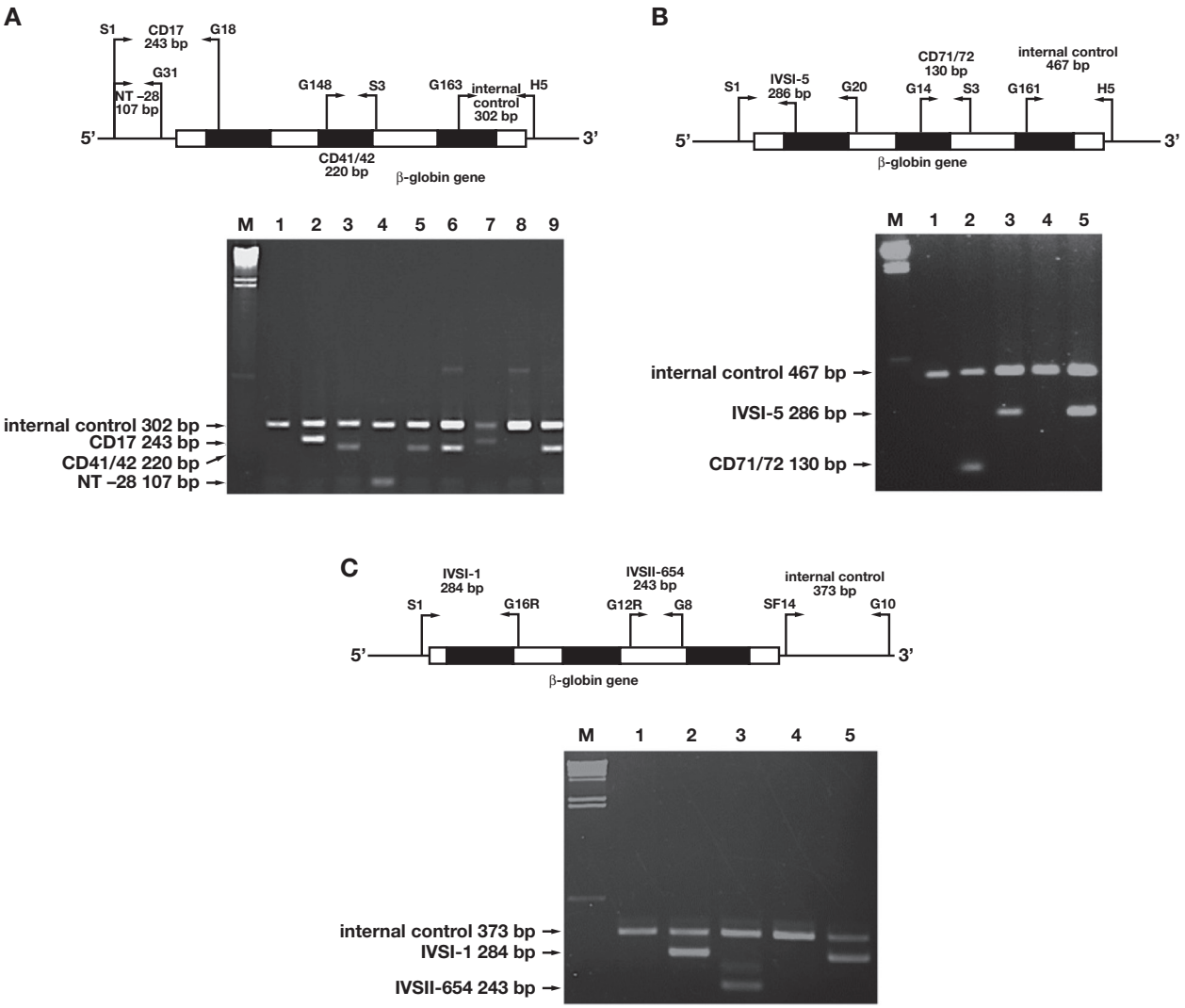

Figure 1

Whole blood PCR for identification of 7 common β-thalassemia mutations. Location and orientation of the primers and a representative 2% agarose gel electrophoresis of PCR product of whole blood PCR assay for identification of β-thalassemia mutations including CD 41/42 (–TTCT), CD 17 (A-T), and NT-28 (A-G) (1A), and CD 71/72 (+A) and IVSI#5 (G-C) (1B), and IVSI#1 (G-T) and IVSII#654 (C-T) (1C).

Each reaction mixture of AF PCR was carried out in a total volume of 50 μL. The PCR mixture contained a high-pH PCR buffer,[10] 8 mM dNTP, 3 mM $MgCl_2$, 1.005 M betaine, 2% dimethyl sulfoxide, 2 units *Taq* DNA polymerase (Biotools, B&M Labs, Madrid, Spain), and 3 μL of the concentrated AF specimen (or 1 μL of the WB mixture). **Table 2** shows the concentration of each primer used in the PCR reaction. The concentrated AF specimen was easily prepared by centrifuged 1.5 mL of AF specimens at 8000 rpm for 10 minutes; we then removed 1450 μL of supernatant and mixed the remaining pellet. Concentrated AF specimens could be added directly to the PCR reaction mixture. The PCR cycling conditions of each reaction mixture are shown in **Table 2**. We conducted the AF PCR assay on a SimpliAmp Thermal Cycler (Applied Biosystems, Waltham, MA, USA). The PCR amplicon was analyzed on 2% agarose gel electrophoresis and visualized under UV light after staining with ethidium bromide (**Figure 2**).

Table 1. Sequences of Oligonucleotide Primers Used in WB PCR Assays for Screening of 7 Common β-Thalassemia Mutations

WB PCR Reactions	Mutations (HGVS names)	Primers (5'→3')	Primer Concentration (μM)	PCR Cycling Conditions
A	NT-28 (A-G)	S1; TGTCATCACTTAGACCTCAC	1.5	1 × 95°C/15 min
	[HBB:c.-78A>G]	S3; TCCCATAGACTCACCCTGAA	0.9	36 × (95°C 1 min/58°C
	CD 17 (A-T)	G18; ACTTCATCCACGTTCACCTA	0.42	1 min/72°C 90 sec)
	[HBB:c.52A>T]	G31; GATGGCTCTCTGCCCTGACTTC	0.3	1 × 72°C 10 min
	CD 41/42 (-TTCT)	G148; CCCTTGGACCCAGAGGTTG	1.5	1 × 10°C hold
	[HBB:c.126_129delCTTT]	G163; CCCTGGCCCACAAGTACTAC	0.18	
		H5; GCAGCCTCACCTTCTTTCATGG	0.18	
B	CD 71/72 (+A)	S1; TGTCATCACTTAGACCTCAC	2.1	1 × 95°C/15 min
	[HBB:c.216_217insA]	S3; TCCCATAGACTCACCCTGAA	0.6	36 × (95°C 1 min/60°C
	IVSI#5 (G-C)	G14; AAAGTGCTCGGTGCCTTTAA	0.6	1 min/72°C 90 sec)
	[HBB:c.92 + 5G>C]	G20; CTGTCTTGTAACCTTGATAG	2.1	1 × 72°C 10 min
		G161; TGAGTCCAAGCTAGGCCCTT	0.6	1 × 10°C hold
		H5; GCAGCCTCACCTTCTTTCATGG	0.6	
C	IVSI#1 (G-T)	S1; TGTCATCACTTAGACCTCAC	0.3	1 × 95°C/15 min
	[HBB:c.92 + 1G>T]	G8; CGAACCTGAGTCTTATTAG	2.1	36 × (95°C 1 min/53°C
	IVSII#654 (C-T)	G10; AGACTAGCACTGCAGATTCC	0.9	1 min/72°C 90 sec)
	[HBB:c.316-197C>T]	G12R; GTAATAATTTCTGGGTTAACGT	2.1	1 × 72°C 10 min
		G16R; CTTGTAACCTTGATACCAAA	0.3	1 × 10°C hold
		SF14; TCCCTCAGAAAAGGATTCAA	0.9	

PCR, polymerase chain reaction; WB, whole blood.

Results

Carrier Screening of 7 Common β-Thalassemia Mutations Using WB PCR

Figure 1, **Image A** shows a representative agarose gel electrophoresis of WB PCR (reaction A). The specific fragments of β^0-thal CD 41/42 (-TTCT), β^0-thal CD 17 (A-T), and β^+-thal NT-28 (A-G) were 220, 243, and 107 base pairs (bps) in length, respectively, and the internal control fragment was 302 bp. **Figure 1**, **Image B** shows a representative agarose gel electrophoresis of WB PCR (reaction B). The specific fragments of β^0-thal CD 71/72 (+A) and β^0-thal IVSI#5 (G-C) were 130 and 286 bps, respectively. **Figure 1**, **Image C** shows a representative agarose gel electrophoresis of WB PCR (reaction C). The specific fragments of β^0-thal IVSI#1 (G-T) and β^0-thal IVSII#654 (C-T) were 284 and 243 bps, respectively. The internal control fragments of reaction B and reaction C were 467 and 373 bps, respectively.

The WB PCR assays had been validated in a blinded trial on 309 β-thalassemia carriers. As shown in **Table 3**, 7 common β-thalassemia mutations were identified in 191 patients (61.8%), including β^0-thal CD 41/42(-TTCT) (n = 57; 18.4%), β^+-thal NT-28 (A-G) (n = 47; 15.2%), β^0-thal CD 17 (A-T) (n = 45; 14.6%), β^0-thal IVSI-1 (n = 14; 4.5%), β^0-thal IVSI-5 (G-C) (n = 12; 3.9%), β^0-thal CD 71/72 (+A) (n = 11; 3.6%), and β^0-thal IVSII-654 (C-T) (n = 5; 1.6%). This showed results that were 100% concordant with routine PCR analysis on purified DNA specimens.

Prenatal Diagnosis of Hb E-β^0-Thalassemia Disease Using AF PCR Assay

Figure 2 shows a representative agarose gel electrophoresis of each AF PCR reaction mixture. **Figure 2**, **Image A** shows multiplex AF PCR reactions for identifying β^0-thal CD 41/42 (-TTCT) and the Hb E gene. The 220 bp fragment was specific for β^0-thal CD 41/42 (-TTCT), and the 400 bp fragment was specific for the Hb E gene. The 302 bp fragment was an internal control fragment. Multiplex AF PCR reactions for identifying β^0-thal CD 17 (A-T) and the Hb E gene are shown in **Figure 2**, **Image B**. The specific fragments of β^0-thal CD 17 (A-T) and the Hb E gene and the internal control fragment were 243, 176, and 373 bp fragments, respectively. **Figure 2**, **Images C through G** show a representative agarose gel electrophoresis of the AF PCR reaction for Hb E-β^0-thalassemia mutations Hb E, CD 71/72 (+A), IVSI#5 (G-C), IVSI#1 (G-T), and IVSII#654, respectively. The specific fragments of Hb E and β^0-thalassemia mutations; CD 71/72 (+A), IVSI#5 (G-C), IVSI#1 (G-T), and IVSII#654 were 400, 130, 286, 284,

DOI: 10.1093/labmed/lmaa117

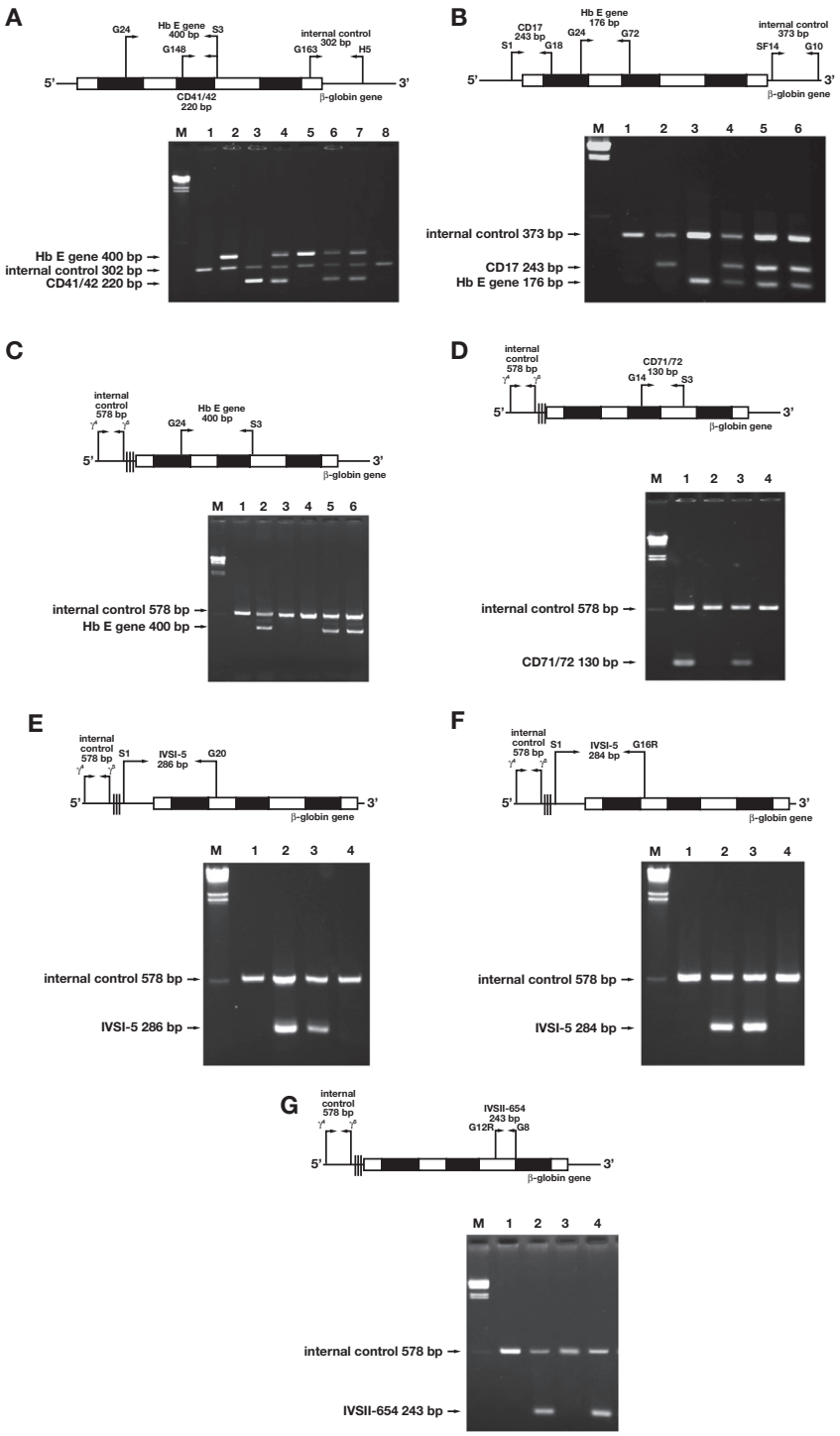

Figure 2

Amniotic fluid PCR for prenatal diagnosis of Hb E-β^0-thalassemia diseases. Location and orientation of the primers and a representative 2% agarose gel electrophoresis of PCR product of 7 sets of amniotic fluid PCR assays. **2A**: Multiplex amniotic fluid PCR for detection of CD 41/42 (– TTCT) & Hb E gene, **2B**: Multiplex amniotic fluid PCR for detection of CD 17 (A-T) & Hb E gene, **2C-2G**: Monoplex amniotic fluid PCR for detection of Hb E gene, CD 71/72 (+A), IVSI#5 (G-C), IVSI#1 (G-T), and IVSII#654, respectively.

Table 2. Sequences of Oligonucleotide Primers Used in AF PCR Assays for Prenatal Diagnosis of Common β^0-Thalassemia/Hb E Diseases

AF PCR Reactions	Mutations (HGVS names)	Primers (5'→3')	Primer Concentration (μM)	PCR Cycling Conditions
A	CD 41/42 (-TTCT)	S3; TCCCATAGACTCACCCTGAA	0.3	1 × 95°C/15 min
	[HBB:c.126_129delCTTT]	G24; CGTGGATGAAGTTGGTGGTA;	0.15	36 × (95°C 1 min/62°C
	Hb E	G148; CCCTTGGACCCAGAGGTTG	1.8	1 min/72°C 90 sec)
	[HBB:c.79G>A]	G163; CCCTGGCCCACAAGTACTAC	0.03	1 × 72°C 10 min
		H5; GCAGCCTCACCTTCTTTCATGG	0.03	1 × 10°C hold
B	CD 17 (A-T)	S1; TGTCATCACTTAGACCTCAC	2.1	1 × 95°C/15 min
	[HBB:c.52A>T]	G10; AGACTAGCACTGCAGATTCC	0.18	36 × (95°C 1 min/61°C
	Hb E	G18; ACTTCATCCACGTTCACCTA	2.1	1 min/72°C 90 sec)
	[HBB:c.79G>A]	G24; CGTGGATGAAGTTGGTGGTA	1.5	1 × 72°C 10 min
		G72; GACCACCAGCAGCCTAAGGG	1.5	1 × 10°C hold
		SF14; TCCCTCAGAAAAGGATTCAA	0.18	
C	Hb E	S3; TCCCATAGACTCACCCTGAA	0.96	1 × 95°C/15 min
	[HBB:c.79G>A]	G24; CGTGGATGAAGTTGGTGGTA	0.96	36 × (95°C 1 min/63°C
		γ4; GGCCTAAAACCACAGAGT	0.3	1 min/72°C 90 sec)
		γ5; CCAGAAGCGAGTGTGTGGAA	0.3	1 × 72°C 10 min
				1 × 10°C hold
D	CD 71/72 (+A)	S3; TCCCATAGACTCACCCTGAA	1.8	1 × 95°C/15 min
	[HBB:c.216_217insA]	G14; AAAGTGCTCGGTGCCTTTAA	1.8	36 × (95°C 1 min/63°C
		γ4; GGCCTAAAACCACAGAGT	0.24	1 min/72°C 90 sec)
		γ5; CCAGAAGCGAGTGTGTGGAA	0.24	1 × 72°C 10 min
				1 × 10°C hold
E	IVSI#5 (G-C)	S1; TGTCATCACTTAGACCTCAC	1.8	1 × 95°C/15 min
	[HBB:c.92 + 5G>C]	G20; CTGTCTTGTAACCTTGATAG	1.8	36 × (95°C 1 min/61°C
		γ4; GGCCTAAAACCACAGAGT	0.12	1 min/72°C 90 sec)
		γ5; CCAGAAGCGAGTGTGTGGAA	0.12	1 × 72°C 10 min
				1 × 10°C hold
F	IVSI#1 (G-T)	S1; TGTCATCACTTAGACCTCAC	1.5	1 × 95°C/15 min
	[HBB:c.92 + 1G>T]	G16R; CTTGTAACCTTGATACCAAA	1.5	36 × (95°C 1 min/60°C
		γ4; GGCCTAAAACCACAGAGT	0.12	1 min/72°C 90 sec)
		γ5; CCAGAAGCGAGTGTGTGGAA	0.12	1 × 72°C 10 min
				1 × 10°C hold
G	IVSII#654 (C-T)	G8; CGAACCTGAGTCTTATTAG	0.6	1 × 95°C/15 min
	[HBB:c.316-197C>T]	G12R; GTAATAATTTCTGGGTTAACGT	0.6	36 × (95°C 1 min/55°C
		γ4; GGCCTAAAACCACAGAGT	0.06	1 min/72°C 90 sec)
		γ5; CCAGAAGCGAGTGTGTGGAA	0.06	1 × 72°C 10 min
				1 × 10°C hold

AF, amniotic fluid; Hb, hemoglobin; PCR, polymerase chain reaction.

and 243 bp fragments, respectively. A 578 bp fragment was an internal control fragment for all PCR reactions.

Validation of the AF PCR assays was done on a total of 448 AF specimens. As expected, the 2 majority mutations of Hb E-β^0-thalassemia disease in our region were β^0-thal CD 41/42 (-TTCT) and CD 17 (A-T), respectively. Among prenatal diagnoses of 448 AF specimens, 116 (25.9%) patients were found to be affected, 247 (55.1%) patients were carriers, and 85 (19.0%) patients were unaffected. A result that was100% concordant with the routine PCR methods on purified DNA specimens was observed, as shown in **Table 4** and **Figure 3**.

Discussion

Hb E-β^0-thalassemia disease is one of the severe thalassemia diseases targeted in a prevention and control program for thalassemia in Thailand.[4] The clinical features of this disease vary from moderate to severe anemia requiring blood transfusion to survive. The prevalence of Hb E- and β-thalassemias are 41.7% and 0.9% in the northeastern Thai population, respectively.[11] Therefore, Hb E-β^0-thalassemia diseases are the most common high-risk diseases in the region.[7] Identification

DOI: 10.1093/labmed/lmaa117

Table 3. Frequency of 7 Common β-Thalassemia Mutations Found Among 309 β-Thalassemia Heterozygotes

β-Thalassemia Mutations		Type	n	%
Mutation	**HGVS Name**			
CD 41/42 (-TTCT)	HBB:c.126_129delCTTT	β^0	57	18.4
NT-28 (A-G)	HBB:c.-78A>G	β^+	47	15.2
CD 17 (A-T)	HBB:c.52A>T	β^0	45	14.6
IVSI#1 (G-T)	HBB:c.92 + 1G>T	β^0	14	4.5
IVSI#5 (G-C)	HBB:c.92 + 5G>C	β^0	12	3.9
CD 71/72 (+A)	HBB:c.216_217insA	β^0	11	3.6
IVSII#654 (C-T)	HBB:c.316-197C>T	β^0	5	1.6
Negative for 6 β-thalassemia mutations		~	118	38.2
Total			309	100

Table 4. Results of a Prenatal Diagnosis for β^0-Thalassemia/Hb E Diseases Using Amniotic Fluid PCR and Routine DNA PCR Assays

Fetal Risks	Number of Patients (%)	Fetal Diagnosis (AF PCR/Routine PCR)		
		Affected	**Carrier**	**Normal**
Hb E/ β^0-thalassemia (CD 41/42)	190 (42.4)	48/48	104/104	38/38
Hb E/ β^0-thalassemia (CD 17)	156 (34.8)	35/35	88/88	33/33
Hb E/ β^0-thalassemia (IVSI#5)	33 (7.4)	9/9	18/18	6/6
Hb E/ β^0-thalassemia (IVSI#1)	26 (5.8)	10/10	12/12	4/4
Hb E/ β^0-thalassemia (CD 71/72)	24 (5.4)	8/8	15/15	1/1
Hb E/ β^0-thalassemia (IVSII#654)	19 (4.2)	6/6	10/10	3/3
Total (448)	448 (100)	116/116	247/247	85/85

AF, amniotic fluid; Hb, hemoglobin; PCR, polymerase chain reaction.

of β-thalassemia mutations is essential for the prevention and control of the disease. Many studies have shown the heterogeneity of β-thalassemia in Thailand.[7,8,12,13] However, 7 mutations—CD 41/42 (-TTCT), NT-28 (A-G), CD 17 (A-T), CD 71/72 (+A), IVSI#1 (G-T), IVSI#5 (G-C), and IVSII#654 (C-T)—are the most common.[7,8] Although β-thalassemia carriers can be confirmed by Hb analysis, identifying β-thalassemia mutations to define the type of mutation (β^0 or β^+) is very important for prenatal diagnosis. Usually, prenatal diagnosis is performed only parents at risk of β^0-thalassemia but not β^+-thalassemia. The β-thalassemia mutations can be identified using many PCR-based techniques as described elsewhere[13-16] that rely on purified DNA specimens. These identification techniques can be laborious in large-scale screening.

Prenatal diagnosis is one of the most critical steps for the prevention and control of severe thalassemia diseases. Fetal specimens, including chorionic villus sampling, AF, and fetal blood, are obtained from at-risk pregnant women according to gestational age. The fetal DNA is prepared from these specimens and subjected to DNA analysis using PCR analysis.[7-9] Although PCR analysis is sensitive and accurate, based on our experience, misdiagnosis was observed because of allele dropout and contamination with PCR inhibitors.[17] Therefore, a double-check method for prenatal diagnosis should be performed.

Furthermore, we also found that some pregnant women begin antenatal care very late. In this case, rapid identification of β-thalassemia mutations and prenatal diagnosis are crucial.

The manual DNA extraction methods commonly used in most molecular laboratories include the phenol-chloroform method and the salting-out method. The yield of DNA obtained from these methods is relatively high. However, these manual methods require the specimen to be transferred to multiple tubes, which is laborious and

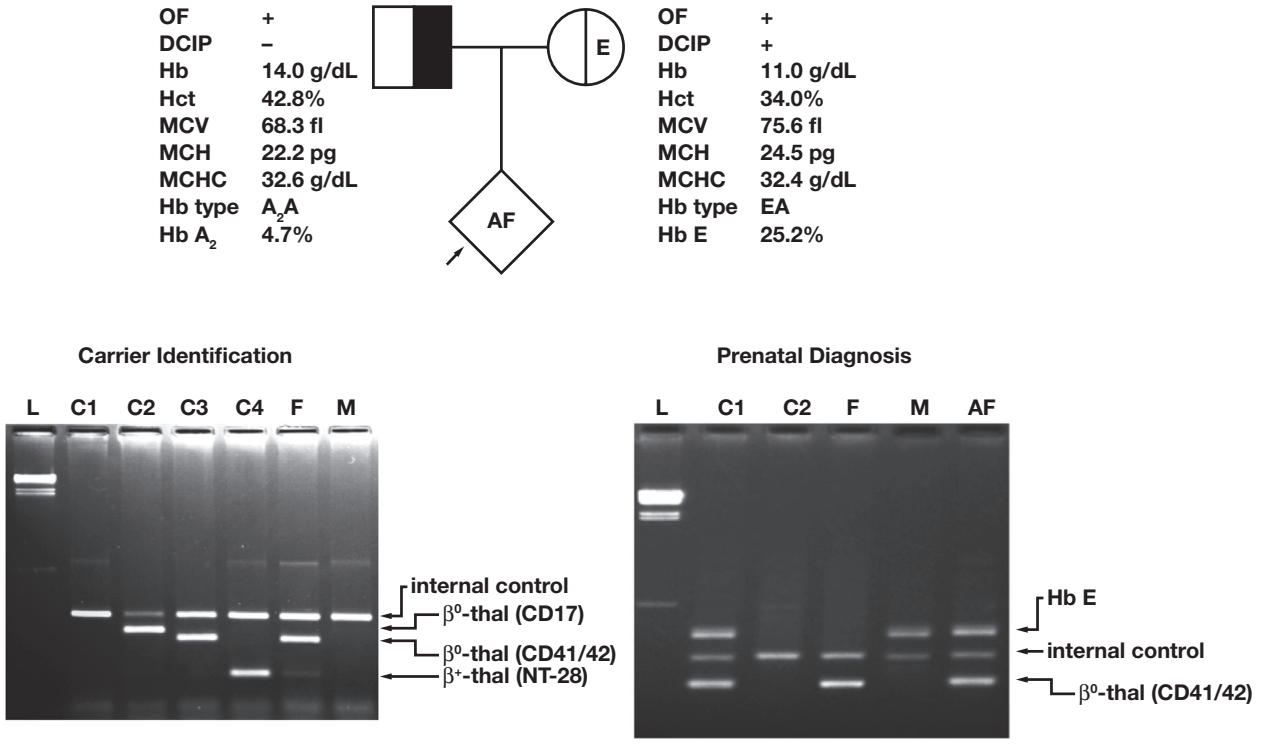

Figure 3

Identification of β-thalassemia mutations and prenatal diagnosis of Hb E-β^0-thalassemia disease in a representative family. Pedigree and hematological profiles of the parent are shown. The father was β-thalassemia carrier whereas the mother was Hb E carrier. The arrow indicate the fetus whose amniotic fluid specimen was obtained at 20 weeks of gestation. Whole blood PCR assays identified that father (F) carries β^0-thalassemia mutations (CD 41/42; – TTCT). The prenatal diagnosis was done using multiplex amniotic fluid PCR for detection of CD 41/42 (– TTCT) & Hb E gene. The fetus (AF) was diagnosed as an affected fetus. The simple, rapid and accurate diagnosis was obtained for this family.

time-consuming. The traditional salting-out method requires incubating the cell lysate overnight at 37°C.[18] The phenol-chloroform method needs at least 2 hours to incubate the cell lysate and involves the use of toxic materials.[19] In addition, there are many commercial DNA extraction kits used regularly in many laboratories. Commercial DNA extraction kits are generally faster and simple to use, but the cost per specimen is higher than that of manual methods. Therefore, we developed a direct PCR method for the identification of β-thalassemia mutations and prenatal diagnosis of Hb E-β^0-thalassemia disease without DNA extraction. An WB mixture could be prepared within 2 steps (less than 1 minute), and a concentrated AF specimen could be prepared within 3 steps (less than 15 minutes). However, these developed techniques also had limitations, including that the WB mixture and the concentrated AF specimen could not be stored and used with other types of PCR-based analysis. As compared to routine methods, our techniques were simple, fast, and cost-effective and required easy steps to prepare the WB mixture and concentrated AF specimen. These techniques can be applied as a rapid second-line or double-check method to identify β-thalassemia mutations and confirm prenatal diagnosis of Hb E-β^0-thalassemia disease.

As shown in **Table 3** and **Table 4**, these newly developed techniques were applied to 309 β-thalassemia carriers and 448 fetuses for the prenatal diagnosis of Hb E-β^0-thalassemia diseases; results that were 100% concordant with the routine PCR system using purified DNA were noted. We also showed an example of applying the developed techniques to 1 family at risk for Hb E-β^0-thalassemia disease. As shown in **Figure 3**, the carrier identification using WB specimens showed that the father was a β^0-thalassemia carrier of the CD 41/42 (-TTCT) mutation. Therefore, prenatal diagnosis using an AF specimen was conducted to

DOI: 10.1093/labmed/lmaa117

identify the Hb E gene and β^0-thalassemia mutation (CD 41/42; -TTCT). The result indicated that the fetus was affected by Hb E-β^0-thalassemia disease.

Although our developed methods can be applied only to the 7 most common β-thalassemia mutations, they could be applied to other rare β-thalassemia mutations. Moreover, in combination with WB PCR for the detection of α^0-thalassemia as reported previously,[10] the prevention and control of 3 severe thalassemia diseases, including Hb Bart's hydrops fetalis syndrome, homozygous β^0-thalassemia, and Hb E-β^0-thalassemia disease, could be easily achieved. The methods would also provide a double-check system for β-thalassemia screening in most PCR laboratories.

Conclusion

The established WB and AF PCR assays should prove useful for the rapid, simple, and reliable prenatal and postnatal diagnosis of Hb E-β0-thalassemia diseases. These developed techniques can also apply to large-scale population screening and are directly relevant to most molecular laboratories in the regions where thalassemia is prevalent. **LM**

Funding Sources

This study was supported by grants from the Centre for Research and Development of Medical Diagnostic Laboratories, Faculty of Associated Medical Sciences, Khon Kaen University, Khon Kaen, Thailand.

References

1. Phanrahan P, Yamsri S, Teawtrakul N, Fucharoen G, Sanchaisuriya K, Fucharoen S. Molecular analysis of non-transfusion dependent thalassemia associated with hemoglobin E-β-thalassemia disease without α-thalassemia. *Mediterr J Hematol Infect Dis.* 2019;11(1):e2019038.
2. Yamsri S, Pakdee N, Fucharoen G, Sanchaisuriya K, Fucharoen S. Molecular understanding of non-transfusion-dependent thalassemia associated with hemoglobin E-β-thalassemia in Northeast Thailand. *Acta Haematol.* 2016;136(4):233–239.
3. Winichagoon P, Thonglairoam V, Fucharoen S, Wilairat P, Fukumaki Y, Wasi P. Severity differences in beta-thalassaemia/haemoglobin E syndromes: implication of genetic factors. *Br J Haematol.* 1993;83(4):633–639.
4. Fucharoen S, Winichagoon P. Thalassemia in SouthEast Asia: problems and strategy for prevention and control. *Southeast Asian J Trop Med Public Health.* 1992;23(4):647–655.
5. Fucharoen G, Sanchaisuriya K, Sae-ung N, Dangwibul S, Fucharoen S. A simplified screening strategy for thalassaemia and haemoglobin E in rural communities in south-east Asia. *Bull World Health Organ.* 2004;82(5):364–372.
6. Sanchaisuriya K, Fucharoen S, Fucharoen G, et al. A reliable screening protocol for thalassemia and hemoglobinopathies in pregnancy: an alternative approach to electronic blood cell counting. *Am J Clin Pathol.* 2005;123(1):113–118.
7. Yamsri S, Sanchaisuriya K, Fucharoen G, Sae-Ung N, Ratanasiri T, Fucharoen S. Prevention of severe thalassemia in northeast Thailand: 16 years of experience at a single university center. *Prenat Diagn.* 2010;30(6):540–546.
8. Yamsri S, Sanchaisuriya K, Fucharoen G, Sae-Ung N, Fucharoen S. Genotype and phenotype characterizations in a large cohort of β-thalassemia heterozygote with different forms of α-thalassemia in northeast Thailand. *Blood Cells Mol Dis.* 2011;47(2):120–124.
9. Yamsri S, Singha K, Prajantasen T, et al. A large cohort of β(+)-thalassemia in Thailand: molecular, hematological and diagnostic considerations. *Blood Cells Mol Dis.* 2015;54(2):164–169.
10. Wichian P, Yamsri S, Sanchaisuriya K, Fucharoen G, Fucharoen S. Whole blood PCR for rapid screening of α0-thalassemia. *Ann Clin Lab Sci.* 2018;48(2):231–235.
11. Tritipsombut J, Sanchaisuriya K, Phollarp P, et al. Micromapping of thalassemia and hemoglobinopathies in diferent regions of northeast Thailand and Vientiane, Laos People's Democratic Republic. *Hemoglobin.* 2012;36(1):47–56.
12. Sirichotiyakul S, Saetung R, Sanguansermsri T. Analysis of beta-thalassemia mutations in northern Thailand using an automated fluorescence DNA sequencing technique. *Hemoglobin.* 2003;27(2):89–95.
13. Nopparatana C, Panich V, Saechan V, et al. The spectrum of beta-thalassemia mutations in southern Thailand. *Southeast Asian J Trop Med Public Health.* 1995;26(Suppl 1):229–234.
14. Tritipsombut J, Phylipsen M, Viprakasit V, et al. A single-tube multiplex gap-polymerase chain reaction for the detection of eight β-globin gene cluster deletions common in Southeast Asia. *Hemoglobin.* 2012;36(6):571–580.
15. Fucharoen S, Fucharoen G, Ratanasiri T, Jetsrisuparb A, Fukumaki Y. A simple non-radioactive assay for hemoglobin E gene in prenatal diagnosis. *Clin Chim Acta.* 1994;229(1–2):197–203.
16. Islam MT, Sarkar SK, Sultana N, et al. High resolution melting curve analysis targeting the HBB gene mutational hot-spot offers a reliable screening approach for all common as well as most of the rare beta-globin gene mutations in Bangladesh. *BMC Genet.* 2018;19(1):1.
17. Wilson IG. Inhibition and facilitation of nucleic acid amplification. *Appl Environ Microbiol.* 1997;63(10):3741–3751.
18. Miller SA, Dykes DD, Polesky HF. A simple salting out procedure for extracting DNA from human nucleated cells. *Nucleic Acids Res.* 1988;16(3):1215.
19. Sambrook J, Russell DW, Russell DW. *Molecular Cloning: A Laboratory Manual*. Cold Spring Harbor, NY: Cold Spring Harbor Laboratory Press; 2001.

Pretreatment of Body Fluid Specimens Using Hyaluronidase and Ultracentrifugation

Sonia L. La'ulu, BS,[1] Devon R. Turner, BS,[2] Emily Zupan, BS,[2] Jonathan R. Genzen, MD, PhD[1,2,3,]*

Laboratory Medicine 2021;52:469-476

DOI: 10.1093/labmed/lmaa115

ABSTRACT

Objective: Viscous body fluids present challenges during clinical laboratory testing. The present study was conducted to evaluate the effectiveness of hyaluronidase (HYAL) and ultracentrifugation (UC) pretreatment for a variety of body fluids before clinical chemistry testing.

Methods: The following body fluids were evaluated: biliary/hepatic, cerebrospinal, dialysate, drain, pancreatic, pericardial, peritoneal/ascites, pleural, synovial, and vitreous. Analytes assessed included amylase, total bilirubin, cancer antigen 19-9, carcinoembryonic antigen, cholesterol, chloride, creatinine, glucose, lactate dehydrogenase, lipase, potassium, rheumatoid factor, sodium, total protein, triglycerides, urea nitrogen, and uric acid.

Results: Observed percentage differences between HYAL treated and untreated fluids were less than ±15% for all analytes investigated, with a small number showing statistical significance ($P < .05$). In addition, UC showed increased variability for limited body fluid/analyte combinations.

Conclusion: The HYAL treatment effectively reduced viscosity for body fluids. Validation of specimen pretreatment processes ensures acceptable analytical performance and the absence of unanticipated interferences.

Keywords: hyaluronidase, ultracentrifugation, viscosity, body fluids, assay interference, validation

Viscous (eg, thick) body fluid specimens are problematic for clinical laboratories because of the challenges that occur during manual pipetting and with specimen aspiration by automated instrumentation. The viscous quality of body fluids is commonly caused by hyaluronic acid (HA; also called hyaluronan), a glycosaminoglycan present in many biological fluids.[1,2] Hyaluronidase (HYAL) has been reported to be an effective treatment for viscous body fluid specimens before analysis.[3-7] By catalyzing the hydrolysis of HA, the addition of HYAL helps liquefy viscous specimens and facilitate aspiration by automated analyzers. Although the clinical laboratory use of HYAL has primarily been focused on liquefying specimens before cellular analysis,[8-13] its utility in regard to the chemical analysis of viscous body fluid specimens has also been described.[4,5,14,15]

A possible alternative approach to enable the chemical analysis of problematic viscous body fluids (eg, when HYAL is ineffective) is ultracentrifugation (UC), a well-known and effective treatment for removing lipemia in serum and plasma.[16,17] Although the lipemic interference of body fluids has previously been investigated,[4] detailed studies on the effect of preanalytical UC of body fluids could be helpful for laboratories considering such processing.

Because body fluids are typically not approved specimen types for most U.S. Food & Drug Administration (FDA)-cleared assays, laboratories must meet applicable regulatory and analytical validation requirements appropriate for testing.[4,18,19] These requirements also include validating pretreatment protocols such as the addition of HYAL or UC to rule out the possibility of assay interferences. For example, prior studies have shown that some commercial HYAL powders (of mammalian testicular origin) contain testosterone,[20] and HYAL pretreatment has previously been shown to cause elevations in lipase (LIP) and total protein (TP).[4]

Abbreviations:

AMY, amylase; CA 19-9, cancer antigen 19-9; CEA, carcinoembryonic antigen; CHOL, cholesterol; CI, chloride; CLSI, Clinical and Laboratory Standards Institute; CREAT, creatinine; FDA, U.S. Food & Drug Administration; GLUC, glucose; HA, hyaluronic acid; HYAL, hyaluronidase; ISE, ion selective electrode; K, potassium; LDH, lactate dehydrogenase; LIP, lipase; Na, sodium; RF, rheumatoid factor; SD, standard deviation; TAE, total allowable error; TBILI, total bilirubin; TP, total protein; TRIG, triglycerides; UA, uric acid; UC, ultracentrifugation; UN, urea nitrogen.

[1]ARUP Institute for Clinical and Experimental Pathology, Salt Lake City, Utah, [2]ARUP Laboratories, Salt Lake City, Utah, [3]Department of Pathology, University of Utah Health Sciences Center, Salt Lake City, Utah

*To whom correspondence should be addressed.
jonathan.genzen@path.utah.edu

The objective of the present report was to evaluate the effect of HYAL treatment and UC on an array of body fluids that a clinical laboratory may encounter. Body fluid/assay combinations were chosen based on previous validation experiments performed by our laboratory on the Roche cobas 8000 platform (Roche Diagnostics, Indianapolis, IN).[21]

Materials and Methods

Testing was performed using Roche cobas 8000 analyzers (c702, c502, e602; Roche Diagnostics, Indianapolis, IN). Residual specimens were deidentified and handled according to an institutional review board–approved protocol. Assays investigated included amylase (AMY; c502), total bilirubin (TBILI; c502), cancer antigen 19-9 (CA 19-9; e602), carcinoembryonic antigen (CEA; e602), cholesterol (CHOL; c502), chloride (Cl; cobas 8000 ion selective electrode [ISE] module), creatinine (CREAT; c502), glucose (GLUC; c502), lactate dehydrogenase (LDH; c502), LIP (c502), potassium (K; cobas 8000 ISE module), rheumatoid factor (RF; c702), sodium (Na; cobas 8000 ISE module), TP (c502), triglycerides (TRIG; c502), uric acid (UA; c502), and urea nitrogen (UN; c502).

Spiking studies were performed using bovine HYAL (catalog number H2126; Sigma Aldrich, St. Louis, MO). Body fluid spiking studies used residual body fluids submitted to the clinical laboratory for patient testing and were subsequently stored at –20ºC. Although single, unique specimens were preferred when available, body fluid–specific specimen pools were created to provide sufficient volume for testing when needed. Body fluids tested (n = 5–10 unique specimens/pools per fluid type) included biliary/hepatic, cerebrospinal, dialysate, drain, pancreatic, pericardial, peritoneal/ascites, pleural, synovial, and vitreous (see Supplemental Table 1 for list of assays evaluated for each respective body fluid). Treatment with HYAL was performed by adding HYAL (~2 mg) into a specimen aliquot (300–500 μL) with 2 disposable wooden applicator sticks and then vortexing to mix the HYAL powder into solution. The specimen was then allowed to sit at ambient temperature for a minimum of 10 minutes. The paired, spiked, and unspiked body fluid specimens were analyzed in singlicate.

The UC of non-HYAL-treated body fluids was performed using an Airfuge (Beckman Coulter, Brea, CA) for 10 minutes at approximately 178,000 x g. Clarified specimen was removed by collecting the portion of the specimen at the bottom of the tube, using a disposable Pasteur pipette, and transferring to a specimen cup for subsequent testing.

The percentage differences between treated (eg, HYAL-spiked or UC) and untreated specimens were calculated as:

$$\% \text{ Difference} = \left(\frac{\text{Treated Result} - \text{Untreated Result}}{\text{Untreated Result}}\right) \times 100$$

We further investigated HYAL for its effectiveness in liquefying HA gels prepared from HA powder (catalog number J66993, Alfa Aesar, Ward Hill, MA) and in reducing the viscosity of viscous body fluid specimens. The HA gels (0.5, 1.0%, 1.5%, and 2.0%) were prepared by dissolving HA powder in distilled H_2O (n = 5 for each gel concentration); HYAL was added to each aliquot of prepared HA gel (~2 mg, as described above).

The effect of HYAL treatment on previously identified viscous body fluids was also assessed. Qualitative (eg, visual) assessment of viscosity was determined by 1 operator by inserting 2 wooden applicator sticks into the specimen, withdrawing them, and then observing whether a "string" of specimen formed between the 2 sticks (ie, the specimen was viscous) or if the specimen came apart cleanly on each stick with separate drops of liquid (ie, it was not viscous). For each specimen, 1 viscosity assessment was made before HYAL treatment and 1 was made after HYAL treatment. Specimens post-HYAL treatment were then loaded onto the cobas 8000 system for Cl (n = 24; cobas 8000 ISE module) to determine whether the instrument would trigger aspiration errors because of increased specimen viscosity. Specimens with aspiration errors (n = 7) were then manually filtered (filter catalog number 6410-FS216, Porex, Fairburn, GA) and reloaded onto the instrument.

Data analysis was conducted using Excel 2016 (Microsoft Corp, Redmond, WA), SigmaPlot 13 (Systat, San Jose, CA), and SPSS Statistics version 25 (IBM Corp, Armonk, NY). Differences between group means were assessed using the paired-samples *t*-test. We considered *P* values <.05 significant. Clinically relevant interference was defined as a statistically significant difference between groups (*P* <.05), with a corresponding average percentage difference that was greater than ±15%, a percentage threshold that was used in percentage recovery experiments for a prior body fluid validation study from members of our team.[22] Data are presented as mean ± standard deviation (SD) unless otherwise indicated.

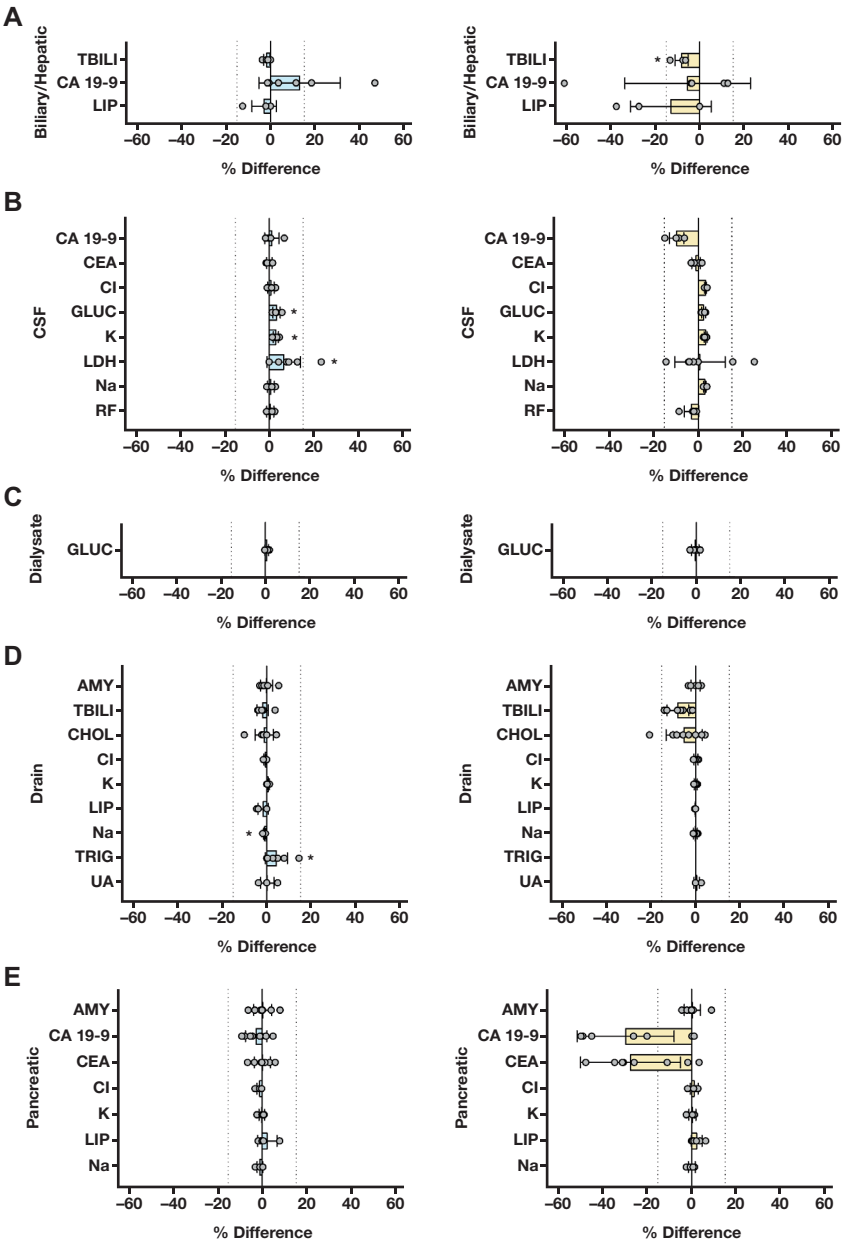

Figure 1

Percentage difference analysis: biliary/hepatic, cerebrospinal (CSF), dialysate, drain, and pancreatic fluids. Graphs are organized per fluid type (**A,** biliary/hepatic; **B,** cerebrospinal; **C,** dialysate; **D,** drain; **E,** pancreatic) showing HYAL (left graph, light blue bars) and UC (right graph, tan bars) for each fluid; bars show mean ± SD. Analytes tested per fluid are shown on corresponding *y* axis labels. All datapoints are plotted in overlying gray circles. Dotted lines show ±15% thresholds. *P <.05. Note that UC was not performed for TRIG.

Specimens with the following pretreatment results were excluded from the percentage difference analysis because of the impact of low quantitative results on the magnitude of the percentage difference calculations: AMY < 10 U/L, TBILI < 0.1 mg/dL, CA 19-9 < 20 U/mL, CEA < 1 ng/mL, CHOL < 10 mg/dL, GLUC < 10 mg/dL, LIP < 5 U/L, and RF < 10 IU/mL. Specimens excluded for percentage difference analysis were alternatively reviewed for absolute quantitative differences in

Lab Medicine 2021;52;469–476
DOI: 10.1093/labmed/lmaa115

results (posttreatment–pretreatment), with the following acceptability limits applied: AMY, ±11 U/L; CA 19-9, ±4 U/mL; CEA, ±0.3 ng/mL; CHOL, ±20 mg/dL; TBILI, ±0.1 mg/dL; GLUC, ±10 mg/dL; LIP, ±6 U/L; and RF, ±4 IU/mL. These acceptability thresholds represented 10% of the upper reference limit of our laboratory's test for each analyte in serum with the exception of RF, which was set at ± 4 IU/mL (approximating 10% of a titer of 40 IU/mL). Finally, TRIG was not evaluated by UC because of the known separation of lipids from aqueous solutions by density during UC.

Results

The HYAL spiking and UC were performed to evaluate for any potential interferences with the body fluid/analyte combinations investigated (**Figure 1**, **Figure 2**, **and Figure 3**). Small albeit statistically significant differences with treatment were observed with HYAL: cerebrospinal—GLUC, K, and LDH (**Figure 1**, **Image B**, left); drain—Na and TRIG (**Figure 1**, **Image D**, left); pericardial—RF and TRIG (**Figure 2**, **Image A**, left); peritoneal—TRIG (**Figure 2**, **Image B**, left); and pleural—Na and TRIG (**Figure 3**, **Image A**, left). Small albeit statistically significant differences were also observed with UC: biliary—TBILI (**Figure 1**, **Image A**, right); cerebrospinal—CA 19-9, Cl, GLUC, K, and Na (**Figure 1**, **Image B**, right); pericardial—Cl, GLUC, Na, RF, and TP (**Figure 2**, **Image A**, right); peritoneal—LDH (**Figure 2**, **Image B**, right); pleural—K and Na (**Figure 3**, **Image A**, right); and vitreous—UN (**Figure 3**, **Image C**, right). Data for HYAL spiking and UC are also presented in tabular format in Supplemental Table 1.

Increased variability (as reflected in SD ≥ 20%) was notable after treatment for several body fluid/analyte combinations using UC: pleural, LIP (**Figure 3**, **Image A**, right); biliary, CA 19-9 (**Figure 1**, **Image A**, right); and pancreatic, CA 19-9 and CEA (**Figure 1**, **Image E**, right). Specimens with low concentration baseline results were not included in the percentage difference analysis but are presented separately in Supplemental Table 2. This analysis showed that HYAL and UC did not impact absolute concentration assessment in low-concentration specimens.

We found that HYAL could liquefy all the prepared HA gels (0.5%, 1.0%. 1.5%, and 2.5% HA; n = 5 each concentration), showing a successful breakdown of HA. **Figure 4** shows a representative example of liquefied 2.0% HA gel after the addition of HYAL. The use of HYAL also effectively reduced the viscosity of previously identified viscous clinical body fluid specimens: Of the 24 specimens that were qualitatively (ie, visibly) viscous before HYAL treatment, all were found to be qualitatively nonviscous post–HYAL treatment. Upon loading these 24 specimens onto analytical instruments, we found that 17 (71%) did not trigger aspiration errors. The remaining 7 (29%) were manually filtered and reloaded on the instrument. All 7 did not trigger aspiration errors upon reloading, suggesting that the prior aspiration error resulted from either particulate matter or other components of the specimen contributing to viscosity (eg, nonliquefied HA) that were removed by subsequent filtration.

Discussion

Body fluid validation requirements may be included as part of a laboratory's accreditation program.[23] This process ensures that testing using modified FDA-cleared or approved assays is conducted according to the 1988 Clinical Laboratory Improvement Amendments regulations for establishing performance specifications.[18] The Clinical and Laboratory Standards Institute (CLSI) has also recently updated its *Analysis of Body Fluids in Clinical Chemistry* standard, which provides additional guidance to clinical laboratories regarding body fluid validations and testing.[6] Note that this CLSI standard emphasizes the importance of specifically incorporating pretreatment techniques in a body fluid validation plan.[6] The use of HYAL to address viscous body fluid specimens and facilitate clinical analysis has previously been reported.[3-6,24] The present study adds to this literature by providing data on multiple body fluid and analyte combinations. It is important to note that body fluid testing should be ordered and conducted only when there is evidence regarding the clinical utility and appropriateness of the body fluid/analyte under investigation.[19] The interpretation of results in the absence of such clear evidence should be conducted with caution.

The present report also highlights the importance and challenge of determining acceptable performance limits for studies, particularly those across multiple analytes.

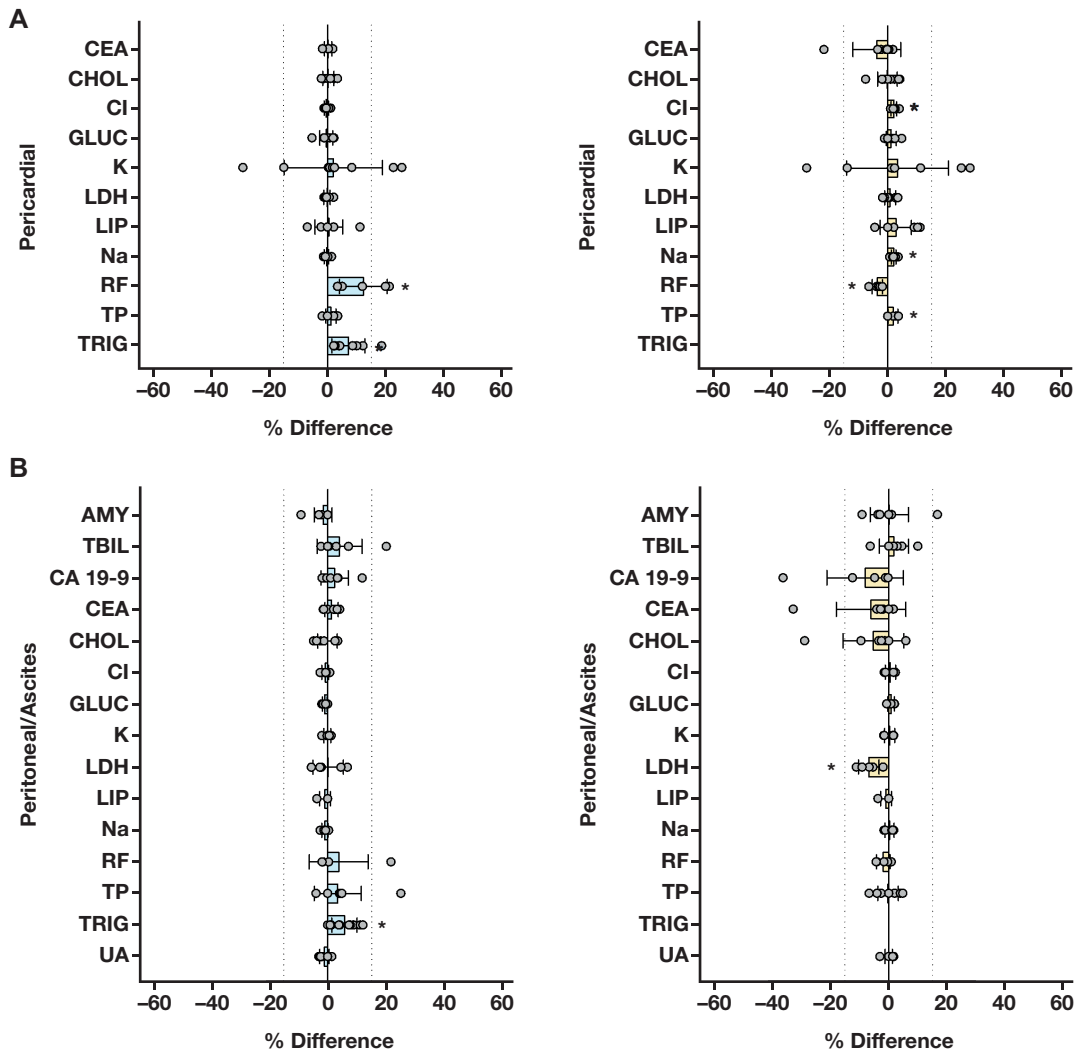

Figure 2

Percentage difference analysis: pericardial and peritoneal/ascites fluids. Graphs are organized per fluid type (**A,** pericardial; **B,** peritoneal/ascites) showing HYAL (left graph, light blue bars) and UC (right graph, tan bars) for each fluid; bars show mean ± SD. Analytes tested per fluid are shown on corresponding *y* axis labels. All datapoints are plotted in overlying gray circles. Dotted lines show ±15% thresholds. **P* <.05. Note that UC was not performed for TRIG.

The 15% threshold was chosen based on its use in recovery studies in a recent body fluid publications for alpha-fetoprotein.[22] Research from our group has also previously used a criterion of 10% in body fluid evaluations.[21] For the present study, we documented 15% acceptability limits during the validation plan as part of an in-house clinical validation. Upon additional analysis, if a 10% criterion was to be applied, then 1 analyte/fluid combination (pericardial fluid, RF) would meet the criterion. Alternatively, if the serum percentage total allowable error (TAE) limits from the Westgard Desirable Biological Variation Database (https://www.westgard.com/biodatabase1.htm) were applied (TAE: AMY, 14.6%; TBILI, 26.94%; CA 19-9, 46.03%; CEA, 24.7%; CHOL, 9.01%; CI, 1.5%; CREAT, 8.87%; GLUC, 6.96%; K, 5.61%; LDH, 11.4%; LIP, 37.88%; Na, 0.73%; RF, 13.5%; TP, 3.63%; TRIG, 25.99%; UA, 11.97%; and UN, 15.55%), then only a few electrolyte/fluid combinations would meet the criterion: Cl (UC—CSF, pericardial, vitreous), Na (UC—CSF, pericardial, pleural), and Na

DOI: 10.1093/labmed/lmaa115

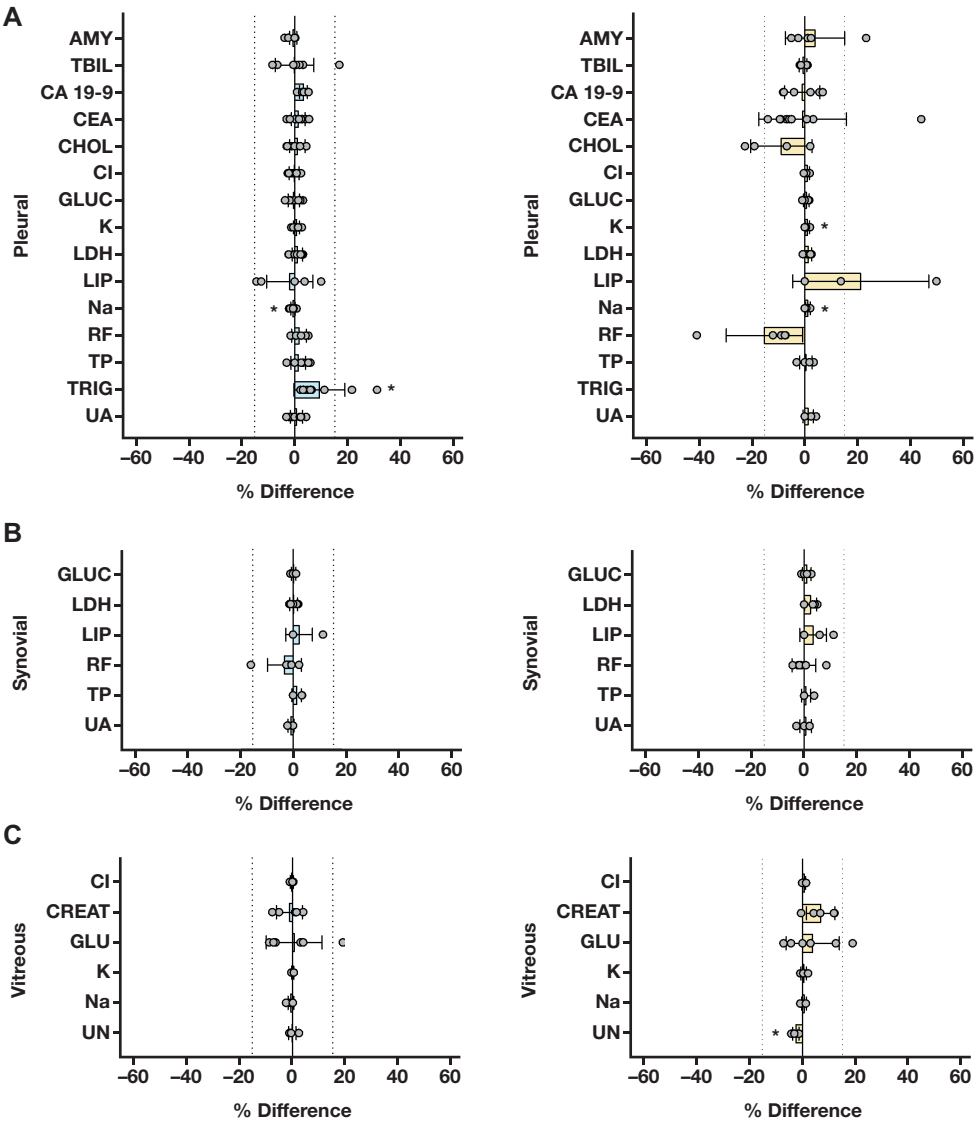

Figure 3

Percentage difference analysis: pleural, synovial, and vitreous fluids. Graphs are organized per fluid type (**A,** pleural; **B,** synovial; **C,** vitreous) showing HYAL (left graph, light blue bars) and UC (right graph, tan bars) for each fluid; bars show mean ± SD. Analytes tested per fluid are shown on corresponding *y* axis labels. All datapoints are plotted in overlying gray circles. Dotted lines show ±15% thresholds. *P <.05. Note that UC was not performed for TRIG.

(HYAL—drain). Given the minimal percentage differences for these analytes with HYAL and UC treatment (**Figure 1**, **Figure 2**, **Figure 3**), these TAE electrolyte limits are likely too restrictive for use with clinical body fluid testing because the differences would almost certainly be clinically irrelevant. However, these results emphasize how critical predefined acceptance criteria are to clinical laboratory validations.

Validation of pretreatment with HYAL for specific analytes can also help identify unexpected reagent contaminants. For example, our laboratory previously used a source of HYAL of bovine testicular origin (Sigma Aldrich catalog number H3506), which has been described by others.[4] In a previous investigation from our laboratory, it was discovered that this particular HYAL powder contained measurable testosterone, presumably carried over from its

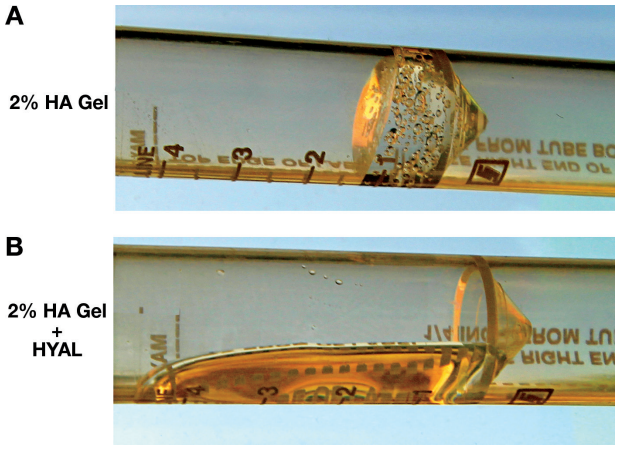

Figure 4

Reduced viscosity of an HA gel by treatment using HYAL. **A,** 2% HA gel, untreated. **B,** 2% HA gel treated with ~2 mg HYAL.

tissue source.[13] Although our laboratory does not perform testosterone measurement on body fluids, an alternative source of HYAL powder was still desired because the instruments used for certain body fluid immunoassays are also used for serum testosterone measurement. The presence of an analyte-containing powder in proximity to such instruments theoretically introduces a contamination risk if a bottle were inadvertently spilled. An evaluation of several sources of HYAL for testosterone contamination was therefore performed, and the HYAL assessed in the present study (catalog number H2126) was selected based on the prior investigation.[20] Although recombinant HYAL is also commercially available, it is generally cost-prohibitive in the amounts required for body fluid testing in clinical laboratories.

Increased percentage differences in TP have previously been reported when using HYAL powder spiked into body fluids (catalog number H3506),[4] possibly because HYAL itself is a protein. Interestingly, the HYAL evaluated in the present study (catalog number H2126) did not show as substantial of a percentage difference in TP for the fluids evaluated (1%–3% difference observed). Although it is still a protein, this bovine HYAL has a more granular characteristic than the previously used light, flaky material, and it is generally easier to scoop in smaller amounts and with a similar overall impact on resolving viscous specimens. These observations reiterate the importance of laboratories evaluating and validating specific HYAL or pretreatment protocols before use to fully understand any potential interferences or unexpected impact on specific assays.

Along with serum and plasma, body fluid specimens are also susceptible to specimen interferences such as hemolysis, icterus, and lipemia. Among the different treatments for clearing lipemia, previous reports have described the effectiveness and benefits of using UC.[16,17,25] In the present study, although not statistically significant, several analytes showed trends toward percentage differences greater than our acceptability criteria with UC: pancreatic CA 19-9 (–29%), pancreatic CEA (–27%), and pleural lipase (21%). However, not all body fluid types showed mean percentage differences greater than our acceptability threshold of 15% for these analytes. Mean percentage differences for the various body fluids ranged from –29% to –1% for CA 19-9, from –27% to 0% for CEA, and from –13% to 21% for lipase. In general, these observations do suggest that increased variability (ie, imprecision) may be seen with UC treatment. Research has shown that CA 19-9 and CEA are membrane-bound glycoproteins that are used clinically as serum tumor markers.[26-28] It is theoretically possible that during UC, the plasma membrane in cellular specimens may be impacted, potentially either releasing or precipitating membrane-bound components. Further studies are required to investigate the variability in CA 19-9 and CEA with UC observed in the present report. Although this study does not definitively explain a mechanism for the trend toward increased pleural LIP, it is interesting to note that a previous study observed elevations in LIP after HYAL pretreatment.[4] Out of an abundance of caution, UC was classified as unacceptable for CA 19-9, CEA, and LIP in our laboratory, regardless of the body fluid type being analyzed.

The limitations of the present report include the fact that specimen viscosity assessment was conducted by 1 operator with viscosity assessments performed in singlicate. The differential ability of instruments to detect specimen clots or hyperviscosity or to provide aspiration error flags was not assessed. Specific recovery studies comparing specimens spiked with HA were not performed but could provide insight into the effect of HA-induced viscosity on assay performance. In addition, this investigation did not evaluate the impact of manual specimen filtration alone, either as a pretreatment step or for any potential impact on analytical results. Determination of statistical significance could be enhanced by studies of individual analyte/fluid combinations with increased numbers of study specimens.

DOI: 10.1093/labmed/lmaa115

Conclusion

A source of HYAL that effectively reduced the viscosity of body fluids was identified and evaluated. Either no or negligible interference for most assays evaluated in this study was observed. Furthermore, UC was classified as unacceptable for CA 19-9, CEA, and LIP. Laboratories should perform verification studies for any pretreatment processes such as HYAL or UC before incorporating them into clinical laboratory protocols. **LM**

Acknowledgments

This work was supported by the ARUP Institute for Clinical and Experimental Pathology. We gratefully acknowledge Taylor Snow for assistance with specimen collection and deidentification.

References

1. Girish KS, Kemparaju K. The magic glue hyaluronan and its eraser hyaluronidase: a biological overview. *Life Sci.* 2007;80(21):1921–1943.
2. Stern R, Kogan G, Jedrzejas MJ, Soltés L. The many ways to cleave hyaluronan. *Biotechnol Adv.* 2007;25(6):537–557.
3. Brunzel NA. *Appendix C: Body fluid diluent and pretreatment solutions. In: Brunzel, NA, ed. Fundamentals of Urine and Body Fluid Analysis*. 3rd ed. St. Louis, MO: Elsevier Saunders; 2012:422–423.
4. Block DR, Ouverson LJ, Wittwer CA, Saenger AK, Baumann NA. An approach to analytical validation and testing of body fluid assays for the automated clinical laboratory. *Clin Biochem.* 2018;58:44–52.
5. Garg U, Althahabi R, Amirahmadi V, Brod M, Blanchard C, Young T. Hyaluronidase as a liquefying agent for chemical analysis of vitreous fluid. *J Forensic Sci.* 2004;49(2):388–391.
6. Clinical and Laboratory Standards Institute. *Analysis of Body Fluids in Clinical Chemistry*. 2nd ed. Wayne, PA: Clinical and Laboratory Standards Institute; 2018.
7. Kjeldsberg C, Hussong J. *Body Fluid Analysis*. 3rd ed. Chicago, IL: ASCP Press; 2015.
8. Sugiuchi H, Ando Y, Manabe M, et al. Measurement of total and differential white blood cell counts in synovial fluid by means of an automated hematology analyzer. *J Lab Clin Med.* 2005;146(1):36–42.
9. Seghezzi M, Buoro S, Manenti B, et al. Optimization of cellular analysis of synovial fluids by optical microscopy and automated count using the Sysmex XN body fluid mode. *Clin Chim Acta.* 2016;462:41–48.
10. Froom P, Diab A, Barak M. Automated evaluation of synovial and ascitic fluids with the Advia 2120 hematology analyzer. *Am J Clin Pathol.* 2013;140(6):828–830.
11. Aulesa C, Mainar I, Prieto M, Cobos N, Galimany R. Use of the Advia 120 hematology analyzer in the differential cytologic analysis of biological fluids (cerebrospinal, peritoneal, pleural, pericardial, synovial, and others). *Lab Hematol.* 2003;9(4):214–224.
12. Moreno MJ, Clayburne G, Schumacher HR Jr. Processing of noninflammatory synovial fluids with hyaluronidase for cytospin preparations improves the accuracy of differential counts. *Diagn Cytopathol.* 2000;22(4):256–258.
13. Buoro S, Seghezzi M, Manenti B, et al. Reliability of automated synovial fluid cell counting with Mindray BC-6800 body fluid mode. *Int J Lab Hematol.* 2017;39(3):337–346.
14. Blana SA, Musshoff F, Hoeller T, Fimmers R, Madea B. Variations in vitreous humor chemical values as a result of pre-analytical treatment. *Forensic Sci Int.* 2011;210(1–3):263–270.
15. Yavorskyy A, Hernandez-Santana A, Shortt B, McCarthy G, McMahon G. Determination of calcium in synovial fluid samples as an aid to diagnosing osteoarthritis. *Bioanalysis.* 2010;2(2):189–195.
16. Nikolac N. Lipemia: causes, interference mechanisms, detection and management. *Biochem Med (Zagreb).* 2014;24(1):57–67.
17. Hunsaker JJH, La'ulu SL, Wyness SP, Genzen JR. Lipemic interference of ceruloplasmin assays—an evaluation of lipid removal methods. *Clin Chim Acta.* 2018;480:71–78.
18. Clinical Laboratory Improvement Amendments of 1988. Laboratory Requirements. 42 CFR §493.1253(b) (2011).
19. Block DR, Algeciras-Schimnich A. Body fluid analysis: clinical utility and applicability of published studies to guide interpretation of today's laboratory testing in serous fluids. *Crit Rev Clin Lab Sci.* 2013;50(4–5):107–124.
20. Genzen JR, La'ulu SL, Wyness SP, Scholes KL, Signorelli HN, Greer RW. Identifying and eliminating laboratory contamination by topical testosterone therapeutics. *Clin Chem*. 2019;65(1):67–73.
21. Owen WE, Thatcher ML, Crabtree KJ, et al. Body fluid matrix evaluation on a Roche cobas 8000 system. *Clin Biochem.* 2015;48(13–14):911–914.
22. Owen WE, Hunsaker JJH, Genzen JR. Alpha-fetoprotein in pericardial, peritoneal, and pleural fluids: a body fluid matrix evaluation. *Clin Biochem.* 2018;56:109–112.
23. College of American Pathologists. Test method validation and verification. COM.40620: body fluid validation. https://appsuite.cap.org/appsuite/learning/LAP/FFoC/ValidationVerificationStudies/story_content/external_files/checklistrequirements.pdf. Accessed December 28, 2020.
24. Block DR, Franke DDH. *Quick Guide to Body Fluid Testing*. Washington, DC: AACC Press; 2015.
25. Saracevic A, Nikolac N, Simundic AM. The evaluation and comparison of consecutive high speed centrifugation and LipoClear reagent for lipemia removal. *Clin Biochem.* 2014;47(4–5):309–314.
26. Magnani JL, Nilsson B, Brockhaus M, et al. A monoclonal antibody-defined antigen associated with gastrointestinal cancer is a ganglioside containing sialylated lacto-N-fucopentaose II. *J Biol Chem.* 1982;257(23):14365–14369.
27. Hammarström S. The carcinoembryonic antigen (CEA) family: structures, suggested functions and expression in normal and malignant tissues. *Semin Cancer Biol.* 1999;9(2):67–81.
28. Diamandis EP, Bast RC Jr, Gold P, Chu TM, Magnani JL. Reflection on the discovery of carcinoembryonic antigen, prostate-specific antigen, and cancer antigens CA125 and CA19-9. *Clin Chem.* 2013;59(1):22–31.

Usage of Plasma Presepsin, C-Reactive Protein, Procalcitonin and Proadrenomedullin to Predict Bacteremia in Febril Neutropenia of Pediatric Hematological Malignancy Patients

Kamile Arıkan, MD[1], Eda Karadag-Oncel, MD, MSc[2], Selin Aytac, MD[3], Mualla Cetin, MD[3], Ali Bülent Cengiz, MD[4], Fatma Gümrük, MD[3], Ates Kara, MD,[4] Mehmet Ceyhan, MD[3]*

Laboratory Medicine 2021;52:477-484

DOI: 10.1093/labmed/lmab002

ABSTRACT

Objective: To investigate the value of presepsin and proadrenomedullin (proADM) as new markers for febrile neutropenia, by comparing them with conventional markers.

Methods: Plasma specimens for presepsin, proADM, C-reactive protein (CRP), and procalcitonin (PCT) were collected every 3 days during each episode of febrile neutropenia.

Results: A total of 39 patients experiencing a collective 47 episodes of febrile neutropenia with hematological malignant neoplasms, as well as 40 healthy control patients without infectious disease, were enrolled in this study. Levels of the studied analytes in the presepsin 1 group (with baseline values taken at admission), presepsin 2 group (values recorded on the 3rd day of febrile neutropenia), and presepsin 3 group (values recorded on the 6th day of hospitalization) were all higher in the subgroups with bacteremia. C-reactive protein 1 (baseline value taken at admission), procalcitonin 1 (as recorded at admission), and procalcitonin 2 (recorded on the 3rd day of febrile neutropenia) were higher in the subroups with bacteremia (P =.03, P = .04, and P = .04, respectively). In multivariate logistic regression analysis, presepsin 1 and/or PCT 1/CRP 1 combined analysis was superior in predicting bacteremia.

Conclusion: Presepsin could be used in combination with other biomarkers to detect bacteremia.

Keywords: febrile neutropenia, bacteremia, presepsin, proadrenomedullin, C-reactive protein, procalcitonin

Febrile neutropenia (FN) represents an important complication that affects the clinical outcomes of patients who receive chemotherapy and/or hematopoietic stem-cell transplantation (HSCT). It is assumed that infectious causes are the reason for 80% of FN episodes.[1] Prediction of bacteremia/sepsis in patients with pediatric hematological malignan neoplasms who have febrile neutropenia still remains a challenge for the medical community due to the lack of reliable biomarkers, especially at the beginning of the infection process. In FN episodes, life-threatening complications can develop in a period of several hours, depending on the pathogen. Thus, an accurate and timely diagnostic work-up is mandatory to yield prompt diagnosis and reveal the correct antibiotic treatment.

C-reactive protein (CRP) and procalcitonin (PCT), as biomarkers, have most often been explored to identify patients at risk for complicated course of febrile neutropenia. CRP and PCT both have some limitations, such as nonspecificity and delayed response. High levels of PCT are observed during systemic bacterial infections, and less-elevated PCT levels are observed during localized bacterial infections.[2] PCT is superior to CRP for predictive

Abbreviations:

FN, febrile neutropenia; HSCT, hematopoietic stem-cell transplantation; CRP, C-reactive protein; PCT, procalcitonin; sCD14, soluble CD14 subtype; ADM, adrenomedullin; SIRS, systemic inflammatory response syndrome; ANC, absolute neutrophil count; IDSA, Infectious Disease Society of America; ECLIA, electrochemiluminescence immunoassay analyzer; ROC, receiver operating characteristics; ALL, acute lymphoblastic lymphoma; AML, acute myeloblastic lymphoma; AUC, area under the curve; CI, confidence interval; min, minimum; max, maximum

[1]Health Sciences University, Izmir Behcet Uz Children's Hospital, Department of Pediatric Infectious Diseases, Izmir, Turkey; [2]Health Sciences University, Izmir Tepecik Research and Training Hospital, Department of Pediatric Infectious Diseases, Izmir, Turkey; [3]Hacettepe University Faculty of Medicine, Pediatric Hematology Unit, Ankara, Turkey; and [4]Hacettepe University Faculty of Medicine, Department of Infectious Diseases, Ankara, Turkey

*To whom correspondence should be addressed.
kamilearikan5@gmail.com

purposes and is slightly more pathogen-dependent, especially in gram negative bacteremia.[2] However, there still is a need for more rapid and accurate markers, which also could be used for deescalation strategies involving broad-spectrum antibiotics.

Soluble CD14 subtype (sCD14), known as *presepsin*, is a biomarker that has been demonstrated as a new, emerging, early indicator for the detection of different infections.[3] When a proinflammatory cascade is activated against infectious agents, sCD14 is released after phagocytosis or released into circulation by breakdown of sCD14 via the proteolytic pathway. After this process, presepsin is generated and released. The molecule occurs as early as within 2 hours of inflammation onset, which is even earlier than PCT and CRP.

Adrenomedullin (ADM) is a 52-amino-acid peptide produced from cultured vascular smooth-muscle cells and vascular endothelial cells; its production is generally augmented by inflammatory agents such as lipopolysaccharide, tumor necrosis factor, and interleukin-1.[3] ADM has regulatory effects on inflammation, infection, angiogenesis, mineralized tissue formation, and development.[4,5]

ADM has been found to be beneficial as a prognostic marker for high sepsis, pneumonia, systemic inflammatory response syndrome (SIRS), and febrile neutropenia. Its precursor molecules are pre–proADM, which consists of 185 amino acids, and proADM, which contains 164 amino acids. After its release, ADM is rapidly eliminated from the serum, so it is hard to measure its serum levels. However, proADM remains stable for longer periods of time.[6,7] To date, to our knowledge, there have been no published studies in pediatric patients with cancer regarding proADM as a biomarker, compared with presepsin, CRP, and PCT.

Herein, we aimed to analyze the utility of presepsin, pro-ADM, CRP, and PCT as biomarkers of bacteremia during febrile episodes that occurred in patients with neutropenia harboring hematological malignant neoplasms. Our goal was to define reliable tools to predict bacteremia and derive the correct prognosis.

Material and Methods

We conducted a prospective, case-control study to examine the utility of presepsin and proADM levels, compared the CRP and PCT levels, for detecting bacterial infections in the FN of pediatric patients in the hematology department. The present study was approved by the ethical committee of the Faculty of Medicine, Hacettepe University, Ankara, Turkey. FN is often defined as having oral temperature of 38.3 or greater, or 38°C or greater, for more than 1 hour, with absolute neutrophil count (ANC) less than 500 per μL or the reduction of ANC to 500 per μL in the next 24 to 48 hours. *Severe neutropenia* has been defined as ANC less than 100 per μL.[8]

The inclusion criteria were age of less than 18 years and presence of hematological malignant neoplasms without a history of antibiotic therapy in the past week. Exclusion criteria were declining to participate in the study, age greater than 18 years, having oncological malignant neoplasms, having nonhematological malignant neoplasms, and not undergoing chemotherapy treatment.

The patients were selected for the study based on the criteria of the Infectious Disease Society of America (IDSA) for the definition of FN. Written consent was given by the parents of each patient to participate in this study. All the patients were subjected to full medical history-taking, thorough clinical examination, and radiological studies (if indicated).

Routine total blood count, biochemical analysis, and blood culture were performed on all patients with febrile neutropenia. Plasma specimens for presepsin, proADM, CRP, and PCT were collected concomitantly during each febrile neutropenic episode at presentation before the first dose of antibiotic treatment (day 0; presepsin 1, proADM1, CRP1, PCT1), at the 3rd day (day 3; presepsin 2, proADM2, CRP2, PCT2) and at the 7th day of antibotic treatment (day 7; presepsin 3, proADM3, CRP3, PCT3). We also checked serum presepsin and proADM levels inm healthy pediatric patients.

None of the included patients had been administered antibiotics before enrollment. *Bacteremia* was defined as a microbial growth in one of the blood culture bottles. For coagulase negative *Staphylococcus* species, 2 positive blood culture results from different sites were required; otherwise, the result was considered to indicate possible contamination. In this study, an individual patient may have had multiple FN events. The serum specimens, taken at the same time as PCT and CRP specimen gathering, were allowed to clot for 10 to 20 minutes at room temperature and then centrifuged (at 492*g* –1107*g*) for 20 minutes. We collected the supernatants carefully. After centrifugation within 2 hours of phlebotomy, the plasma was preserved at –80°C until measurement.

We measured plasma presepsin levels using a rapid chemiluminescent enzyme immunoassay on the fully automated PATHFAST immunoanalyzer (Mitsubishi Chemical Europe GmbH). ProADM was measured via quantitative sandwich enzyme immunoassay technique, using the Human Pro-ADM ELISA Kit. ProADM levels were measured by ELISA (pg/mL). PCT levels were measured by electrochemiluminescence immunoassay analyzer (ECLIA; ng/mL; local inflammation/infection, 0–0.5; moderate systemic inflammatory response, 0.5–2.0; severe systemic inflammatory response, 2.1–10.0; severe bacterial sepsis/septic shock, >10.0). CRP levels were measured by immunoturbidimetry (mg/L; threshold >5).

Statistical Analysis

The data were analyzed using SPSS Statistics, version 20.0 (IBM Corporation). Comparisons between measures (mean [SD]) of the 2 groups were performed using the Student *t* test, and comparisons between measures (mean [SD]) of multiple groups were performed by 1-way ANOVA testing (*F*). Kruskall-Wallis test (*K*) was used instead of ANOVA in nonparametric data (SD >50% mean).

Mann-Whitney testing was used for nonparametric data, and χ^2 testing was used for comparing categorical variables. We used correlation coefficient rank testing to rank different variables against each other in linear correlation, which was positive or negative. The capacity of CRP, PCT, presepsin, pro-ADM, and serum thrombocyte values were analyzed using ROC (receiver operating characteristics) curve analysis. When we observed a significant cutoff value, sensitivity, specificity, and positive and negative predictive values were presented. While we investigated the associations between non-normally distributed and/or ordinal variables, we calculated the correlation coefficients and their significance using the Spearman test. A *P* value of less than .05 was considered statistically significant, and a *P* value of .05 or greater was considered statistically insignificant.

Results

A total of 29 patients with acute lymphoblastic lymphoma (ALL; 33.3%), 18 with acute myeloblastic lymphoma (AML; 20.7%), and 40 control individuals (46.0%) with no known underlying disease or fever were included in this study. The median age of the patients with hematological malignant neoplasms was 77 months (21–216 months), and the median age of the control group was 71.5 months (10.0–215.0 months; *P* = .72).The median age of the 47 patients with hematological malignant neoplasms was 77 months (21–216 months), and the median age of the control group was 71.5 months (10–215 months; *P* = .72). In total, 23 of the 47 patients (48.9%) and 18 of 40 (45.0%) in the control group were male (*P* = .44). The median (minimum–maximum) duration of hospitalization was 13 days (6–75 days). Patients with AML were more prone to longer hospitalization than patients with ALL: 19 days (6–75) vs 10 days (6–38; *P* = .01). In 36 FN episodes (41.4%), patients had severe neutropenia (ANC <100/μL).

In 26 of 47 FN episodes (55.3%), at least 1 infectious cause was found: 18 (69.2%) were due to bacteria, 5 (19.2%) were due to viruses, and 3 (11.6%) were due to fungal infections (**Table 1**). Patients with FN who had severe neutropenia more commonly had bacteriemia: of 8 of 9 (88.9%) patients with gram negative bacteremia, 7 of 9 (77.8% patients with gram positive bacteremia) had severe neutropenia.

The median (minimum–maximum) presepsin levels of control individuals were statistically significantly higher than those levels in the patient group (2555 pg/mL [670–7010] vs 1870 pg/mL [140–7010], respectively [*P* = .04]). Median (minimum–maximum) presepsin levels were higher in patients with FN episodes caused by bacterial infections than in patients with FN episodes with no underlying infectious etiology; however, the difference was not statistically significant (*P* = .10, *P* = .67, and *P* = .75, respectively; **Table 2**). In 9 patients with gram negative bacteriemia, median presepsin 1, -2, and -3 levels were all higher than in the patients with gram-positive bacteremia (*n* = 9); however, the difference was not statistically significant (*P* = .13, *P* = .89, and *P* = .42, respectively; **Table 3**, **Figure 1**).

Serum proADM1 levels of patients with FN who harbored bacteremia was statistically significantly higher than those in the control group: 58.24 pg per mL (58.24–69.13) vs 46.13 pg/mL (20.16–70.45), respectively (*P* <.001.) Median (minimum–maximum) proADM levels were similar between patients with bacteremia and those without bacteremia (*P* = .90, *P* = .67, and *P* = .70, respectively; **Table 2**). Median serum proADM levels (1, 2, and 3) of patients with gram positive bacteremia were not statistically different from those levels in patients with gram negative bacteremia (**Table 3**).

Lab Medicine 2021;52;477–484 479
DOI: 10.1093/labmed/lmab002

Median CRP1, -2, and -3 levels of patients with FN were 5.82 mg/dL (0.16–31.5 mg/dL), 5.99 mg/dL (0.42–52.1 mg/dL), and 1.67 mg/dL (0.18–51.1 mg/dL), respectively; change was statistically significant during hospitalization (*P* <.001).

Table 1. Patient Characteristics[a]

Hematological Malignancy, No. (%)	
Acute myeloid leukemia	18 (61.7)
Acute lymphoblastic leukemia	29 (38.3)
Absolute Neutrophil Count During FN (Day 0), No. (%)	
<100/μL	36 (76.6)
100–500/μL	11 (23.4)
Focus of Infection, No. (%)	
No focus of infection	21 (44.7)
Bacteriemia	18 (38.3)
Viral upper respiratory infection	5 (10.6)
Fungal infection	3 (6.4)
Pathogens Identified in Blood Cultures, No.	
Gram negative Bacteria	
Escherichia coli	3
Klebsiella pneumonia	2
Pseudomonas aeruginosa	1
Citrobacter freundii	1
Klebsiella oxytoca	1
Gram positive Bacteria	
Staphylococcus epidermidis	5
Staphylococcus hominis	2
Enterococcus faecium	1
Streptococcus mitis	1

FN, febrile neutropenia.
[a]No. refers to number of episodes of febrile neutropenia.

Median CRP2 levels were statistically significantly higher (*P* = .02), but CRP1 and CRP3 levels were similar in patients with bacteremia and without bacteremia (*P* = .68 and *P* = .45, respectively). Median CRP2 levels of patients with FN who harbored gram-negative bacteremia were statistically significantly higher than those levels in patients with FN who harbored gram-positive bacteremia (*P* = .02; **Table 3**, **Figure 1**).

Median (minimum–maximum) PCT1, -2, and -3 levels of patients with FN were 0.43 ng per mL (0.05–40.4 ng/mL), 0.29 ng per mL (0.04–17.6 ng/mL), and 0.22 ng per mL (0.04–11.4 ng/mL), respectively; the change was statistically significant during hospitalization (*P* <.001). Median PCT1 and -2 values of patients with FN who had documented bacterial infections were higher than in patients with FN who did not have underlying infectious etiology (each *P* = .04) (**Table 2**). Median PCT1 and -2 values were higher in patients with gram-negative bacteremia than those with gram-positive bacteremia (*P* = .01 and *P* = .008, respectively; **Table 3**). A cutoff value of serum pro-ADM1 level of 57.95 pg/mL was found to diagnose FN attacks, with sensitivity of 98% and specificity of 75% (area under the curve [AUC], 0.78; 95% confidence interval [CI], .66–.90; *P* <.001). A cutoff value of serum presepsin 3 level of 750 pg/mL was found to diagnose bacteremia in FN, with sensitivity of 85% and specificity of 64 % (AUC, 0.74; 95% CI, 0.55-0.93; *P* = .03).

A cutoff value of serum PCT1 level of 0.36 ng/mL was found to detect bacteremia in patients with FN, with sensitivity of 82%

Table 2. Biomarker Changes in Bacteremic and Nonbacteriemic FN Groups

Variable	Group with Bacteremia, Median (Min–Max)[a]	Group without Bacteremia Median (Min–Max)[b]	*P* Value[c]
Age (mo)	78 (21–216)	81 (21–213)	.85
Presepsin 1 (pg/mL)	2210 (250–7010)	1700 (140–6920)	.10
Presepsin 2 (pg/mL)	2540 (130–7010)	1560 (100–6920)	.67
Presepsin 3 (pg/mL)	4550 (170–6920)	1880 (100–7010)	.75
Pro–ADM 1 (pg/mL)	58.24 (58.24–69.13)	52.44 (53.56–70.45)	.90
Pro–ADM 2 (pg/mL)	56.24 (58.24–70.45)	49.40 (48.55–70.45)	.60
Pro–ADM 3 (pg/mL)	54.44 (58.24–70.45)	48.40 (53.01–70.45)	.70
CRP 1 (mg/dL)	7.00 (0.20–18.80)	8.45 (0.49–31.50)	.68
CRP 2 (mg/dL)	8.25 (0.46–52.10)	5.08 (0.47–17.60)	**.03**
CRP 3 (mg/dL)	6.00 (0.30–18.50)	0.98 (0.40–28.9)	.45
PCT 1 (ng/mL)	0.53 (0.15–10.80)	0.20 (0.05–40.40)	**.04**
PCT 2 (ng/mL)	1.81 (0.08–17.60)	0.20 (0.04–3.67)	**.04**
PCT 3 (ng/mL)	0.23 (0.11–11.40)	0.20 (0.04–3.60)	.26

FN, febrile neutropenia; min, minimum; max, maximum; No., refers to the number of episodes of FN; pro-ADM, proadrenomedullin; CRP, C-reactive protein; PCT, procalcitonin.
[a]n = 18.
[b]n = 29.
[c]Bolding indicates statistical significance.

Table 3. Biomarker Changes in Gram Positive and Gram Negative Bacteriemic FN Groups

Variable	Group with Gram Positive Bacteremia[a]	Group with Gram Negative Bacteremia[a]	*P* Value[b]
	Median (Min-Max)		
Presepsin 1 (pg/mL)	1960 (470–4470)	4590 (250–7010)	.13
Presepsin 2 (pg/mL)	2030 (250–5890)	3990 (130–7010)	.89
Presepsin 3 (pg/mL)	2090 (210–6920)	6920 (170–6920)	.42
Pro–ADM 1 (pg/mL)	52.34 (58.24–64.20)	58.24 (58.24–64.20)	.93
Pro–ADM 2 (pg/mL)	52.30 (58.24–66.83)	56.40 (58.24–70.45)	.99
Pro–ADM 3 (pg/mL)	49.45 (58.24–65.06)	52.30 (58.24–70.45)	.68
CRP 1 (mg/dL)	7.31 (0.2–18.8)	5.79 (1.67–16.29)	.89
CRP 2 (mg/dL)	7.01 (0.46–21.1)	18.2 (6.11–52.10)	**.02**
CRP 3 (mg/dL)	2.01 (0.3–17.1)	10.85 (0.47–18.50)	.48
PCT 1 (ng/mL)	0.41 (0.34–40.4)	1.00 (0.15–10.80)	**.01**
PCT 2 (ng/mL)	0.55 (0.08–3.67)	4.40 (1.63–17.60)	**.008**
PCT 3 (ng/mL)	0.22 (0.11–1)	0.48 (0.17–11.40)	.18
Thrombocyte 1, $\times 10^3/\mu L$	41 (11–257)	22.50 (14.00–52.00)	**.004**
Thrombocyte 2, $\times 10^3/\mu L$	49 (16–273)	20.50 (15.00–62.00)	.19
Thrombocyte 3, $\times 10^3/\mu L$	35 (23–376)	40.50 (18.00–183.00)	.09

min, minimum; max, maximum; pro-ADM, proadrenomedullin; CRP, C-reactive protein; PCT, procalcitonin.
[a] *n = 9.*
[b] *Bolding indicates statistical significance.*

and specificity of 62% (AUC, 0.74; 95% CI, 0.58-0.90; *P* = .01). A cutoff value of serum CRP2 level of 6.6 mg/dL was found to detect bacteremia in FN, with sensitivity of 67% and specificity of 69% (AUC, 0.70; 95% CI, 0.54-0.86; *P* = .02).

A cutoff value of serum thrombocyte 1 level of 40.5 × 10^3 μL was found to detect bacteremia in patients with FN, with sensitivity of 80% and specificity of 74% (AUC, 0.28; 95% CI, .09–.46; *P* = .04). A cutoff value of serum thrombocyte 2 level of 54.5 × 10^3 μL was found to detect bacteriemia in patients with FN, with sensitivity of 80% and specificity of 61% (AUC, 0.21; 95% CI, .02–.40; *P* = .01). The optimal cutoff values for proADM, presepsin, PCT, CRP, and thrombocytes were identified by plotting ROC curves. ROC curves of all patients with febrile neutropenia and bacteremia vs patients with febrile neutropenia who did not have bacteremia are depicted in **Figure 2**.

In multivariate logistic regression analysis, presepsin 1 and PCT1 combined analysis was superior in detecting bacteriemia than PCT1 by itself (R^2: 0.18 vs 0.09, respectively). Presepsin 2 and PCT2 combined analysis was superior in detecting bacteremia, compared with PCT1 by itself (R^2: 0.58 vs 0.05, respectively). Presepsin 2 and PCT2 combined analysis was superior in detecting gram negative bacteremia, compared with PCT 1 by itself (R^2: 0.15 vs 0.002, respectively). In multivariate logistic regression analysis, presepsin 1 and CRP1 combined analysis was superior in detecting bacteremia, compared with CRP1 by itself (R^2: 0.34 vs 0.05, respectively). Presepsin 1 and CRP1 combined analysis was superior in detecting gram negative bacteremia, compared with CRP1 by itself (R^2: 0.13 vs 0.08, respectively).

Discussion

In the results of this study, we discovered that presepsin, when combined with CRP and PCT, can discriminate among bacterial infections, especially gram negative bacteriemia, in FN episodes of pediatric hematological malignancy. Also, presepsin 1 and -2, when combined with PCT1 and PCT2, were superior predictors of bacteremia, especially in gram negative bacteriemia. Median plasma presepsin levels were statistically significantly higher in the control group than in the FN group. This difference of serum presepsin levels between the control and FN groups might be explained by the fact that CD14 is expressed in neutrophils or monocytes and neutropenia in patients with FN, hence the lower serum presepsin levels. It was reported[9] that patients with hemophagocytic syndrome had higher levels of serum presepsin than those patients without hemophagocytic syndrome.

DOI: 10.1093/labmed/lmab002

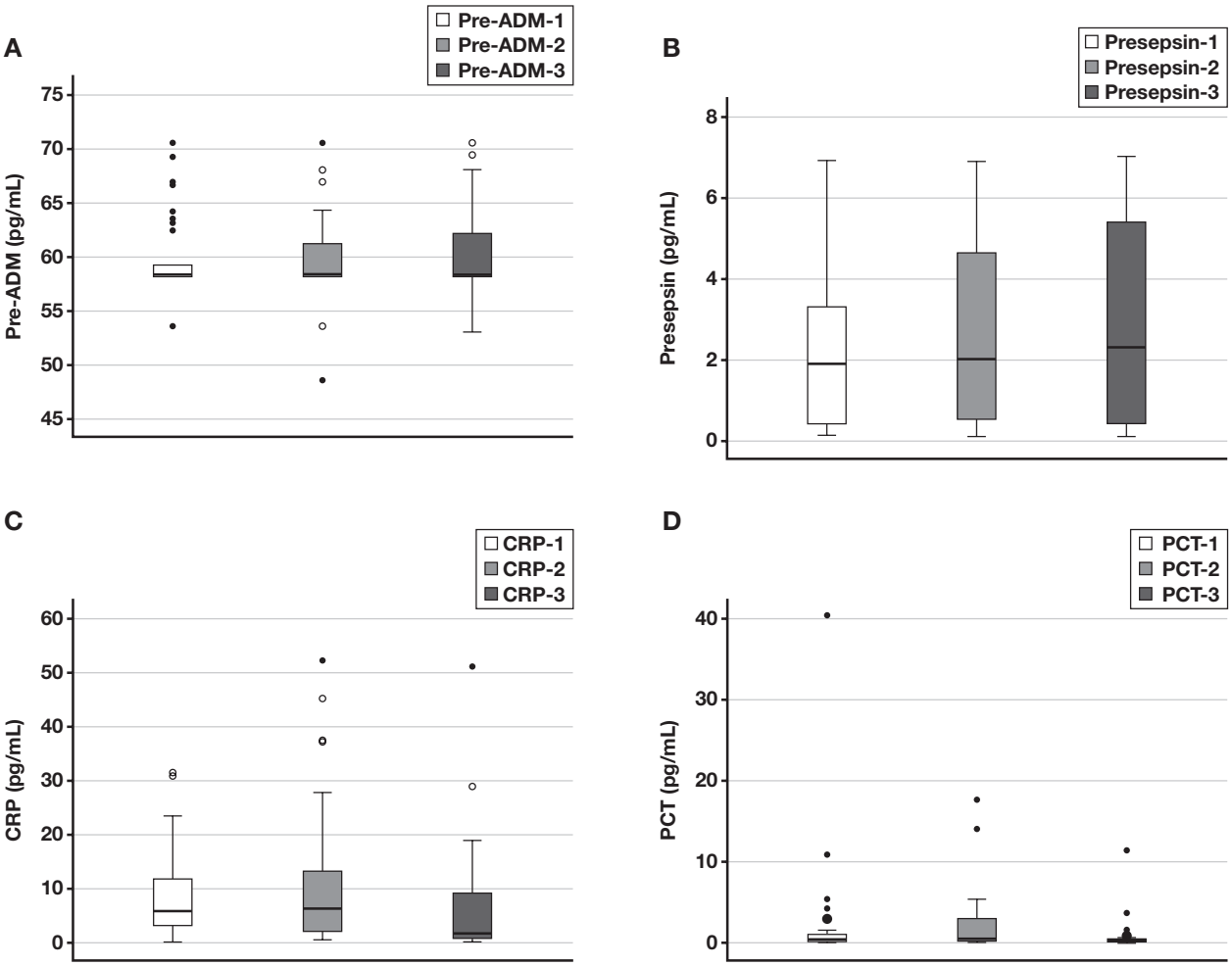

Figure 1

Box-and-whisker plots showing levels of various analytes in patients with febrile neutropenia. Plots show the median (solid black line), 25th and 75th percentiles (ends of boxes), and range (whiskers). **A**, Proadrenomedullin (proADM). **B**, Presepsin. **C**, C-reactive protein (CRP). **D**, Procalcitonin (PCT) levels of patients with febrile neutropenia.

These results show that serum presepsin might have less diagnostic value in patients with neutropenia because of less phagocytosis. However, in our study findings, the baseline and the lowest plasma presepsin levels were not extremely low, as we had expected in patients with severe neutropenia. Thus, we can say that presepsin stays at an appropriate level even in cases of severe neutropenia. This theory might be explained by the recent finding[9] that monocytes, rather than neutrophils, are the dominant producer of presepsin. Production from tissue macrophages or resident monocytes might play a role in maintaining plasma presepsin levels. Another result is that plasma presepsin levels were elevated in the early phase of most bacteremia episodes.

The data have shown a clear relationship between presepsin level and CRP, suggesting the sensitivity and validity of presepsin testing in the evaluation of infection. Median presepsin levels were higher in FN episodes caused by bacterial infections than in FN episodes with no underlying infectious etiology. Correlations between presepsin and CRP values were also discovered in an other study conducted by Koizumi et al.[10] In those study results, serum presepsin level and very low neutrophil count were reliable markers of FN, similar to our findings.

However, the reliability of presepsin in febrile neutropenia has not been well demonstrated so far in the literature. In

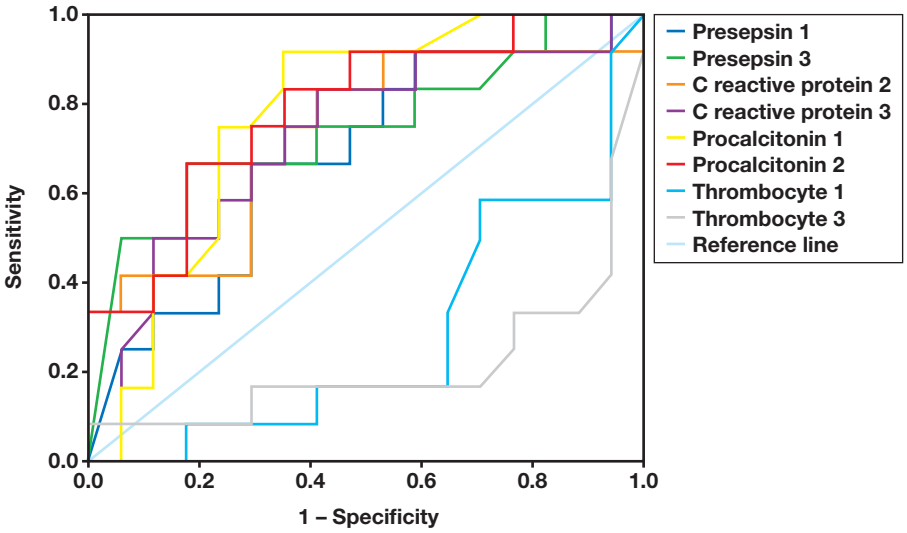

Area Under the Curve

Test Result Variable(s)	Area	Std. Error[a]	Asymptotic Sig.[b]	Asymptotic 95% Confidence Interval	
				Lower bound	Upper bound
Presepsin 1	0.694	0.099	0.080	0.499	0.888
Presepsin 3	0.743	0.098	0.028	0.550	0.935
C reactive protein 2	0.740	0.099	0.030	0.546	0.935
C reactive protein 3	0.723	0.099	0.044	0.528	0.918
Procalcitonin 1	0.775	0.089	0.013	0.601	0.948
Procalcitonin 2	0.789	0.086	0.009	0.621	0.958
Thrombocyte 1	0.277	0.097	0.044	0.087	0.467
Thrombocyte 3	0.213	0.098	0.010	0.021	0.405

Figure 2

Receiver operating characteristics (ROC) of biomarkers in patients with bacteriemic febrile neutropenia, compared with those in patients with nonbacteremic febrile neutropenia. CRP indicates C-reactive protein; PCT, procalcitonin.

the report of a study conducted in adult patients with FN, Koh et al[11] revealed that plasma presepsin level was a reliable marker of FN, even during aggressive chemotherapy in patients with a very low white blood cell count.

In the findings of another study conducted in patients with FN who were older than 16 years, the authors concluded that in patients with FN, presepsin levels were elevated significantly earlier than were PCT levels. Also, they discovered that presepsin may be a more sensitive indicator of bacterial infection than other analytes. Nevertheless, the ability of presepsin to discriminate septic shock from other conditions was inferior to that of PCT.[12]

We also concluded that procalcitonin is a faster-increasing marker, compared with CRP, in FN. Median PCT1 and PCT2 were statistically significantly higher in bacteriemia-induced FN episodes than in FN episodes without identified bacterial etiology. Median PCT1 and -2 levels were also statistically significantly higher in patients with gram negative bacteriemia than patients with gram positive bacteriemia. In a study of patients with FN pediatric hematologic and oncologic manifestations, it was concluded that a significant elevation of presepsin level was statistically significantly higher in bacteremia than clinically proven infection and fever of unknown origin,[13] as in our study findings. These investigators also reported a significant increase in CRP and PCT, as in our study. However, in contrast with the aforementioned study, we checked serum CRP, PCT, and presepsin levels 3 days apart in patients with FN. In multivariate logistic regression analysis, presepsin 1–CRP1, presepsin 1–PCT1, and presepsin 2–PCT2 combinations

DOI: 10.1093/labmed/lmab002

were superior in distinguishing bacteriemia from nonbacterial FN episodes and gram-negative bacteriemia from gram-positive bacteriemia than CRP or PCT by themselves.

To our knowledge, ours is the first study on using serum proADM levels to predict bacteriemia in pediatric patients with FN who harbor hematologic malignant neoplasms. In a published pediatric study report,[14] serum adrenomedullin was not superior or equal to CRP and/or PCR in detecting the severity of infection in patients with FN. However, in an other published study report[15] on pediatric patients with FN who harbored solid tumors, the authors concluded that increased plasma ADM was correlated with high-risk neutropenic fever and culture-positive results.

Despite those findings, in our study, we did not find any difference between bacterial and nonbacterial FN episodes, nor between gram negative and gram positive bacterial FN episodes. Serum proADM1 levels in patients with FN who had bacteriemia were statistically significantly higher than those levels in the control group (P <.001). Serum proADM levels in patients with FN may alert physicians to bacteremic febril neutropenic episodes in pediatric patients with hematological malignant neoplasms; however, further studies are needed to verify or disprove this hypothesis.

In conclusion, plasma presepsin level is a reliable marker of bacteremic FN episodes, even in patients with extremely low neutrophil counts. Evaluation of the increase rate can aid in early diagnosis of bacteremia in FN, in myeloid and lymphoid disorders. Closer monitoring of this molecule, concomitantly with CRP and/or procalcitonin, may guide physicians to select antibiotics in treatment of patients with FN. Serum presepsin levels may be used and combined with serum CRP and/or PCT levels to predict bacteriemia, especially gram negative bacteriemia, in pediatric patients with hematologic malignant neoplasms. **LM**

Personal and Professional Conflicts of Interest

None reported.

References

1. Sharma A, Lokeshwar N. Febrile neutropenia in haematological malignancies. *J Postgrad Med.* 2005;51(5):42–48.
2. Chirouze C, Schuhmacher H, Rabaud C, et al. Low serum procalcitonin level accurately predicts the absence of bacteremia in adult patients with acute fever. *Clin Infect Dis.* 2002;35(2):156–161.
3. Bufler P, Stiegler G, Schuchmann M, et al. Soluble lipopolysaccharide receptor (CD14) is released via two different mechanisms from human monocytes and CD14 transfectants. *Eur J Immunol.* 1995;25(2):604–610.
4. Hirata Y, Mitaka C, Sato K, et al. Increased circulating adrenomedullin, a novel vasodilatory peptide, in sepsis. *J Clin Endocrinol Metab.* 1996;81(4):1449–1453.
5. El Haddad H, Chaftari AM, Hachem R, Chaftari P, Raad II. Biomarkers of sepsis and bloodstream infections: the role of procalcitonin and proadrenomedullin with emphasis in patients with cancer. *Clin Infect Dis.* 2018;67(6):971–977.
6. Ueda S, Nishio K, Minamino N, et al. Increased plasma levels of adrenomedullin in patients with systemic inflammatory response syndrome. *Am J Respir Crit Care Med.* 1999;160(1):132–136.
7. Al Shuaibi M, Bahu RR, Chaftari A-M, et al. Pro-adrenomedullin as a novel biomarker for predicting infections and response to antimicrobials in febrile patients with hematologic malignancies. *Clin Infect Dis.* 2013;56(7):943–950.
8. Taplitz RA, Kennedy EB, Bow EJ, et al. Outpatient management of fever and neutropenia in adults treated for malignancy: American Society of Clinical Oncology and Infectious Diseases Society of America Clinical Practice Guideline Update. *J Clin Oncol.* 2018;36(14):1443–1453.
9. Arai Y, Mizugishi K, Nonomura K, Naitoh K, Takaori-Kondo A, Yamashita K. Phagocytosis by human monocytes is required for the secretion of presepsin. *J Infect Chemother.* 2015;21(8):564–569.
10. Koizumi Y, Shimizu K, Shigeta M, et al. Plasma presepsin level is an early diagnostic marker of severe febrile neutropenia in hematologic malignancy patients. *BMC Infect Dis.* 2017;17(1):27.
11. Koh H, Aimoto M, Katayama T, et al. Diagnostic value of levels of presepsin (soluble CD14-subtype) in febrile neutropenia in patients with hematological disorders. *J Infect Chemother.* 2016;22(7):466–471.
12. Baraka A, Zakaria M. Presepsin as a diagnostic marker of bacterial infections in febrile neutropenic pediatric patients with hematological malignancies. *Int J Hematol.* 2018;108(2):184–191.
13. Demirkaya M, Tugcu D, Akcay A, et al. Adrenomedullin–a new marker in febrile neutropenia: comparison with CRP and procalcitonin. *Pediatr Hematol Oncol.* 2015;32(7):482–489.
14. Kesik V, Ataş E, Gülcan Kurt Y, et al. Adrenomedullin predicts high risk and culture positivity in children with solid tumors suffering from neutropenic fever. *J Infect Chemother.* 2016;22(9):617–621.
15. Agnello L, Bivona G, Parisi E, et al. Presepsin and midregional proadrenomedullin in pediatric oncologic patients with febrile neutropenia. *Lab Med.* 2020;51(6):585–591.

Need for Confirmatory Neutralization Tests for Hepatitis B Surface Antigen Tests in Populations with Intermediate Prevalence

Min Young Lee, MD, PhD, So Young Kang, MD, PhD, Woo In Lee, MD, PhD, Myeong Hee Kim, MD, PhD*

Laboratory Medicine 2021;52:485-492

DOI: 10.1093/labmed/lmab006

ABSTRACT

Objective: Hepatitis B surface antigen (HBsAg) is known as the hallmark of hepatitis B virus (HBV) infection. This study aimed to determine whether an HBsAg neutralization test is necessary to accurately interpret HBsAg test results.

Methods: Initially reactive HBsAg specimens from a 5-year period, with cutoff index values between 1.0 and 2.0, were subjected to neutralization confirmatory testing using an Elecsys HBsAg Confirmatory test kit (Roche Diagnostics GmbH. Mannheim, Germany).

Results: The neutralization test showed 46.1% positive (confirmed positive group) and 53.9% negative (confirmed negative group) results from the total specimens. Among the confirmed negative group, 79.5% of patients were confirmed to be negative for the current infection, whereas 4 patients in the chronic hepatitis B subgroup showed a neutralization percentage close to 40%. More than half of patients in the confirmed positive group were considered to be in the hepatitis B e antigen-negative inactive HBsAg carrier phase.

Conclusion: In populations with intermediate HBV prevalence, a neutralization test is necessary to confirm an HBsAg result and reduce the false positive and false negative rates of initial HBsAg tests.

Keywords: immunology, HBsAg test, neutralization test, confirmatory assay, inactive carrier, false positivity

According to World Health Organization (WHO) 2016 data, an average of 240 million people worldwide have chronic hepatitis B (CHB), and more than 686,000 die each year from complications of hepatitis B virus (HBV) infection, such as cirrhosis and hepatocellular carcinoma (HCC).[1] The epidemiology of hepatitis B can be described in terms of hepatitis B surface antigen (HBsAg) prevalence in a population, broadly classified into low- (<2%), intermediate- (2%–7%), and high- (>8%) prevalence areas.[2] South Korea is an intermediate endemic area for HBV, with an estimated prevalence of 2.6% according to the 2018 Korea National Health and Nutrition Examination Survey.[3]

The diagnosis and monitoring of HBV infection are usually done through laboratory testing for hepatitis B viral markers. In diagnostic virology, HBsAg is the hallmark of active HBV infection. However, the detection of HBsAg for diagnosing HBV infections can present ambiguous false positive reactions that are close to the cutoff values. To overcome this limitation, laboratories utilize several different strategies, such as retest, the 2-assay method, or neutralization confirmatory assay. Many available commercial HBsAg detection kits, such as those of Siemens, Abbott, Bio-Rad, Diasorin, and Roche, use neutralization assay as the gold standard confirmatory assay. However, neutralization assays are usually difficult for clinical use because they require subsequent retest and complex preparations. This study aimed to investigate the role of an HBsAg neutralization test in the diagnosis of chronic HBV infection and the identification of inactive carriers and to assess whether the neutralization test is essential as a confirmatory test for HBsAg test in intermediate endemic areas for HBV.

Abbreviations:

HBsAg, hepatitis B surface antigen; HBV, hepatitis B virus; WHO, World Health Organization; CHB, chronic hepatitis B; HCC, hepatocellular carcinoma; COI, cutoff index; anti-HBs, anti-hepatitis B surface antibody; anti-HBc, anti-hepatitis B core antibody; HBeAg, hepatitis B e antigen; anti-HBe, anti-hepatitis B e antibody; ALT, alanine aminotransferase.

Department of Laboratory Medicine, Kyung Hee University School of Medicine and Kyung Hee University Hospital at Gangdong, Seoul, Korea

*To whom correspondence should be addressed.
sykangmd@daum.net

Materials and Methods

Patients and Study Design

Blood specimens from initially reactive patients with HBsAg, with HBsAg cutoff index (COI) values between 1.0 and 2.0 using an electrochemiluminescent immunoassay analyzer, were taken from 179 participants from January 2015 to December 2019. These specimens were subjected to neutralization confirmatory testing at Kyung Hee University Hospital at Gangdong (Seoul, Korea). If a patient had multiple test results, then the most recent one was included. Individuals with indeterminate or nonvalid results from the neutralization test were excluded. All patients were assessed for their characteristics, medical history, and laboratory findings, including HBV serum markers, HBV DNA, and liver function tests, by chart review. Based on their neutralization test results, the patients were grouped into confirmed positive and confirmed negative groups. Each patient was then further classified into "CHB," "other disease," "indeterminate," and "past infection" subgroups through a review of their clinical information, such as history of HBV infection and HBV test results (Figure 1 and Figure 2). Patients who had a history of CHB or who had a result corresponding to CHB in the HBV test were classified under the CHB group. Patients who had no history of HBV infection and HBV tests, other than the reactive HBsAg test, were classified under the other disease subgroup. However, patients who were HBsAg-reactive who had no history of HBV infection with inconsistent serial HBsAg results and those who were uncertain of their HBV infection history and did not have enough additional HBV tests were classified under the indeterminate subgroup. Among the patients who were HBsAg-reactive, patients positive for anti-hepatitis B surface antibody (anti-HBs) and anti-hepatitis B core antibody (anti-HBc) were classified under the past infection group.

This study was performed in accordance with the principles of the Declaration of Helsinki and was approved by the Gangdong Kyung Hee University Hospital Ethics Committee (IRB number KHNMC 2020-04-013).

HBsAg Screening

The blood specimens were centrifuged at 3000 rpm for 10 minutes, followed by screening for HBsAg using

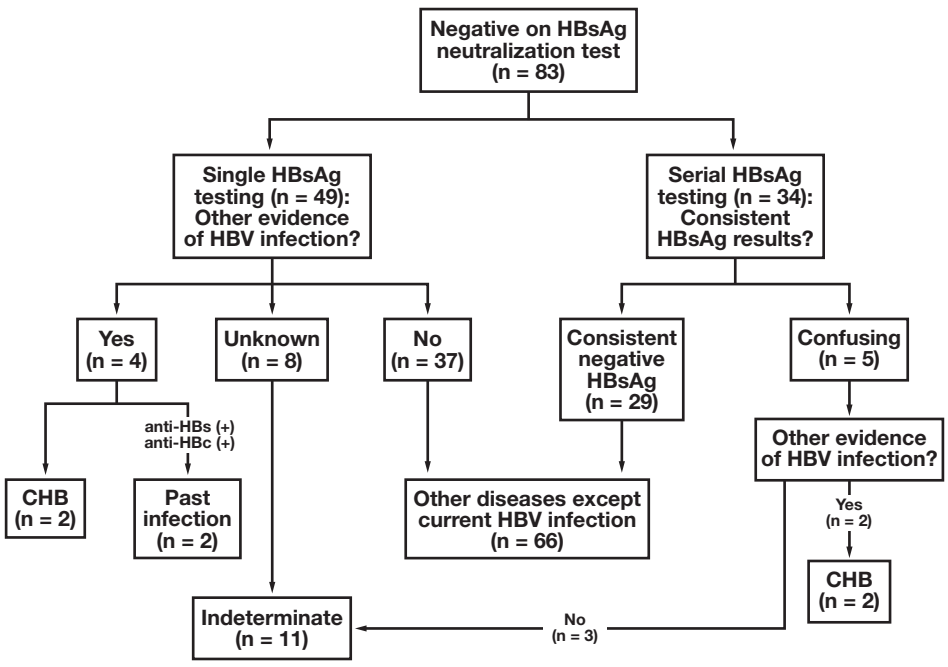

Figure 1

Flow chart of the HBsAg confirmed negative group for diagnosis of CHB. anti-HBc, anti-hepatitis B core antibody; anti-HBs, anti-hepatitis B surface antibody; CHB, chronic hepatitis B; HBsAg, hepatitis B surface antigen; HBV, hepatitis B virus.

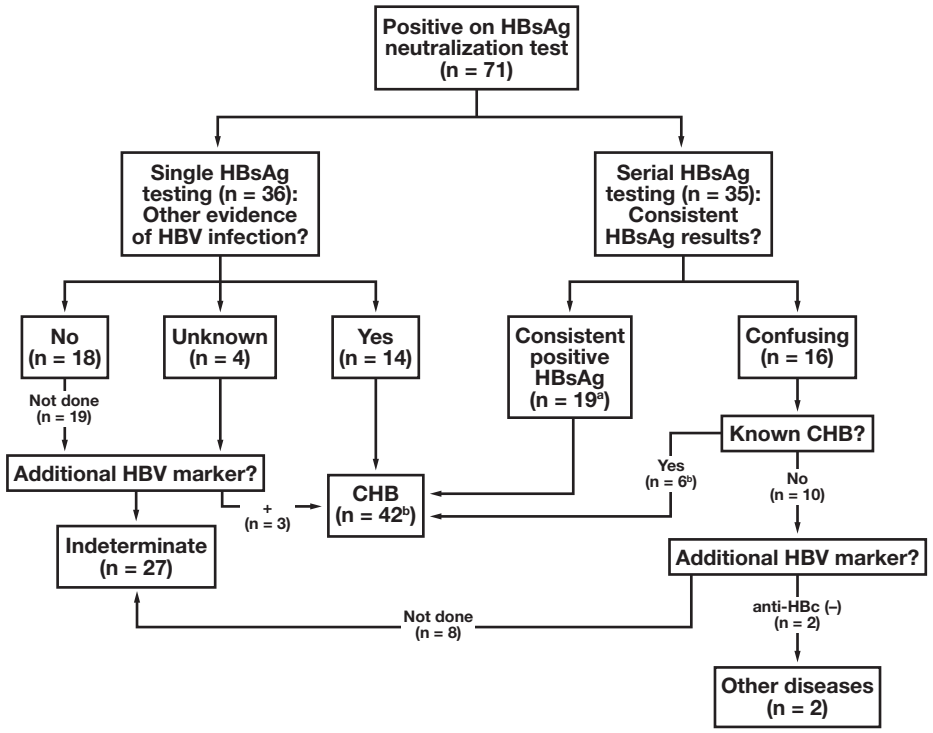

Figure 2

Flow chart of the HBsAg confirmed positive group for diagnosis of chronic hepatitis B infection. AHB, acute hepatitis B; anti-HBc, anti-hepatitis B core antibody; CHB, chronic hepatitis B; HBsAg, hepatitis B surface antigen; HBV, hepatitis B virus.

the Roche Cobas e801 module, with reagents from the Elecsys HBsAgII kit (Roche Diagnostics GmbH, Mannheim, Germany) in accordance with the manufacturer's recommendations. The result from a specimen was shown as either nonreactive (COI < 0.90), borderline (0.90 ≤ COI < 1.0), or reactive (COI ≥ 1.0). Retesting in duplicates of specimens with an initial COI ≥ 0.9 was automatically performed in the system.

HBsAg Neutralization Assay

HBsAg confirmatory testing was performed using the Roche Cobas e801 module and the Elecsys HBsAg Confirmatory test kit (Roche Diagnostics GmbH). According to the manufacturer's recommendation, the results were interpreted as follows. To confirm a positive result, the COI of the specimen with the confirmatory reagent (confirmatory COI value) was set to ≤ 60% of the control reagent (the control COI value), with a cutoff index of ≥ 0.81. Specimens were considered to have nonreactive (ie, negative) results if the control COI value was ≥ 0.81 and the ratio of the confirmatory COI value to the control COI was > 60%. If the control COI was < 0.81 and the ratio was ≤ 60%, then the specimen was considered indeterminate. If the ratio was > 60% and the control CI was < 0.81, the value was nonvalid. The percentage of neutralization was obtained by the equation {1- (the confirmatory COI value / the control COI value)} × 100.

Statistical Analysis

SPSS version 20.0 software (SPSS Inc., Chicago, IL) was used for data analysis. Data were tested for normal distribution using the Kolmogorov-Smirnov test. Data were then presented as mean ± standard deviation. Statistical comparisons were calculated using the Kruskal-Wallis test and the Mann-Whitney *U* test, and the number of patients with CHB according to neutralization percentage was analyzed using the χ^2 test for trend (linear by linear association).

Lab Medicine 2021;52;485–492
DOI: 10.1093/labmed/lmab006

Results

Patient Characteristics

Of the 179 participants with initial HBsAg COI values of 1.0 to 2.0, those with indeterminate (n = 3), nonvalid (n = 5), and multiple test (n = 17) results were excluded, leaving 154 participants for the study. The neutralization test as a confirmatory test yielded 71 (46.1%) positive results and 83 (53.9%) negative results. The median of the neutralization percentages obtained from the confirmed positive and negative groups were 60% and 0.1%, respectively. No statistically significant differences were observed between men and women within the confirmed negative and positive groups. The mean age and HBsAg COI value in the confirmed positive group were 57 years and 1.47, respectively, which were higher than those of the confirmed negative group (35 years and 1.28, respectively; **Table 1**).

Confirmed Negative Group

Among the confirmed negative group (n = 83), 66 patients (79.5%) were classified under the other disease subgroup, 11 (13.3%) under the indeterminate subgroup, 4 (4.8%) under the CHB subgroup, and 2 (2.4%) under the past infection subgroup (**Table 2**). The distribution of neutralization percentages is summarized in **Table 2** and **Figure 3**. Most of the patients who had negative results in the neutralization test were classified under the other disease group. All of the other disease patients showed a neutralization percentage of < 10%. On the other hand, 4 patients in the CHB subgroup who had negative results in the neutralization test showed neutralization percentages close to 40%, which was the cutoff of the neutralization test. There were 7 patients with neutralization percentages of > 10%: 4 in the CHB subgroup (27.7%, 34.2%, 37.1%, and 39.7%), 2 in the past infection subgroup (15.4% and 27.8%), and 1 in the indeterminate subgroup (34.2%). A negative neutralization test result was considered as a false negative, at least in the 4 patients with CHB, because they showed significantly higher percentages (34.7 ± 2.58; P <.001) than the other patients in the negative group (2.5 ± 0.60). In addition, in the disease course of hepatitis B infection, HBsAg and anti-HBs generally exist mutually exclusively. The serial test results of anti-HBs and HBsAg helped determine whether HBsAg was actually negatively converted. Clinical information and the results of the HBV tests for the 4 patients with CHB are summarized in **Table 3**.

In the indeterminate subgroup (n = 11), 8 patients had anti-HBs whereas 10 showed a very low neutralization percentage of < 5%. Therefore, most patients in the indeterminate subgroup were considered not to have HBV infection.

Confirmed Positive Group

In the confirmed positive group (n = 71), 42 patients (59.2%) were classified under the CHB subgroup (including 1 patient with acute hepatitis B), 27 (38%) under the indeterminate subgroup, and the remaining 2 under the other disease subgroup (**Table 2**). Among the 42 patients in the CHB subgroup, hepatitis H e antigen (HBeAg)/anti-hepatitis B e antibody (anti-HBe) and HBV DNA tests were performed for 23 and 15 patients, respectively. There were 22 patients with HBeAg-negative/anti-HBe-positive results and 1 with HBeAg-negative/anti-HBe-negative results. We did not detect HBV DNA in 7 of the 15 patients, and low levels of HBV DNA were detected in the remaining 8. Viral loads were 3.20×10^1 IU/mL, 5.50×10^1 IU/mL, 6.06×10^1 IU/mL, and 1.99×10^2 IU/mL for 4 patients, respectively, and was < 20 IU/mL in the remaining 4 patients. The CHB patients with HBeAg-negative/anti-HBe-positive and low or undetected HBV DNA were considered to be in the HBeAg-negative inactive carrier phase.

The patients in the indeterminate subgroup with positive neutralization results were those who had undergone HBsAg/anti-HBs testing during health screening, checkup for operation, or hospitalization, without any additional HBV tests or history of HBV infection. Of the 27 patients in this subgroup, 19 reported undergoing the HBsAg/anti-HBs test once, whereas the remaining 8 patients reported having undergone the test twice or more consecutively over the months, showing inconsistent results. These patients were mainly older adults, with a mean age of 55 years, and had alanine aminotransferase (ALT) values within the reference range except for 1 patient with HCC (data not shown). Two patients in the other disease subgroup showed positive neutralization results, with neutralization percentages within 50% to 60%. However, they both had no history of HBV infection and showed negative results in the repeated HBsAg and additional HBV tests. For both patients, follow-up HBsAg results performed 3 months later showed values near the cutoff, with negative results. Therefore, the initial reactive HBsAg and

Table 1. Clinical characteristics of HBsAg negative and positive groups confirmed by neutralization test

	HBsAg Confirmed-Negative Group (n = 83; 53.9%)	HBsAg Confirmed-Positive Group (n = 71; 46.1%)	*P* Value
Sex, M:F	1:0.66	1:0.69	
Age, y, mean ± SD	35 ± 19.0	57 ± 16.1	.14
COI, mean ± SD	1.28 ± 0.26	1.47 ± 0.32	.004
Median	1.22	1.50	
Percentage of neutralization, mean ± SD (%)	4.1 ± 8.7	60.6 ± 11.0	<.001
Median	0.1	60.0	
Range	0-39.7	41.2-83.5	
Results for HBV viral markers			
Anti-HBs, number of patients			
Positive	53 (63.9%)	12 (16.9%)	<.001
HBeAg/anti-HBe, number of patients			
Negative/positive	2[a]	22[b]	
Negative/negative	1[c]	3[d]	
Not done	80	46	
Anti-HBc, number of patients			
Negative	3	25	
Positive	4	14	
Not done	76	55	
HBV DNA, Number of patients			
Negative	2	9[e]	
Positive	0	8	
Not done	84	54	
Results for ALT			
Median, U/L	14	21	.44
Number of patients with higher ALT level than cutoff value	8/79	9/70	
Diagnosis for HBV infection			
CHB	4	42[f]	
Past HBV infection	2	0	
Other diseases except current HBV infection	66	2	
Indeterminate	11	27	

AHB, acute hepatitis B; ALT, alanine aminotransferase; anti-HBc, anti-hepatitis B core antibody; anti-HBe, anti-hepatitis B e antibody; anti-HBs, anti-hepatitis B surface antibody; CHB, chronic hepatitis B; COI, cutoff index; HBeAg, hepatitis B e antigen; HBsAg, hepatitis B surface antigen; HBV, hepatitis B virus; SD, standard deviation.
[a]*Known CHB patients.*
[b]*Known CHB patients.*
[c]*Past HBV infection.*
[d]*Two patients with other disease except current HBV infection and 1 known patient with CHB patient.*
[e]*Seven known patients with CHB and 2 patients with other diseases except current HBV infection.*
[f]*Including 1 patient with AHB.*

positive neutralization test results were both considered to be false positives (**Table 3**).

The distribution of neutralization percentages is summarized in **Table 2** and **Figure 3**. The distribution of patients was as follows: 15, 23, 17, and 16 patients in the 40% to 50%, 50% to 60%, 60% to 70%, and > 70% neutralization percentages, respectively. In particular, the patients with CHB were distributed as 5 (33.3%), 14 (60.9%), 11 (64.7%), and 12 (75%) patients in the 40% to 50%, 50% to 60%, 60% to 70%, and > 70% of neutralization percentages, respectively. As the neutralization percentage increased, the number of patients in the CHB subgroup tended to increase, although statistical significance was not observed ($P = .071$).

Discussion

Infection with HBV is a potentially life-threatening disease that shows a variety of viral marker profiles depending on the phase of the disease. There is currently no diagnostic marker that has proven to be complete, clear, and easy to interpret. In 2017, the WHO recommended adopting a testing strategy for diagnosing CHB according to national seroprevalence.[4] In populations with an HBsAg seroprevalence of ≥ 0.4%, a single serological assay for detection of HBsAg is recommended. In populations with a low HBsAg seroprevalence of < 0.4%, confirmation

Lab Medicine 2021;52;485–492 489
DOI: 10.1093/labmed/lmab006

Table 2. Distribution of diagnosis for HBV infection according to the percentage of neutralization

Percentage of Neutralization	Number of Patients (%)	Mean COI of HBsAg	Diagnosis			
			Other Diseases (n)	CHB (n)	Indeterminate (n)	Past HBV Infection (n)
Confirmed-negative group (%)						
0	41 (49.4)	1.31	36	0	5	0
0.1-10	35 (42.2)	1.26	30	0	5	0
10-20	1 (1.2)	1.40	0	0	0	1
20-30	2 (2.4)	1.37	0	1	0	1
30-40	4 (4.8)	1.11	0	3	1	0
Total	83		66	4	11	2
Confirmed-positive group (%)						
40-50	15 (21.1)	1.30	0	5	10	0
50-60	23 (32.4)	1.28	2	14	7	0
60-70	17 (23.9)	1.56	0	11	6	0
>70	16 (22.5)	1.77	0	12	4	0
Total	71		2	42	27	0

CHB, chronic hepatitis B; COI, cutoff index; HBsAg, hepatitis B surface antigen; HBV, hepatitis B virus.

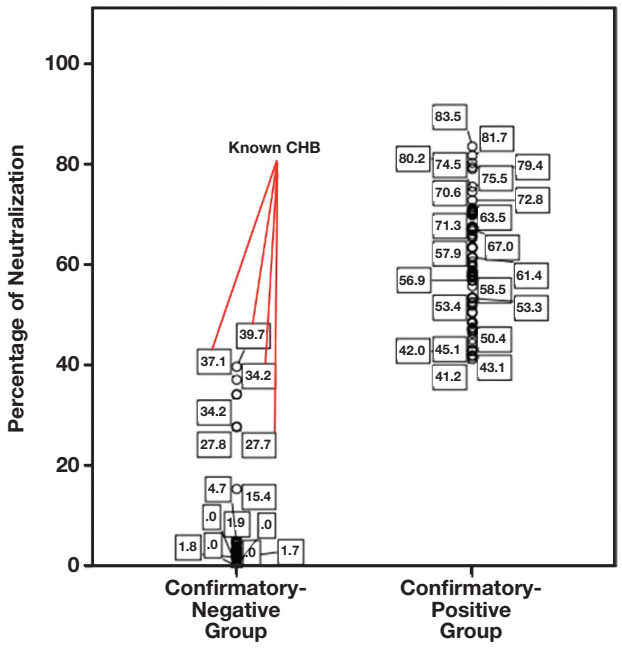

Figure 3

The percentage of neutralization for the HBsAg confirmed negative group and the confirmed positive group. Four known patients with CHB, indicated by the red line in the confirmed negative group, had high neutralization percentages of 25% to 40%. CHB, chronic hepatitis B virus; HBsAg, hepatitis B surface antigen.

of HBsAg positive result with a neutralization step or a second rapid diagnostic test assay for HBsAg detection may be considered.[4] South Korea has a seroprevalence of > 0.4%; thus, a single assay method for testing can be applied according to WHO recommendations. However, available commercial HBsAg detection kits emphasize the necessity to confirm HBsAg reactivity using neutralization tests. Because of this contradiction between statements, clinical laboratories are using policies that are not uniform.

Table 3. Summary of patients with false neutralization test results

Sex/age (y)	Mean COI of HBsAg	Percentage of Neutralization (%)	Diagnosis	Anti-HBs	Anti-HBc	HBV DNA	HBeAg/ anti-HBe	ALT (U/L)	Serial HBsAg/ anti-HBs
False-negatives									
M/57	0.99	27.7	CHB	N	ND	ND	N/P	23	P<u>N</u>[a]N/N<u>N</u>[a]P
F/71	1.08	34.2	CHB	N	ND	ND	ND	18	PP<u>N</u>[a]/NN<u>N</u>[a]
M/58	1.16	37.1	CHB	N	ND	ND	N/P	47	ND
F/47	1.15	39.7	CHB	N	ND	ND	ND	14	ND
False-positives									
M/61	1.28	53.3	KTP donor	N	N	N	N/N	25	P[a]N/N[a]N
M/20	1.55	58.5	Crohn disease	N	N	N	N/N	9	P[a]N/N[a]N

ALT, alanine aminotransferase; anti-HBs, anti-hepatitis B surface antibody; anti-HBc, anti-hepatitis B core antibody; anti-HBe, anti-hepatitis B e antibody; CHB, chronic hepatitis B; COI, cutoff index; HBeAg, hepatitis B e antigen; HBsAg, hepatitis B surface antigen; N, negative; ND, not done; P, positive; KTP, kidney transplantation.
[a]*The results of tests conducted during the study period.*

In this study, 83 (54%) patients who were HBsAg-reactive with low COI values between 1.0 and 2.0 showed negative results in neutralization tests, whereas 66 patients (43%) were considered not to have HBV infection. This finding means that at least 43% of the reactive HBsAg tests with a low COI between 1.0 and 2.0 were false positives and would be reported as positive if the neutralization test was not performed. A study[5] conducted in China, which has a higher HBsAg seroprevalence than Korea, reported similar results to this study wherein approximately 42.2% of the results were confirmed negative (false positives) by using a neutralization assay on blood specimens with an initial COI of between 1.0 and 2.0.

Among the confirmed positive patients with low COI values between 1.0 and 2.0, 59% had CHB. Based on their long history of HBV infection, older age (60.02 ± 2.10 years), and other laboratory testing results, including HBeAg/anti-HBe and HBV DNA results, most patients were considered to be in the HBeAg-negative inactive HBsAg carrier phase with an undetectable or low viral load, even though not all patients had HBeAg/anti-HBe and/or HBV DNA test results. In addition, 27 patients (38%) in the confirmed positive group were classified under the indeterminate subgroup, all of whom lacked sufficient information to determine whether or not they had HBV infection other than a reactive HBsAg and a positive neutralization result. These patients, with their older age (54.35 ± 3.03 years) and ALT values within the reference range, were likely to be accidentally discovered inactive HBsAg carriers even without any medical records and test results for HBV infection.

Patients who are HBeAg-negative inactive HBsAg carriers have persistent HBV infection of the liver without continuous significant necroinflammatory disease; such patients have good prognosis with low risk of complication. On the other hand, patients with active CHB who are HBeAg-negative have active liver disease with a high risk of progression to liver cirrhosis or HCC.[6] Prolonged biochemical and virological follow-up are mandatory to distinguish between the 2 conditions. To be diagnosed as an inactive HBV carrier, it is required that ALT levels and HBV DNA levels be followed up for a minimum of 1 year. Subsequently, once a patient is diagnosed as an inactive HBV carrier, periodic lifelong measurement of ALT and HBV DNA is necessary.[7, 8] Therefore, if a patient with a low reactive HBsAg result shows a normal serum ALT level and undetected HBV DNA, then the HBsAg result should not be considered as a false positive and should not be overlooked without a neutralization test. According to the results of this study, there were many newly diagnosed patients who were HBV carriers and patients who were known inactive HBV carriers. It is necessary to accurately evaluate patients with low reactive HBsAg by neutralization test to avoid missing HBV carriers.

There are some limitations in this study. First, there were many patients in the indeterminate subgroup because additional viral marker tests were not performed for all included patients. Thus, true diagnostic accuracy, such as the positive/negative predictive value of the neutralization test, could not be calculated. Second, the neutralization tests were performed only on HBsAg-reactive specimens with a limited COI range of 1.0 to 2.0. Shao et al[5] showed that when the COI of the initial test was within the range of 1.0 to 2.0, the confirmed rate was only 57.78%, which increased to 83.3% when the initial COI was between 2 and 4. Further studies will be needed by conducting neutralization tests for enough patients and with a wide range of COI to determine the COI range that should be confirmed by neutralization test. Third, there may have been some false positives or false negatives on the neutralization tests as shown in **Table 3**. However, the evaluation of the accuracy

DOI: 10.1093/labmed/lmab006

for the cutoff (40%) of the neutralization test applied to this study was not performed.

Conclusion

In this study, we evaluated the significance and importance of neutralization tests as confirmatory tests for low reactive HBsAg with values close to the COI cutoff and analyzed patients identified as confirmed-negative and confirmed-positive. In patients with low reactivity in the initial HBsAg test, > 40% were false positives. Therefore, the neutralization test significantly reduces the false positive rate of the initial HBsAg test. Because additional viral marker testing and continuous follow-up are essential for inactive HBV carriers, confirmation of the patient's HBsAg status by neutralization tests is important to help classify the disease stage. In conclusion, if the initial HBsAg test shows a low COI value, then the neutralization test is still necessary to confirm a positive or negative HBsAg result in populations with intermediate HBV prevalence. **LM**

Acknowledgments

SYK and WIL designed the study and MYL wrote the article. SYK, MYL, and MHK carried out the data management and analysis. All authors have agreed with the final version of the article.

References

1. Global hepatitis report, 2017. World Health Organization website. https://www.who.int/hepatitis/publications/global-hepatitis-report2017/en/. Published April 2017. Accessed January 24, 2021.
2. Previsani N, Lavanchy D, Zuckerman A. Hepatitis B. 2002. *Perspect Med Virol.* 2002;10:31–98.
3. Kweon S, Kim Y, Jang MJ, et al. Data resource profile: the Korea National Health and Nutrition Examination Survey (KNHANES). *Int J Epidemiol.* 2014;43(1):69–77.
4. Guidelines on hepatitis B and C testing. World Health Organization website. https://www.who.int/hepatitis/publications/guidelines-hepatitis-c-b-testing/en/ Published February 2017. Accessed January 24, 2021.
5. Shao H, Li Y, Xu W-Z, et al. Increased need for testing to confirm initial weakly reactive results for hepatitis B virus surface antigen. *Lab Med*. 2012;43(4):15–17.
6. Puoti C. HBsAg carriers with normal ALT levels: healthy carriers or true patients? *Brit J Gen Prac*. 2013;6(1):4–6.
7. Liver EAFTSOT. EASL clinical practice guidelines: management of chronic hepatitis B virus infection. *J Hepatol.* 2012;57(1):167–185.
8. Papatheodoridis GV, Manolakopoulos S, Liaw YF, Lok A. Follow-up and indications for liver biopsy in HBeAg-negative chronic hepatitis B virus infection with persistently normal ALT: a systematic review. *J Hepatol.* 2012;57(1):196–202.

Clinical Utility of Midregional Proadrenomedullin in Patients with COVID-19

Bruna Lo Sasso, PhD,[1,2] Caterina Maria Gambino, PhD,[1] Nicola Scichilone, MD,[3] Rosaria Vincenza Giglio, PhD,[1] Giulia Bivona, MD,[1] Concetta Scazzone, BS,[1] Roberto Muratore, BS,[2] Salvatore Milano, BS,[2] Mario Barbagallo, MD,[4] Luisa Agnello, PhD,[1] Marcello Ciaccio, MD[1,2,]*

Laboratory Medicine 2021;52:493-498

DOI: 10.1093/labmed/lmab032

ABSTRACT

Objective: The aim of the study was to assess the role of midregional proadrenomedullin (MR-proADM) in patients with COVID-19.

Methods: We included 110 patients hospitalized for COVID-19. Biochemical biomarkers, including MR-proADM, were measured at admission. The association of plasma MR-proADM levels with COVID-19 severity, defined as a requirement for mechanical ventilation or in-hospital mortality, was evaluated.

Results: Patients showed increased levels of MR-proADM. In addition, MR-proADM was higher in patients who died during hospitalization than in patients who survived (median, 2.59 nmol/L; interquartile range, 2.3–2.95 vs median, 0.82 nmol/L; interquartile range, 0.57–1.03; $P < .0001$). Receiver operating characteristic curve analysis showed good accuracy of MR-proADM for predicting mortality. A MR-proADM value of 1.73 nmol/L was established as the best cutoff value, with 90% sensitivity and 95% specificity ($P < .0001$).

Conclusion: We found that MR-proADM could represent a prognostic biomarker of COVID-19.

Keywords: biomarker, COVID-19, inflammation, MR-proADM, respiratory disease

COVID-19 is caused by SARS-CoV-2, which primarily infects the respiratory system in humans. It is characterized by a broad spectrum of clinical manifestations with varying degrees of severity, from asymptomatic form to pneumonia, which can evolve into acute respiratory distress syndrome and multiorgan failure syndrome, until death.[1-4]

SARS-CoV-2 internalization occurs by the viral spike glycoprotein that binds to angiotensin-converting enzyme 2 (ACE2), which is mainly expressed on type II alveolar epithelial cells, myocardial cells, proximal tubule cells of the kidney, bladder urothelial cells, and enterocytes.[5,6] This interaction results in the downregulation of ACE2 expression and excessive angiotensin production, enhancing an inflammatory response that contributes to acute organ injury.[7]

The clinical course of the disease is unpredictable, and there is an urgent need for biomarkers that could reliably stratify patients into different classes of risk. Early identification of hospitalized patients who are more vulnerable to clinical deterioration could guide clinicians for risk stratification and monitoring.

The hallmark of SARS-CoV-2 infection is the activation of the immune system, which can lead to an uncontrolled and

Abbreviations:

MR-proADM, midregional proadrenomedullin; ACE2, angiotensin-converting enzyme 2; IL, interleukin; CRP, C-reactive protein; PCT, procalcitonin; ADM, adrenomedullin; ICU, intensive care unit; LOS, length of stay; ALT, alanine aminotransferase; AST, aspartate aminotransferase; CK, creatine kinase; LDH, lactate dehydrogenase; sCR, serum creatinine; hs-TnT, high-sensitivity troponin T; eGFR, estimated glomerular filtration rate; IQR, interquartile range; ROC, receiver operating characteristic; CI, confidence interval; AUC, area under the curve.

[1]Department of Biomedicine, Neurosciences and Advanced Diagnostics, Institute of Clinical Biochemistry, Clinical Molecular Medicine and Laboratory Medicine, University of Palermo, Palermo, Italy, [2]Department of Laboratory Medicine, AOUP P. Giaccone, Palermo, Italy, [3]Department of Health Promotion Sciences, Maternal and Infant Care, Internal Medicine and Medical Specialties, University of Palermo, Palermo, Italy, [4]Department of Internal Medicine and Geriatrics, Geriatric Unit, University of Palermo, Italy

*To whom correspondence should be addressed.
marcello.ciaccio@unipa.it

generalized inflammatory response and to the so-called cytokine storm.[8] Indeed, patients with COVID-19 have significantly increased circulating levels of inflammatory biomarkers, such as interleukin (IL)-6, C-reactive protein (CRP), and procalcitonin (PCT). Moreover, several biochemical parameters, such as D-dimer, cardiac troponin, and homocysteine, are altered.[9-13] These biomarkers have been associated with disease severity and mortality.[2,14,15] However, there is ongoing research for biomarkers to better define the biochemical phenotype of COVID-19 patients to improve their management.

Midregional proadrenomedullin (MR-proADM) is a surrogate biomarker of adrenomedullin (ADM), a 52–amino acid peptide belonging to the Calc gene family. Under physiological conditions, ADM levels are very low. Several factors, including catecholamines, hypoxia, oxidative stress, inflammatory mediators, and cytokines, induce their increase.[16] Thus, it has been evaluated in several inflammatory conditions.[17,18] However, the measurement of ADM has several technical issues, such as a short half-life and rapid degradation by proteases. The more stable MR-proADM provides a solution to these problems. The latter is secreted in equimolar amounts with ADM and is more stable in vitro. Moreover, it can be easily measured on a fully automated platform.

Research has recently proposed MR-proADM as a biomarker of organ failure.[19-22] Specifically, increased MR-proADM levels have been associated with short- and long-term mortality in patients with community-acquired pneumonia and sepsis.[23-26] In addition, MR-proADM has emerged as a prognostic biomarker in critically ill patients admitted to the intensive care unit (ICU) independently by their underlying clinical conditions.[23,24] Considering that patients with COVID-19 are at high risk of developing organ failure, MR-proADM could represent a useful prognostic biomarker.

The aim of the present study was to evaluate the potential prognostic value of MR-proADM to predict in-hospital mortality in patients with COVID-19.

Methods

Study Population

In this retrospective observational study, we enrolled all consecutive adult patients admitted to the COVID-19 units at the University Hospital P. Giaccone in Palermo, Italy, from September to October 2020. A SARS-CoV-2 infection was confirmed by a positive real-time reverse-transcription polymerase chain reaction mainly using naso-oropharyngeal swabs, in accordance with guidelines.[27]

Demographical and clinical information, including the length of stay (LOS), in-hospital mortality, and admission to ICU, was recorded for each patient. The primary endpoints for assessing COVID-19 severity were the requirement for mechanical ventilation and in-hospital mortality.

The local ethics committee approved the study, and all the clinical and biological assessments were carried out in accordance with the Declaration of Helsinki. For privacy respect, each patient was identified with an alphanumeric code. Informed consent was not required because the blood specimen used for study procedures was residual material that would have otherwise been discarded.

Hematological and Biochemical Analysis

All laboratory analyses were performed at the Laboratory Medicine Unit of the University Hospital P. Giaccone in Palermo. Routine hematological and biochemical parameters were measured upon admission. Specifically, hematological tests, including red and white blood cells, platelets, neutrophils, lymphocytes, and monocytes, were performed using the UniCel DxH 900 hematology analyzer (Beckman Coulter's Inc., Brea, CA).

Serum biochemical parameters, including alanine aminotransferase (ALT), aspartate aminotransferase (AST), total bilirubin, creatine kinase (CK), lactate dehydrogenase (LDH), serum creatinine (sCR), high-sensitivity troponin T (hs-TnT), vitamin D, high-sensitivity CRP, IL-6, and PCT were measured on the Cobas 8000 (Roche, Basel, Switzerland), according to the manufacturer's procedures. The estimated glomerular filtration rate (eGFR) was calculated using the Chronic Kidney Disease EPIdemiology collaboration equation expressed for specified race, sex, and sCR in mg/dL.[28]

After the routine analyses were performed, an aliquot of plasma was collected within 3 hours of blood collection and stored at –80°C. The MR-proADM was measured by the time-resolved amplified cryptate emission technology (TRACE-Kryptor MR-proADM; BRAHMS AG, Henningsdorf, Germany), as previously described.[19,24] The MR-proADM

assay has a limit of detection of 0.05 nmol/L and a limit of quantification of 0.23 nmol/L, as declared by the manufacturer.

Statistical Analysis

Statistical analysis was performed using MedCalc v12.1.4.0 statistical software (MedCalc Software, Mariakerke, Belgium). Demographic and clinical characteristics were expressed as frequencies (percentage) for categorical data and median with interquartile ranges (IQR) for continuous data.

A Spearman correlation coefficient was used to assess the relationships between plasma MR-proADM levels and several clinical and laboratory parameters. Finally, receiver operating characteristic (ROC) curves with 95% confidence intervals (CI) were calculated to assess the prognostic ability of MR-proADM. A *P* value <.05 was considered statistically significant in all the calculations.

Results

Demographic and Clinical Features

One hundred ten patients admitted to converted COVID-19 units for SARS-CoV-2 infection were included in the study. Demographic and baseline clinical characteristics of patients are shown in **Table 1**.

Overall, 92 (84%) patients had pneumonia, and none of the patients at admission required intubation; 60 (55%) had more severe infections and needed noninvasive ventilation with positive airway pressure, and 50 (45%) had moderate respiratory symptoms. The median LOS was 13 days (IQR, 8–19). According to the clinical course of the disease, 2 (2%) patients were transferred to the ICU, and 14 patients (13%) died during hospitalization. The median (IQR) time to death was 9 (8–10) days.

Laboratory Findings

Table 2 shows the laboratory test findings. In the overall study population, we observed lymphocytopenia (lymphocytes <1.50 × $10^3/\mu L$). On admission, most patients showed normal levels of AST, ALT, total bilirubin, sCR, LDH, and CK. A weak increase in serum D-dimer and hs-TnT concentrations were observed in 37% and 51% of patients, with a median level of 850 ng/mL (IQR, 477–1420) and 19 pg/mL (IQR, 16–35), respectively. In addition, a moderate decrease in vitamin D levels in most patients (76%) was found, with a median level of 23 ng/mL (IQR,15.5–30). Similarly, eGFR values were reduced in only 24% of patients.

Table 1. General Characteristics, Comorbidities and Clinical Outcomes in the Study Population (n = 110)

Demographic Characteristics	
Median age, (IQR), y	62 (52–76)
Male sex, n (%)	61 (55)
Comorbidities	
Chronic respiratory disease, n (%)	93 (84)
Chronic kidney disease, n (%)	6 (5)
Diabetes, n (%)	8 (7)
Hypertension, n (%)	19 (17)
Severe cardiovascular disease, n (%)	2 (2)
Clinical outcomes	
Hospital stay, median (IQR), d	13 (8–19)
Hospital discharge, n (%)	29 (26)
ICU transfer, n (%)	2 (2)
Death, n (%)	14 (13)

ICU, intensive care unit; IQR, interquartile range.

As reported in **Table 2**, inflammation was the prominent feature of our studied population, with significantly higher CRP and IL-6 levels. In particular, CRP was >40 mg/L in nearly half of patients (47%), and IL-6 was elevated in 81 (74%) patients with a median level of 19 pg/mL (IQR, 7–38). The PCT was increased in 17 (15%) patients (median levels 0.103 ng/mL; IQR, 0.05–0.17).

In addition to classical inflammatory biomarkers, MR-proADM plasma levels were also significantly increased in 79 (72%) patients, with a median level of 0.93 nmol/L (IQR, 0.58–1.09).

We found that MR-proADM levels were correlated with biochemical parameters reflecting inflammation. In particular, we observed a statistically significant correlation between MR-proADM and CRP (r = .49; 95% CI, 0.30–0.64; P <.0001), LDH (r = .56; 95% CI, 0.39–0.69; P <.0001), IL-6 (r = .50; 95% CI, 0.29–0.66; P <.0001), PCT (r = .58; 95% CI, 0.39–0.73; P <.0001), and hs-TnT (r = .80; 95% CI, 0.68–0.88; P <.0001) values. Moreover, MR-proADM had a weakly positive correlation with total bilirubin (r = .28; 95% CI, 0.01–0.48; P = .01)

DOI: 10.1093/labmed/lmab032

Table 2. Laboratory Findings of Study Population (n = 110)

	Median (IQR)	Reference Interval	
Hematological parameters		**M**	**F**
White blood cell count, $10^3/\mu L$	8.0 (5.96–10.8)	3.6–10.2	3.8–11.8
Neutrophils, $10^3/\mu L$	6.2 (3.90–8.90)	1.7–8.2	
Lymphocytes, $10^3/\mu L$	0.90 (0.68–1.30)	1.0–3.2	
Monocytes, $10^3/\mu L$	0.55 (0.20–0.70)	0.2–1.1	
Eosinophils, $10^3/\mu L$	0 (0–0.02)	0–0.5	
Basophils, $10^3/\mu L$	0.01 (0–0.02)	0–0.1	
Red cells, $10^6/\mu L$	4.5 (4.1–4.8)	4.0–5.6	3.6–4.9
Hemoglobin, g/dL	13.4 (12–14)	12.5–16.0	11.0–14.0
MCV, fL	85 (82–90)	75–95	
MCH, pg	29 (28–31)	30–36	
RDW, fL	42 (39–44)	36.5–50.3	
Platelets, $10^3/\mu L$	222 (155–307)	150–400	
Biochemical parameters			
ALT, U/L	34 (21–51)	0–41	
AST, U/L	27 (20–40)	0–37	
Bilirubin, mg/dL	0.6 (0.4–0.8)	<1.20	
CK, U/L	70 (41–181)	26–192	
sCR, mg/dL	0.7 (0.55–0.8)	0.50–1.20	
D-dimer, ng/mL	850 (477–1420)	0–800	
eGFR, mL/min	82.5 (67–92.3)	>90	
LDH, U/L	228 (181–325)	50–250	
hs-TnT, pg/mL	19 (16–35)	<14	
Vitamin D, ng/mL	23.0 (15.5–30)	≥30	
Inflammatory parameters			
CRP, mg/dL	33 (18–79)	<5	
IL-6, pg/mL	19 (7–38)	<7	
PCT, ng/mL	0.103 (0.05–0.17)	<0.05	
MR-proADM, nmol/L	0.93 (0.58– 1.09)	<0.55	

ALT, alanine aminotransferase; AST, aspartate aminotransferase; CRP, C-reactive protein; CK, creatine kinase; eGFR, estimated glomerular filtration rate; hs-TnT, high-sensitivity troponin T; IL-6, interleukin-6; IQR, interquartile range; LDH, lactate dehydrogenase; MCH, mean corpuscular hemoglobin; MCV, mean corpuscular volume; MR-proADM, midregional proadrenomedullin; PCT, procalcitonin; RDW, red cell distribution width; sCR, serum creatinine.

and sCR (r = .25; 95% CI, 0.04–0.45; P = .02) and a negative correlation with vitamin D (r = –.37; 95% CI, –0.61 to –0.07; P = .01) and lymphocytes % (r = –.46; 95% CI, –0.66 to –0.20; P = .0009). No significant correlation was found between MR-proADM and ALT (r = .007; 95% CI, –0.21 to 0.23; P = .95), AST (r = .18; 95% CI, –0.04 to 0.38; P = .10), and CK (r = –.01; 95% CI, –0.23 to 0.20; P = .91).

MR-proADM in Risk Stratification of Patients with SARS-CoV-2

We found that MR-proADM was significantly associated with in-hospital mortality but not with LOS (r = .19; 95% CI, –0.13 to 0.48; P = .23). Indeed, patients who died (n = 14) during hospitalization had higher MR-proADM levels than patients who survived (n = 96; median, 2.59; IQR, 2.3–2.95 nmol/L; range, 1.89–10.58 nmol/L vs median, 0.82; IQR, 0.57–1.03 nmol/L; range, 0.44–2.63 nmol/L; P <.0001). According to the ROC curve analysis, the area under the curve (AUC) of MR-proADM for predicting mortality was 0.95 (95% CI, 0.86–0.99; Figure 1). An MR-proADM value of 1.73 nmol/L was identified as the optimal cutoff value for mortality prediction, with 90% sensitivity and 95% specificity (P <.0001).

Discussion

In this study, we sought to evaluate the prognostic value of MR-proADM in patients with COVID-19. Only a few studies have evaluated the role of such a biomarker in patients with SARS-CoV-2 infection.[29,30]

In our study, most patients showed altered levels of inflammatory biomarkers, such as lymphocytopenia, reduced vitamin D levels, and eGFR, along with increased D-dimer, hs-TnT, IL-6, CRP, and PCT levels, in accordance with the literature.[10,31] Notably, MR-proADM was significantly increased in 72% of patients. In addition, nonsurvivors

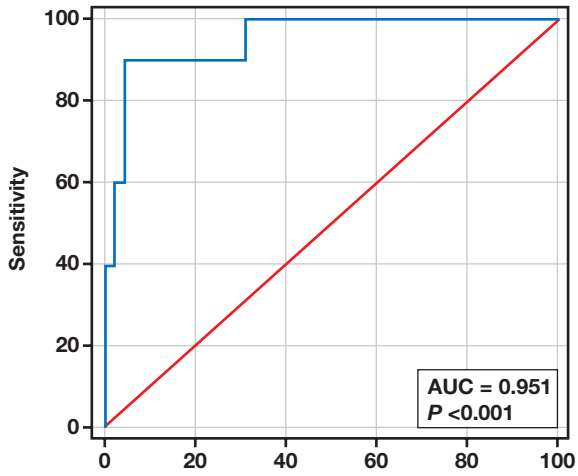

Figure 1

ROC curve analysis of MR-proADM for predicting in-hospital mortality. MR-proADM showed sensitivity of 90% and specificity of 95%; the cutoff value was 1.73 nmol/L. MR-proADM, midregional proadrenomedullin; ROC, receiver operating characteristic.

showed higher MR-proADM levels than survivors. The ROC analysis revealed a good accuracy of MR-proADM for predicting mortality with an AUC of 0.95 at a cutoff value of 1.73 nmol/L.

Finally, we found a significant correlation between MR-proADM and inflammatory biomarkers, as previously shown by studies performed in patients with other clinical conditions, such as pneumonia.[32-36] Overall, our findings suggest that the measurement of MR-proADM upon hospital admission could provide important prognostic information in patients with COVID-19.

To date, the role of different biomarkers in COVID-19 management, from diagnosis to treatment monitoring, has been assessed.[37] However, contrasting results have been achieved.[38-40] Indeed, COVID-19 is a disease about which much is still unknown, and there is active research to understand its pathogenesis and consequently to identify useful biomarkers. Among all the biomarkers currently studied, a role for hypovitaminosis D has been reported. Recently, Hernández et al[41] showed that more than 80% of patients hospitalized with COVID-19 had vitamin D deficiency, which was associated with inflammatory biomarkers. In accordance with such evidence, we found an association between reduced vitamin D levels and higher levels of MR-proADM. In addition, a recent review highlighted that approximately one-third of patients with COVID-19 showed neurological manifestations, particularly seizures and status epilepticus.[42-45]

In this study, we found an optimal MR-proADM cutoff value of 1.73 nmol/L, which is slightly lower than that established by Spoto et al[29] (2 nmol/L) but higher than that reported by Gregoriano et al[30] (0.93 nmol/L). Larger studies are required before introducing such a biomarker into clinical practice to confirm these preliminary findings and establish a unique cutoff value. Moreover, the mechanism underlying the increase of MR-proADM in patients with COVID-19 should be elucidated.

Our study presents some limitations. First, it is a single, monocenter, and retrospective study. Thus, it provides a snapshot of the biomarker within patients with COVID-19, allowing us to draw some conclusions mainly about the distribution of MR-proADM in our study population. In addition, the low rate of mortality could affect the robustness of the ROC curve analysis findings. Our strength is that we first evaluated the role of MR-proADM in a large population of patients with COVID-19.

Conclusion

The identification of biomarkers to define patients who are likely to deteriorate during their hospitalization could help clinicians to improve their clinical management. In this study, at hospital admission, patients with more severe COVID-19 showed higher levels of MR-proADM, together with other inflammatory biomarkers. Noteworthy, a variability in MR-proADM levels in COVID-19 patients exists. Our results agree with those of Spoto et al[29] but are different from those of Gregoriano et al,[30] who reported lower MR-proADM concentrations. Thus, further studies to determine a cutoff value are imperative.

Our findings encourage further investigation to confirm the usefulness of MR-proADM as a prognostic biomarker in patients with COVID-19. Such a biomarker can be easily and rapidly measured on a fully automated platform. Thus, MR-proADM could be part of a panel of biomarkers to evaluate the prognosis and assess the risk of developing complications.[46-50] **LM**

References

1. Wang C, Horby PW, Hayden FG, Gao GF. A novel coronavirus outbreak of global health concern. *Lancet.* 2020;395(10223):470–473.
2. Huang C, Wang Y, Li X, et al. Clinical features of patients infected with 2019 novel coronavirus in Wuhan, China. *Lancet.* 2020;395(10223):497–506.
3. Lai CC, Ko WC, Lee PI, Jean SS, Hsueh PR. Extra-respiratory manifestations of COVID-19. *Int J Antimicrob Agents.* 2020;56(2):106024.
4. Coz Yataco AO, Simpson SQ. Coronavirus disease 2019 sepsis: a nudge toward antibiotic stewardship. *Chest.* 2020;158(5):1833–1834.
5. Hamming I, Timens W, Bulthuis ML, Lely AT, Navis G, van Goor H. Tissue distribution of ACE2 protein, the functional receptor for SARS coronavirus. A first step in understanding SARS pathogenesis. *J Pathol.* 2004;203(2):631–637.
6. Zou X, Chen K, Zou J, Han P, Hao J, Han Z. Single-cell RNA-seq data analysis on the receptor ACE2 expression reveals the potential risk of different human organs vulnerable to 2019-nCoV infection. *Front Med.* 2020;14(2):185–192.
7. Zhou P, Yang XL, Wang XG, et al. A pneumonia outbreak associated with a new coronavirus of probable bat origin. *Nature.* 2020;579(7798):270–273.
8. Gu J, Korteweg C. Pathology and pathogenesis of severe acute respiratory syndrome. *Am J Pathol.* 2007;170(4):1136–1147.
9. Ciaccio M, Agnello L. Biochemical biomarkers alterations in coronavirus disease 2019 (COVID-19). *Diagnosis (Berl).* 2020;7(4):365–372.

DOI: 10.1093/labmed/lmab032

10. Kermali M, Khalsa RK, Pillai K, Ismail Z, Harky A. The role of biomarkers in diagnosis of COVID-19—a systematic review. *Life Sci.* 2020;254:117788.
11. Lippi G, Plebani M. Laboratory abnormalities in patients with COVID-2019 infection. *Clin Chem Lab Med*. 2020;58:1131–1134.
12. Ponti G, Ruini C, Tomasi A. Homocysteine as a potential predictor of cardiovascular risk in patients with COVID-19. *Med Hypotheses.* 2020;143:109859.
13. Vivona N, Bivona G, Noto D, et al. C-reactive protein but not soluble CD40 ligand and homocysteine is associated to common atherosclerotic risk factors in a cohort of coronary artery disease patients. *Clin Biochem.* 2009;42(16–17):1713–1718.
14. Li J, Gong X, Wang Z, et al. Clinical features of familial clustering in patients infected with 2019 novel coronavirus in Wuhan, China. *Virus Res.* 2020;286:198043.
15. Wang D, Hu B, Hu C, et al. Clinical characteristics of 138 hospitalized patients with 2019 novel coronavirus-infected pneumonia in Wuhan, China. *JAMA.* 2020;323(11):1061–1069.
16. Tang Y, Liu J, Zhang D, Xu Z, Ji J, Wen C. Cytokine storm in COVID-19: the current evidence and treatment strategies. *Front Immunol.* 2020;11:1708.
17. Elsasser TH, Kahl S. Adrenomedullin has multiple roles in disease stress: development and remission of the inflammatory response. *Microsc Res Tech.* 2002;57(2):120–129.
18. De La Torre-Prados MV, Garcia-De La Torre A, Enguix A, et al. Mid-regional pro-adrenomedullin as prognostic biomarker in septic shock. *Minerva Anestesiol*. 2016;82:760–766.
19. Agnello L, Bivona G, Parisi E, et al. Presepsin and midregional proadrenomedullin in pediatric oncologic patients with febrile neutropenia. *Lab Med.* 2020;51(6):585–591.
20. Spoto S, Fogolari M, De Florio L, et al. Procalcitonin and MR-proadrenomedullin combination in the etiological diagnosis and prognosis of sepsis and septic shock. *Microb Pathog.* 2019;137:103763.
21. Angeletti S, Spoto S, Fogolari M, et al. Diagnostic and prognostic role of procalcitonin (PCT) and MR-pro-adrenomedullin (MR-proADM) in bacterial infections. *APMIS.* 2015;123(9):740–748.
22. Valenzuela-Sánchez F, Valenzuela-Méndez B, Rodríguez-Gutiérrez JF, Estella-García Á, González-García MÁ. New role of biomarkers: mid-regional pro-adrenomedullin, the biomarker of organ failure. *Ann Transl Med.* 2016;4(17):329.
23. Spoto S, Nobile E, Carnà EPR, et al. Best diagnostic accuracy of sepsis combining SIRS criteria or qSOFA score with procalcitonin and mid-regional pro-adrenomedullin outside ICU. *Sci Rep.* 2020;10(1):16605.
24. Bellia C, Agnello L, Lo Sasso B, et al. Mid-regional pro-adrenomedullin predicts poor outcome in non-selected patients admitted to an intensive care unit. *Clin Chem Lab Med.* 2019;57(4):549–555.
25. Krüger S, Ewig S, Giersdorf S, Hartmann O, Suttorp N, Welte T; German Competence Network for the Study of Community Acquired Pneumonia (CAPNETZ) Study Group. Cardiovascular and inflammatory biomarkers to predict short- and long-term survival in community-acquired pneumonia: results from the German Competence Network, CAPNETZ. *Am J Respir Crit Care Med.* 2010;182(11):1426–1434.
26. Saeed K, Wilson DC, Bloos F, et al. Correction to: The early identification of disease progression in patients with suspected infection presenting to the emergency department: a multi-centre derivation and validation study. *Crit Care.* 2019;23(1):255.
27. World Health Organization. Clinical management of severe acute respiratory infection when novel coronavirus (nCov) infection is supsected: interim guidance, 25 January 2020. https://apps.who.int/iris/handle/10665/330854. Accessed March 30, 2021.
28. Levey AS, Stevens LA, Schmid CH, et al. A new equation to estimate glomerular filtration rate. *Ann Intern Med*. 2009;150:604–612. Published correction appears in *Ann Intern Med.* 2011;155(6):408.
29. Spoto S, Agrò FE, Sambuco F, et al. High value of mid-regional proadrenomedullin in COVID-19: a marker of widespread endothelial damage, disease severity and mortality. *J Med Virol*. Published online November 16, 2020. doi: 10.1002/jmv.26676.
30. Gregoriano C, Koch D, Kutz A, et al. The vasoactive peptide MR-pro-adrenomedullin in COVID-19 patients: an observational study. *Clin Chem Lab Med*. Published online January 8, 2021. doi: 10.1515/cclm-2020-1295.
31. Henry B, Cheruiyot I, Vikse J, et al. Lymphopenia and neutrophilia at admission predicts severity and mortality in patients with COVID-19: a meta-analysis. *Acta Biomed.* 2020;91(3):e2020008.
32. Giulia B, Luisa A, Concetta S, Bruna LS, Chiara B, Marcello C. Procalcitonin and community-acquired pneumonia (CAP) in children. *Clin Chim Acta.* 2015;451(Pt B):215–8. doi:10.1016/j.cca.2015.09.031
33. Agnello L, Bellia C, Di Gangi M, et al. Utility of serum procalcitonin and C-reactive protein in severity assessment of community-acquired pneumonia in children. *Clin Biochem.* 2016;49(1–2):47–50.
34. Florin TA, Ambroggio L, Brokamp C, et al. Proadrenomedullin predicts severe disease in children with suspected community-acquired pneumonia. *Clin Infect Dis.* Published August 6, 2020. doi: 10.1093/cid/ciaa1138.
35. Pilotto A, Dini S, Veronese N, et al. Multidimensional Prognostic Index and pro-adrenomedullin plasma levels as mortality risk predictors in older patients hospitalized with community-acquired pneumonia: a prospective study. *Panminerva Med.* 2018;60(3):80–85.
36. Kakareko K, Rydzewska-Rosołowska A, Rygasiewicz K, et al. Prognostic value of midregional proadrenomedullin in critically ill patients. *Pol Arch Intern Med.* 2019;129(10):673–678.
37. Lo Sasso B, Giglio RV, Gambino CM, et al. SARS-CoV-2: new perspectives for the clinical laboratory diagnostics. *Biochimica Clinica.* 2020;44:023–024.
38. Huang L, Zhao X, Qi Y, et al. Sepsis-associated severe interleukin-6 storm in critical coronavirus disease 2019. *Cell Mol Immunol.* 2020;17(10):1092–1094.
39. Lippi G, Plebani M. The critical role of laboratory medicine during coronavirus disease 2019 (COVID-19) and other viral outbreaks. *Clin Chem Lab Med.* 2020;58:1063–1069.
40. Xu P, Zhou Q, Xu J. Mechanism of thrombocytopenia in COVID-19 patients. *Ann Hematol.* 2020;99(6):1205–1208.
41. Hernández JL, Nan D, Fernandez-Ayala M, et al. Vitamin D status in hospitalized patients with SARS-CoV-2 infection. *J Clin Endocrinol Metab.* 2021;106(3):e1343–e1353.
42. Narula N, Joseph R, Katyal N, et al. Seizure and COVID-19: association and review of potential mechanism. *Neurol Psychiatry Brain Res.* 2020;38:49–53.
43. Holló A, Clemens Z, Kamondi A, Lakatos P, Szűcs A. Correction of vitamin D deficiency improves seizure control in epilepsy: a pilot study. *Epilepsy Behav.* 2012;24(1):131–133.
44. Bivona G, Gambino CM, Iacolino G, Ciaccio M. Vitamin D and the nervous system. *Neurol Res.* 2019;41(9):827–835.
45. Bivona G, Lo Sasso B, Iacolino G, et al. Standardized measurement of circulating vitamin D [25(OH)D] and its putative role as a serum biomarker in Alzheimer's disease and Parkinson's disease. *Clin Chim Acta.* 2019;497:82–87.
46. Silberstein M. Correlation between premorbid IL-6 levels and COVID-19 mortality: potential role for Vitamin D. *Int Immunopharmacol.* 2020;88:106995.
47. Bellia C, Zaninotto M, Cosma C, et al. Definition of the upper reference limit of glycated albumin in blood donors from Italy. *Clin Chem Lab Med.* 2017;56(1):120–125.
48. Parveen R, Sehar N, Bajpai R, Agarwal NB. Association of diabetes and hypertension with disease severity in covid-19 patients: a systematic literature review and exploratory meta-analysis. *Diabetes Res Clin Pract.* 2020;166:108295.
49. Wicaksana AL, Hertanti NS, Ferdiana A, Pramono RB. Diabetes management and specific considerations for patients with diabetes during coronavirus diseases pandemic: a scoping review. *Diabetes Metab Syndr.* 2020;14(5):1109–1120.
50. Nishiga M, Wang DW, Han Y, Lewis DB, Wu JC. COVID-19 and cardiovascular disease: from basic mechanisms to clinical perspectives. *Nat Rev Cardiol.* 2020;17(9):543–558.

Case Study

Achondroplasia—First Report from India of a Rare *FGFR3* Gene Variant

Chakshu Chaudhry, MD,[1] Prabakaran G, MD,[1] Priyanka Srivastava, PhD,[1,] Reena Das, MD,[2] Jasbir Kaur, BSc,[2] Inusha Panigrahi, DM,[1] Anupriya Kaur, DM[1]*

Laboratory Medicine 2020;52:499-502

DOI: 10.1093/labmed/lmaa116

ABSTRACT

The clinical manifestations of *FGFR3* sequence variations can vary from mild unnoticed short stature to neonatal lethal dwarfism and can be causative of phenotypes including achondroplasia, hypochondroplasia, and thanatophoric dysplasia. Clinical data describe an 11 month old girl with restricted growth and preserved intellect. She had rhizomelic short stature with peculiar facies but no Acanthosis nigricans. In view of the absence of the hotspot mutation c.1138 G>A/G>C (p.Gly380Arg), complete gene sequencing was done that revealed a rare sequence variation, NM_000142.4:c.1043C>G (p.Ser348Cys) in *FGFR3*. This sequence variation has not been reported from India so far. This report emphasizes the benefit of sequencing the whole gene in individuals who are negative for hotspot mutation of achondroplasia with strong clinical suspicion.

Keywords: pediatrics, genetics, molecular diagnostics, bone, bioinformatics

A multitude of skeletal dysplasias, ranging from benign prototypic achondroplasia (OMIM#100800) to severe lethal thanatophoric dysplasia (OMIM#187600), can be caused by functionally activating mutations of *FGFR3*. These are all short-limb skeletal dysplasias, inherited in an autosomal dominant fashion. One of the classic examples of genetic disorders with an excellent genotype and phenotype correlation is *FGFR3*-associated skeletal dysplasia. Although most (98%) individuals with achondroplasia have the common mutation (p.Gly380Arg), other rare mutations have been reported but no other hotspot mutation has been identified. However, novel mutations presenting with atypical clinical and radiological features pose a challenge in clinical diagnosis and genetic counseling in day-to-day practice. A rare mutation, c.1043C>G (p.Ser348Cys), has been reported in 3 separate publications as contributing to the variety of mutations causing achondroplasia/hypochondroplasia.[1-3] One of the reported patients had Acanthosis nigricans without evidence of hyperinsulinem.[2] Recently, this rare variant was also reported in a fetus with type I thanatophoric dysplasia by Wu et al.[4]

We present a report of an infant who was managed as failure to thrive at multiple centres but eventually turned out to have achondroplasia. She was the first patient from India and the fourth patient worldwide with the mutation; NM_000142.4:c.1043C>G (p.Ser348Cys) in *FGFR3.*

[1]Genetic Metabolic Unit, Department of Pediatrics, Advanced Pediatrics Centre, Post Graduate Institute of Medical Education and Research, Chandigarh, India, [2]Department of Hematology, Post Graduate Institute of Medical Education and Research, Chandigarh, India

*To whom correspondence should be addressed.
srivastavapriy@gmail.com

Case Report

The index case, an 11 month old girl, was brought with complaints of delay in achieving motor milestones since birth but with a preserved intellect. She was the firstborn girl of a nonconsanguineously married healthy couple. She was born full-term with a birth weight of 2.5 kg. She had an uneventful perinatal period. Her weight, length, and head circumference were at 0.1Z, –3Z, and 4.6Z scores, respectively. She had a disproportionately short stature, a large head with a flat nasal bridge, upper and lower limb rhizomelia with redundant skin folds, and hypotonia. Radiological examination was classical for achondroplastic phenotype (**Figures 1A–1C**; informed consent received from parents). A common

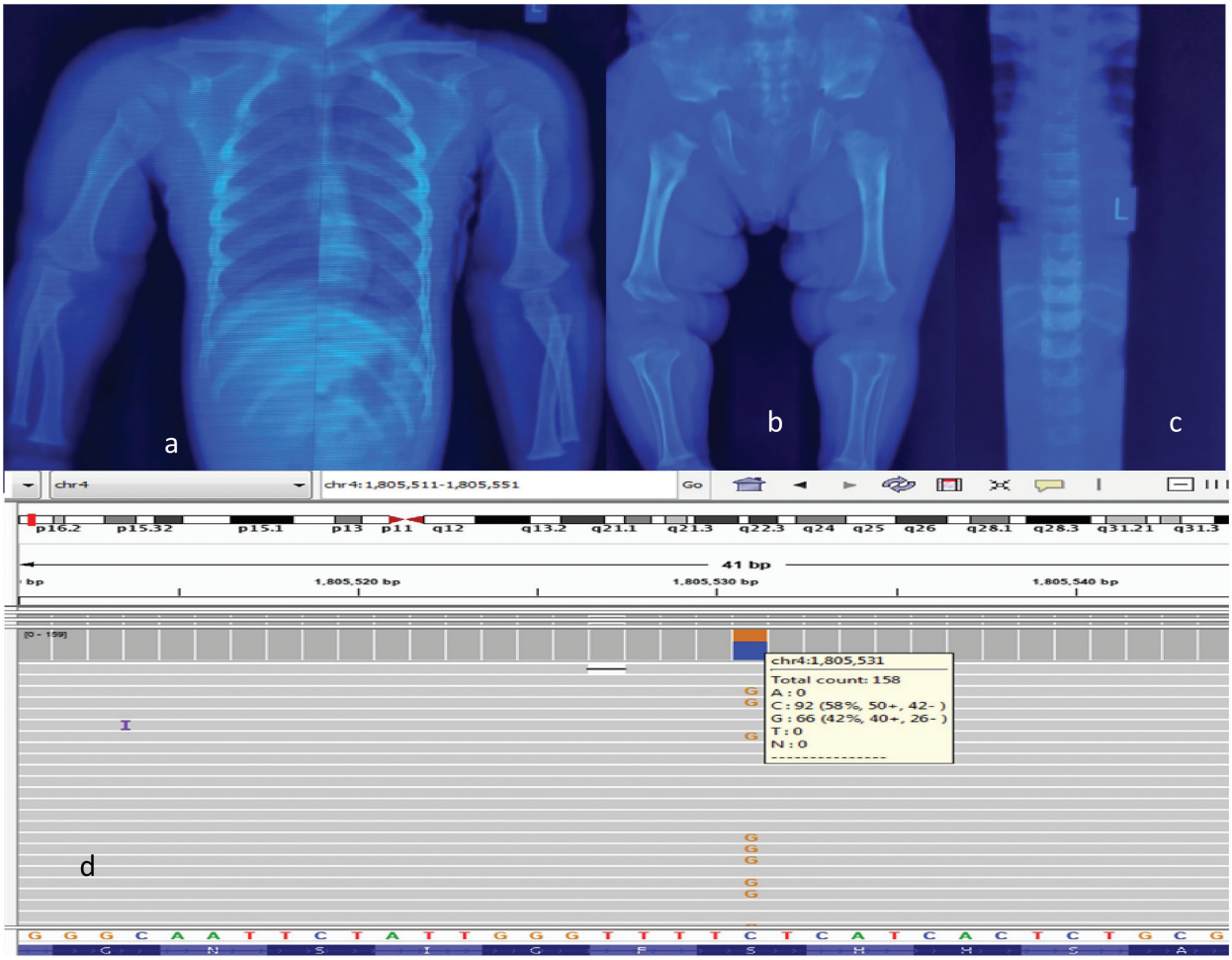

Figure 1

A, Radiographs of patient showing short tubular bones with metaphyseal flaring. **B,** The iliac bones appear squarish with horizontal acetabula and a narrow sacrosciatic notch. **C,** Decreased vertebral interpedicular distance in the caudal spine. **D,** Snapshot of the Integrative Genomics Viewer showing heterozygous variant c.1043C>G (chr4:1805531C>G; depth: 158×).

mutation causing achondroplasia, c.1138G>A/G>C, was first tested for using polymerase chain reaction restriction fragment length polymorphism. When the mutation was found to be absent, the radiographs of the child were reassessed. Because they were very suggestive of achondroplasia, focused exome sequencing covering *FGFR3* was performed using the Ion Torrent platform (Ion-Torrent, Thermo Fisher Scientific-India). We analyzed all coding exons and exon-intron boundaries of *FGFR3* and found a heterozygous missense variation in exon 8, NM_000142.4:c.1043C>G (chr4:1805531C>G; Depth: 158x; **Figure 1D**). This base change resulted in an amino acid change at the 348th position from serine to cysteine (Ser348Cys) in the FGFR3 protein. The Sanger sequencing of exon 8 of *FGFR3* in the child's parents did not reveal any variation, suggesting a de novo origin of the variation seen in the child although germline mosaicism could not be excluded.

Discussion

Achondroplasia, an autosomal dominantly inherited skeletal dysplasia, typically manifests as rhizomelic short stature with facial dysmorphism. Children display frontal bossing,

Table 1. Comparison of Clinical Features of Achondroplasia in Reported Patients of the Variation c.1043C>G in the *FGFR3*

	Present Patient (age 11 months)	Bengur et al[1] (age 8 months)	Couser et al[2] (age 8 years)	Hasegawa K et al[3] (age 11 months)
Rhizomelic shortening	✓	✓	✓	✓
Brachydactyly	✓	✓	✓	✓
Macrocephaly	✓	✓	✗	✗
Frontal bossing	✓	mild	✗	✓
Acanthosis nigricans	✗	✗	✓	✗
Flat nasal bridge	✓	✗	✗	✓
Short femur and tibia	✓	✓	✓	✓
Short squared ilia	✓	✓	✓	✓
Interpedicular narrowing of lower lumbar spine	✓	✓	✓	✓
Short, thick humerus	✓	✓	✓	✓
Brachydactyly of hands	✓	✓	✓	✗
Flat cranial base	…	✓	✗	✓
Long distal portion of fibula	…	✓	✓	✗

macrocephaly, and midface retrusion. In addition to the rhizomelic short stature, other major skeletal manifestations are brachydactyly with the hand showing trident configuration and exaggerated lumbar lordosis. Radiographs show short tubular bones with metaphyseal flaring. Iliac bones appear squarish with horizontal acetabula and a narrow sacrosciatic notch. There is decreased vertebral interpedicular distance in the caudal spine. All these typical features were well appreciated in our patient (**Figures 1A–1C**).

Motor delay in achondroplasia is commonly seen and is attributed to difficulty in supporting a large head along with hypotonia. Delay in fine motor development results from small hands with joint laxity. Other areas of development are usually preserved.[5]

FGFR3 hotspot mutation screening is the first-line test in individuals with suspected achondroplasia. Most cases (98%) of achondroplasia are caused by the FGFR3 amino acid change p.Gly380Arg. Other mutations such as p.Ser217Cys, p.Ser279Cys, p.Ser344Cys, and p.Gly375Cys account for the remaining 1% of patients with achondroplasia.[6-9] The mutation found in our patient, p.Ser348Cys, has previously been found in only 3 patients: an 11-month-old girl,[3] a 8-year-old boy,[2] and a 8-month-old from Turkey.[1] A comparison of the clinical features of these 3 patients with our patient is shown in **Table 1**.

As previously reported, all the other uncommon mutations have an amino acid change to cysteine.[10] Hasegawa et al[3] proposed that this change probably leads to the formation of an abnormal disulfide bond, resulting in the constitutive activation of *FGFR3.* Whereas Hasegawa et al[3] described their patient as having achondroplasia, Bengur et al[1] postulated the diagnosis of mild achondroplasia/hypochondroplasia. The characteristic craniofacial features of achondroplasia have been mild or absent in other patients but were present in our patient. The patient reported by Hasegawa et al[3] had frontal bossing and a flat nasal bridge. Acanthosis nigricans has also been reported in other patients but was absent in our patient. Follow-up of our patient will be conducted considering the possibility of late onset of Acanthosis nigricans. A recent study on prenatal cases by Wu et al[4] showed the same variation (Ser348Cys) in a fetus with type I thanatophoric dysplasia. A large series of 477 individuals with achondroplasia postulated that Acanthosis nigricans arises in approximately 10% of individuals with achondroplasia.[11] Follow-up of our patient is important for phenotype-genotype correlation.

Conclusion

We have described the first report of the rare pathogenic variation NM_000142.4:c.1043C>G p.Ser348Cys in *FGFR3* causing achondroplasia in a child from India, emphasizing the genetic heterogeneity in achondroplasia and reinforcing the need for a complete analysis of *FGFR3* in a strongly

DOI: 10.1093/labmed/lmaa116

suspected case of achondroplasia without the common mutation. **LM**

Acknowledgments

We sincerely thank the cooperation of the patient's family. Prabakaran G and Chakshu Chaudhry wrote the manuscript. Priyanka Srivastava contributed the interpretation of the exome sequencing. Reena Das and Jasbir Kaur performed the common mutation testing. Inusha Panigrahi was involved in patient care and management. Anupriya Kaur was involved in patient care and management and in final drafting and approval of the manuscript.

References

1. Bengur FB, Ekmekci CG, Karaarslan E, et al. p.Ser348Cys mutation in *FGFR3* gene leads to "mild ACH /severe HCH" phenotype. *Eur J Med Genet.* 2020;63:103659.
2. Couser NL, Pande CK, Turcott CM, Spector EB, Aylsworth AS, Powell CM. Mild achondroplasia/hypochondroplasia with acanthosis nigricans, normal development, and a p.Ser348Cys FGFR3 mutation. *Am J Med Genet A.* 2017;173(4):1097–1101.
3. Hasegawa K, Fukuhara R, Moriwake T, et al. A novel mutation p.Ser348Cys in FGFR3 causes achondroplasia. *Am J Med Genet A.* 2016;170A(5):1370–1372.
4. Wu QC, Wang WB, Sun L, et al. Mutation analysis of the fibroblast growth factor receptor 3 gene in fetuses with thanatophoric dysplasia, type I. *Clin Exp Obstet Gynecol.* 2020;47(1):7–11.
5. Ireland PJ, Donaghey S, McGill J, et al. Development in children with achondroplasia: a prospective clinical cohort study. *Dev Med Child Neurol.* 2012;54(6):532–537.
6. Ikegawa S, Fukushima Y, Isomura M, Takada F, Nakamura Y. Mutations of the fibroblast growth factor receptor-3 gene in one familial and six sporadic cases of achondroplasia in Japanese patients. *Hum Genet.* 1995;96(3):309–311.
7. Heuertz S, Le Merrer M, Zabel B, et al. Novel FGFR3 mutations creating cysteine residues in the extracellular domain of the receptor cause achondroplasia or severe forms of hypochondroplasia. *Eur J Hum Genet.* 2006;14(12):1240–1247.
8. Zhang SR, Zhou XQ, Ren X, et al. Ser217Cys mutation in the Ig II domain of FGFR3 in a Chinese family with autosomal dominant achondroplasia. *Chin Med J (Engl).* 2007;120(11):1017–1019.
9. Takagi M, Kouwaki M, Kawase K, et al. A novel mutation Ser344Cys in FGFR3 causes achondroplasia with severe platyspondyly. *Am J Med Genet A.* 2015;167A(11):2851–2854.
10. Naski MC, Wang Q, Xu J, Ornitz DM. Graded activation of fibroblast growth factor receptor 3 by mutations causing achondroplasia and thanatophoric dysplasia. *Nat Genet.* 1996;13:233–237.
11. Smid CJ, Modaff P, Alade A, Legare JN, Pauli RM. Acanthosis nigricans in achondroplasia. *Am J Med Genet.* 2018;176(12):2630–2636.

Analysis of Multiple Bands on Serum Protein Immunofixation Electrophoresis: Challenge in Interpretation of Clonality in a Patient with Light Chain–Predominant Multiple Myeloma

Okechukwu V. Nwogbo, MD, Yulan Jin, MD, Taylor Sliker, MD, Dorian Wilhite, MD, Gurmukh Singh, MD, PhD, MBA[*]

Laboratory Medicine 2021;52:503-508

DOI: 10.1093/labmed/lmab001

ABSTRACT

Sera from patients with multiple myeloma usually display a single monoclonal immunoglobulin band on serum protein immunofixation electrophoresis. Multiple bands may be seen if the myeloma is bi- or triclonal or if the monoclonal immunoglobulin has rheumatoid factor activity. We describe a patient with light chain–predominant IgA lambda myeloma; the patient's serum displayed 2 spatially distinct bands reacting for alpha heavy and lambda light chains. The methods used to establish monoclonality are addressed.

Keywords: Monoclonal gammopathy, light chain predominant multiple myeloma, immune-subtraction, polymeric immunoglobulin chains, multiple bands in SIFE, serum free light chains

Serum protein electrophoresis (SPEP) and serum protein immunofixation electrophoresis (SIFE) are used routinely for evaluation of serum proteins in general and for diagnosis of monoclonal immunoglobulins in particular. Multiple bands may be seen if the myeloma is bi- or triclonal or if the monoclonal immunoglobulin has rheumatoid factor activity.[1-7] Monoclonal immunoglobulins usually produce a single sharp band on protein electrophoresis.[4,5] However, interpretation is complicated on occasion by the observation of multiple bands.[3] We present an illustrative case with multiple bands and the interpretive resolution of the issue.

Abbreviations:

SPEP, serum protein electrophoresis; SIFE, serum protein immunofixation electrophoresis; UIFE, urine immunofixation electrophoresis; SFLC, serum free light chains; DTT, dithiothreitol; QUIET, quantitative ultrafiltration immunofixation electrophoresis test; IS-SIFE, immune-subtraction serum protein immunofixation electrophoresis; LCPMM, light chain–predominant multiple myeloma; I/UI ratio, involved light chain and uninvolved light chain ratio.

Department of Pathology, Medical College of Georgia at Augusta University, Augusta, Georgia, USA

*To whom correspondence should be addressed.
gurmukhsinghmdphd@yahoo.com

Clinical History

The patient was an 88 year old White male with multiple medical problems including mitral stenosis, coronary artery disease, Wenckebach atrioventricular block, and hyperlipidemia with IgA lambda multiple myeloma diagnosed 4 years earlier at an outside hospital.

Two years after initial diagnosis, oncology care for the patient was referred to a tertiary care institution, at which point bone marrow biopsy revealed 20% plasma cells. Cytogenetic analysis showed a normal male karyotype, but fluorescence in situ hybridization evaluation showed an abnormal clone with a gain of 1q21 and 5q and a loss of *DLEU1* in chromosome 13. Since the initial diagnosis, laboratory test values showed a gradual increase in lambda light chain levels. Follow-up of the patient 1 year later revealed 40% plasma cells in the marrow with a negative positron emission tomography scan, and the patient was subsequently restaged. Treatment was initiated with bortezomib, lenalidomide, and dexamethasone, which were well tolerated.

Laboratory test results showed pancytopenia with macrocytosis, hypogammaglobulinemia, hypoproteinemia,

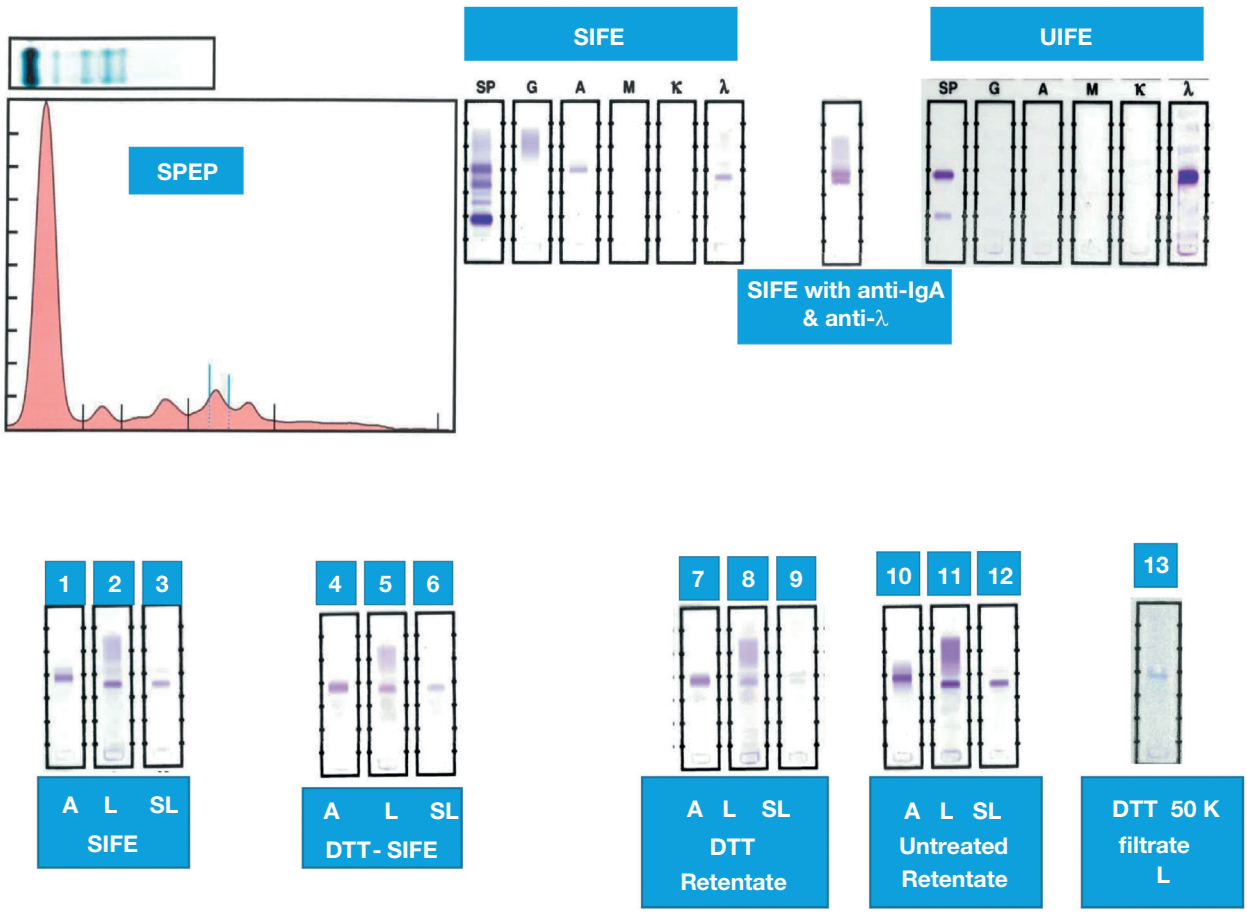

Figure 1

Serum protein electrophoresis (SPEP) did not reveal a monoclonal spike in the gamma region. Gamma globulins and total proteins are low. SIFE revealed a band reactive with antiserum to IgA, co-migrating with transferrin, and a slightly anodal band reactive with antiserum to lambda light chains. There is a barely perceptible band in the anti-lambda lane at the same level as the monoclonal IgA band. The difference in the migration pattern of the IgA and lambda bands is obvious in the serum protein stained with both anti-IgA (cathodal band) and anti-lambda (anodal band) in the same lane. UIFE revealed a prominent monoclonal lambda light chain band. Lower part of Figure 1: Details of the various manipulations are given in the text. In short, lanes 1–3 are SIFE with antibodies to IgA, conventional anti-lambda and Sebia anti-lambda to free light chains (A, L SL). Lanes 4–6 were stained like lanes 1–3 for serum treated with DTT. Lanes 7–9 are SIFE of retentate of 50 kDa filter from serum treated with DTT and demonstrate staining for IgA and Lambda documenting that the retained immunoglobulin is in fact IgA lambda and not just alpha heavy chain. Free monoclonal lambda light chains were filtered out as demonstrated by the lack of staining with Sebia antiserum to free lambda light chains in lane 9. Lanes 10–12 are from retentate of untreated serum. Each set of three lanes was stained with antibodies as for lanes 1–3. Lane 13 reflects the DTT treated, 50 KDa filtrate of serum, stained for lambda light chains and reveals monoclonal lambda light chains only. Briefly, the light chains with intact IgA were not accessible to antisera to lambda light chains, in SIFE, due the polymeric nature of IgA. The free lambda light chains were also polymeric and present in sufficient concentration to qualify the lesion being classified as light chain predominant IgA lambda multiple myeloma. DTT, dithiothreitol; SIFE, serum protein immunofixation electrophoresis.

and proteinuria. Kappa free light chains ranged from 0.4 mg/L to 1.04 mg/L over the previous 4 years, and lambda free light chains ranged from 23.55 mg/L to 247.51 mg/L in the same time period.

Initially, no monoclonal immunoglobulin band was detectable in the gamma region on SPEP or SIFE. Upon further evaluation, a monoclonal IgA band was determined to overlap the transferrin band in the beta region on SIFE;

however, because of the low concentration of the monoclonal Ig a monoclonal spike was not detected on SPEP. On biochemical analysis, gammaglobulins and total serum proteins were depressed. The use of SIFE revealed a band reactive with antiserum to IgA and a slightly anodal band reactive with antiserum to lambda light chains. There was a barely perceptible band in the anti-lambda lane at the same level as the monoclonal IgA band (**Figure 1**).

The difference in the mobility of the IgA and lambda bands was evident in the elecrophoretic evaluation stained with both anti-IgA (cathodal band) and anti-lambda (anodal band) in the same lane, as depicted in the upper part of **Figure 1**. Urine immunofixation electrophoresis (UIFE) revealed a prominent monoclonal lambda light chain band, confirming the renal clearance of monoclonal free light chains.

Preliminary Analysis

Aggregate interpretation of the SPEP, SIFE, UIFE, and serum free light chains (SFLC) data suggested at least 3 possible scenarios: (1) IgA lambda multiple myeloma, per the patient's clinical diagnosis; (ii) a biclonal lesion of alpha heavy chains and lambda light chains; or (iii) a light chain–predominant IgA lambda multiple myeloma with multimeric monoclonal proteins.[8]

Additional Testing

To resolve these issues, results of conventional SPEP/SIFE were compared to the results with SIFE using antiserum selective for free lambda light chains (Sebia), for native serum, and for serum reduced with dithiothreitol (DTT). The retentate and filtrate from 50 kDa filtration of serum with saline and 0.1 M DTT solutions were also analyzed by SIFE with antisera to IgA, by conventional antiserum to lambda light chains, and by Sebia antiserum for free lambda light chains. The results are depicted in **Figure 1**. In addition, the analytical technique of immune-subtraction was also employed to bolster the evidence that the band staining of IgA was in fact IgA lambda and that excess free lambda light chains produced a spatially distinct lambda chain band, anodal to the IgA band.

We found that SIFE studies stained with antisera to IgA, standard immunofixation antiserum to lambda light chain, and selective antiserum to free lambda light chain (Sebia) failed to reveal lambda chains at the mobility of the IgA band. This result suggested that circulating monoclonal IgA immunoglobulin is likely a dimer or higher-order polymer whereby either the light chains are not accessible to the anti-lambda antisera or the immunoglobulin represents strictly an alpha heavy chain protein. The bands stained with conventional anti-lambda and Sebia antiserum to free lambda light chains likely represent free light chains in the specimen not treated with DTT (lanes 1–3). This estimate is corroborated by the results in lanes 4, 5, and 6 (**Figure 1**). On reduction with 0.1 M DTT, the band staining for IgA shifted further anodal to comigrate at the same mobility as the bands stained with conventional anti-lambda and Sebia antiserum to free lambda light chains (**Figure 1**, lanes 4–6).

The initial interpretation that in its native state the lambda chains associated with IgA are not accessible to the anti-lambda serum in SIFE was further substantiated in the results shown in **Figure 1**, lanes 7–12. For this analysis, serum, with and without reduction with DTT, was subjected to size-exclusion filtration with a nominal cutoff size of 50 kDa as described for the quantitative ultrafiltration immunofixation electrophoresis test (QUIET).[4,9]

Lanes 7, 8, and 9 represent the SIFE of the retentate from the serum specimen processed in the reduced, DTT-treated state. Lane 7 was stained with antiserum to IgA, and lane 8 was stained with conventional antiserum to lambda light chains and showed staining at the same mobility as IgA. Lane 9 was stained with Sebia antiserum to free lambda light chains, the specimen was essentially depleted of free light chains, and the lambda light chains associated with IgA were not stained. The lambda light chain staining with conventional antiserum resulted from reactivity with IgA-associated lambda light chains on reduction of the polymeric IgA. This finding documents that the immunoglobulin staining for IgA in conventional SIFE is in fact IgA lambda and not uncomplexed alpha heavy chain proteins. The findings, in association with those in lanes 10–12, are consistent with the free lambda light chains being dimers. When reduced with DTT to their monomeric tertiary state, the dimers were filtered out through the 50 kDa filter as

Lab Medicine 2021;52;503–508 505
DOI: 10.1093/labmed/lmab001

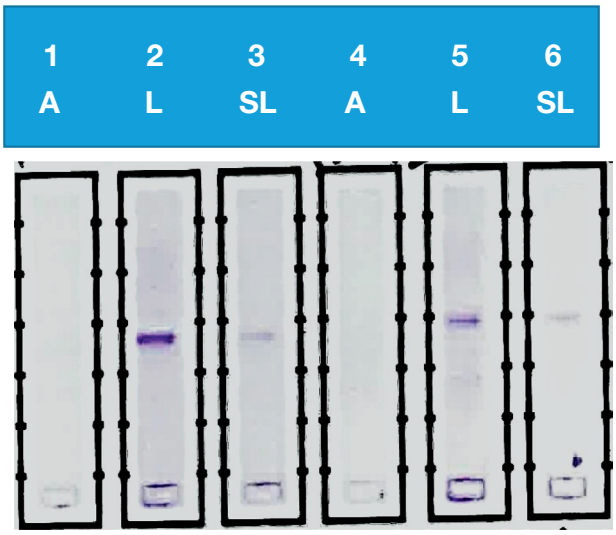

Figure 2

Immune-subtraction SIFE. Patient's serum was subjected to depletion of IgA and the supernatant was used for SIFE (lanes 1–3) after 1:2 dilution with saline. The supernatant was treated with an equal volume of 0.2 M DTT reducing agent and used for SIFE (lanes 4–6). Depleting IgA removed the band reacting with the antibody to the alpha chains (lanes 1 and 4), but the free lambda light chains persisted in the lanes stained with the Helena anti-lambda (lanes 2 and 5) and the lanes stained with the Sebia antibody to the free lambda light chains (lanes 3 and 6). The protein bands in lanes 5 and 6 have a slightly more cathodic location, as was seen in the reduction of whole serum shown in **Figure 1**. DTT, dithiothreitol; SIFE, serum protein immunofixation electrophoresis.

evidenced by the lack of reactivity with the Sebia anti-lambda antiserum in lane 9 and were detectable in the filtrate as shown in lane 13.

Serum was further subjected to immune-subtraction SIFE (IS-SIFE) with antiserum to the alpha heavy chain. The depleted specimen was processed for immunofixation with conventional antiserum to IgA lambda light chains and with Sebia antiserum to free lambda light chains. For the depletion of alpha chains, a manufacturer reagent antiserum to IgA (Helena Laboratories, Beaumont, TX), provided for use in SIFE, was used: 50 μL of antiserum was added to 10 μL of patient serum and the specimen was incubated overnight at 4ºC. The resultant serum was centrifuged at 16,600 g for 5 minutes and the supernatant was collected. Aliquots of the supernatant were diluted with an equal volume of saline and 0.2 M DTT solution and subjected to SIFE as illustrated in **Figure 2**.

A second aliquot was subjected to depletion of the lambda chain and lambda chain–associated immunoglobulins using manufacturer reagent antiserum to lambda light chains. Next, 25 μL of patient serum was incubated overnight, with 225 μL of antiserum to lambda light chains (Helena Laboratories). The solution was centrifuged at 16,600 g for 5 minutes and the supernatant was tested without further dilution by immunofixation electrophoresis using manufacturer reagent kits (Helena Laboratories). Both IgA and lambda chain bands were eliminated by this immune subtraction. The supernatant did not react with antisera to either IgA or lambda light chains (data not shown), showing again that the band reacting for IgA in conventional SIFE is in fact IgA lambda. It is likely that the prolonged overnight incubation with antiserum to lambda light chains was effective in binding to the light chains in the dimeric IgA lambda globulins. Results comparing the patient data with criteria of light chain–predominant multiple myeloma (LCPMM)-lambda are given in **Table 1**.[8]

Table 1. Patient Data and Criteria for LCPMM-Lambda

	SFLC- L	I/UI	SFLC/g	I/UI/g
Patient	247.51	257.82	2097.54	2184.94
LCPMM-L	36.75	44.87	43.5	51.61

The patient's lesion met the criteria for classification as LCPMM.

Discussion

The concentration of monoclonal IgA could not be determined by conventional SPEP because of overlap of the monoclonal Ig with transferrin. The combined concentration of the 2 proteins was 0.29 g/dL. For the purpose of this comparison, the total IgA level (0.121 g/dL) was used instead to provide a more conservative estimate for comparison with LCPMM lambda criteria. The SFLC lambda concentration, the ratio of the serum free light chain concentrations of involved light chain and uninvolved light chain (I/UI ratio), the values of SFLC/g of monoclonal Ig, and the I/IU ratio/g of monoclonal Ig

for the patient are given in **Table 1**. The second row lists the criteria for LCPMM lambda lesions.[8] The patient conformed to the classification as LCPMM-lambda in that the comparators exceeded all criteria for classification as LCPMM-lambda.

Serum IgA is usually in monomeric form, whereas IgA in mucosal secretions is normally dimeric. Mulitmeric forms of IgA have been shown to enhance antimicrobial activity of IgA and occur under physiological states.[10] The close juxtaposition of multiple light chains in a multimeric IgA may render such light chains inaccessible to reagent antibodies for immunofixation of light chains in SIFE. A complex of multimers could alter both the mobility and the antigenicity of the molecule.

It is known that IgA monoclonal immunoglobulins may migrate in the beta region, as in this case report, and this phenomenon affects the densitometric quantification of the monoclonal Ig. Using a heavy/light measurement of relevant immunoglobulin has been proposed as a means to improve the quantification of beta-migrating monoclonal IgA.[11,12] However, this modality is not in common use, and the measurement of total IgA is generally used in monitoring the course of disease.

In this study we present a variation on the QUIET method for determining the clonality of the abnormal IgA; however, nanobody enrichment and MALDI-TOF mass spectrometry is an alternative method that has been used to ascertain the monoclonality of immunoglobulins.[13,14]

In summary, the patient's serum contained low levels of intact, polymeric, monoclonal IgA lambda comigrating with the transferrin peak and abundant free monoclonal lambda light chains, also in polymeric (at least dimeric) form. Thus, the 2 bands noted in the initial SIFE pattern seemed to suggest a biclonal pattern of alpha heavy chains and lambda chains. The results are explainable by quaternary structural parameters and the polymeric nature of both IgA and excess free lambda light chains. The lambda light chains in the polymeric IgA were not accessible to the antisera to lambda light chains in SIFE, although overnight incubation with anti-lambda antiserum allowed the depletion of IgA and the exposure of the antigenic epitope. This finding prompts a general caution in interpreting immunofixation studies because quaternary structural features may obscure epitopes required for effective immunofixation with standard reagents. In addition, the relative concentration of SFLC and other parameters supports the classification of the lesion as LCPMM, whereas initial evaluation may have suggested a biclonal gammopathy.[8] **LM**

Takeaways

1. Light chains in polymeric/dimeric IgA may not be accessible to immunofixation antisera reagents for light chains in SIFE.
2. Circulating SFLC may be present in multimeric/dimeric form.
3. In patients with light chain–predominant IgA MM, the intact IgA and free light chain bands may not migrate in the same location.
4. Reducing the serum specimen with DTT can resolve the otherwise confusing protein electrophoretic findings. Size-exclusion filtration of the native and DTT-treated serum though a 50 kDa filter may be required to confirm the polymeric nature of free light chains.
5. Use of free light chain–specific antisera is helpful in patients with LCPMM.
6. IS-SIFE may be helpful in resolving monoclonality.

Funding

There is no external funding source.

Disclosures/Conflicts of interest

GS serves as a consultant to Diazyme Inc. and HealthTap.

References

1. Nikolova-Vlahova M, Kamburova M, Hristove J, et al. Biclonal myeloma in renal failure. *Centr Eur J Immunol* 2020;45:122–124.
2. Kancharla P, Patel E, Hennrick K, Ibrahim S, Goldfinger M. A rare presentation of biclonal gammopathy in multiple myeloma with simultaneous extramedullary involvement: a case report. *Case Rep Oncol.* 2019;12(2):537–542.
3. Larsen R, Allen S, Thompson TZ, Bollag R, Singh G. Challenges in interpreting multiple monoclonal bands on serum protein electrophoresis and serum immunofixation electrophoresis: an illustrative case report. *J Appl Lab Med.* 2019;4(3):455–459.

DOI: 10.1093/labmed/lmab001

4. Tate JR. The paraprotein—an enduring biomarker. *Clin Biochem Rev.* 2019;40(1):5–22.
5. Singh G. Serum and urine protein electrophoresis and serum-free light chain assays in the diagnosis and monitoring of monoclonal gammopathies. *J Appl Lab Med.* 2020;5(6):1358–1371.
6. O'Connell TX, Horita TJ, Kasravi B. Understanding and interpreting serum protein electrophoresis. *Am Fam Physician.* 2005;71(1):105–112.
7. Le Carrer D. *Serum Protein Electrophoresis Immunofixation: Illustrated Interpretations*. Evry, France: Laboratoires Sebia; 2005.
8. Singh G, Xu H. Light chain predominant intact immunoglobulin monoclonal gammopathy disorders. shorter survival in light chain predominant multiple myelomas. *Lab Med*. 2020;52(4):390–398.
9. Singh G, Bollag R. Quantification by ultrafiltration and immunofixation electrophoresis testing for monoclonal serum free light chains. *Lab Med.* 2020;51(6):592–600.
10. Terauchi Y, Sano K, Ainai A, et al. IgA polymerization contributes to efficient virus neutralization on human upper respiratory mucosa after intranasal inactivated influenza vaccine administration. *Hum Vaccin Immunother.* 2018;14(6):1351–1361.
11. Katzmann JA, Willrich MA, Kohlhagen MC, et al. Monitoring IgA multiple myeloma: immunoglobulin heavy/light chain assays. *Clin Chem.* 2015;61(2):360–367.
12. Paolini L. Quantification of β region IgA paraproteins—should we include immunochemical "heavy/light chain" measurements? Counterpoint. *Clin Chem Lab Med.* 2016;54(6):1059–1064.
13. Kohlhagen MC, Dasari S, Vanderboom PM, et al. Comprehensive assessment of M-proteins using nanobody enrichment coupled to MALDI-TOF mass spectrometry. *Clin Chem*. 2016;62:1334–1344.
14. Sepiashvili L, Kohlhagen MC, Snyder MR, et al. Direct detection of monoclonal free light chains in serum by use of immunoenrichment-coupled MALDI-TOF mass spectrometry. *Clin Chem*. 2019;65:1015–1022.

Loss and Reappearance of A Antigen After Chemotherapy Leading to Blood Group Discrepancy in Acute Myeloid Leukemia: A Case Report

Satya Prakash, MD,[1] *Sonali Mohapatra, MD, DM,*[1,2] *M. Sree Bhagavathi, MBBS,*[1] *Niladri Das, MBBS,*[1] *Gopal Krushna Ray, MD,*[1] *Somnath Mukherjee, MD*[1,*]

Laboratory Medicine 2021;52:509-513

DOI: 10.1093/labmed/lmab008

ABSTRACT

A male patient aged 11 years diagnosed with acute myeloid leukemia presented with complaints of fever, lethargy, and bleeding manifestations. On ordering red blood cells and platelet transfusion, his blood group was tested. Blood group discrepancy was observed in that forward grouping showed the O Rh D positive blood group and reverse grouping revealed the A Rh D positive. The patient's previous blood group record was O Rh D positive, and he had a transfusion history of O Rh D positive red blood cells and platelets in other hospital. Initial immunohematological workup results, including adsorption and heat elution, were consistent with the O Rh D-positive blood group, but further workups on follow-up after the commencement of chemotherapy showed that his original blood group was A Rh D positive, in which the A antigen expression was previously masked by the underlying disease condition of the patient. Hence, the correlation of laboratory results with clinical details and case history is an essential step in resolving such blood group discrepancies.

Keywords: acute myeloid leukemia, blood group discrepancy, hypomethylating agents, ABO blood group system, H antigen, chemotherapy, secretor status

A blood group system is classified based on the antigens that are attached to the red blood cell (RBC) membrane, being either proteins or carbohydrates. The ABO blood group system is the most important clinically significant system in transfusion practice. The alleles of the ABO gene code for glycosyltransferase, which acts on the precursor H antigen and subsequently adds carbohydrate residues on the H antigen. The A, B, and H antigens are usually present on the surface of most epithelial cells, endothelial cells, and RBCs. The H antigen in the RBCs is determined by the *FUT1* gene, which codes for fucosyltransferase.[1, 2]

Abbreviations:

RBC, red blood cell; AML, acute myeloid leukemia; RDP, random donor platelets; CML, chronic myelocytic leukemia.

[1]Department of Transfusion Medicine, All India Institute of Medical Sciences, Bhubaneswar, Odisha, India, [2]Department of Medical Oncology Hematology, All India Institute of Medical Sciences, Bhubaneswar, Odisha, India

*To whom correspondence should be addressed.
som.mukherjee2011@gmail.com

Blood group, which are complex carbohydrate structures, are inherited and constant in an individual throughout life. Blood group discrepancies are encountered when there is a mismatch between forward and reverse grouping. This mismatch may occur because of problems associated with the patient's serum or the patient's RBCs. Blood group discrepancies can result from clerical error; physiological or pathological conditions such as hematological malignancies, including acute myeloid leukemia (AML); or other solid organ malignancies such as carcinoma of the bladder, lungs, colon, or stomach.[2, 3]

Sometimes blood group discrepancies exist because of a mismatch between the current blood group and the historical blood group report.[4] However, blood group discrepancy because of underlying malignancy, especially hematological malignancy, is rare. Here we report a case of ABO discrepancy in a boy with AML who had a loss of expression of the A antigen during the acute leukemic phase followed by the reappearance of the A blood group after completion of the consolidation phase of chemotherapy.

Case Report

Admission and Diagnosis

A male patient aged 11 years presented to the hemato-oncology outpatient department with complaints of fever for 2 months, lethargy for 1 month, bleeding from the mouth, swelling, and blackish discoloration around the eyes. On clinical examination, his weight was 25 kilograms, and he had severe pallor, purpura, ecchymosis, conjunctival hemorrhage, and hepato-splenomegaly. His hematological parameters revealed anemia, thrombocytopenia, and leukocytosis with 97% blasts (hemoglobin 5.2 g/dL, platelet count 13,000/μL, white blood cell count 260.46 x 10^3/μL). Flow cytometry showed positivity for CD34, human leukocyte antigen-DR isotype, cytoplasmic myeloperoxidase, CD13, CD33, and CD117 and was abnormal expression for CD7. This pattern is consistent with AML. The Leukemia Translocation Panel for AML including FLT3, *CEBPA, Inv 16, NPM1, AML1/ETO,* and *PML/RARa* was performed and only a single mutation was detected in the coding region of the *CEBPA* gene, which did not bear any prognostic significance.

The blood group history of the patient was revealed as O Rh D-positive, and there was a history of transfusion of 5 units of RBCs and multiple units of platelet concentrates in the past 4 months. The treating oncologist ordered RBC and platelet concentrates for transfusion with a transfusion trigger of low hemoglobin (<8 gm/dL) and thrombocytopenia (<20,000/μL). The patient's blood group was tested by column agglutination technique (Gel Card, Tulip Diagnostics Pvt. Limited, Goa, India). A blood group discrepancy was noted in that cell grouping showed blood group O Rh D-positive but serum grouping showed a positive reaction with only B cells (**Figure 1A**, **Table 1**). Blood grouping was repeated using the tube technique and a similar result was obtained. To rule out missing an anti-A antibody in the serum, blood grouping was repeated in the test tube after 4°C incubation for 1 hour. There was no missing anti-A antibody observed in reverse grouping even with incubation at 4°C.

Further immunohematological workup, including the adsorption of the patient's cells with polyclonal anti-A serum followed by heat elution, was done as per the AABB Technical Manual,[5] but the elute failed to reveal any missing A antigen. Hence, the patient's blood group was considered to be O Rh D-positive with a missing anti-A antibody, and O Rh D-positive RBCs and random donor platelets (RDP) were transfused without any evidence of adverse transfusion reaction. The absence of the A antigen in the patient's RBCs could explain the lack of signs and symptoms of hemolysis after the transfusion of O Rh D-positive RDP units. Anti-A antibodies in the RDP units may have been diluted in a blood volume of approximately 1750 mL (70 mL × 25 kg body weight) in the patient.

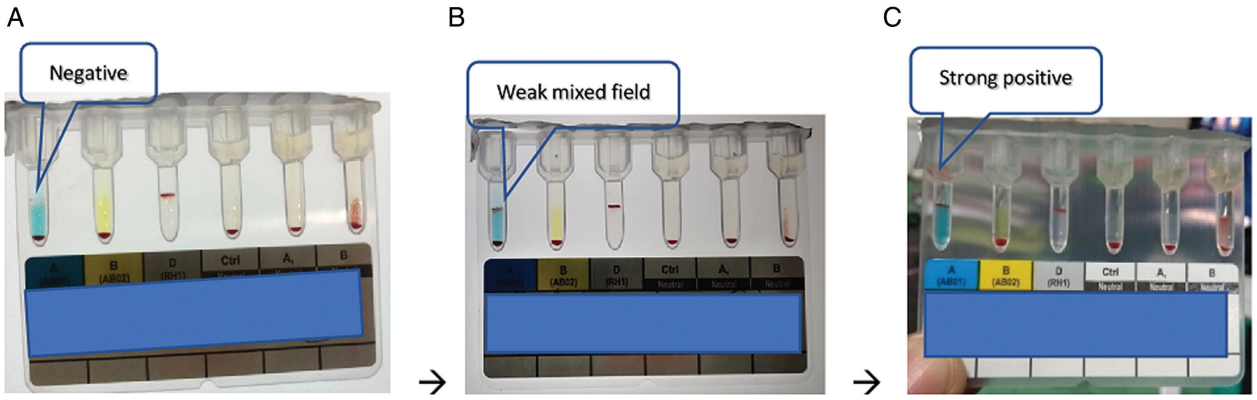

Figure 1

Eventual progress in A antigen expression with treatment for AML. AML, acute myeloid leukemia.

Table 1. Summary of Findings of Blood Group Typing of the Patient at Different Time Intervals

Method	At AML Diagnosis								
	Forward Grouping						Reverse Grouping		
	Anti-A	Anti-B	Anti-D	Anti-A1	Anti-AB	Anti-H	Control Cells	A Cells	B Cells
Gel card	0	0	4+	…	…	…	0	0	3+
Tube (RT incubation)	0	0	4+	…	…	4+	0	0	3+
Tube (4°C incubation)	0	0	4+	…	…	4+	0	0	4+
After 2 cycles of induction-phase chemotherapy									
Gel card	Mf (vw)[a]	0	4+	…	…	…	0	0	2+
Tube (RT incubation)	Mf (vw)[b]	0	4+	0	Mf (vw)	4+	0	0	2+
Tube (4°C incubation)	Mf (vw)	0	4+	0	Mf (vw)	4+	0	0	3+
After consolidation phase of chemotherapy									
Gel card	4+	0	4+	…	…	…	0	0	3+

AML, acute myeloid leukemia; Mf, mixed field reaction; RT, room temperature; vw: very weak reaction.
[a]*Mixed field reaction.*
[b]*Very weak reaction.*

After Second Cycle of Induction-Phase Chemotherapy

After the diagnosis of AML, the patient was started on chemotherapy as per the United Kingdom Medical Research Council protocol, which includes cytarabine, daunorubicin, etoposide, triple intrathecal therapy (methotrexate, cytarabine, hydrocortisone) as induction, and high-dose cytarabine as consolidation regimens. The patient attained complete remission after the first induction chemotherapy. He was administered 2 cycles of induction and 2 cycles of consolidation chemotherapy. After the second cycle of induction, an order for RBC and platelet transfusion was sent. The blood group was evaluated using the same column agglutination method as mentioned before. This time, the patient's cell grouping showed a weak mixed field reaction with anti-A antisera and a very weak reaction with B cells in the reverse group (**Figure 1B**, **Table 1**).

The blood group evaluation was repeated using the test tube method both at room temperature and during incubation at 4°C. The tube technique showed a similar pattern along with weak or mixed field reactions with anti-AB antisera in the forward grouping as well. Consequently, a weak subgroup of A (blood type A antigen) was suspected and a secretor study was performed per the method described in the AABB Technical Manual,[6] which showed that the patient was a secretor of A substance (**Figure 2**). Therefore, the possibility of a weak subgroup of A was confirmed and the patient was issued O Rh D-positive RBCs and A Rh D-positive platelets to avoid any untoward transfusion event. The transfusion was uneventful, and the patient had good posttransfusion platelet recovery.

After 4 Months of Follow-Up (Patient Completed Consolidation Phase of Chemotherapy)

After the second cycle of consolidation chemotherapy and approximately 4 months after diagnosis, the patient needed RBC transfusions. His blood group was evaluated using the same column agglutination technique and indicated the A blood group in both forward and reverse grouping with a strong 4+/3+ strength of reaction in the cell and serum groupings, respectively (**Figure 1C**, **Table 1**). Therefore, this time the patient's blood group was confirmed to be A Rh D-positive because there was no discrepancy observed between the forward and the reverse grouping. The patient had been transfused uneventfully with 2 units of A Rh D-positive RBCs.

Discussion

In this case report, the patient had a complete loss of expression of the A antigen in the RBCs since the onset of the disease process followed by the gradual recovery of antigen expression after the initiation of chemotherapy. This loss or

Lab Medicine 2021;52;509–513 511
DOI: 10.1093/labmed/lmab008

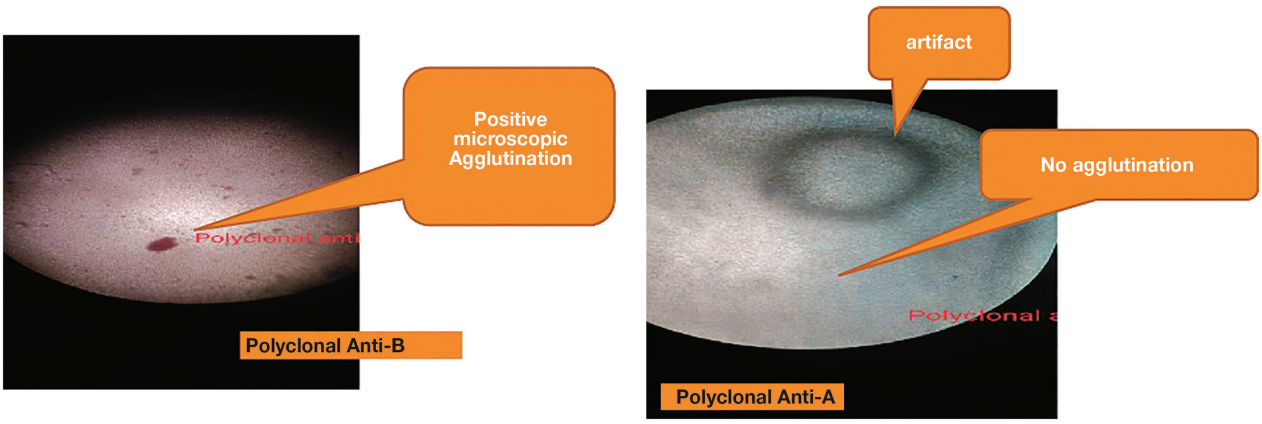

Figure 2

Saliva testing to determine presence/absence of A substance in secretions.

alteration of expression of blood group ABH antigens is a rare phenomenon but has been observed in hematological or solid organ malignancies.[7] The loss or weak expression of antigens results in ABO discrepancy in forward and reverse blood grouping. Research has shown that ABO antigens have the most frequently observed blood group antigen variation because ABO blood grouping is a mandatory requirement for any patients requiring blood transfusion.[8] In myeloid malignancy, the loss of ABH antigens is seen mainly in the RBCs because other hematopoietic cells do not express ABH antigens. Moreover, malignant stem cells often have the potential to differentiate into the erythroid lineage. Therefore, the loss of expression of ABH antigens in RBCs could be an indicator of genetic changes that have occurred in malignant stem cells.[9, 10]

Few possible mechanisms have been described in the literature on the altered expression of ABH antigens in hematologic malignancies. For example, there could be strongly decreased A or B transferase activity resulting in the reduced expression of the A or B antigens with a concurrent increased expression of the H antigens. Hence, in this situation the H antigen is not converted to the A or B antigen because of a lack of A or B transferase activity. Another mechanism is the inactivation of H transferase because of the loss of expression of one or both alleles of the gene (*FUT1* in erythroid precursors) code for the H antigen, thus eventually causing loss of all the H, A, and B antigens.[10] Sometimes, in myeloid malignancy, recurrent deletion on the chromosome band 9q23-31 region, which may even extend to the 9q34 region—the loci for the ABO gene—leads to a decreased expression of the A or B antigen.[11] However, the expression of the H antigen remains unaltered because the *FUT1* gene is present on chromosome band 19q13. In this patient, we observed a presentation similar to the loss of expression of the A antigen in the patient's RBCs with consistent expression of the H antigens. The loss of ABO antigens has also been reported very rarely in chronic myelocytic leukemia (CML) because the A or B transferase genes are located on chromosome 9, which may be inactivated by 9:22 translocation in CML. However, A or B transferase gene inactivation is not directly attributed to chromosomal translocation, otherwise, it would be observed in CML more frequently.[4]

Another proposed mechanism of the alteration or loss of ABO allelic expression is the silencing of the ABO promoter region by DNA methylation. Rarely, hematological and solid malignancies like gastric carcinoma cause hypermethylation of the CpG (cytosine and guanine rich bases in the regions of DNA where a cytosine nucleotide is followed by a guanine nucleotide in the linear sequence) sites in the ABO gene promoter region, leading to the inhibition of ABO genes by silencing either H transferase or A/B transferase.[3, 12] Upon therapy with hypomethylating agents, the ABO genes that were hypermethylated during the disease process begin to regain their function and encode to secrete their corresponding enzymes, revealing the original blood group of patients with malignancy.[12] We encountered a similar situation in our patient; initially, there was a complete loss of the A antigen, which was gradually restored after treatment with demethylating agents including methotrexate as one of the drugs used during chemotherapy.[13]

The approach for transfusion support is crucial in this type of blood group discrepancy where the patient needs repeated blood transfusions because of the underlying condition. Transfusion of ABO-identical or ABO-compatible blood components should be considered when there is blood group discrepancy. The type-specific RBCs or other blood components can be given only after confirmation of both cell and serum grouping.

Conclusion

Any loss or alteration of ABO antigens gives rise to ABO blood group discrepancy. Variation of ABO antigen expression should raise the suspicion of underlying disease, especially hematological malignancy, and also reflect the status of the malignant disease. Therefore, the importance of integrating laboratory results with clinical details and case history plays an important role in resolving blood group discrepancy and deciding on transfusion support of various blood components. **LM**

References

1. Kominato Y, Sano R, Takahashi Y, Hayakawa A, Ogasawara K. Human ABO gene transcriptional regulation. *Transfusion.* 2020;60(4):860–869.
2. Yamamoto M, Lin XH, Kominato Y, et al. Murine equivalent of the human histo-blood group ABO gene is a cis-AB gene and encodes a glycosyltransferase with both A and B transferase activity. *J Biol Chem.* 2001;276(17):13701–13708.
3. Bianco-Miotto T, Hussey DJ, Day TK, O'Keefe DS, Dobrovic A. DNA methylation of the ABO promoter underlies loss of ABO allelic expression in a significant proportion of leukemic patients. *PLoS One.* 2009;4(3):e4788.
4. Chenna D, Mohan G, Reddy VR, Shastry S. The disappearance of blood group antigens: a clue to the clinical diagnosis of leukemia. *Transfus Apher Sci.* 2019;58(1):48–49.
5. Technical manual, 20th edition: methods and appendices. Method 2.7. AABB website. https://www.aabb.org/aabb-store/resources/technical-manual-methods. Accessed January 25, 2021.
6. Technical manual, 20th edition: methods and appendices. Method 2.8. AABB website. https://www.aabb.org/aabb-store/resources/technical-manual-methods. Accessed January 25, 2021.
7. Reid ME, Bird GW. Associations between human red cell blood group antigens and disease. *Transfus Med Rev.* 1990;4(1):47–55.
8. Nambiar RK, Narayanan G, Prakash NP, Vijayalakshmi K. Blood group change in acute myeloid leukemia. *Proc (Bayl Univ Med Cent).* 2017;30(1):74–75.
9. Suciu S, Zeller W, Weh HJ, Hossfeld DK. Immunophenotype of mitotic cells with clonal chromosome abnormalities demonstrating multilineage involvement in acute myeloid leukemia. *Cancer Genet Cytogenet.* 1993;70(1):1–5.
10. Bianco T, Farmer BJ, Sage RE, Dobrovic A. Loss of red cell A, B, and H antigens is frequent in myeloid malignancies. *Blood.* 2001;97(11):3633–3639.
11. Evdokiou A, Webb GC, Peters GB, et al. Localization of the human growth arrest-specific gene (GAS1) to chromosome bands 9q21.3-q22, a region frequently deleted in myeloid malignancies. *Genomics.* 1993;18(3):731–733.
12. Kominato Y, Hata Y, Takizawa H, Tsuchiya T, Tsukada J, Yamamoto F. Expression of human histo-blood group ABO genes is dependent upon DNA methylation of the promoter region. *J Biol Chem.* 1999;274(52):37240–37250.
13. Wood GS, Wu J. Methotrexate and pralatrexate. *Dermatol Clin.* 2015;33(4):747–755.

DOI: 10.1093/labmed/lmab008

Case Study

Contradictory Phenomenon Between Serum Separator Tube and Plasma Tube: A Case Report

Lu Pang, MD,[1] Ying Xing, MD,[1] Lingsheng Xing, MD,[1] Linzi Miao, MD,[1] Chongwen An, MD,[1] and Haixia Li, MD, PhD[1,]*

Laboratory Medicine 2021;52:e125-e128

DOI: 10.1093/labmed/lmab003

ABSTRACT

Separator gels in blood collection tubes are used to separate serum from clotted whole blood or plasma from cells. Here we present a case of a patient with a contradictory phenomenon between the serum separator tube and the plasma tube. The serum separator tube showed mixed serum and separator gel and distinctly less serum. However, the plasma tube showed fewer cells. Laboratory study revealed an IgG level of 78.9 g/L. Serum immunofixation electrophoresis analysis identified the abnormal pattern as a dense IgG band with a corresponding dense light chain band of λ. Bone marrow smear showed 53% proplasmacytes. The patient was diagnosed with multiple myeloma. The marked hyperproteinemia, especially hyperimmunoglobulinemia, may have resulted in the density alteration of serum that was mixed or located above the separator gel. This phenomenon is also seen in patients injected with iodinated radiologic contrast media such as iohexol and in patients on hemodialysis with a concentrated sodium citrate solution.

Keywords: case report, serum separator tube, plasma tube, multiple myeloma, density, hyperimmunoglobulinemia

Clinical History

A female patient aged 57 years was referred to our hospital with 1 month of fatigue. She had a history of type 2 diabetes mellitus and hypertension. When performing laboratory analysis, we found a contradictory phenomenon between the serum separator tube (BD Vacutainer, Becton, Dickinson and Company, NJ, USA) and the plasma tube with heparin (BD Vacutainer) even with correct centrifugation (2000 g for 10 minutes at room temperature). The serum separator tube showed mixed serum and separator gel and distinctly less serum, which indicated polycythemia vera (**Image 1A**). However, the plasma tube showed fewer cells, which was in accordance with a hematocrit level of 23.5% (reference interval, 35.0%–45.0%; **Image 1B**). Repeat centrifugation did not yield any change.

Abbreviations:

SPE, serum protein electrophoresis; IFE, immunofixation electrophoresis; MM, multiple myeloma.

[1]Department of Clinical Laboratory, Peking University First Hospital, Beijing, China

*To whom correspondence should be addressed.
bdyylhx@126.com

In view of this contradictory phenomenon, further laboratory studies were performed. Laboratory studies (plasma specimen) revealed a hemoglobin level of 7.7 g/dL (reference interval, 11.5 g/dL–15.0 g/dL), a total calcium level of 11.92 mg/dL (2.98 mmol/L; reference interval, 8.44 mg/dL–10.08 mg/dL [2.11 mmol/L–2.52 mmol/L]), a total protein level of 110 g/L (reference interval, 65 g/dL–85 g/L), an IgG level of 78.9 g/L (reference interval, 7.23 g/L–16.85 g/L), and a β2-microglobulin level of 6.13 μg/mL (upper reference limit, <3.4 μg/mL). Serum protein electrophoresis (SPE) and the corresponding densitometry scan showed an abnormal band with γ globulin increased to 44.3 % (reference interval, 10.3%–18.2%; **Image 1C**). Further serum immunofixation electrophoresis (IFE) analysis, shown in **Image 1D**, identified the abnormal pattern as a dense IgG band with a corresponding dense light chain band of λ. A peripheral blood smear showed a rouleaux formation (red arrow, **Image 1E**).

After communication with the clinician, bone marrow puncture was requested. Bone marrow smear showed 53% proplasmacytes (red arrow, **Image 1F**). Flow cytometric immunophenotyping of plasma cells from the bone marrow showed diminished CD19 and CD27 expression, with aberrant expression of CD56 and CD20 and monoclonal cytoplasmic lambda light chain expression. The patient was

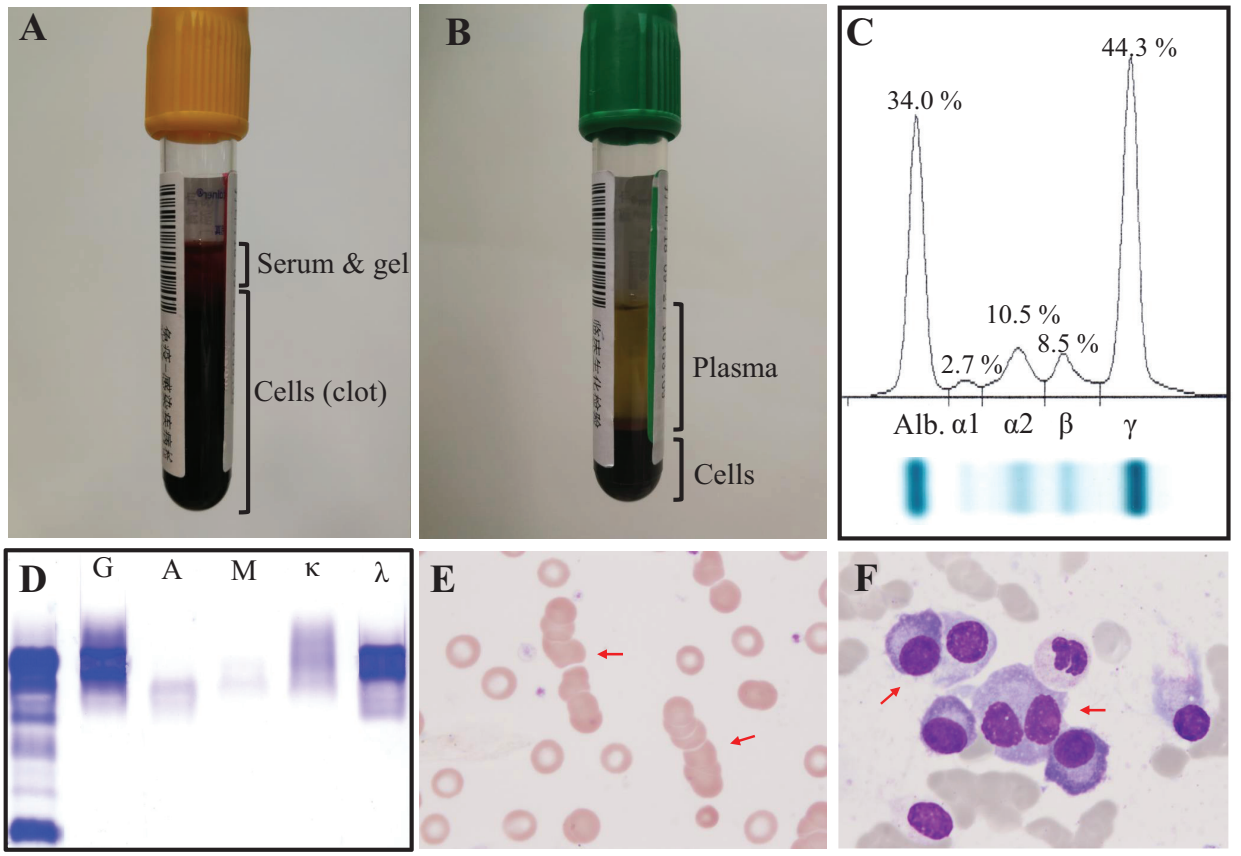

Image 1

Laboratory findings associated with patient. **A,** The serum separator tube showed mixed serum and separator gel and distinctly less serum, indicating polycythemia vera. **B,** The plasma tube showed fewer cells, in accordance with the hematocrit (23.5%). **C,** SPE and the corresponding densitometry scan showed an abnormal band with γ globulin increased to 44.3%. **D,** IFE analysis identified the abnormal pattern as a dense IgG band with a corresponding dense light chain band of λ. **E,** A peripheral blood smear showed a rouleaux formation (red arrow). **F,** A bone marrow smear showed 53% proplasmacytes. IFE, immunofixation electrophoresis; SPE, serum protein electrophoresis.

diagnosed with multiple myeloma (MM) based on the results of SPE, IFE, peripheral blood smear, bone marrow smear, and flow cytometric immunophenotyping of plasma cells.

Discussion

This case report presents an incidental finding during the routine work of centrifugation in the clinical laboratory. The phenomenon is influenced by many variables, such as patient characteristics, tube features, and laboratory factors (Table 1).

Components from blood collection tubes, such as additives, stoppers, surfactants, and separator gels, can alter analyte stability from a specimen. Because of the interference with blood specimens, blood collection tubes are a potential source of preanalytical error in laboratory testing. Blood specimen tubes that contain a separator gel are often used to obtain serum for laboratory tests. During centrifugation, the thixotropic gel in these tubes is located between packed cells and the top serum layer.[1] The migration of the separator gel during centrifugation is mainly determined by the density rather than the viscosity of the specimen because dextran solutions with very high viscosity but normal density allow proper behavior of the separator gel.[2] After centrifugation,

Lab Medicine 2021;52;e125–e128
DOI: 10.1093/labmed/lmab003

the separator gel at the bottom of the tube normally occupies the middle position between the cells (clot) and the serum, because its density (1.04 g/cm^3) is intermediate between their densities (1.09 g/cm^3 and 1.03 g/cm^3, respectively). The separator gel then acts as a barrier to separation and prevents contamination of the serum with cells (clot).[3] The dislocation of the separator gel, cells (clot), and serum indicates the density alteration of the serum. The marked hyperproteinemia, especially hyperimmunoglobulinemia, which is a characteristic of MM, may result in the density alteration of serum, which therefore mixes or is located above the separator gel.[4] Hyperimmunoglobulinemia can lead to this phenomenon. Wang et al[5] showed that serum migrated below the separator gel when the IgG concentration exceeded 50 g/L. In addition to the advanced MM, this phenomenon has also been seen in patients injected with iodinated radiologic contrast media[6-8] such as iohexol[6] and in patients on hemodialysis with a concentrated sodium citrate solution[9] because the presence of high-density molecules such as iodinated contrast media increases the density of serum. When the density of the serum exceeds that of the separator gel, the latter no longer forms a barrier between the serum and the cells (clot) but floats partially or completely to the top of the serum.

Different separator tubes from different manufacturers have different kinds of separator gels. Faught et al[2] observed remarkable differences in the density of separator gels contained in serum separator tubes from different manufacturers, with a consequent difference in the frequency of this issue. This dislocation phenomenon was observed at a lower specific gravity of serum in Greiner Vacuette tubes than in BD Vacutainer tubes.[2] Furthermore, the main composition of the separator gel in the BD Vacutainer SST II is acrylic, which is easily affected by environmental temperature, but the separator gel in the BD Vacutainer SST is polyester, which is not easily affected. Wang et al[5] found that this dislocation phenomenon was observed in the BD Vacutainer SST II but not in the BD Vacutainer SST, which indicates that the different kinds of separator gels were responsible for the anomalous separator gel barrier formation.

Table 1. Representative Lists of Potential Causes of Dislocation of Separator Gel, Cells (clot), and Serum

Patient characteristics	Hyperproteinemia
	Hyperimmunoglobulinemia
	Injected with iodinated radiologic contrast media
	Injected with iohexol
	Patients on hemodialysis with sodium citrate solution
	Heparin therapy
Tube features	Density of separator gel
	Yield stress of separator gel
	Composition of separator gel
Laboratory factors	Centrifugation speed
	Temperature
	Acceleration and deceleration conditions of centrifugation
	Storage conditions of tubes

This case report reminds researchers and clinicians to consider MM or clinical operation whenever this phenomenon is seen. Laboratory tests should not be performed; the results may be falsely low because of dilution with iodinated radiologic contrast media and sodium citrate, or they may be wrong owing to the interference of these substances or separator gel on assay because an inappropriate amount of serum would have been analyzed.[10] The probes of the instrument may be occluded by the aspiration of separator gel, especially in clinical laboratories with a high degree of preanalytical and analytical automation, where vacuum blood collection tubes may be introduced to an automated centrifugation and specimen delivery system without direct visual inspection. The peripheral blood specimen should be collected at least 1 elimination half-life (approximately 2 hours) after clinical operation[8] and checked visually to determine the accuracy of barrier formation after centrifugation. **LM**

Acknowledgments

The study was performed in accordance with the tenets of the Helsinki principles and was approved by the ethics committee of our hospital. The significance of the research was explained to the patient and informed consent was obtained.

References

1. Bowen RA, Remaley AT. Interferences from blood collection tube components on clinical chemistry assays. *Biochem Med (Zagreb).* 2014;24(1):31–44.
2. Faught RC, Marshall J, Bornhorst J. Solution densities and estimated total protein contents associated with inappropriate flotation of separator gel in different blood collection tubes. *Arch Pathol Lab Med.* 2011;135(9):1081–1084.
3. Maire B, Schlüter K. Problem with the separating gel in a blood sample tube in a patient with multiple myeloma. *Dtsch Arztebl Int.* 2017;114(29–30):507.
4. Fatás M, Franquelo P, Franquelo R. Anomalous flotation of separator gel: density or viscosity? *Clin Chem.* 2008;54(4):771–772.

5. Wang ZE, Song XF, Zou JW, et al. The usage of separating gel vacuum tube with different IgG concentration. *Ann Clin Lab Sci.* 2015;45(4): 438–440.
6. Kaleta EJ, Jaffe AS, Baumann NA, Block DR. A case of floating gel. *Clin Chem.* 2012;58(11):1604–1605.
7. Daves M, Lippi G, Cosio G, et al. An unusual case of a primary blood collection tube with floating separator gel. *J Clin Lab Anal.* 2012;26(4):246–247.
8. Spiritus T, Zaman Z, Desmet W. Iodinated contrast media interfere with gel barrier formation in plasma and serum separator tubes. *Clin Chem.* 2003;49(7):1187–1189.
9. Srivastava R, Murphy MJ, Card J, Severn A, Fraser CG. The case of the floating gel. *J Clin Pathol.* 2004;57(12):1333–1334.
10. van den Ouweland JM, Church S. High total protein impairs appropriate gel barrier formation in BD Vacutainer blood collection tubes. *Clin Chem.* 2007;53(2):364–365.

DOI: 10.1093/labmed/lmab003

Case Study

Sky High or Undetectable? A Patient with Discordant Hemoglobin A1c

Patricia Lee, DO, JD,[1] *Allison B. Chambliss, PhD,*[1] *Maximo J. Marin, MD*[1,*]

Laboratory Medicine 2021;52:e129-e132

DOI: 10.1093/labmed/lmab012

ABSTRACT

A female patient aged 47 years presented with a hemoglobin A1c (HbA1c) level of 54.6%, as measured by ion-exchange high-performance liquid chromatography (HPLC), and a glucose level of 106 mg/dL. The HbA1c was re-evaluated using a turbidimetric inhibition immunoassay and found below the level of detection. Hemoglobinopathy testing led to the identification of a hemoglobin variant consistent with Hb Raleigh, in which a valine → alanine substitution on the beta chain effects a charge difference, resulting in coelution with HbA1c on HPLC and a spuriously high reading. Many Hb variants may interfere with HbA1c measurement and generate misleading results. The unique properties of Hb Raleigh may give rise to analytical errors when evaluating HbA1c using 2 different methods—molecular charge–based (eg, HPLC) and molecular structure–based (eg, immunoassay)—yielding diametrically opposed results. Consequently, recognition and diagnosis of this entity are essential in patients with Hb Raleigh, especially when monitoring long-term glucose control.

Keywords: hemoglobin, variant, immunoassay, high-performance liquid chromatography, A1c, Hb Raleigh

Clinical History

A female patient aged 47 years who was obese (body mass index [BMI], 32.5 kg/m^2) with no previous diagnosis of diabetes mellitus presented to the clinic complaining of dyspnea on exertion, occasionally accompanied by left-sided facial tingling, for several months. In addition to a cardiac workup for the patient's chief complaint, a hemoglobin A1c (HbA1c) measurement was ordered because of her BMI. Her HbA1c level, measured by ion-exchange high-performance liquid chromatography (HPLC), was biologically implausible at 54.6% (clinical reportable range, 4.0%–16.9%) and incongruous given the patient's glucose level of 106 mg/dL (reference range, 70–99 mg/dL) at the same visit. Her HbA1c level was re-evaluated using a turbidimetric inhibition immunoassay and was determined to be below the assay's limit of detection. These unusual results increased suspicion for an interfering substance, including a hemoglobin (HB) variant, and prompted further investigation. Hemoglobinopathy evaluation detected an abnormal beta Hb variant (46.9%) consistent with Hb Raleigh.

Abbreviations:

HbA1c, hemoglobin A1c; HPLC, high-performance liquid chromatography; BMI, body mass index; Hb, hemoglobin; HbA, hemoglobin A; VAL, valine; ALA, alanine.

[1]Department of Pathology, Keck School of Medicine, University of Southern California, Los Angeles, California, USA

*To whom correspondence should be addressed.
maximo.marin@med.usc.edu

Discussion

The red-pigmented protein Hb, located in erythrocytes, acts to transport oxygen and carbon dioxide in blood. The hemoglobin molecule is composed of 4 globin chains, each with a heme moiety to which oxygen binds. Normal adult hemoglobin (Hb A) is composed of 2 pairs (two alpha and two beta) of globin chains. Further, Hb consists of various subfractions and derivatives; the most common and nonpathological fractions are HbA, hemoglobin F (contains 2 alpha and 2 gamma chains), and hemoglobin A2 (contains

2 alpha and 2 delta chains). Hemoglobinopathies consist of structural Hb variants and thalassemias. Structural Hb variants are typically the result of a point mutation and the subsequent amino acid substitution in a globin chain, whereas thalassemias are the result of insufficient or absent globin chain synthesis. There are hundreds of Hb variants, including but not limited to hemoglobin S (results in sickle cell trait or disease), hemoglobin C (responsible for mild hemolytic anemia), and hemoglobin E.[1]

Glycohemoglobin is blood glucose bound to Hb. Glycated hemoglobin is formed by a nonenzymatic process within red blood cells during their 120-day circulating lifespan. In patients who are hyperglycemic, an increase in glycohemoglobin results in an increase in HbA1c. HbA1c is formed by the glycation of or nonenzymatic addition of a glucose molecule to the N-terminal valine (VAL) on the beta-globin chain of HbA. The glycation of the N-terminal VAL on the beta-globin chain of HbA alters the structure and decreases the positive charge of the protein. Other glycohemoglobins include HbA1a and HbA1b and occur naturally; these have charges distinct from HbA1c. Described as a fraction or percentage of total hemoglobin, HbA1c reflects the mean blood glucose levels of the previous 3 months (the normal, average lifespan of erythrocytes) and is used for the screening and diagnosis of diabetes mellitus and for monitoring long-term glycemic control in those with an established diagnosis of that condition.[2] Any event or condition that affects the structure of Hb or red blood cells, or their turnover, may affect the level of serum HbA1c. Rapid erythrocyte turnover and a prolonged erythrocyte life span alters the time available for glycation and can thus result in HbA1c measurements that underestimate or overestimate glycemic control.[3] It has been well-documented that misleading HbA1c results may be seen in patients with both common and rare Hb variants.[4, 5]

Although many causes of HbA1c interference are associated with clinical signs and symptoms (eg, uremia, chronic alcohol abuse, hyperbilirubinemia, iron deficiency anemia, massive bleeding, pregnancy induced anemia), most Hb variants are clinically silent.[6] Suspicion of an Hb variant should arise if (1) the HbA1c result is wholly unexpected, (2) the HbA1c result is above 15%, (3) the HbA1c result is radically different from a previous measurement using a different methodology, or (4) the HbA1c result does not correlate with the patient's self-monitoring of blood glucose.[2]

In this patient, an inordinately high HbA1c fraction (54.6%) was found on ion-exchange HPLC and led to re-evaluation using an immunoassay. When an undetectable HbA1c level on immunoassay was observed, suspicion of an Hb variant increased and prompted hemoglobinopathy evaluation. The patient's Hb was subsequently characterized using cytometry and HPLC, and a variant consistent with Hb Raleigh was identified. Research has shown that Hb Raleigh is a variant of the beta chain, in which alanine (ALA) is substituted for VAL at the second base of the codon encoding the first amino acid. After translation, the N-terminal ALA undergoes acetylation, which in turn prevents glycation.[7, 8]

A rare Hb variant, Hb Raleigh was first described in 1977.[9] A review of the literature shows that fewer than 10 patients with this variant have been documented.[7, 9, 10] All prior reports on Hb Raleigh describe spuriously high HbA1c measured by HPLC; however, whereas researchers have suggested that immunoassay methods may underestimate glycated Hb, there have been no previous reports of HbA1c below the level of detection.[5,7-10]

Laboratory Role in Diagnosis

Analytical assays developed to measure HbA1c rely on techniques that detect changes in either molecular charge (eg, HPLC) or molecular structure (eg, immunoassay). In our laboratory, HbA1c analysis was performed using 2 methods in accordance with the manufacturers' instructions: ion-exchange HPLC (Tosoh G8, Keck Medical Center, Los Angeles, CA) and turbidimetric inhibition immunoassay (Roche cobas 8000, LAC+USC Medical Center, Los Angeles, CA). Results from HPLC showed an HbA1c fraction of 54.6% (**Figure 1**). The immunoassay results were below the assay's level of detection: Its limit of quantitation for patient reporting of HbA1c is 4.2%, but the analyzer detected no HbA1c signal with this specimen and thus could not calculate a result.

Studies have shown that HPLC separates Hb species based on surface charge differences. The output from the analyzer, displayed as a chromatogram, consists of peaks indicating the presence of glycated, fetal, or Hb variants.[11] Further, HbA1c is separated from HbA because glycation of the N-terminal VAL decreases the positive charge. In the Hb variant Hb Raleigh, ALA is substituted for VAL at position 1 of the Hb beta chain. The effect is a decrease in the positive

surface charge, similar to that of HbA glycated at the N-terminal of the beta chain.[7, 8] The resulting coelution with HbA1c in the ion-exchange HPLC explains the exceptionally high measurement seen in our patient.

Immunoassays use antibodies to target the N-terminal glycated amino acids of the first 4 to 10 amino acids of the beta chain of Hb to quantify HbA1c. This technique does not directly report the presence of Hb variants; however, any factor that prevents the glycation or identification of these amino acids may interfere with HbA1c immunoassays.[12] In Hb Raleigh, the substitution of VAL with ALA occurs at the same site that is most commonly glycated within the Hb tetramer. This substitution at the N-terminal residue leads to posttranslational modification by acetylation and prevents glycation.[13] As shown by the undetectable concentration of HbA1c in this patient, the antibody kinetics do not favor binding (**Figure 2**).

The inordinately high HbA1c fraction on HPLC and a concentration below the level of detection on immunoassay increased the suspicion of an Hb variant and prompted further investigation. Hemoglobinopathy evaluation performed by a reference laboratory using cytometry and

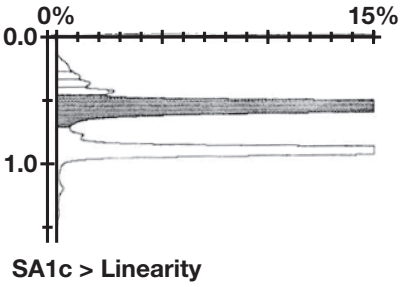

Name	%	Time	Area
FP	0.0	0.00	0.00
A1A	0.6	0.23	10.73
A1B	0.7	0.30	11.94
F	1.0	0.37	17.35
LA1C+	1.7	0.44	28.39
SA1C	54.6	0.56	771.17
A0	50.3	0.90	831.14
			1,670.72

Figure 1

HPLC results

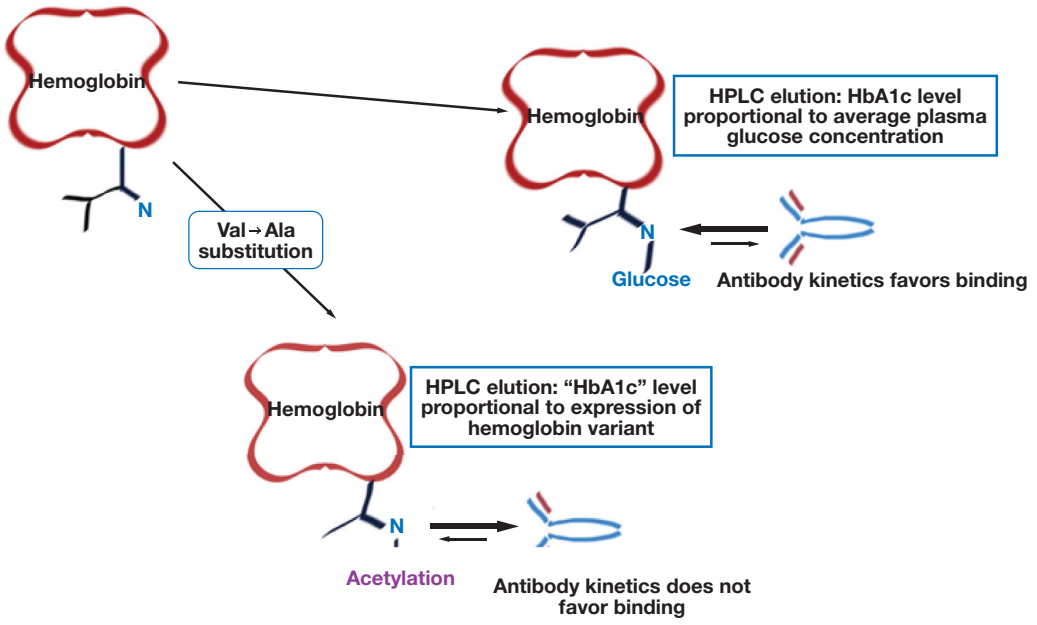

Figure 2

HPLC coelution and antibody kinetics.

Lab Medicine 2021;52;e129–e132
DOI: 10.1093/labmed/lmab012

HPLC revealed an abnormal Hb variant consistent with Hb Raleigh.

Patient Follow-Up

The use of HbA1c measurements to diagnose diabetes mellitus or to monitor glycemic control in patients with diabetes with Hb Raleigh will be ineffective because the variant confounds interpretation of the common analytical methods. Given the unreliability of HbA1c analysis in patients with this Hb variant, it is important that such variants are detected and documented on the patient's electronic medical record for future reference. In addition, clinicians should be advised to consider alternative measures of glycemic control that are not affected by the turnover of erythrocytes or hemoglobinopathies. One alternative measure that has been suggested is fructosamine, which reflects the binding of glucose to proteins (primarily albumin) and is a measure of plasma glucose over the previous 2 to 3 weeks.[3, 5, 10] **LM**

Acknowledgments

This work was not supported by grant from any funding agency in the public, commercial, or not-for-profit sectors. The authors declare that they have no known competing financial interests or personal relationships that could have appeared to influence the work reported in this article.

References

1. Troxler H, Kleinert P, Schmugge M, Speer O. Advances in hemoglobinopathy detection and identification. *Adv Clin Chem.* 2012;57:1–28.
2. Klonoff DC. Hemoglobinopathies and hemoglobin A1c in diabetes mellitus. *J Diabetes Sci Technol.* 2020;14(1):3–7.
3. Fisher SJ. Commentary. *Clin Chem.* 2011;57(2):157.
4. Little RR, Roberts WL. A review of variant hemoglobins interfering with hemoglobin A1c measurement. *J Diabetes Sci Technol.* 2009;3(3):446–451.
5. Chandrashekar V. Hb A1c separation by high performance liquid chromatography in hemoglobinopathies. *Scientifica (Cairo).* 2016;2016:2698362.
6. Jain N, Kesimer M, Hoyer JD, Calikoglu AS. Hemoglobin Raleigh results in fictitiously low hemoglobin A1c when evaluated via immunoassay analyzer. *J Diabetes Complications.* 2011;25(1):14–18.
7. Singha K, Fucharoen G, Chaibunruang A, Netnee P, Fucharoen S. A spurious haemoglobin A(1c) result associated with double heterozygote for haemoglobin Raleigh (β1[NA1]Val → Ala) and α(+)-thalassaemia. *Ann Clin Biochem.* 2012;49(Pt 5):445–449.
8. Sofronescu AG, Williams LM, Andrews DM, Zhu Y. Unexpected hemoglobin A1c results. *Clin Chem.* 2011;57(2):153–156.
9. Moo-Penn WF, Bechtel KC, Schmidt RM, et al. Hemoglobin Raleigh (beta1 valine replaced by acetylalanine). Structural and functional characterization. *Biochemistry.* 1977;16(22):4872–4879.
10. Vandewiele A, Genbrugge K, Delanghe J. Spuriously high HbA1c due to the presence of haemoglobin Raleigh: a case report and review of the literature. *Acta Clin Belg.* 2010;65(5):336–340.
11. Manley S, Stratton I, Gough S. *HbA1c in Diabetes: Case Studies Using IFCC Units*. 1st ed. Chichester, UK and Hoboken, NJ: Wiley-Blackwell; 2010.
12. Bry L, Chen PC, Sacks DB. Effects of hemoglobin variants and chemically modified derivatives on assays for glycohemoglobin. *Clin Chem.* 2001;47(2):153–163.
13. Chen D, Crimmins DL, Hsu FF, Lindberg FP, Scott MG. Hemoglobin Raleigh as the cause of a falsely increased hemoglobin A1C in an automated ion-exchange HPLC method. *Clin Chem.* 1998;44(6 Pt 1):1296–1301.

Case Study

Lymphocyte Aggregation in Low-Grade B-Cell Lymphoma

Eric A Walradth, MA, MLS(ASCP)[CM] *SH*[CM*]

Laboratory Medicine 2021;52:e133-e136

DOI: 10.1093/labmed/lmab010

ABSTRACT

Platelet and erythrocyte agglutination is known to happen in vitro due to EDTA or temperature-induced cold antibodies. Leukocyte agglutination is far less common, and its etiology is not always known. The 2 cases presented herein are of low-grade B-cell lymphomas consistent with splenic marginal-zone lymphoma that presented with lymphocyte agglutination. In Case A, the lymphocyte aggregates were not resolved by warming the sample or by non-EDTA anticoagulation. In Case B, the lymphocyte aggregates were largely resolved by warming the specimen at 37°C for 15 minutes. The 2 cases presented herein further show that the etiology of lymphocyte aggregation can have multiple causes, even within the same disease process.

Keywords: splenic marginal zone lymphoma, lymphocyte aggregates, lymphocyte agglutination, low grade B-cell lymphoma, lymphocytosis, leukocytosis, atypical lymphocytes

Case A

An 86 year old caucasian man presented for evaluation for lymphocytosis. He has a history of hypertension, low back pain, and generalized anxiety disorder. The patient only reported mild fatigue, saying that, overall, he felt well. In October 2019, his absolute lymphocyte count had been at 5.0 $\times 10^3/\mu L$. Repeat counts in September 2020 showed his absolute lymphocyte count to be 12.7 $\times$ $10^3/\mu L$.

During this same time period, the white blood cell (WBC) count of the patient increased from 8.1 $\times$ $10^3/\mu L$ to 14.9 $\times$ $10^3/\mu L$. His platelet counts showed mild thrombocytopenia (113 $\times$ $10^3/\mu L$ and 110 $\times 10^3/\mu L$, respectively); hemoglobin (12.0 g/dL and 11.6 g/dL, respectively) and hematocrit (36.0% and 35.7%, respectively) levels showed mild anemia. On arrival at our office, a complete blood count (CBC) was run. The WBC count was 20.8 $\times$ $10^3/\mu L$ (4.0–10.0 $\times$ $10^3/\mu L$), and the absolute lymphocyte count was 16.67 $\times$ $10^3/\mu L$ (1.2–3.4 $\times$ $10^3/\mu L$). The platelet count was 110 $\times$ $10^3/\mu L$ (150–400 $\times$ $10^3/\mu L$); hemoglobin, 12.8 g/dL (13.5–18.0 g/dL); and hematocrit, 39.7% (41.0%–53.0%). Quantitative immunoglobulins were as follows: immunoglobulin (Ig)G, 975.0 g/dL (650–1600 mg/dL); IgM, 43.2 mg/dL (50–300 mg/dL); and IgA, 161.5 mg/dL (40–350 mg/dL). Serum protein electrophoresis was not performed.

Peripheral blood smear review showed a subpopulation of his lymphocytes, which were smaller in size with moderately condensed chromatin, had occasional singular but prominent nucleoli and pale blue cytoplasm with bipolar tufts, and appeared in aggregates of 2 to 6. Suspecting that the aggregates could be a possible cold-activated antibody, the EDTA tube was warmed at 37°C for 15 minutes, a CBC was performed again, and another peripheral blood smear was performed. The results of the CBC did not change. The lymphocyte aggregates were still present.

The laboratory research team and I were unable to test whether the agglutination would resolve with anti-IgM treatment because we do not keep the supplies for such testing in stock. These findings were noted in the report and discussed with the treating medical oncologist.

Flow cytometry was also performed at this new consult visit. The results returned with the diagnosis of low-grade B-cell lymphoma, with a differential diagnosis that includes marginal-zone lymphoma (including splenic marginal-zone lymphoma) and lymphoplasmacytic lymphoma. The pathologist reviewing the case for flow cytometry noted similar

Abbreviations:

WBC, white blood cell; CBC, complete blood count; Ig, immunoglobulin; CLL, chronic lymphocytic leukemia

Hematology Oncology Associates of Central New York, East Syracuse, NY

*To whom correspondence should be addressed.
ewalradth@hoacny.com

lymphocyte morphology and requested molecular studies for MYD88 and cytogenetics. Testing results for MYD88 came back negative. Testing results for cytogenetics came back positive for Deletion 7q, which has been associated with splenic marginal-zone lymphoma.[1]

On return to our office 2 weeks later for an abdominal CT scan, a new CBC was ordered. On this visit, a peripheral blood specimen was drawn into a sodium citrate tube, to rule out a possible EDTA mechanism causing the lymphocyte aggregation. We noted the same lymphocyte morphology and aggregation on the EDTA and sodium citrate peripheral smears; similar CBC results were obtained as during the initial visit. The CT scan showed a substantially enlarged spleen with a 7-mm indeterminate focal exophytic nodule off the posterior inferior aspect of the spleen. A diagnosis of low-grade B-cell lymphoma consistent with splenic marginal-zone lymphoma was made.

Case B

An 86 year old caucasian woman was admitted to a local hospital for a bleeding rectal prolapse. A CBC was performed; lymphocytosis with abnormal-appearing lymphocytes were noted and sent to a pathologist for review. Pathology review noted atypical lymphocytes consistent with lymphoma. The WBC count of the patient was 27.9 × 10^3/μL, with an absolute lymphocyte count of 25.9 × 10^3/μL. At that time, the patient was seen for a hematology consultation. Flow cytometry and cytogenetics testing were ordered.

The flow cytometry report showed a diagnosis of B-cell leukemia/lymphoma with a phenotype that could be consistent with prolymphocytic leukemia or marginal-zone lymphoma. The cytogenetics report was positive for translocation (10;14) and deletion of IgH in 3.5% of cells. FISH results were negative for t(11;14). Multiple small mobile nodes in the spleen were noted during the physical examination. A CT scan showed moderate splenomegaly. A diagnosis of low-grade B-cell lymphoma consistent with splenic marginal-zone lymphoma was made.

Two weeks after being seen in the hospital, the patient was seen in our office for hospital follow-up of her initial consultation visit. She has a history of dementia, diabetes, hypercholesterolemia, hypertension, gastroesophageal reflux, and mutlifactoral anemia caused by chronic kidney disease and iron deficiency. Her WBC count was 41.0 × 10^3/μL, with an absolute lymphocyte count of 35.67 × 10^3/μL. Her hemoglobin was 8.9 g/dL (13.5–18.0 g/dL), and her hematocrit was 29.1% (41.0%–53.0%). Her platelet count was 134 × 10^3/μL. It was noted on the peripheral smear review that several lymphocytes were larger, with pale blue cytoplasm, occasionally having singular but prominent nucleoli, and had clefted nuclei.

Four weeks after being seen in the hospital, the patient was seen in our office for a routine follow-up, for continuation of attempts to ameliorate her anemia and further monitor her lymphoma. Her WBC count was 60.5 × 10^3/μL, with an absolute lymphocyte count of 57.49 × 10^3/μL. Her hemoglobin was 9.4 g/dL (13.5–18.0 g/dL) and her hematocrit was 30.4% (41.0%–53.0%). Her platelet count was 159 × 10^3/μL. On review of her peripheral blood smear, most of her lymphocytes were noted to be larger, with pale blue cytoplasm, occasionally having singular but prominent nucleoli and some clefted nuclei, and appeared in aggregates of 3 to 15.

Due to the lymphocyte aggregates, the EDTA tube was placed into a 37°C water bath for 15 minutes. Then, the laboratory reran the CBC and performed a new peripheral blood smear. The CBC results did not change; however, the lymphocyte aggregates were largely resolved. A few lymphocyte aggregates remained but they consisted of only 2 to 5 lymphocytes each. Quantitative immunoglobulins and serum protein electrophoresis were not ordered.

Discussion

Pseudothrombocytopenia caused by EDTA-induced platelet agglutination and erythrocyte agglutination caused by cold-induced IgM antibodies are relatively common and well-studied.[2–6] However, leukocyte agglutination is far less documented. Clumping has been documented in benign and malignant lymphocytes, including chronic lymphocytic leukemia (CLL) and lymphoma, and is thought to be temperature dependent, EDTA dependent, or of unknown cause.[2–6]

In Case A, temperature-dependent cold agglutination was ruled out on the first specimen by warming it at 37°C for 15 minutes. An EDTA mechanism was also ruled out as the possible source for the lymphocyte aggregation by drawing a subsequent specimen into a sodium citrate tube. A manual WBC estimate was performed on all slides; the results confirmed the automated WBC counts. IgA and IgG levels were within normal limits, and IgM levels were slightly decreased. These findings suggest that there is no polyclonal or monoclonal process; however, such a result cannot be ruled out due to the fact that serum electrophoresis had not been ordered. At this point, the etiology of the lymphocyte agglutination is unknown in this case.

In Case B, a temperature-dependent mechanism seemed to be the cause of the lymphocyte agglutination, although erythrocyte agglutination was not seen in this patient. The 4-week follow-up after the initial consult was the only CBC in which lymphocyte aggregates were noted. The results from the prewarmed and warmed specimens did not differ, despite that most of the lymphocyte agglutination had been resolved. The manual WBC estimate and differential matched the automated counts as well, leading us to believe that the lymphocyte agglutination was not causing erroneous results. We were not able to note the presence of a possible polyclonal or monoclonal process due to quantitative immunoglobulins and serum protein electrophoresis not being ordered.

Leukocyte agglutination has been shown,[4–6] in some instances, to cause spurious pseudoleukopenia. In the 2 cases presented herein, this does not appear to be occurring. Attempts were made to resolve the lymphocyte aggregates with the 2 most common methods of resolution. We were unable to resolve Case A by warming or using a different anticoagulant; however, we were able to resolve Case B by warming. Manual WBC estimates and differentials were performed on all peripheral smears where lymphocyte aggregation was present. The manual WBC estimates agreed with the automated WBC counts for all specimens. The lymphocytes that were morphologically consistent with lymphoma cells in both patients were counted as a mixture of lymphocytes and monocytes, on the automated differential for both patients on all blood specimens collected, due to the gating algorithms of the Sysmex XN 2000 hematology analyzer. Therefore, manual differentials were performed and released on all CBCs that were ordered.

It has been documented that approximately 25% to 40% of patients with splenic marginal-zone lymphoma have an underlying monoclonal paraprotein.[7,8] We postulated that, although we are unable to confirm the presence of clonal immunoglobulins, they may be a product of the low-grade B-cell lymphoma cells and may be the cause of the lymphocyte aggregation. These immunoglobulins may have be diluted out or rendered functionless by the reagents when we ran the specimens through the Sysmex XN 2000 analyzer (Sysmex Corporation).

This same compensation mechanism resolving the lymphocyte aggregates would not be present when preparing peripheral smears for modified Wright-Giemsa staining. This could account for the lymphocyte aggregates being present on the peripheral-blood films and the automated WBC and differential counts matching manual WBC estimates and differentials. We believe that pseudoleukopenia was not caused by the lymphocyte aggregates in these 2 cases.

In conclusion, we did not see pseudoleukopenia due to the lymphocyte agglutination. In both cases, the diagnosis of low-grade B-cell lymphoma consistent with splenic marginal-zone lymphoma was made, and only the lymphocytes that were morphologically consistent with lymphoma cells appeared in aggregates. One was shown to be a temperature-dependent mechanism; the mechanism causing lymphocyte agglutination in the other is still unknown. Lymphocyte aggregation may suggest an underlying lymphoproliferative disorder such as low-grade B-cell lymphoma—specifically, splenic marginal-zone lymphoma—as in these 2 cases. **LM**

Personal and Professional Conflicts of Interest

None reported.

References

1. Salido M, Baró C, Oscier D, et al. Cytogenetic aberrations and their prognostic value in a series of 330 splenic marginal zone B-cell lymphomas: a multicenter study of the Splenic B-Cell Lymphoma Group. *Blood.* 2010;116(9):1479–1488.
2. Deol I, Hernandez AM, Pierre RV. Ethylenediamine tetraacetic acid-associated leukoagglutination. *Am J Clin Pathol.* 1995;103(3):338–340.
3. Shelton JB Jr, Frank IN. Splenic B cell lymphoma with lymphocyte clusters in peripheral blood smears. *J Clin Pathol.* 2000;53(3):228–230.
4. Yang D, Guo X, Chen Y, Xu G. Leukocyte aggregation in vitro as a cause of pseudoleukopenia. *Lab Medicine*. 2008;39(2):89–91.

DOI: 10.1093/labmed/lmab010

5. Bowen K. Clinical pathology rounds: erroneous leukocyte counts and cold agglutinins. *Lab Medicine*. 1997;28:247–250.
6. Goyal P, Agrawal D, Kailash J, et al. Cold-induced pseudoneutropenia in human immunodeficiency virus infect: first case report and review of related articles. *Indian J Hematol Blood Transfus*. 2014;30(Suppl 1):148–150.
7. Zinzani PL. The many faces of marginal zone lymphoma. *Hematology Am Soc Hematol Educ Program.* 2012;2012(1):426–432.
8. King R, Kurtin P. *Small B-Cell Lymphomas. Hematopathology: A volume in Foundations in Diagnostic Pathology*. 3rd ed. Elsevier, Inc.; 2019.

Science

Cross-Institutional Evaluation of the Abbott ARCHITECT SARS-CoV-2 IgG Immunoassay

Joesph R. Wiencek, PhD,[1] Lorin M. Bachmann, PhD,[2] Kelly Dinwiddie,[3] Greg W. Miller, PhD,[2] Lindsay A. L. Bazydlo, PhD[1,]*

Laboratory Medicine 2021;52:e137-e146

DOI: 10.1093/labmed/lmab011

ABSTRACT

Objective: To describe a cross-institutional approach to verify the Abbott ARCHITECT SARS-CoV-2 antibody assay and to document the kinetics of the serological response.

Methods: We conducted analytical performance evaluation studies using the Abbott ARCHITECT SARS-CoV-2 antibody assay on 5 Abbott ARCHITECT i2000 automated analyzers at 2 academic medical centers.

Results: Within-run and between-run coefficients of variance (CVs) for the antibody assay did not exceed 5.6% and 8.6%, respectively, for each institution. Quantitative and qualitative results agreed for lithium heparin plasma, EDTA-plasma and serum specimen types. Results for all SARS-CoV-2 IgG-positive and -negative specimens were concordant among analyzers except for 1 specimen at 1 institution. Qualitative and quantitative agreement was observed for specimens exchanged between institutions. All patients had detectable antibodies by day 10 from symptom onset and maintained seropositivity throughout specimen procurement.

Conclusions: The analytical performance characteristics of the Abbott ARCHITECT SARS-CoV-2 antibody assay within and between 2 academic medical center clinical laboratories were acceptable for widespread clinical-laboratory use.

Keywords: antibody, COVID-19, EUA, immunoassay, SARS-CoV-2, serology

Coronavirus disease 2019 (COVID-19) was characterized as a global pandemic by the World Health Organization (WHO) on March 11, 2020, after first appearing in Wuhan, China in December 2019.[1] The highly contagious COVID-19 virus was identified to be a phylogenetic sister to the severe acute respiratory syndrome coronavirus (SARS-CoV) and has been named *severe acute respiratory coronavirus 2* (SARS-CoV-2).[2] As of March 8, 2021, there are over 29 million people in the United States and over 117 million people around the world who have been confirmed as having SARS-CoV-2 infection. As of July 17, 2020, nearly 3.5 million people in the United States and nearly 14 million people around the world have been confirmed as having SARS-CoV-2 infection.[3] However, the full extent of the outbreak has yet to be determined, due to limited testing to detect current or past exposure to the novel contagion.[4,5]

In an effort to slow the spread of COVID-19 and to avoid straining vital health care resources, numerous countries around the world have implemented social behaviorial restrictions for their citizens (ie, social distancing, lockdowns). Now, after a year of disrupted living and an economic crisis, government and scientific strategists are requesting accurate estimates of COVID-19 infection rates and immunity status as they prepare approaches to gradually lift these restrictions.[6] Consequently, a critical discussion point in returning to normal daily life has been centered on testing for human antibodies to SARS-CoV-2, to determine exposure rates and possible resistance to the virus.[6,7]

Abbreviations:

COVID-19, coronavirus disease 2019; WHO, World Health Organization; SARS-CoV, severe acute respiratory syndrome coronavirus; SAR-CoV-2, severe acute respiratory coronavirus 2; Ig, immunoglobulin; EUA, Emergency Use Authorization; PMA, premarket approval; N, nucleocapsid; S, spike surface; CMIA, chemiluminescent microparticle immunoassay; IRB, institutional review boards; UVA, University of Virginia; VCU, Virginia Commonwealth University; S/C, signal-to-calibrator; RT, real-time; CLSI, Clinical and Laboratory Standards Institute; CV, coefficient of variation; CI, confidence interval; IVD, in-vitro diagnostic

[1]Department of Pathology, University of Virginia (UVA) School of Medicine, Charlottesville, Virginia [2]Department of Pathology, Virginia Commonwealth University, Richmond, Virginia [3]Medical Laboratories, University of Virginia Health System, Charlottesville, Virginia

*To whom correspondence should be addressed.
LAL2S@virginia.edu

Recent preliminary reports[8–10] have attempted to quickly document the timeframe to detect antibodies to SARS-CoV-2 in infected individuals. Symptomatic individuals with SARS-CoV-2 infection typically did not demonstrate detectable antibodies to the virus in the first 7 days after symptoms.[8,9] In most hospitalized patients with a confirmed RNA viral load, detectable immunoglobulin (Ig)G antibodies appeared 14 to 28 days after symptoms onset.[10] Serology characteristics of IgM to SARS-CoV-2 has also been studied[8,11] and it appears to rise several days before IgG or simultaneously as previously described.[8,11]

Hundreds of SARS-CoV-2 antibody tests have rapidly emerged during the pandemic.[11,12] In the United States, manufacturers of these tests were not required by the FDA to go through their formal approval process.[13] However, this policy was changed, and now the FDA requires manufacturers to submit assay-performance data for review under the FDA Emergency Use Authorization (EUA) process.[14] However, due to the dynamic and evolving situation, typical assay validation and patient cohort studies through cross-institutional studies are still not being rigorously performed. These limitations have led to various questions regarding analytical performance characteristics that are typically vetted by the FDA 510(K) or premarket approval (PMA) review processes.[15]

The 2 most common analytical methods available to detect antibodies to SARS-CoV-2 rely on lateral flow immunochromatography or noncompetitive immunoassay technology.[11] These methods predominantly were designed to identify antibodies towards the SARS-CoV-2 nucleocapsid (N) or spike surface (S) proteins. A primary target for several assay developers has been directed towards the nonconserved S1 subunit of the SARS-CoV-2 spike protein. The S1 subunit is considered to be specific to each coronavirus strain, which could possibly mitigate cross-reactivity with the 4 common coronaviruses (eg, HKU1, NL63, OC43, 229E).[11] Initially large commercial manufacturers of laboratory tests started to distribute SARS-CoV-2 antibody tests for use on their automated immunoassay platforms, with or without EUA.[11]

Abbott Diagnostics recently developed a chemiluminescent microparticle immunoassay (CMIA) used for the qualitative detection of IgG antibodies to SARS-CoV-2 in human serum and plasma, which is run on the ARCHITECT i System.[16] Several performance evaluations of the assay[17–22] were published recently. However, the studies were conducted at single institutions, multiple analyzers were not evaluated, and only 1 study evaluated different specimen-collection tube types. Therefore, the aim of this study is to report on a cross-institutional approach for validating the Abbott Architect SARS-CoV-2-IgG immunoassay, evaluate assay performance for different specimen-collection tube types, and to document the kinetics of the serological response.

Methods and Materials

The study was considered to constitute research on nonhuman subjects, as defined by the institutional review boards (IRBs) of both institutions. Performance evaluation studies were conducted using the Abbott ARCHITECT qualitative SARS-CoV-2 IgG antibody assay, implemented on 2 Abbott ARCHITECT i2000SR immunoassay analyzers in the clinical laboratory at University of Virginia (UVA), and 3 ARCHITECT i2000SR immunoassay analyzers implemented in the clinical laboratory at Virginia Commonwealth University (VCU). Although the Abbott ARCHITECT SARS-CoV-2 IgG assay is a qualitative assay, quantitative evaluations of assay results were also performed using the numerical signal-to-calibrator (S/C) values. The assay cutoff for a positive result is 1.4 S/C or greater.

Blood was collected into BD Vacutainer SST II Advance tubes for serum-specimen studies, BD Vacutainer EDTA tubes for EDTA plasma studies, and BD Vacutainer PSTTM II tubes (all products by Becton, Dickinson and Company) for lithium heparin plasma specimens. Residual specimens were from patients with SARS-CoV-2 real-time (RT)–PCR results measured at VCU using the Xpert Xpress SARS-CoV-2 (Cepheid), BD SARS-CoV-2 (Becton, Dickinson and Company), or cobas SARS-CoV-2 (F. Hoffman-La Roche Ltd.) analytical systems. RT-PCR testing at UVA was performed by ABI 7500 (CDC assay) and Abbott m2000 (AbbVie Inc.). Prepandemic specimens had been collected in 2018 and 2019 and stored at –70°C and were categorized as having SARS-Cov-2–negative results.

For the studies conducted at UVA, 105 specimen from 8 individual patients who had positive results via SARS-CoV-2 PCR testing and 54 specimens from 34 patients with negative results via SARS-CoV-2 PCR tesing were collected.

Of those, 24 specimens from 4 patients tested positive for non–SARS-CoV-2 coronaviruses. To compare tube types, specimens from 20 patients were included when heparin lithium and EDTA plasma were available from the same phlebotomy draw: 40 specimens total.

UVA precision studies were performed as follows. Between-run imprecision was assessed by analyzing 2 levels of Abbott Architect SARS-CoV-2 IgG quality-control materials during a 5-day period; within-run imprecision was assessed by analyzing 10 replicates each of a SARS-CoV-2 IgG-positive and -negative patient specimen during a single run.

For the studies conducted at VCU, 116 specimens from 57 individual patients with positive results via SARS-CoV-2 PCR, 33 specimens from 32 patients testing negative via SARS-CoV-2 PCR, and 15 specimens collected before the pandemic were included. Fifteen of the specimens with negative SARS-CoV-2 PCR results were from 14 patients with positive results for the following non–SARS-CoV-2 respiratory viruses: 1 adenovirus, 1 influenza A, 4 rhinovirus/enterovirus, 4 coronavirus OC43 (3 individual patients), 3 coronavirus NL63, and 2 coronavirus HKU1. To compare tube types, specimens from 20 patients were included when heparin lithium and serum (red-top tube) were available from the same phlebotomy draw: 40 specimens total. VCU within-run and between-run precision studies were performed according to Clinical and Laboratory Standards Institute (CLSI) EP15.[23]

Because this study utilized residual specimens, the time duration between specimen collection for PCR testing and serology specimen collection varied. For all serology specimens except those collected in patients with other coronaviruses, specimens were collected between 1 and 26 days from non–SARS-CoV-2 PCR testing. For specimens from patients who tested positive for other coronaviruses, 7 of 33 serology specimens were collected the same day that the corresponding non–SARS-CoV-2 coronavirus PCR specimens were collected.

Box and whisker, Passing Bablok Regression Fit, and difference plots were constructed using R statistical software. Also, sum of least squares linear regression and difference plots were generated by Microsoft Excel version for Mac 2011 version 14.7.7 (Microsoft Corporation). Imprecision studies and statistical analyses among analyzers and study groups were performed by ANOVA using GraphPad statistical software (GraphPad Software) and Analyse-it (a statistical-analysis add-in for Microsoft Excel).

Results

Results of Imprecision and Among-Instrument Comparisons Studies for the Abbott ARCHITECT SARS-CoV-2 IgG Assay

The Abbott ARCHITECT SARS-CoV-2 IgG antibody assay exhibited similar performance characteristics during independent EUA verification studies conducted at both institutions. In **Table 1**, we show the results of imprecision assessments using S/C values for ARCHITECT SARS-CoV-2 IgG quality-control materials or patient specimens categorized as having positive or negative results via SARS-CoV-2 PCR. We obtained 100% qualitative agreement vs expected value for all results. For quantitative S/C values, imprecision did not exceed 5.6% for within-run coefficient of variation (CV) estimates and 8.6% for between-run CV estimates.

Table 1. Imprecision Study Results[a]

Institution	Negative SARS-CoV-2 IgG Result		Positive SARS-CoV-2 IgG Result	
	Within-run CV% (S/C)	Between-run CV% (S/C)	Within-run CV% (S/C)	Between-run CV% (S/C)
UVA	0.0% (0.02)	8.6% (0.05)	1.6% (4.10)	3.4% (3.14)
VCU	5.6% (0.05)	5.6% (0.05)	2.1% (3.35)	3.2% (3.35)

SARS-CoV-2, severe acute respiratory syndrome coronavirus 2; IgG, immunoglobulin G; CV, coefficient of variation; S/C, signal-to-calibrator; UVA, University of Virginia; VCU, Virginia Commonwealth University.

[a]Control specimens that tested negative and positive via Abbott ARCHITECT SARS-CoV-2 IgG assay were analyzed at UVA for between-run and at VCU for within-run and between-run imprecision estimates, the results are the average of the calculated imprecision values. A patient specimen with positive and negative results via SARS-CoV-2 IgG PCR testing i was analyzed at UVA for within-run imprecision estimates.

Lab Medicine 2021;52;e137–e146 e139
DOI: 10.1093/labmed/lmab011

A specimen-collection tube-type evaluation was performed independently at the 2 institutions. EDTA plasma specimens and corresponding lithium heparin plasma specimens collected from the same patients were analyzed at UVA. Lithium heparin plasma specimens and corresponding serum specimens collected from the same patients were analyzed at VCU. All qualitative results among tube types were 100% concordant, and the quantitative S/C results agreed (**Figure 1**). The difference plots showed average bias of –0.01 S/C, with maximum differences of 0.17 to –0.21 S/C for EDTA and lithium plasma; the slope of the linear regression for S/C values was 0.997 (95% confidence interval [CI], 0.985–1.008), with an intercept of 0.002 (–0.046 to 0.049). For serum and lithium plasma, the difference plots showed average bias of –0.04 S/C with maximum differences of 0.20 to –0.28 S/C for EDTA; the slope of the linear regression for S/C values was 0.984 (95% CI, 0.968–0.999), with an intercept of 0.008 (–0.051 to 0.067).

Among-instrument comparison studies were performed independently at each institution, using multiple analyzers, and evaluated for qualitative and quantitative agreement. Qualitative measurements at UVA for 2 ARCHITECT i2000 analyzers were concordant, with the exception of 1 specimen. One specimen, from a patient who tested positive for SARS-CoV-2 via PCR assay, tested negative via the ARCHITECT SARS-CoV-2 IgG assay on a single analyzer, with an S/C value below the 1.4 cutoff for positivity, as confirmed by repeat analysis. This specimen had been collected from a patient 11 days after symptoms; the patient experienced seroconversion on day 6 after symptoms, with all other specimens testing positive after day 6.

Quantitative S/C values for IgG-positive and IgG-negative results are shown in **Figure 2**. Median S/C values for IgG-positive results at UVA (**Figures 2A** and **2B**) were 4.86 and 4.72, respectively, and 0.06 and 0.06, respectively, for IgG-negative results via each analyzer. The results of

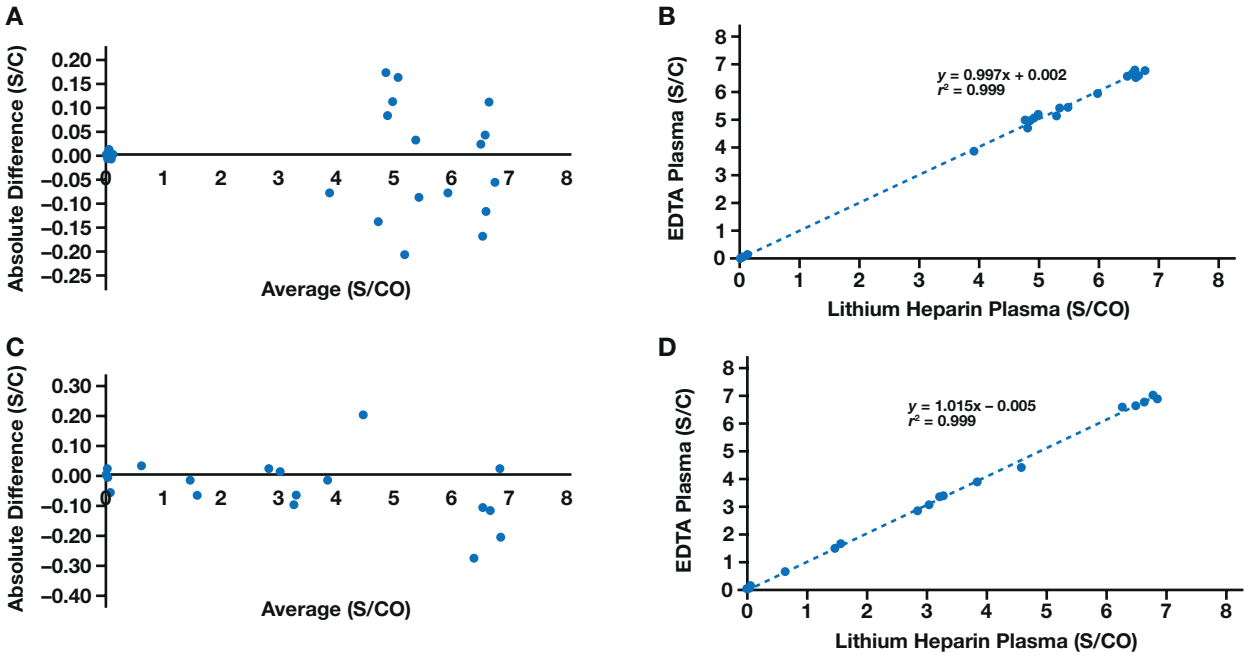

Figure 1

Comparison of the means of the signal-to-calibrator (S/C) values obtained from different specimen-collection tube types. S/C values from 30 specimen of lithium heparin plasma and corresponding EDTA-plasma specimen (from the same patients) were measured on analyzer A (**A**) and analyzer B (**B**) at the University of Virginia (UVA). S/C values from 21 specimens of lithium heparin plasma (**C**) and corresponding serum specimens from the same patients (**D**) were analyzed at Virginia Commonwealth University (VCU) on the same analyzer. Absolute-difference plots and ordinary least-squares regressions were calculated.

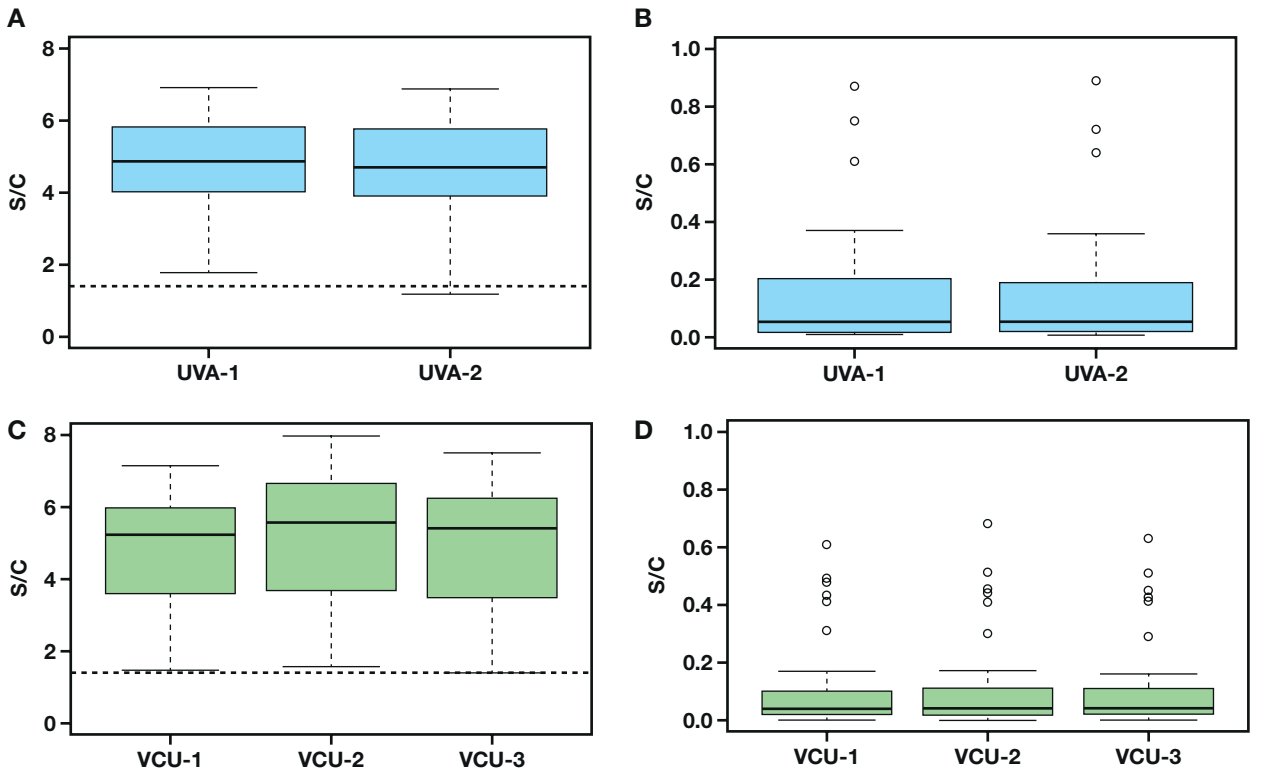

Figure 2

Lithium heparin specimens were analyzed on different analyzers at the University of Virginia (UVA) and Virginia Commonwealth University (VCU). At UVA, 64 severe acute respiratory syndrome coronavirus 2 (SARS-CoV-2) immunoglobulin (IgG)-positive specimens (**A**) and 59 IgG-negative (**B**) specimens were analyzed on 2 analyzers. At VCU, 78 IgG-positive specimens (**C**) and 86 IgG-negative specimens (**D**) were assayed on 3 analyzers. The dotted line at the bottom of panels A and C represent the assay cutoff of signal-to-calibrator (S/C) results, of 1.4. The heavy line is the median, the ends of the boxes are the 25th- and 75th-percentile values, and the end caps represent the maximum and minimum S/C values observed, with the open circles representing potential outliers.

among-instrument comparison studies performed at VCU demonstrated 100% qualitative agreement among 3 analyzers. Median S/C values at VCU (**Figures 2C** and **2D**) were 5.23, 5.56, and 5.40, respectively, for positive results, and 0.04, 0.04, and 0.04, respectively, for negative results via each analyzer.

For quantitative results, there were no statistically significant differences for median S/C values among analyzers for IgG-positive results at UVA (P = .66) or VCU (P = .30), or IgG-negative results at UVA (P = .91) or VCU (P = .97). Also, there were no statistically significant differences for median IgG S/C values among the 2 independent sample sets for IgG-positive specimens (P = .51) or among the 2 independent sample sets for IgG-negative specimens (P = .15).

To evaluate agreement of results for the IgG assay implemented at 2 different institutions, 9 lithium heparin specimens from patients with positive results via SARS-CoV-2 PCR and 10 lithium heparin specimens from patients with negative results via SARS-CoV-2 PCR were exchanged between the institutions; the S/C values were then compared. There was 100% concordance for qualitative IgG results for all specimens.

Figure 3 shows Passing-Bablok regression and an absolute difference plot of the S/C results of the exchanged specimens. S/C results showed quantitative agreement and no biases for specimens with S/C values less than 6.29. The slope of the regression was 0.990 (95% CI, 0.942–1.000), with an intercept of 0 (0–0.012), and the average bias was –0.08 S/C. One specimen exhibited a

DOI: 10.1093/labmed/lmab011

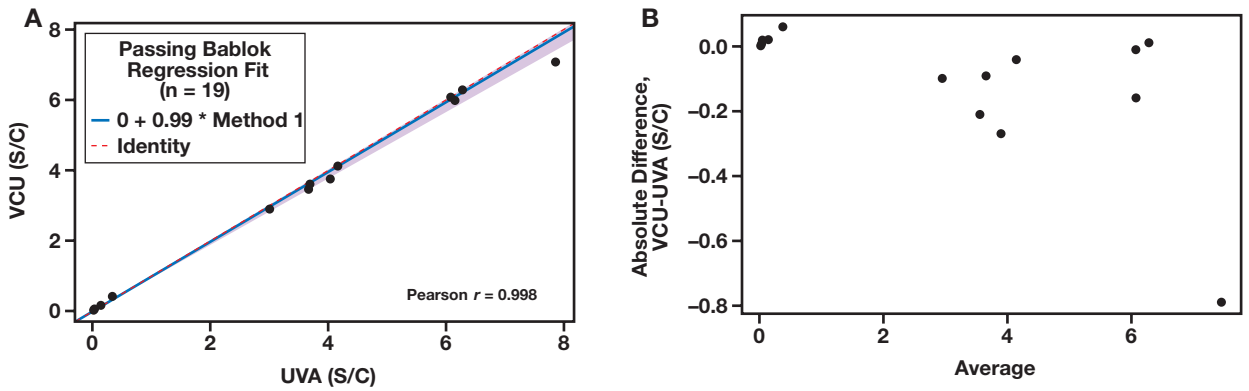

Figure 3

Comparison of results from specimens run at the University of Virginia (UVA) and Virginia Commonwealth University (VCU). Lithium heparin specimens (*n* = 19) were exchanged between institutions; the results are shown as Passing Bablok regression (**A**) and absolute-difference (**B**) plots.

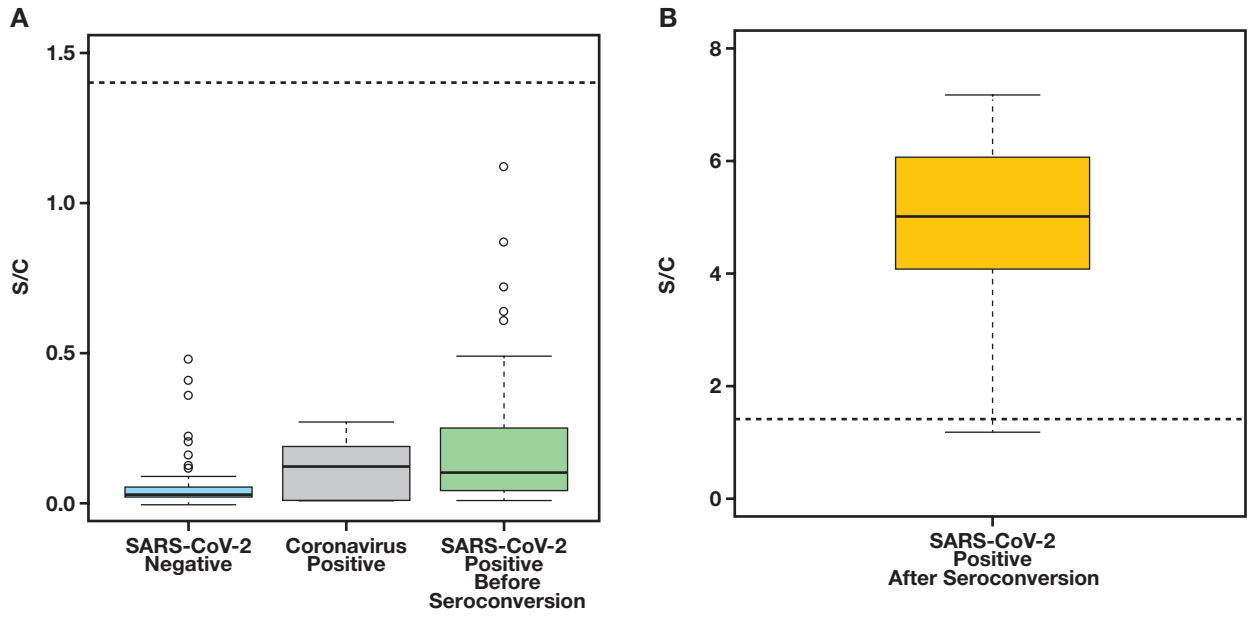

Figure 4

Comparison of signal-to-calibrator (S/C) results from patient specimens. Specimens were categorized based on patient severe acute respiratory syndrome coronavirus 2 (SARS-CoV-2) status. A box-and-whiskers plot shows the specimens with negative results (**A**), which are grouped by specimens testing SARS-CoV-2 negative (negative via PCR testing and collected before the pandemic: 68 patients, 68 specimens), specimens testing negative via SARS-CoV-2 PCR testing and others that tested positive for coronavirus via PCR testing (12 patients, 33 specimens), and specimens from patients who had tested positive for SARS-CoV-2 via PCR testing but had not yet experienced seroconversion (13 patients, 37 specimens). The specimens testing positive for SARS-CoV-2 via PCR (**B**) included all specimens collected after the first positive IgG result from patients in whom serial specimens were collected (9 patients, 65 specimens). The dotted lines at the bottom of the plots represent the positivity cutoff at S/C of 1.4. The heavy line is the median, the ends of the boxes are the 25th- and 75th-percentile values, and the end caps represent the maximum and minimum S/C values observed, with the open circles representing potential outliers.

bias of −0.80 S/C for VCU vs UVA at a S/C of 7.5; however, the bias did not affect the qualitative interpretation of the result.

Performance of the Abbott ARCHITECT SARS-CoV-2 IgG Antibody Assay in Different Patient Populations

Data from the independent method-comparison studies at each institution were combined to evaluate the IgG antibody assay performance for different patient populations. **Figure 4** shows S/C results of specimens that were classified into 1 of the following 4 categories: negative results via SARS-CoV-2 PCR (n = 68); negative results via SARS-CoV-2 PCR but positive results for non–SARS-CoV-2 coronaviruses via PCR (n = 33); serial specimens from patients with positive SARS-CoV-2 results via PCR but who had IgG-negative results and presumably had not yet experienced seroconversion (n = 37 specimens from 13 patients); and serial specimens from patients with SARS-COV-2 positivity via PCR, who had positive IgG results (n = 65). The median S/C values for the different patient groups were as follows: patients with SARS-CoV-2 negativity via PCR, 0.03; patients with other coronaviruses, 0.12; patients that had SARS-CoV-2 positivity via PCR but did not reach the cutoff for IgG positivity, 0.10; and SARS-CoV-2 positivity via PCR along with IgG positivity, 5.01.

Of the patients who tested negative for SARS-CoV-2 via PCR (**Figure 4A**), all had S/C results less than 1.12 (median, 0.04), and those results were well below the cutoff of 1.4, including specimens that tested positive for other coronaviruses. **Figure 4B** shows all specimens used in this study that had positive results via IgG for SARS-CoV-2, via IgG, including all specimens collected after the first positive IgG result was obtained from serial specimens. There was 1 discrepant specimen (**Figure 2**) that had false negativity via 1 analyzer and positivity via the other analyzer, after the patient experienced seroconversion (as mentioned in first section of the Results). Otherwise, all other data were greater than the cutoff for a positive result.

The medians were significantly different for patients with negative SARS-CoV-2 results via PCR testing (P <.01), patients with non–SARS-CoV-2 coronaviruses (P <.01), and those with SARS-CoV-2 positivity via PCR testing (P <.01) (**Figure 4A**). However, those values did not reach the cutoff for IgG positivity, compared with SARS-CoV-2 positivity via PCR and IgG positivity (**Figure 4B**). Also, median results for patients with other coronaviruses (0.12) and SARS-CoV-2 positivity via PCR but for whom values did not reach the cutoff for IgG positivity (0.10) were significantly larger than the median for patients with SARS-CoV-2 negativity via PCR (0.03; P <.05 and P <.01, respectively; **Figure 4A**). We note that the median S/C value for specimens from patients who positive for other coronaviruses (0.12) and positive for SARS-CoV-2 via PCR (0.10), but for whom values were below the cutoff for IgG positivity, were not significantly different (P = .27).

Seroconversion Across Serial Specimens in Patients with Positive Results Via PCR

Results from serial specimens from patients testing SARS-CoV-2 positive via PCR, beginning at the date of symptom onset, were examined to characterize the kinetics of seroconversion. The data were collected independently at the 2 institutions and were combined to generate **Figure 5**. We included 13 different patients in the evaluation, and by onset of symptoms after day 10, all patients had detectable IgG and maintained seropositivity for the remainder of the specimen-collection period.

Discussion

Before an in-vitro diagnostic (IVD) clinical assay is cleared by the FDA, the assay will go through an extensive, multisite clinical evaluation period.[24,25] This evaluation is performed to ensure that the analytical performance characteristics of the assay provide equivalent results among instruments and correspond to clinical outcomes in specified patient populations and clinical settings. In emergency situations, such as the current worldwide COVID-19 pandemic, the FDA provides IVD companies with the option to submit their tests through an EUA process.[26] This route is provided to expedite measurement technologies that can be rapidly deployed in a clinical setting for rapidly evolving medical conditions. However, the accelerated authorization may not identify performance issues that might otherwise have been identified during a normal review process.

We conducted a cross-institutional and multianalyzer evaluation of the Architect SARS-CoV-2 IgG antibody test implemented on the Abbott ARCHITECT i2000 platform

DOI: 10.1093/labmed/lmab011

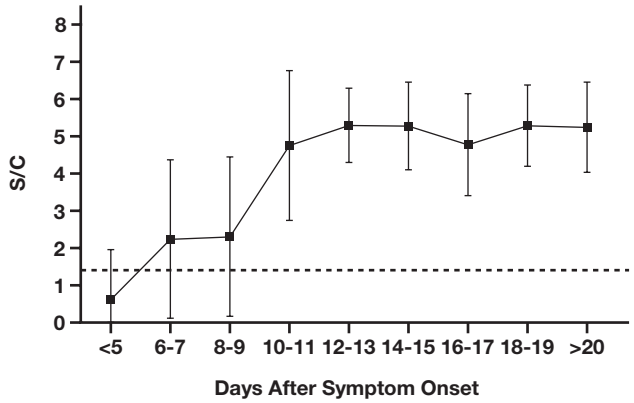

Figure 5

Serial specimens collected from 13 patients at different institutions and graphed by signal-to-calibrator (S/C) result. The x-axis represents postsymptom onset during a period of days; the sample size is ≤5 days (n = 18), 6–7 days (n = 15), 8–9 days (n = 13), 10–11 days (n = 10), 12–13 days (n = 7), 14–15 days (n=12), 16–17 days (n = 6), 18–19 days (n = 8) and ≥20 days (n = 17). The error bars indicate SD.

with 2 separate study-patient populations. Evaluations of the Abbott SARS-CoV-2 IgG antibody test have been published.[17–21] However, in each of these study reports, the authors do not evaluate assay performance among multiple ARCHITECT analyzers, and only 1 study evaluated different specimen-collection tube-type comparisons.

Similar to the findings of previously published studies, our assessment showed excellent analytical performance within and between both of our institutions. Assay imprecision was acceptable across both institutions for IgG antibody-negative and -positive specimens. Our specimen-tube evaluation demonstrated equivalent assay performance for lithium heparin plasma, EDTA plasma, and serum specimens. This finding is consistent with the updated manufacturer-provided instructions-for-use claims that all 3 specimen types are acceptable.[16] In contrast, the findings of a recent study[22] showed significant differences between plasma- and serum-based testing in other commercially available antibody assays; these findings highlight the importance of performing specimen-type verification studies.

For within-institution method comparison studies, all IgG antibody results were concordant among analyzers or with patient SARS-CoV-2 PCR result, with the exception of 1 specimen at 1 institution. For that specimen, the IgG antibody result was below the assay cutoff; however, but the patient had a positive result via SARS-CoV-2 PCR testing, and positive IgG results had been obtained for specimens collected before that specimen, which suggests a preanalytical error, false-negative assay result, or technical error. Analysis of the same 19 specimens at both institutions yielded 100% qualitative concordance among the 5 analyzers at both institutions, demonstrating equivalent assay performance across institutions and analyzers. Also, no statistically significant differences were obtained for S/C results within institutions, suggesting equivalent quantitative performance.

Cross-reactivity in SARS-CoV-2 antibody tests has been a concern from the medical community. In our study, we included specimens from patients who had tested negative via SARS-CoV-2 PCR, had tested positive for other coronaviruses via PCR, and had had specimens collected before the pandemic. All of these 101 specimens had negative qualitative results via the Abbott ARCHITECT assay, supporting lack of cross-reactivity with immunoglobulins produced in response to other viral infections.

One finding that interested us was a slightly larger median S/C value for patients diagnosed with non–SARS-CoV-2 coronaviruses compared to specimens obtained from patients with a negative SARS-CoV-2 result via PCR. This result could suggest partial interference from non–SARS-CoV-2 IgG antibodies. However, if there was potential interference, it was not substantial enough to affect the qualitative result. Also, the S/C values for patients with positive results via PCR before seroconversion had significantly larger values, compared with patients having negative results via PCR. This finding suggests the possible presence of SARS-CoV-2 IgG antibodies at a concentration lower than the cutoff for the assay. This observation

agrees with previously published findings.[18] Our results are consistent with those of previously published studies[17–21] evaluating the specificity of the Abbott ARCHITECT SARS-CoV-2 assay.

Seroconversion studies included specimen from both institutions. For all 13 patients who tested positive for SARS-CoV-2 via PCR testing who were included in the seroconversion study, seroconversion was detected by the IgG antibody assay within 10 days of symptom onset. This finding is consistent with those of previous studies.[8,9,18]

The present study has some limitations. A limitation of the cross-reactivity assessment was that for 6 patients who tested positive via PCR for non–SARS-CoV-2 coronaviruses, specimens were collected for serological testing within 4 days of specimen collection for the viral PCR assay and an unknown time period from the time of symptom onset. Therefore, the patients from whom the specimens were obtained may have had insufficient time to develop a robust IgG response and, thus, the specimen may not have been suitable for assessment of cross-reactivity in the ARCHITECT SARS-CoV-2 IgG antibody assay.

Another limitation is the relatively small number of specimens included in the seroconversion study. Because the specimens were obtained from among specimens submitted for purposes other than this research, our ability for specimen acquisition was limited. It is possible that seroconversion kinetics may have differed if specimens had been obtained on a daily basis for all patients. Also, the number of serial specimens and time of specimen collection for IgG antibody testing relative to PCR testing varied, and time of symptom onset was unknown for the specimens from other patients in this study. These factors could complicate comparison of S/C values among the different patient categories shown in **Figure 4**. Further research is needed to define the relationships of S/C values in patients infected with non–SARS-CoV-2 coronavirus, as well as in patients testing positive for SARS-CoV-2 via PCR before seroconversion vs after seroconversion.

In conclusion, the Abbott ARCHITECT SARS-CoV-2 IgG assay performed similarly for 3 specimen types and across 5 analyzers at 2 different institutions. This finding suggests acceptable performance of this assay and analyzer for widespread clinical laboratory use. **LM**

Personal and Professional Conflicts of Interest

None reported.

References

1. WHO Director-General's opening remarks at the media briefing on COVID-19. Published March 11, 2020. Accessed Febuary 20, 2021. https://www.who.int/dg/speeches/detail/who-director-general-s-opening-remarks-at-the-media-briefing-on-covid-19---11-march-2020
2. Gorbalenya AE, Baker SC, Baric RS, et al. The species *severe acute respiratory syndrome-related coronavirus*: classifying 2019-nCoV and naming it SARS-CoV-2. *Nat Microbiol.* 2020;5:536–544.
3. COVID-19 Map. Johns Hopkins Coronavirus Resource Center. Last updated February 20, 2021. Accessed February 20, 2021. https://coronavirus.jhu.edu/map.html. Accessed March 8, 2021.
4. IDSA Releases Antibody Testing Primer. Updated April 20, 2020. Accessed February 20, 2021. https://www.idsociety.org/news--publications-new/articles/2020/emphasizing-need-for-more-information-idsa-releases-antibody-testing-primer2/
5. The New York Times website. Mandavilli A. Coronavirus Antibody Tests: Can You Trust the Results? Published April 24, 2020. Accessed February 20, 2021. https://www.nytimes.com/2020/04/24/health/coronavirus-antibody-tests.html
6. The New York Times website. Eder S, Twohey M, Mandavilli A. Antibody Test, Seen as Key to Reopening Country, Does Not Yet Deliver. Accessed February 20, 2021. https://www.nytimes.com/2020/04/19/us/coronavirus-antibody-tests.html
7. Weitz JS, Beckett SJ, Coenen AR, et al. Intervention Serology and Interaction Substitution: Modeling the Role of 'Shield Immunity' in Reducing COVID-19 Epidemic Spread. Published April 3, 2021. Accessed February 20, 2021. https://www.medrxiv.org/content/10.1101/2020.04.01.20049767v1
8. Lou B, Li T-D, Zheng S-F, et al. Serology characteristics of SARS-CoV-2 infection since the exposure and post symptoms onset. Published March 27. 2020. Accessed February 20, 2021. https://www.medrxiv.org/content/10.1101/2020.03.23.20041707v1
9. Liu L, Liu W, Zheng Y, et al. A preliminary study on serological assay for severe acute respiratory syndrome coronavirus 2 (SARS-CoV-2) in 238 admitted hospital patients. Accessed February 20, 2021. https://www.medrxiv.org/content/10.1101/2020.03.06.20031856v1
10. Wölfel R, Corman VM, Guggemos W, et al. Virological assessment of hospitalized patients with COVID-2019. *Nature.* 2020;581(7809):465–469.
11. Long Q-X, Liu B-Z, Deng H-J, et al. Antibody responses to SARS-CoV-2 in patients with COVID-19. *Nat Med.* 2020;26(6):845–848.
12. Torres R, Rinder HM. Double-edged spike: are SARS-CoV-2 serologic tests safe right now? *Am J Clin Pathol.*. 2020;aqaa071.
13. Wall Street Journal. Burton TM. FDA sets standards for coronavirus antibody tests in crackdown on fraud. Updated May 4, 2020. Accessed February 20, 2021. https://www.wsj.com/articles/fda-sets-standards-for-coronavirus-antibody-tests-in-crackdown-on-fraud-11588605373
14. FDA. Insight into FDA's Revised Policy on Antibody Tests: Prioritizing Access and Accuracy. Updated May 4, 2020. Accessed February 20, 2021. https://www.fda.gov/news-events/fda-voices/insight-fdas-revised-policy-antibody-tests-prioritizing-access-and-accuracy
15. FDA. Center for Devices and Radiological Health. Policy for Coronavirus Disease-2019 Tests During the Public Health Emergency (Revised). Published May 2020. Accessed February 20, 2021. https://www.fda.

DOI: 10.1093/labmed/lmab011

gov/regulatory-information/search-fda-guidance-documents/policy-coronavirus-disease-2019-tests-during-public-health-emergency-revised

16. Farnsworth CW, Anderson NW. SARS-CoV-2 serology: much hype, little data. *Clin Chem.* 2020;66(7):875–877.
17. Abbott. SARS-CoV-2 Immunoassays: Advancing Diagnostics of COVID-19. Accessed February 20, 2021. https://www.corelaboratory.abbott/us/en/offerings/segments/infectious-disease/sars-cov-2
18. Bryan A, Pepper G, Wener MH, et al. Performance characteristics of the Abbott Architect SARS-CoV-2 IgG assay and seroprevalence in Boise, Idaho. *J Clin Microbiol*. 2020;58(8):e00941-20.
19. Tang MS, Hock KG, Logsdon NM, et al. Clinical performance of two SARS-CoV-2 serologic assays. *Clin Chem*. 2020;66(8):1055–1062.
20. Kohmer N, Westhaus S, Rühl C, Ciesek S, Rabenau HF. Brief clinical evaluation of six high-throughput SARS-CoV-2 IgG antibody assays. *J Clin Virol.* 2020;129:104480.
21. Nicol T, Lefeuvre C, Serri O, et al. Assessment of SARS-CoV-2 serological tests for the diagnosis of COVID-19 through the evaluation of three immunoassays: two automated immunoassays (Euroimmun and Abbott) and one rapid lateral flow immunoassay (NG Biotech). *J Clin Virol.* 2020;129:104511.
22. Theel ES, Harring J, Hilgart H, Granger D. Performance characteristics of four high-throughput immunoassays for detection of IgG antibodies against SARS-CoV-2. *J Clin Microbiol*. 2020;58(8):e01243-20.
23. Haselmann V, Kittel M, Gerhards C, et al. Comparison of test performance of commercial anti-SARS-CoV-2 immunoassays in serum and plasma samples. *Clin Chim Acta.* 2020;510:73–78.
24. Carey RN, Durham AP, Hauck WW, et al. *User Verification of Precision and Estimation of Bias; Approved Guideline*. Clinical Laboratory Standards Institute; 2014.
25. FDA. Overview of IVD Regulation. Updated September 16, 2019. Accessed February 20, 2021. https://www.fda.gov/medical-devices/ivd-regulatory-assistance/overview-ivd-regulation
26. FDA. *Regulatory Controls*. Published March 27, 2018. Accessed February 20, 2021. https://www.fda.gov/medical-devices/overview-device-regulation/regulatory-controls
27. FDA. *Emergency Use Authorization. Updated February 19, 2021.* Accessed February 20, 2021. https://www.fda.gov/emergency-preparedness-and-response/mcm-legal-regulatory-and-policy-framework/emergency-use-authorization